SYNTHESIS AND CHARACTERIZATION OF PHOSPHINE OXIDE CONTAINING MONOMERS AND OF THE FLAME RESISTANT POLYMERS PREPARED THEREFROM

by

Charles N. Tchatchoua

Dissertation submitted to the Faculty of the

Virginia Polytechnic Institute and State University

in partial fulfillment of the requirements for the degree of

DOCTOR OF PHILOSOPHY

in

Chemistry

APPROVED:

Dr. James E. McGrath, Chairman

Dr. Allan R. Shultz

Dr. Gary L. Long

Dr. Judy S. Riffle

Dr. James P. Wightman

Dr. James F. Wolfe

December 21, 1999

Blacksburg, Virginia

SYNTHESIS AND CHARACTERIZATION OF PHOSPHINE OXIDE CONTAINING MONOMERS AND OF THE FLAME RESISTANT POLYMERS PREPARED THEREFROM

by

Charles N. Tchatchoua

Dr. James E. McGrath, Committee Chairman

Chemistry

(ABSTRACT)

This thesis has focused on the synthesis and characterization of amino functional monomers, principally monomers containing aryl phosphine oxide units. Utilization of these monomers was demonstrated in various types of linear and network polymerizations. The diamines monomers included bis(3-aminophenyl) methyl phosphine oxide (DAMPO), bis(3-aminophenyl) phenyl phosphine oxide (DAPPO), bis(3-aminophenoxy phenyl) phenyl phosphine oxide (BAPPO) and bis(3-aminophenoxy phenyl) methyl Phosphine oxide (BAMPO). From these monomers high molecular weight poly(ether imides), polyurea-urethanes, poly(arylene ether ketones) poly(arylene ether sulfones) and poly(arylene ether phosphine oxides) were. Internal and external fire testing methodologies showed that the new polymers containing phosphine oxide units were fire resistant while maintaining the desirable physical characteristics of carefully selected control systems.

In addition, suitable curing schedules for epoxy networks were determined by using dielectric monitoring techniques. The curing rates varied with the structure of the monomers and were slowest for the deactivated control (4,4'aminophenyl sulfone). Epoxy networks containing aryl phosphine oxide units had higher char yields in dynamic thermogravimetric analyses than control specimens. This correlated with their superior flame resistance.

The brittle epoxy matrices were subsequently modified with reactive or non-reactive thermoplastic polymers in order to improve their fracture toughness. Poly(ether

imides) and poly(ether sulfones) showed good phase separation behavior with tetrafunctional epoxy matrices during the curing reactions, as confirmed by scanning electron microscopy (SEM) and dynamic mechanical analysis (DMA). Mechanical tests showed that reactive thermoplastic modification of the epoxy networks improved the fracture toughness of the systems, without noticeable decreases in other characteristics such as flexural modulus. Reactive systems also maintained chemical resistance in contrast to non-reactive thermoplastic controls.

ACKNOWLEDGMENTS

I will not thank anybody. I would rather not. These past years have been absolutely marvelous to me, with the encouragements and blessings of too many people for me to remember. I have been very comfortable in this town (my other home town) and it would be sad if I forget any of the people who have been so wonderful to me. I would not thank anybody. It would be regrettable if I forgot my graduate committee with Professor McGrath who has supported me in every possible way during the completion of my program. It would be sad to omit Dr. James Wightman who went as far as to learn the basis of my own native language so he would make me feel at home. It is always a very pleasant surprise to hear someone shouting hello from a distance in my own language, with my uncle's accent. Professor Riffle taught me the basis of organic chemistry and has been very supportive to me. Her encouragements lead me to study polymer chemistry. I rather not thank anybody. I could not afford to forget Dr. Allan Shultz who turned all of my scratches into scientific articles. Dr. Wolfe was right across the hall and would always be one of my favorite advisors. Dr. Gary Long taught me something that I probably could not learn from anybody else (analytical spectroscopy)! May God bless such a diligent professor?

O Lord! I always literally forget about the secretaries, Laurie Good, Esther Brann, Millie Ryan, and Joyce Mosher who would work way past the quitting time to make sure that my late abstract is eventually submitted, sometimes ten days past the deadline. They have been writing my resume lately. I will not thank anybody. I mean it. It would be sad to forget any of my fellows graduate students, Nazan Gunduz, Debi Dunson, Jeff Meacham, Dave Polk, Elena Bonaplata, Emre Isin, Dave Porter and many others, all of who have contributed a lot in the work I seem to do. Dr. Sheng Wang scanned all of my images into computer files. Dr. Hong Zhuang made sure I never starved, even if it took for her to cook again after her diner. Her son Wilson took it upon himself to teach me some of his computer games. What slow learners chemists are, he might think.

Professor Robert Hoehn (my host family) took me to his house from the first week I came to this town. How could I afford to forget Johnnie Hoehn? She would pay my debts for me if that were what it takes to make me feel happy. Julie and Andrew would wrap specials gifts for me for any occasions that come to their mind. This makes it very difficult for me to leave this town. Christmas would not be over until I unwrap the gift from David and Annie Hoehn.

Dr. Sankar and Dr. Ajit Banthia are sitting across from me while I am writing these lines, and may heaven forgive me, I had forgotten about them. They are always here to help me.

How could I afford to omit Professor Hohenboken (my other advisor) and Linda Hohenboken (she makes the best pies in the world)? I will not thank anybody. It would not be fair to forget Dr. Paul Siegel and Dr. Ron Pearson, both genetic professors, for the patience and kindness that they have shown to me.

Dr. LaBerge (the international student advisor) refers to me as his Cameroonian brother. He served in Cameroon as a Peace Corps volunteer. I am grateful to the Almighty that I had brothers in the international office. I do not know how else they could have put up with me in the last ten years. Dr. McKeon probably has other things to do than fixing the visas that I always forget to renew. And now I forgot about Monica Gibson. She is also tired of fixing the same visa over and over again. She now calls me to remind me that my visa will be expiring in the next few days.

How could I afford to forget Mr. Jim Brown in the accounting office at Burruss Hall? He had designed a tuition payment plan for a poor and absent-minded student, without which my life would have been very miserable. This had saved me hundreds of dollars in late payment fees. May Mother Africa someday reap the benefits of these savings.

Margie Lawrence, Jim Jones, John Stimpson and other residence and housing employees have been very helpful to me during my earlier years in this town. Dave and Katherine Aho carried my stuffs everywhere with their big truck. Jim and Caty Nelson used to fix the old looking cars that I used to have. It would not be nice to omit any of them.

Professor Frank Van Damme and Andy Mollick made all of the strange types of glassware that I used. Shame on me, should I forget Ronna Cadorette who taught me how to behave like a good organic laboratory instructor. Joe Fagan has been very helpful in discussing the laboratory sessions. Dr. Glanville, Dr. Sanzone and Dr. Harold Bell were always there to help me. Dr. Merola is an outstanding professor. I wish he had taught me physical chemistry. Professor Larry Taylor would even notice it when I am out of town for a few days. It would be sad if I forget any of them.

Dr. Jim Shuler may be a great politician to most of you. Dr. Jim and Margaret Shuler are wonderful people, to say the least. Their generosity has left me speechless in several occasions. Curse on me if I forget to thank them.

It is always a pleasure to run into my laboratory students on campus, some of who have even invited me to their wedding. My stay on this campus would be meaningless without them. Shame on me if I forget to thank any of them.

I could not honestly afford to forget all the children of this town, who always shine light on my confused mind. I will forever remember the late Milena Conte for her generous hugs and kisses. She was a sweet little angel.

Dr. Greg Lyle has taught me how to set up a polymer chemistry laboratory. He is very patient, kind and knowledgeable.

I have had the rare privilege to work side by side with many outstanding scientists from all over the world and it would be very ungrateful to omit any of them: Dr. Hu Yang and his most wonderful wife, Dr. Attila Gungor, Dr. Lin, Dr. Maria Martinez, Dr. Hossein Ghassemi, Dr. Satya Srinivasan, Dr. Biao Tan, Dr. Dan Knauss, Dr. Dan Riley, Dr. Sue Mecham and her wonderful children Michael and Shane. I would rather not thank any of them.

What Lord if I forget about Rose Muggli and all the delicious Austrian dishes that she made for me. Sometimes she would cook African food, if that would make me feel at home or for any other reason of her choice. Mark Muggli and his children, Florian, Janika, Joseph and Peter made my stay here extremely pleasant. I nearly forgot about his parents and siblings who make of Minnesota the place to visit (during summer time).

How could I afford to forget Maxime Smith, Juanita Knott, Mary English and Charles Williams? They know who they are.

How could I afford to forget the pleasant Sundays with my campus ministers Peter McCourt, Marlene McGrath and Cate O'Hare.

It would be sad to omit Dick and Kathleen Harshberger, Peter Hastings, Gary and Leslie Whitings, and other wishful minded people of the University Club.

My family have given me everything they had so I could study abroad. It would be a punishable crime to forget any of the collective efforts that have been invested into me. May God bless them and bless Mother Africa.

I owe this world too much o Lord, and rather than omitting any of my creditors, I would not thank anybody. I can live with that.

Table of Contents

List of Tables

List of Schemes

List of Figures

1 CHAPTER 1 INTRODUCTION

1.1 An Overview Of Aryl Phosphine Oxide Containing Diamines

Organic polymers are increasingly applicable to a wide variety of material systems, ranging from household utensils to high performance aerospace structures. However, it is well known that limitations exist in areas which require high thermal and flame resistance. Thermal properties of polymers can be improved by introducing heterocyclic or aromatic rings into their backbone, such as in the case of polyimides. Modification of epoxy networks to improve their thermal properties have received increasing attention during recent years.[1-4]

Physical blending of flame retardant compounds into polymeric systems is a widely practiced approach. It has long been known that phosphorus, either as a component of the polymer chemical structure, or as a phosphorus additive can significantly improve the flame resistance of polymeric materials.[5,6] However, literature reveals that the most common pathway by which phosphorus-containing polymers have been synthesized employs phosphorus-oxygen-carbon bonds. Unfortunately, though economical, these materials are very hydrolytically unstable and will hydrolyze even in the presence of atmospheric moisture. The general approach of incorporating phosphorus in polymeric materials by simple physical blending with flame retardant additives often further embrittles both thermosets and tough engineering thermoplastics. Moreover, in the case of textile fibers and fabrics, simple laundering with detergents could hydrolyze the flame retardant additive or extract it from the textile fabric system. Indeed, one must also be concerned with possible toxicological effects of the extracted additives. In contrast, one may synthesize molecules, such as triphenyl phosphine or triphenyl phosphine oxide, with phosphorus-carbon bonds that are both hydrolytically and thermally stable.[7] Until recently, the study of polymeric materials whose structures contained the aryl phosphine oxide unit attached by chemical bonds has been extremely limited.

During the past few years our research group has been very active in the effort to demonstrate many unique characteristics of the phosphine oxide moiety in polymeric materials.[8,9,10] These characteristics can be summarized in these terms:

- Thermooxidative and hydrolytic stability
- Improved miscibility with other polymers through polar hydrogen bonding
- High char yields which impart fire resistance
- Improved adhesion to metals
- Superior optical properties (high refractive index)
- Enhanced structure modification possibilities, e.g., sulfonation, nitration, reduction
- Higher glass transition temperatures

A wide variety of triphenyl phosphine oxide containing polymers, including polyimides, polyamides, polyesters, polyarylene ethers, polysiloxane copolymers and thermosets, such as epoxy or bismaleimides, have been synthesized. Several triphenyl phosphine oxide derivatives were synthesized in an effort to find candidate phosphine oxide containing curing agents for epoxy resins. It was found that those compounds as a rule had high melting points (sometimes above 300°C) and low solubilities in common solvents as well as in the epoxy resins. These difficulties were overcome by introducing heteroatoms, e.g. and by isomeric design.

Preparations of diamines containing phosphine oxide units were reported as early as 1963.[11,12] One important synthesis involved the nitration of diphenyl methylphosphine oxide, followed by the reduction of the nitro compound to give the bis(3-aminophenyl) methyl phosphine oxide (DAMPO) in good yield. Diamine functional phenyl substituted phosphine oxides have been less studied in the literature than any other phosphine oxide containing monomers. This is probably due to the nature of the P-C bond formation. Grignard techniques have been used for the preparation of triphenyl phosphine oxide monomers, but amine or nitro group substitutions on aromatic rings render the Grignard route useless, unless impractical protective groups are used.

The Friedel Crafts reactions of phenyl rings with either phosphines or phosphine sulfides (P=S) is another process involved in the formation of P-C bonds. These materials can be subsequently oxidized to the corresponding phosphine oxides with commonly

used reagents such as hydrogen peroxide (H_2O_2) or potassium permanganate ($KMnO_4$).[13] Once again, problems exist with nitro group deactivation of aromatic rings to Friedel-Crafts catalysts.

Another possible route to the synthesis of aminated phosphine oxide containing monomers is the nitration of triphenylphosphine oxide, followed by the reduction of the resulting nitro compound. Earlier studies showed that this route was extremely challenging, because of the formation of several isomeric forms of the nitro intermediate. Separation of these isomers was possible only by very precise chromatographic procedures.[14] Another diamine of similar structure, bis(4-aminophenyl) phenyl phosphine oxide was reportedly synthesized through a single step procedure[15] that involved a reaction between 4,4'-dichlorodiphenyl phosphine oxide and aniline hydrochloride (48 hours at 140-190°C). A polymer grade diamine was reported to be obtained in low yields after recrystallization from ethanol. Unfortunately, these findings were incorrect and simply produced a diamide.[16, 17]

The synthesis of bis(3-aminophenyl) phenyl phosphine oxide has recently been reported .[18] The compound was obtained in high yield and excellent purity by nitrating commercially available triphenylphosphine oxide and subsequently reducing the nitro derivative to the corresponding diamine. However, the amount of nitric acid used in the nitration step was crucial to substantially reduce the formation of the trinitro side product. The synthesis of bis(4-aminophenyl) phenyl phosphine oxide has also been reported in our research group.[19] In one approach, a bromo substituted phenyl ring was attached to dichlorophenyl phosphine with Grignard techniques, followed by the oxidation of the phosphine unit and a subsequent amination of the bromophenyl unit via a Gabriel synthesis.[17, 19] Both the yield and the purity were satisfactory.

1.2 Thesis Objectives

A major goal of the proposed research was to synthesize phosphine oxide containing diamine monomers which possess low melting points, or which were at the least soluble in the systems in which they were intended to be used. Those systems included polyimides, epoxy networks and polyurea-urethanes. Another objective of this

work was to use high performance thermoplastics, poly(ethersulfones) and poly(etherimides), to improve the fracture toughness of epoxy networks.

In collaborative studies[20] suitable curing conditions of epoxy networks were investigated via dielectric analysis.

Preliminary work in our laboratory had pointed out that many triphenyl phosphine oxide diamines have high melting points. The melting points of these compounds could however be drastically reduced and their solubility significantly improved either by extending the phenyl rings with ether linkages or by replacing one of the phenyl rings with an alkyl chain. Within this framework, the synthesis of suitable diamines and determining their efficacy in linear and network polymerization were high priority.

Although some of the monomers had already been previously reported in the literature, either their yield or purity was not adequate. Moreover the synthetic steps often employed exotic reactions, which later proved to be inappropriate when attempting to expand the scale of the synthesis.

It is very important to indicate that our research group has been involved in flame resistance testing of polymeric materials. Some of the techniques used for this purpose, such as cone calorimetry, use rather large samples with precise dimensions and require several replicates for validity. A consciensus effort was therefore made to avoid chemistry which would produce only moderate to poor yields or involved multi-step pathways.

1.3 Phosphorus Chemistry

There has been a spectacular increase in the synthetic organic chemistry of phosphorus during the last decade.[21, 22, 23] The importance of this chemistry can be easily understood on the basis that phosphorus compounds play a vital role in living processes. The importance of phosphate esters in nucleic acid synthesis and in the formation of carbon-carbon bonds in terpene and steroid synthesis is particularly well known. Furthermore, a wide range of applications has been found for trivalent phosphorus and for phosphonium salts, most of which are derived from the Wittig reaction.

Phosphorus containing polymers are relatively few in number compared to other organic polymers. Polyphosphazene, which is also known as “inorganic rubber” was

perhaps the first known synthetic phosphorus containing polymer.[24] Although its synthesis was reported by the end of the past century, the technological potential for this class of polymers has only been recently realized. Interest in polyphosphazenes specialty elastomers range from aerospace, marine technologies and oil exploration to a few other industries.[26,27] Several other phosphorus containing polymers have now been prepared, but not many are yet industrially important. These polymers include polyimides,[8] poly(ether sulfones),[10] polyphosphonates,[27, 28, 29] polybenzimidazoles,[30] and phenoxaphosphine ring containing polymer.[31,32,33] Most of these polymers are not only flame resistant but are also thermostable. However, polymers containing P-N and P-O-C linkages suffer from hydrolytic instability.[34]

The chemistry of phosphorus and its derivatives follows closely the electronic structure of the atom and is sometimes compared with that of nitrogen or even chromium (a typical transition element). Of course elements like nitrogen and phosphorus differ considerably from transition elements in which 4*s*, 4p and 3d levels also exist. Consequently, d-orbital bonding is very important in transition metal complexes and determines their stereochemistry and chemical stability. In the case of nitrogen and phosphorus, the d-orbitals are less defined hence other high energy states (4s, 4p, 5s) may make similar contributions to the 3d-level in stabilizing these systems. The contributions of these high energy orbitals will affect the polarizability of the atom, and hence the reactivity, but it is unlikely that the 3d-orbitals of phosphorus can influence the stereochemistry of the 5- and 6- coordinated compounds significantly.[35]

The 3s - 3d promotional energy for phosphorus (17eV) is, however, significantly less than that of nitrogen (23eV) and consequently the contribution of higher energy levels will be greater. This lead to a reduced electronegativity and greater polarizability. These differences are responsible for many of the different structures and reactions of the compounds of nitrogen and phosphorus. Elemental phosphorus shows very interesting structural properties, and several allotropic modifications have been described. The physical chemistry of the allotropes has been widely investigated. Of the two common forms, white and red phosphorus, the former is metastable (with a high vapor pressure) and consists of cubic packed tetrahedra whereas the red, violet and metallic forms are largely amorphous, highly polymeric solids with very low vapor pressures.

Derivatives of trivalent phosphorus are very nucleophilic owing to the relatively low ionization potential of the 3s-electrons and the strong sp^3 bonds in the product. However they are also very electrophilic, because of the relatively low electronic repulsion exerted towards a nucleophilic reagent. This follows from the greater radius of polarizability of phosphorus compared with a first-row element. Displacement reactions of tervalent phosphorus are therefore extremely rapid and thus, P-P and P-S bonds, but not C-C bonds are rapidly broken by both nucleophilic and electrophilic reagents. The high energy of d-orbitals contributes to the reduced electronegativity and the greater polarizability of phosphorus compared to that of nitrogen. The chemistry of phosphorus generally lies much closer to that of arsenic, and therefore a given phosphorus compound often resembles its arsenic analog in structure and in many of its properties. In general, phosphorus compounds prefer to react by electron pair mechanisms, utilizing the nucleophilic reactivity of the lone pair electrons in the case of trivalent compounds and the electrophilicity of the phosphorus atom in the pentavalent derivatives. However, some phosphorus reactions proceed also by a free radical mechanism.[36, 37]

Bimolecular substitution on phosphorus proceeds via a trigonal bipyramidal transition state (S_N2-reaction) as with carbon. In the case of phosphorus compounds, the intermediate trigonal bipyramid has a finite lifetime ($\sim 10^{-13}$s), and it can be observed and sometimes isolated as a definite compound, compared to the transitory ($<10^{-13}$s) trigonal bipyramid of carbon. In carbon compounds however, the S_N2-reaction is stereospecific but this is not always true with phosphorus compounds. The other common mechanism for substitution, i.e., S_N1, is similar to that for carbon compounds.

Nucleophilic substitution on pentavalent phosphorus clearly has no parallel in carbon chemistry. There is evidence that these reactions proceed via tetrahedral phosphonium ions or octahedral transition states.[38]

Phosphorus forms binary compounds with most elements except antimony, bismuth and, of course, the noble gases. It forms various polymeric (oligomeric) compounds having P-P, P-C, P-N and P-O-C linkages. From the bond strength values in table 1.3-1 it is expected that P-C, P-O and P-N linkages in the main chain may give rise to thermostable polymers. The P-O bond is stronger than N-O or C-O bonds. The P-C bond is very resistant to oxidation and hydrolysis, and in this respect is more stable than

the C-C bond. The phosphoryl P=O linkage is quite strong and stable but when the oxygen atom is involved in the bridge, e.g., in P-O-P or P-O-C linkages, this generally results in hydrolytic instability.[34] The P-O-C linkage is, however, more stable than the P-O-P and P-O-Si linkages. P-S linkages reduce the stability of the compound both thermally and hydrolytically relative to P-O linkages. P-O and P-N bonds show various degrees of π-bonding in different compounds. The bond energy of P=O is greater than $N^{+}O^{-}$, indicating extra bonding in the case of phosphorus compounds. The bond strengths of P-O, P-C and P-N are generally greater than those of analogous linkages where P is replaced by N (table 1.3-1).

Bond	Bond energy (kJ/mol)	Bond	Bond energy (kJ/mol)	Bond	Bond energy (kJ/mol)
P-H	322	N-H	389	C-H	414
P-F	527	N-F	272	C-F	440
P-Cl	331	N-Cl	193	C-Cl	327
P-Br	264			C-Br	276
P-I	184			C-I	240
P-C	272	N-C	306	C-C	355
P-N	230				
P-O	360	N-O	209	C-O	356
P=P	352	N=N	435	C=C	222
P=O	586	N=O	628	C=O	750
P=C	578	N=C	812		
P≡P	490	N≡N	946	C≡C	837

Table 1.3-1 Various bond energies of phosphorus, nitrogen and carbon.[34]

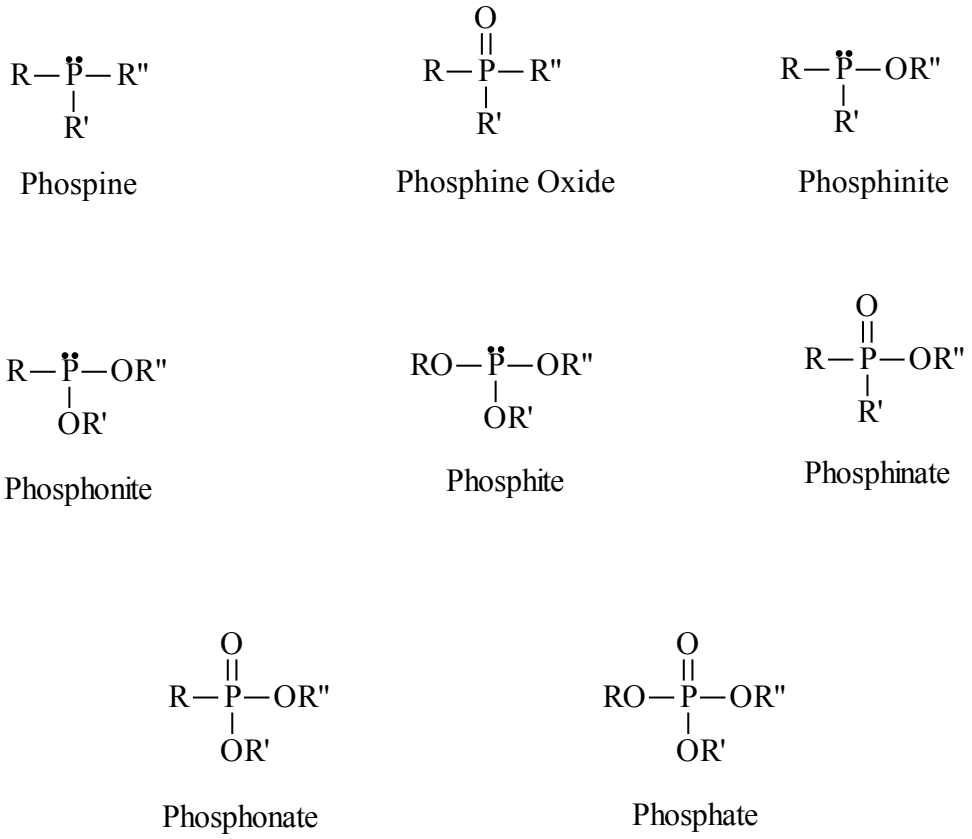

Figure 1.3-1 Types of Organic Phosphorus Structures.

1.4 Chemistry of Flame Resistance

Most organic polymers will burn if they are exposed to a flame under oxygen atmosphere. With the imminent introduction of stringent legislation, the polymer industry is faced with a serious challenge: designing materials with reduced flammability. Although society has always been accustomed to the presence and use of flammable matter in the form of, for instance, building, clothing and auxiliary material, the problem at issue has become acute. Today people are crowded into confined spaces (sometimes of great height), such as blocks of flats, office buildings, department stores, hospitals and jumbo jets with all the hazards this implies.[39] A fundamental issue in the chemistry of flame resistance is predicting the flammability of a material solely based on its structure. The limiting oxygen index (LOI) test has been used as a measure of flammability for a wide range of materials since its introduction.[40] It is defined as the minimum oxygen concentration of an atmosphere in which a specific polymer can just start and sustain burning for a short period of time. This index is known to be dependent on a number of sample and test parameters. These include the moisture content of the sample, dimensions of the sample, chimney effects, gas flow measurement and control, gas composition, specific heat of the gas, pressure, temperature, igniter gas and ignition application time, mode of ignition and sample flow properties.[41]

If the above parameters are kept constant, polymer flammability can be related to a number of factors such as polymer composition and structure, bond strength, nature of pyrolysis products, exposure environment and more.[42]

Technologically, a material is considered flammable if its LOI value is less or equal to 0.26. Table 1.4-1 provides the Limiting Oxygen Index values for a number of polymers.[39]

1.4.1 Fundamentals of Flammability

Four processes are involved in the polymer combustion cycle: (i) heating, (ii) decomposition, (iii) ignition, and (iv) combustion.[39] A simple description of these processes is represented in figure 2. Q_l is the heat provided from an

Polymer	LOI	Polymer	LOI
Polyformaldehyde	0.15	Wool	0.25
Poly(ethylene oxide)	0.15	Polycarbonate	0.27
Poly(methyl methacrylate)	0.17	Nomex®	0.285
Polyacrylonitrile	0.18	PPO®	0.29
Polyethylene	0.18	Polysulphone	0.30
Polyisoprene	0.185	Phenol-formaldehyde resin	0.35
Polybutadiene	0.185	Neoprene®	0.40
Cellulose	0.19	Polybenzimidazole	0.415
Poly(ethylene terephthalate)	0.21	Poly(vinyl choride)	0.42
Poly(vinyl alcohol)	0.22	Poly(vinylidene fluoride)	0.44
Nylon-6,6	0.23	Poly(vinylidene chloride)	0.60
Penton®	0.23	Carbon	0.60
		Poly(tetrafluoro ethylene)	0.95

Table 1.4-1 Limiting oxygen indices of various polymers[43]

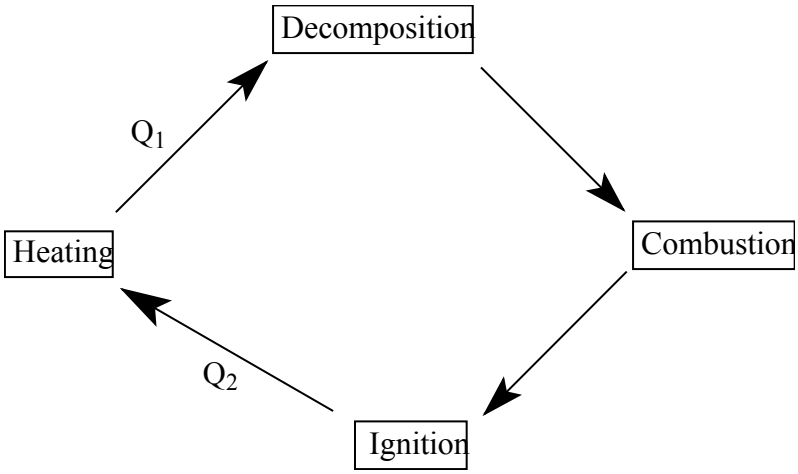

Figure 1.4-1 Processes involved in polymer combustion[39]

external source to the polymer. Q_1 must be greater than the weakest bond strength within the polymer structure for the polymer to decompose. As the polymer decomposes, two types of products may be formed: flammable volatile products and highly crosslinked char. The combustible volatile products are able to ignite. After ignition, if the necessary concentration of combustible gases and the availability of oxygen are maintained, oxidation is sustained and the polymer will burn. The exothermic burning process generates additional heat Q_2, which is transferred to the polymer. If Q_2 is greater than Q_1, the polymer undergoes further decomposition, further ignition and further combustion. This cycle continues until the polymer is completely consumed. To be flame resistant a material should have a high Q_1 and a low Q_2.

1.4.2 Approaches to Flame Retardation.

In order to increase the flame resistance of a polymer, the above mentioned polymer combustion cycle must be interrupted. Flame resistant materials yield products that are more difficult to ignite than the initial polymer when they are exposed to heat. Also, they should not propagate flame as readily. Flame resistant materials function through one or several of the following pathways:

- They have strong bonds, which decrease the decomposition rate. The stronger the bond, the higher the heat Q_1 to cause decomposition. Thus aromatic polymers or polymers with multiply bonded structures usually show much less flammability than aliphatic polymers of corresponding structures.
- They yield non-flammable char during pyrolysis, which reduces the diffusion of flammable gaseous products through the char layer. Also, the efficiency of heat transfer and oxygen penetration to the inner polymer is reduced.
- They may have enhanced decomposition of the substrate, thereby accelerating melting at lower temperatures so that the material drips or flows away from the flame front.
- They produce flame inhibitors such as carbon dioxide, water vapor, and hydrogen halides… Carbon dioxide and water vapor not only protect the

burning polymer from contact with oxygen but also remove heat from the burning system so that there will be less heat Q_2 transferred to the polymer.

- They release hydrogen halides which are well known as efficient radical scavengers for $H^{\cdot}$ and $HO^{\cdot}$ radicals in the flame region.[44, 45, 46] The relationship between radical scavengers and the reduced flammability of materials has now been well documented..[47, 48, 49]

In fact, the residue of pyrolysis (or the sum of this residue and the weight of carbon dioxide and water produced may be used as a measure of non-flammability.[39] It has been reported that there is a significant correlation between the char yield (CY) and the limiting oxygen index of polymers[50] This linear relationship is the following:

$$LOI \times 100 = 17.5 + 0.4CY \qquad \text{Equation 1.4-1}$$

where CY is the char yield in weight % at 850º C.

In practice, flame retardation of polymers is achieved by one of the following ways:

- Incorporation of a suitable flame retardant additive system.
- Coating the finished product with flame retardants.
- Developing new polymer systems with inherent flame resistance by virtue of their chemical structure and composition, e.g. copolymerizing with a flame retardant comonomer such as the copolycarbonates of bisphenol-A and 4,5,6,7-tetrabromophenolphthalein.

1.4.2.1 Flame Retardant Additives

Flame retardant additives may negatively affect the mechanical properties of the polymers especially when large quantities are required. Also, they may be leached or evaporate from the material in use environments.

1.4.2.1.1 Organohalogens

The principal inhibition reactions involve radical scavenging of the critical chain-branching radicals. Halogen inhibition reactions using HBr and Br_2 as examples are provided below.[51]

with HBr

$$HBr + {}^{\cdot}OH \text{ ------}\rightarrow H_2O + Br^{\cdot}$$

$$H^{\cdot} + HBr \text{ -------}\rightarrow H_2 + Br^{\cdot}$$

$$HBr + {}^{\cdot}O^{\cdot} \text{ -------}\rightarrow HO^{\cdot} + Br^{\cdot}$$

with Br_2

$$^{\cdot}O^{\cdot} + Br_2 \text{ -------}\rightarrow BrO^{\cdot} + Br^{\cdot}$$

$$^{\cdot}O^{\cdot} + Br^{\cdot} \text{ ------- }\rightarrow BrO^{\cdot}$$

$$Br^{\cdot} + H^{\cdot} + M \text{ ---------}\rightarrow HBr + M$$

Where M is an energy absorbant of arbitrary nature.

The above reactions destabilize the flame and reduce the thermal feedback to the substrate surface. This reduces the rate of volatile combustible gas formation which further destabilizes the flame. If enough halogen were introduced into the flame, the system would become self-extinguishing. Examples of halogenated flame retardant additives are chlorinated paraffins, chlorinated cycloaliphatics, and brominated aromatics. Reactive retardants include chlorendic acid, chlorendic anhydride, tetrabromobisphenol A and tetrabromophthalic anhydride.[52]

1.4.2.1.2 Antimony Oxides[53]

Antimony trioxide, Sb_2O_3, and antimony pentoxide, Sb_2O_5 are used as flame retardants often in a synergistic interaction with organohalogens. In the absence of halogens, antimony oxides function only as fillers. The combined system is always more effective than halogens alone. Organohalogens decompose at the flame front and provide the necessary reactant, HX, which combines with the

antimony oxide species to afford the volatile, nonflammable compound and water as depicted in the scheme below.[51]

$$6HX + Sb_2O_3 \rightarrow 2SbX_3 + 3H_2O$$

The volatile nonflammable antimony species generated may act as a diluent for the oxygen in the flame, in addition to the cooling effect of the other product, water. It is presumed that antimony pentoxide works the same way as the trioxide, but in some applications the pentoxide is thought to be more effective. Antimony oxides are used in all classes of polymers either as additives or with reactive organohalogens. Ordinarily the amount of antimony oxide used would be 25 to 50% of that of the organohalogen. In additive systems, the antimony oxide is melt mixed with the organohalogen to ensure thorough blending. In reactive systems, the antimony oxide may be added during or after the polymerization.

1.4.2.1.3 Phosphorus Compounds[54, 55, 56]

Phosphorus compounds (mainly organophosphorusrus) have long been known to impart flame resistance to materials. Several flame resistant polymers containing phosphorus or a mixture of halogens and phosphorus have been prepared.[57, 58] Mechanistic aspects of flame retardancy with phosphorus compounds and some other compounds have been described.[51] Briefly, these may be summarized in these terms: phosphorus containing compounds reduce flammability by promoting char formation, which in turn inhibits glowing.[59] Some other work pointed out that phosphorus compounds inhibit chain depolymerization, thereby reducing fuel gas generation and Q_2. The following mechanism has been suggested for triphenyl phosphine oxide and triphenyl phosphate containing compounds:[60]

$$R_3P = O \rightarrow PO^{\cdot}, P^{\cdot}, P_2$$

$$H^{\cdot} + PO^{\cdot} \rightarrow HPO + M$$

$$HO^{\cdot} + PO^{\cdot} \rightarrow HPO + {}^{\cdot}O^{\cdot}$$

$$HPO + H^{\cdot} \rightarrow H_2 + PO$$

$$P_2 + \cdot O \cdot \rightarrow P \cdot + PO \cdot$$

The key points of the above reactions are:

- the promotion of hydrogen recombination
- the scavenging of oxygen radicals by molecular phosphorus.[61]

The mechanism of the halogen-phosphorus synergy for flame resistance has been published elsewhere.[62, 63] Simultaneous addition of halogenated compounds and phosphorus compounds, or addition of halo-phosphorus compounds, provides improved flame retardancy. Synergistic action may originate from the fact that these mixed compounds can produce radical traps and reduce the amount of flammable gas formed on the one hand and also promote char formation that reduces glowing.[64]

1.5 REFERENCES

1. Martinez, P.A., W. Cadiz, A. Mantecon and A. Serra (1985) *Angew. Makromol. Chem.*, **133,** 97.
2. Ichino, T., and Y. Hasuda (1987) *J. Appl. Polym. Sci.,* **34**, 1667.
3. Soler, H., V. Cadiz and A. Serra (1987) *Angew. Makromol. Chem.,* **152**, 55.
4. Shau, M.D. and W. K. Chin (1993) *J. Polym. Sci. Part A. Polym. Chem.*, **31**, 1653.
5. Kourtides, D.A. and J. Parker (1978) *Poly. Eng. Sci.* **18(11)**, 855.
6. Weil, E.D. (1986) Encylopedia of Polymer Science and Technology (H.F. Mark, et. al. Eds), vol. II, Wiley Interscience, New York.
7. Bailey, W.J., W. M. Muir and F. Marktscheffel (1962) *J. Org. Chem.,* **27**, 4404.
8. Tan, B., C. N. Tchatchoua, L. Dong and J. E. McGrath (1998) *Polym. Adv. Technol*. **9**. 83-93.
9. Smith, C.D., H.J. Grubbs, H.F. Webster, A. Gungor, J.P. Wightman and J.E. McGrath (1991) *High Perform. Polym.,***4**, 211.
10. Riley, D. J., A. Gungor, S. A. Srinivasan, M Sankarapandian, C. Tchatchoua, M. W. Muggli, T. C. Ward, T. Kashiwagi and J. E. McGrath (1997) *Polym. Eng. and Sci*. Vol 37, **9**, 1501.
11. Medved, T.Y., T.M. Frunze, K.C. Mei, V.V. Kurashev, V.V. Korshak, and M.I. Kabachnik (1964) *Polym. Sci. USSR,* **5**, 386.
12. Korshak, V.V., T.M. Frunze, V.V. Kurashev, T.Y. Medved, Y.M. Polikarpov, C.M. Hu and M.I. Kabachnik (1965) *Chem. Abstr.,* **62**, 6507.

13. Kosalapoff, G.M. and L. Maier (1972) Organic phosphorus compounds, Vol 1, John Wiley & Sons, New York.

14. Pavlov, G.P., V.A. Kukhtin, N.A. Kukhtin, N. A. Golynina and V.V. Kormachev (1981) *Chem. Abstr.,* **94**, 15816.

15. Androva, N.A., M.M. Koton and L.K. Prokhorova (1971) *Chem. Abstr.,* **75**, 21174.

16. Smith, C. (1991) Ph.D. Thesis, Viginia Polytechnic Institute and State University.

17. Grubbs, H. J. (1993) Ph. D. Thesis, Virginia Polytechnic Institute and State University.

18. Martinez-Nunez, M.F., V. N. Sekharipuram and J.E. McGrath (1994) *ACS Polym Prep.,* **35**, 709.

19. Yang, H., M.E. Rogers and J.E. McGrath (1995) *ACS Polym. Prep.,* **36**, 205.

20. Muggli, M. W. (1998) Ph. D. Thesis, Virginia Polytechnic Institute and State University.

21. Rosescu, L., F. Popescu and O. Petreus (1998) *Angew. Makromol. Chem.: Appl. Macromol. Chem. Phys*., **257**, 7-12.

22. Levchik, S. V., G. Camino, and M. P. Luda (1998) *Polym. Degrad. Stabil*. **60**: (1) 169-183.

23. Zhang, Y., J. C. Tebby and J. W. Wheeler (1997) *J. Polym. Sci. A: Polym. Chem*. **35**, 2865-2870.

24. Stokes, H.N. (1897) *Am. Chem. J.*, **19**, 782.

25. Allcock, H.R. (1988) *Inorganic and Organometallic Polymers* (M. Zeldin, K.J. Wynne and H.R. Allcock Eds), p. 250, ASC Symposium, Series No. 360, Washington, D.C.

26. Penton, H.R. (1988) *Inorganic and Organometallic Polymers* (M. Zeldin, K.J. Wynne and H.R. Allcock Eds), p. 277, ACS Symposium, Series No. 360, Washington, D.C.

27. Millich, F. and L.L. Lambing (1980) *J. Polym. Sci. Polym. Chem.* **18**, 2155.

28. Imai, Y., N. Sato and M. Ueda (1980) *Makromoek. Chem. Rapid Commun.* **1**, 419.

29. Kim, K.S. (1983) *J. Appl. Polym. Sci.* **28**, 1119.

30. Sivrev, H., and G. Borissov (1977) *Eur. Polym. J.* **13**, 25.

31. Sato, M., and M. Yokoyama (1980) *Eur. Polym. J.* **16**, 79.

32. Sato, M., Y. Tada and M. Yokoyama (1980) *Eur. Polym. J.* **16**, 671.

33. Sato, M., and M. Yokoyama (1980) *J. Polym. Sci., Polym. Chem. Ed.* **18**, 2751.

34. Maiti, S., S. Banerjee and S.K. Palit (1993) *Prog. Polym. Sci.* **18**, 227.

35. Hudson, R.F. (1965) Structure and Mechanism in Organo-Phosphorus Chemistry, Academic Press, London.

36. Hartley, F. R. (1990) The Chemistry of Organophosphorus Compounds, Vol 1, John Wiley and Sons, New York.

37. Engel, R. (1992) Handbook of Organophosphorus Chemistry, Marcel Dekker, New York.

38. Corbridge, D.E.C. (1985) Phosphorus: An outline of its chemistry, biochemistry and technology, *Studies in Inorganic Chemistry,* **6**, Elsevier, Amsterdam.

39. van Krevelen, D.W. (1975) *Polymer,* 16, 615.

40. Fenimore, C.P. and F.J. Martin (1966) *Mod. Plast.,***44**, 141.

41. Wharton, R.K. (1979) Fire and Material, Heyden, Lond, Vol. 3, p. 39.

42. Lin, M.S. and E.M. Pearce (1981) *J. Polym. Sci. Polym. Chem. Ed.,* **19**, 2659.

43. Landrock, A.H. (1983) Handbook of Plastics Flammability and Combustion Toxicology, Noyes Publications, Park Ridge, NJ.

44. Wise, H. and W.A. Rosser (1963) *Proc. 9th Int. Symp., Combustion,* 733.

45. Rosser, W.A. H. Wise and J.Miller (1959) *Proc. 7th Int. Symp., Combustion,* 175.

46. Hastie, J.W. (1973) *J. Res. Natl. Bur. Stand. U.S.,* **77A**, 733.

47. Ram, A. and Calahorra (1979) *J. Appl. Polym. Sci.,* **23**, 814.

48. Sanders, H.J. (1978) *Chem. Eng. News, ACS, April,* p. 22.

49. Johnson, P.R. (1974) *J. Appl. Polym. Sci.,* **18**, 491.

50. van Krevelen, D.W. (1974) *Chimia* **28**, 504.

51. Gann, R.G., R.A. Dipert and M.J. Drews (1987) Encyclopedia of Polymer Science and Engineering, J.I. Kroschwitz, Ed., John Wiley & Sons, Vol. 7, p. 154.

52. Tanaka, Y. (1988) Epoxy Resins Chemistry and Technology, 2nd ed., Dekker, New York, p. 719.

53. Potter, W.G. (1970) Epoxide resins, Iliffe, London.

54. Koutinas, A.A. and N.K. Kalfoglou (1983) *J. Appl. Polym. Sci.* **28**, 123.

55. Marom, A.M. and L.A. Razleenbach (1983) *J. Appl. Polym. Sci.* **28**, 2411.

56. Granzow, A. and C. Savides (1980) *J. Appl. Polym. Sci.* **25**, 2195.

57. Ballisteri, A., G. Montaudo, C. Puglisi, E. Scamporrino and D. Vitalini (1983) *J. Appl. Polym. Sci.* **28**, 1743.

58. Katsuma, K., and N. Inagki (1980) *J. Appl. Polym. Sci.* **25**, 2195.

59. Larsen, E.R. and R.B. Ludwing (1979) *J. Fire Flammability* **10**, 69.

60. Drews, M.J. and R.H. Barker (1985) Cellulose Chemistry and its Application (T.P. Nevell and S.H. Zeromian, Eds), p. 266, Ellis Horwood, Chichester.

61. Rosser, W.A., S.H. Imami and H.Wise (1966) *Combust. Flame* **10**, 287.

62. Brauman, S.K. (1980) *J. Fire Retard. Chem.* **7**, 1.

63. Larsen, E.R. and R.B. Ludwing (1979) *J. Fire Retard. Chem.* **6**, 182.

64. Yang, C.P. and T.W.Lee (1986) *J. Appl. Polym. Sci.* **32**, 3005.

2 CHAPTER 2 MONOMER SYNTHESIS AND ANALYSIS

2.1 Basic philosophies

It has been our observation[1, 2, 3] that compounds that contain triphenyl phosphine oxide (or related) units were difficult to crystallize, even when they were already fairly pure. This is consistent with findings from molecular modeling performed in our research group and elsewhere. Molecular modeling simulations suggest that the rings in the triphenyl phosphine oxide unit are not coplanar (see model below) and the angles between the P-C bonds reduce the propensity for the molecules to form organized structures and therefore to crystallize.

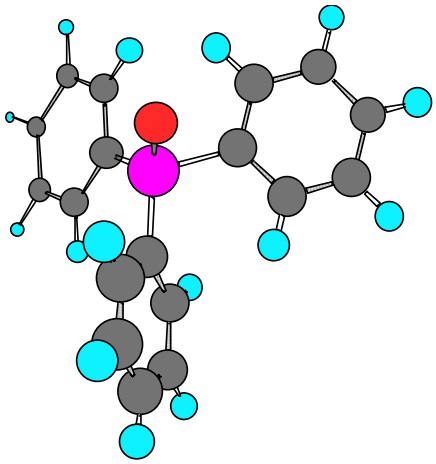

Even if they do form crystals, there often is little difference, if any, between the purity of the original product and that of the recrystallized adduct. From these observations it appears that the synthesis of monomers containing phosphine oxide units presents a considerable challenge. In general, the following rules must be observed:

- The starting materials and the intermediate products must be purified.

- Distillation is preferred to recrystallization if possible.

- Whenever several pathways are accessible to achieve a given structure, preference must be given to the one that produces the lesser amount of unusual side products, even if a lower yield is obtained. Traces of phosphorus containing impurities are often difficult to remove from the major product.

- Recrystallization benefits from prior analysis of the compound and the efficacy of solvent mixture can be very dependent on the nature and percentage of the specific impurities.

2.2 Analytical Techniques

2.2.1 Instrumentation

2.2.1.1 Liquid Chromatography

HPLC was a major tool for the determination of the purity of the monomers and the synthetic intermediates. The instrumentation for this purpose consisted of a Varian VISTA 5500 liquid chromatograph monitor equipped with a DuPont Zobax ODS (C_{18} inverse stationary phase) analytical column (4.6 mm I.D. x 25cm). HPLC grade methanol was used as the mobile phase. Approximately 10 μl of samples (monomer dissolved in methanol) were injected at a mobile phase flow rare of 1ml/minute.

2.2.1.2 Nuclear Magnetic Resonance Spectroscopy

Nuclear magnetic resonance spectroscopy (^{1}H, ^{13}C, ^{31}P) was used to elucidate the structure of the monomers synthesized and of their synthetic intermediates. Samples were dissolved in a deuterated solvent, either DMSO-d_6 or $CDCl_3$, at approximately 10%

solids concentration. The NMR tubes were filled to about one third of their full capacity with the solution.. Proton spectra were obtained on a Varian Unity Spectrometer operating at 400 MHz. Proton and carbon spectra were referred to tetramethylsilane (TMS); phosphorus spectra used H_3PO_4 as reference.

2.2.1.3 Melting Point Measurements

Capillary melting points of highly purified monomers and their intermediates were determined using a Melt-Temp II apparatus manufactured by Laboratory Devices USA. A heating rate of approximately 1^oC/minute was employed. Samples were finely ground before being introduced into the capillaries and the beginning of the liquefaction of the powder was usually taken as the practical melting points even though in several instances melting point ranges were provided.

2.2.1.4 Mass Spectrometry Data

Mass spec data were essential in the structure determinations of the novel compounds synthesized in the course of this research. Small amounts of samples were dissolved in methanol and injected into a VG QUATTRO GC 800 series Quattro 5155 instrument from FISONS Instruments. Electron impact ionization was used in most of the cases.

2.2.1.5 Titration Expriments.

The amine curing agents, the novel epoxides synthesized and the commercially available epoxides were titrated either to determine the molecular weights of the former or the epoxy equivalent weights (EEW) of the latter. Approximately 0.1g of sample was dissolved in a mixture of chloroform and acetic acid (5:1 v/v). Acetic acid may enhance

the basicity of the amine and intensify the end point. The titrant was a solution of hydrogen bromide previously standardized with potassium hydrogen phthalate (KHP). The titration experiments were performed on an MCI GT- (COSA Instruments Corp.) automatic potentiometric titrator. The end points were determined from the maximum of the first derivative of the potential as a function of the volume of the titrant used.

For the tetrafunctional epoxy resins, the equivalent epoxy number was determined by disolving 0.4g of the novel resins into 150 ml of acetone and 3 ml of 36.5% HCl solution. The titrant used was a 0.1N sodium hydroxide solution with methyl red as the indicator.

2.2.1.6 Fourier Transform Infrared Spectroscopy (FTIR).

FTIR has now become a common practice in our laboratory and elsewhere. It was used essentially to detect the anticipated functional groups in the novel compounds synthesized, and particularly the P=O stretch. Liquid samples were smeared between two NaCl salt plates and placed in a holder. The holder was then inserted into the FTIR spectrometer. Solid samples were placed on a salt plate and put into an oven until melting occurred. In some cases the samples had to be dissolved in chloroform or ground with potassium bromude, especially if they had high melting points. For each spectrum 32 scans were averaged with a resolution of $4cm^{-1}$, on a Nicolet Impact 400 FTIR spectrometer.

2.2.1.7 X-Ray Diffraction

A wedge was cut from a large trapezoidal crystal grown from slow evaporation of the recrystallization solvent (ethanol for DAMPO). The crystal was mounted on a glass fiber with epoxy and centered on the the goniometer of a Siemens (Bruker) P4 diffractometer. Unit cell parameters were determined by least squares refinement of 42 reflections that had been automatically centered on the diffractometer[4]. Intensity data were collected,

processed and corrected for absorption.[2] The approximate structure was solved by direct methods and refined using the SHELXTL-PC v5.03 program package.[5] The final refinement involved an anisotropic model for all non-hydrogen atoms and a riding model for all hydrogen atoms. The program package SHELXTL-PC was used for the ensuing molecular graphic generation.[5]

2.2.2 Chemicals

Hydrazine Monohydrate:

Supplier:	Acros, 99%
Empirical Formula:	H_6N_2O
Molecular Weight:	50.06
Boiling Point, ^oC:	113.5
Melting Point, ^oC:	-51.7
Structure:	$H_2NNH_2 \cdot H_2O$
Purification:	Used as received

Methyltriphenylphosphonium Bromide:

Supplier:	Aldrich, 98%
Empirical Formula:	$C_{19}H_{18}PBr$
Molecular Weight:	357.23
Melting Point, ^oC:	230-234

Structure:

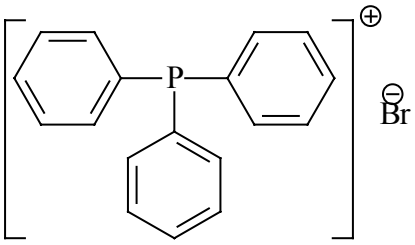

Purification: Used as received

Nitric Acid:

Supplier: Fisher, Certified, 69.5%

Empirical Formula: HNO_3

Molecular Weight: 63.01

Purification: Used as received

Palladium on Activated Carbon (Pd/C):

Supplier: Aldrich

Empirical Formula: Pd(5%) and C

Purification: Used as received

Sodium Hydroxide:

Supplier: Mallinckrod, AR, 99.4%

Empirical Formula: NaOH

Molecular Weight: 40.00

Purification: Used as received

Sulfuric acid:

Supplier: Mallinckrodt, AR, 96.2%

Empirical Formula: H_2SO_4

Molecular Weight: 98.07

Purification: Used as received

Ethanol:

Supplier: AAPER, 200-proof

Empirical Formula: C_2H_6O

Molecular Weight: 46.07

Boiling Point, ^oC: ` 78

Melting Point, ^oC: -130

Structure: CH_3CH_2-O-H

Purification: Used as received

Triphenylphosphine Oxide:

Supplier: Elf Atochem, AR, 98% by HPLC

Empirical Formula: $C_{18}H_{15}PO$

Molecular Weight: 278.29

Melting Point, ^{o}C: 156-158

Structure:

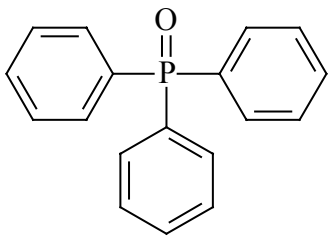

Purification: Used as received

Phenylphosphonic Dichloride:

Supplier: Acros, 97%

Empirical Formula: $C_6H_5Cl_2PO$

Molecular Weight: 194.985

Boiling, Point ^{o}C: 258

Structure:

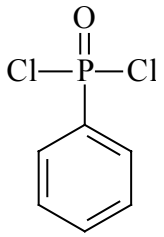

Purification: This material was purified by vacuum distillation

4-Bromofluorobenzene:

Supplier: Acros 99%

Empirical Formula: C6H4BrF

Molecular Weight: 175.00

Boiling Point, ^{o}C: 153

Melting Point, ^{o}C: -16

Structure:

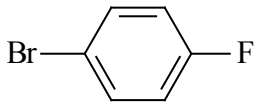

Purification: Used as received

Dimethyl Methylphosphonate:

Supplier: Aldrich 97%

Empirical Formula: $C_3H_9O_3P$

Molecular Weight: 124.08

Boiling Point, ^{o}C: 181

Structure:

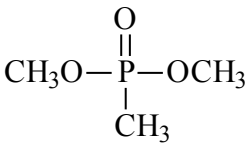

Purification: Used as received

Thionyl Chloride:

Supplier: Aldrich

Empirical Formula: $SOCl_2$

Molecular Weight: 118.97

Boiling Point, ^oC: 79

Melting Point, ^oC: -105

Purification: Used as received

N,N-Dimethylformamide:

Supplier: Fisher, 99%

Empirical Formula: C_3H_7NO

Molecular Weight: 73.09

Boiling Point, ^oC: 153

Melting Point, ^oC: -61

Structure:

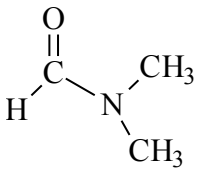

Purification: Used as received

Magnesium:

Supplier:	Fisher, turnings, 99.9%
Empirical Formula:	Mg
Molecular Weight:	24.31
Boiling Point ^{o}C:	1107
Melting Point, ^{o}C:	651
Purification:	Dried in the vacuum oven

Ether, anhydrous:

Supplier:	Mallinckrodt, AR, 99%
Empirical Formula:	$C_4H_{10}O$
Molecular Weight:	74.12
Boiling Point, ^{o}C: `	34.6
Melting Point, ^{o}C:	-116
Structure:	CH_3CH_2-O-CH_2CH_3
Purification:	Used as received

Chloroform:

Supplier:	EM, HPLC Grade
Empirical Formula:	$CHCl_3$
Molecular Weight:	119.38
Boiling Point, ^{o}C:	61

Melting Point, ^{o}C: -63

Purification: Used as received

Magnesium Sulfate Anhydrous:

Supplier: Mallinckrodt, AR, 97%

Empirical Formula: $MgSO_4$

Molecular Weight: 120.37

Purification ` Used as received

Tetrahydrofuran (THF):

Supplier: Fisher (stabilized)

Empirical Formula: C_4H_8O

Molecular Weight: 72.11

Boiling Point, ^{o}C: 66

Melting Point, ^{o}C: -103.4

Structure:

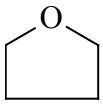

Purification Dried over sodium and benzophenone (one crystal), refluxed until the benzophenone turned purple before the distillation could start.

m-Aminophenol:

Supplier: Acros, 99%

Empirical Formula: $H_2NC_6H_4OH$

Molecular Weight: 109.13

Boiling Point, ^oC: 164(11mm)

Melting Point, ^oC: 124-126

Structure:

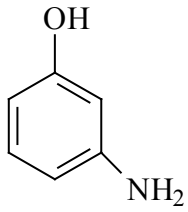

Purification: Two times sublimed (110^{o}C, ~2 mm Hg)

Potassium Carbonate:

Supplier: Fisher 99%

Empirical Formula: K_2CO_3

Molecular Weight: 138.21

Melting Point, ^oC: 891

Purification: Dried in a vacuum oven at 180^{o}C for 24 hours prior to use.

N,N-Dimethylacetamide:

Supplier: Fisher

Empirical Formula: C_4H_9NO

Molecular Weight: 87.12

Boiling Point, ^{o}C: 166

Melting Point, ^{o}C: -20

Structure:

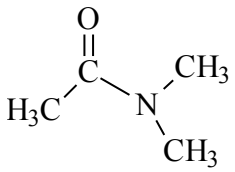

Purification: Vacuum distilled over calcium hydride.

Toluene:

Supplier: Fisher

Empirical Formula: $C_6H_5CH_3$

Molecular Weight: 92.14

Boiling Point, ^{o}C: 111

Melting Point, ^{o}C: -93

Structure:

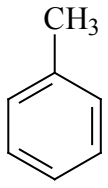

Purification Used as received

Sodium Bicarbonate:

Supplier: Mallinckrodt, AR

Empirical Formula: $CHNaO_3$

Molecular Weight: 84.01

Purification Used as received

Methanol:

Supplier: EM, HPLC Grade

Empirical Formula: CH_3OH

Molecular Weight: 32.04

Boiling Point, ^oC: 64.7

Melting Point, ^oC: -98

Purification Used as received

Epichlorohydrin:

Supplier: Acros, 99%

Empirical Formula: C_3H_5ClO

Molecular Weight: 92.52

Boiling Point, ^oC: 116

Melting Point, ^oC: -57

Structure:

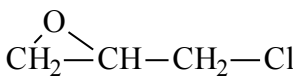

Purification: Used as received

Phenol:

Supplier:	Fisher, 99%
Empirical Formula:	C_6H_5OH
Molecular Weight:	94.11
Boiling Point, ^oC:	182
Melting Point, ^oC:	41

Structure:

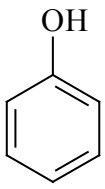

Purification	Vacuum distilled

Potassium hydroxide

Supplier:	Mallinckrodt, AR, Pellets, 87.6%
Empirical Formula:	KOH
Molecular Weight:	56.11
Melting Point, ^oC:	
Purification:	Used as received

Dimethyl sulfoxide

Supplier:	Fisher, 99.9%
Empirical Formula:	C_2H_6SO

Molecular Weight: 78.3

Boiling Point, ^{o}C: ` 189

Melting Point, ^{o}C: 18.4

Structure:

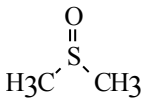

Purification: Used as received

Hydrochloric acid

Supplier: Fisher, 36.5%

Empirical Formula: HCl

Molecular Weight: 36.46

Purification: Used as received

Ethylene carbonate

Supplier: Aldrich, 98%

Empirical Formula: $C_3H_4O_3$

Molecular Weight: 88.06

Boiling Point, ^{o}C: ` 244

Melting Point, ^{o}C: 37-39

Structure:

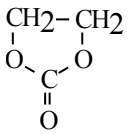

Purification: Used as received

Tetraethylammonium iodide

Supplier: Aldich

Empirical Formula: $C_8H_{20}NI$

Molecular Weight: 257.16 `

Melting Point, ^oC: > 300

Structure: $(CH_3CH_2)_4N^+I^-$

Purification: Used as received

2.3 Bis(3-Aminophenyl) Methyl Phosphine Oxide (DAMPO)

2.3.1 Molecular Modeling

Molecular modeling of DAMPO was performed using the CAChe Molecular Modeling Package. CAChe uses a built-in library of computational chemistry tools and provides a dramatic visualization of the three-dimensional structure of the lowest conformational energy of a given molecule, where computer visualizations clearly surpass physical models.[6, 7, 8]

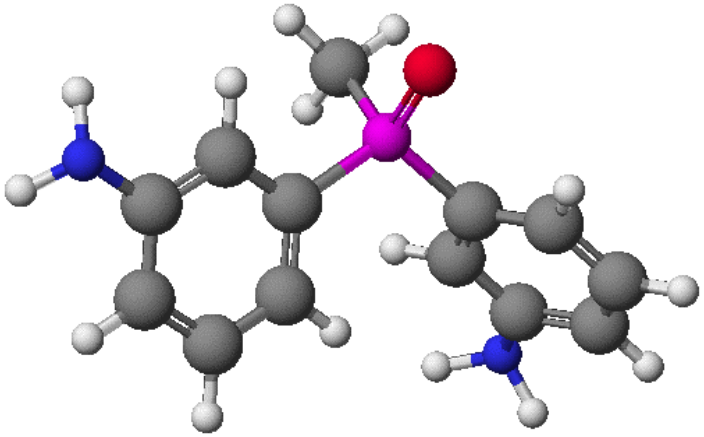

Figure 2.3-1 Lowest energy conformation structure of DAMPO by CAChe

2.3.2 Previous Synthesis Of DAMPO

The synthesis of this molecule can be found in the literature at least as early as 1962[9]. This synthesis was accomplished by disproportionation of (dichloro) phenyl phosphine ($PhPCl_2$) with aluminum chloride ($AlCl_3$) and benzene to give $(Ph)_2PCl_2$. This substitution was followed by a methanolysis to give $(Ph)_2POCH_3$. Then a quantitative alkylation of the phosphorus by the well-known Michaelis-Arbuzov reaction followed this sequence. A mechanism for that alkylation is shown below.[10]

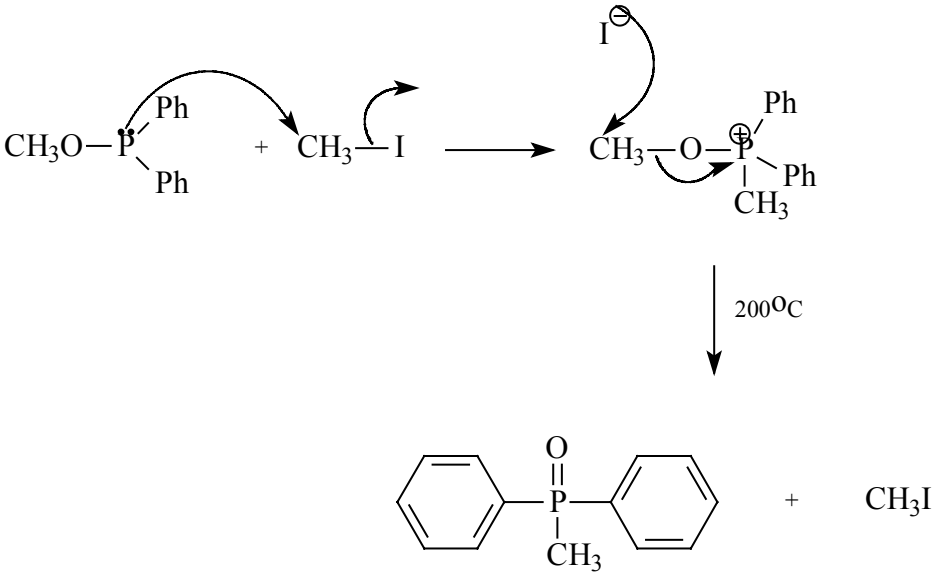

Scheme 2.3-1 Mechanism for the Michaelis-Arbusov reaction

The first step for this reaction is apparently rate determining.[11] Nitration, followed by the reduction of this adduct gave the desired diamine. This monomer (DAMPO) has a considerable synthetic advantage on its triphenyl homolog (DAPPO) because the tri(nitrophenyl) phosphine oxide impurity which often plagues the synthesis of the latter is not a conceivable problem in the synthesis of DAMPO. This is because the methyl group which makes up for one of the phenyl rings in the triphenyl derivative cannot undergo nitration under our experimental conditions. This particular trifunctional impurity in DAPPO is of considerable importance, given the fact that even traces of triamino monomers in the polymerization of a system intended to be linear could cause gelation.

The methyl diphenyl phosphine oxide intermediate of the above reaction could likely be prepared by the reaction of the Grignard reagent of bromobenzene with dichloro methyl phosphine oxide as shown below.

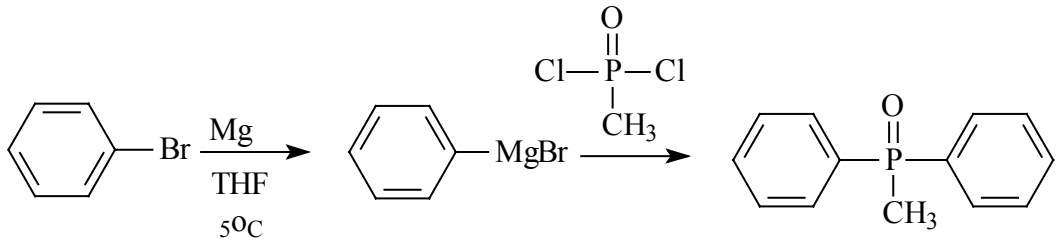

This procedure has been performed in our laboratory and the resulting product was obtained with both high yield and high purity. The monomer DAMPO has been synthesized and used in a number of applications.[12, 13, 14, 15] In all of these cases, high molecular weight materials were not obtained even though some of the applications did not require highly purified monomers (curing of epoxy resins for example). Some workers suggested that the reactivity of that particular amine in the meta position to an electron withdrawing group (phosphine oxide in this case) was inherenly low,[13] but this seems not to be the case.

2.3.3 Motivations

Our goal was to make this diamine (DAMPO) available in a purity high enough to achieve the synthesis of high performance macromolecules pertaining to our reseach objectives. Our starting material was somewhat original, that is methyltriphenylphosphonium bromide (structure in 2.2.2). This compound is best known for its use in stereoselective vinylation of amino aldehydes using 2-trimethylsilylethylidenetriphenylphosphorane.[15] This Wittig reagent could be prepared from the reaction of triphenylphosphine and bromoalkane in a non polar solvent such as benzene or toluene.

2.3.4 Preparation of Methyl Diphenyl Phosphine Oxide

Methyltriphenylphosphonium bromide (200g, 0.56 mole) was charged to a 5L three-necked round bottom flask equipped with an overhead stirrer, a reflux condenser and a nitrogen inlet. Water (1L) was then added and the mixture was heated with stirring to reflux (~100^{o}C) for about 30 minutes. This produced a cloudy suspension. Sodium hydroxide (112g, 2.8 moles, 5 times the stoichiometric amount) was dissolved in 1L of water in a beaker and then transferred to the suspension. Immediately after the addition of the sodium hydroxide solution, a clear organic layer (benzene) formed on top of the reaction mixture. The reaction was further refluxed for an additional two hours and its completion was confirmed by TLC (chloroform:methanol, 9:1). The crude product was extracted with chloroform, washed several times with water, dried over magnesium sulfate and the chloroform solvent was evaporated by rotary evaporation. The compound was further dried at ~70^{o}C in a vacuum oven for 12 hours and the yield was quantitative.

A plausible mechanism for the reaction is depicted in scheme2.3-2. It has been shown, using very similar reactions (with other phosphonium salts), that the reaction rate is that of a third order kinetic process as written below:[16, 17]

$$\frac{d[Ph_2(CH_3)P=O]}{dt} = k_{obs}\left[Ph_3P^{+}CH_3Br^{-}\right][NaOH]^2$$

The above equation clearly shows that the reaction is a second order kinetic process with respect to the sodium hydroxide reagent. This was taken into account in our experiments by using five times the stichiometric amount of sodium hydroxide. While our experimental conditions gave a product within minutes, it was previously reported that the reaction took hours.[12, 13] A close look at the reaction mechanism that we proposed (scheme 2.3-2) would suggest that more than one mole of sodium hydroxide would be needed to convert the phosphonium salt into the desired intermediate. One mole of base is needed for the formation of the phosphorus ylid while the other mole is required to complete the reaction. It is worthwile mentioning that when a stoichiometric amount of sodium hydroxide was used no methyl diphenyl phosphine oxide was formed.

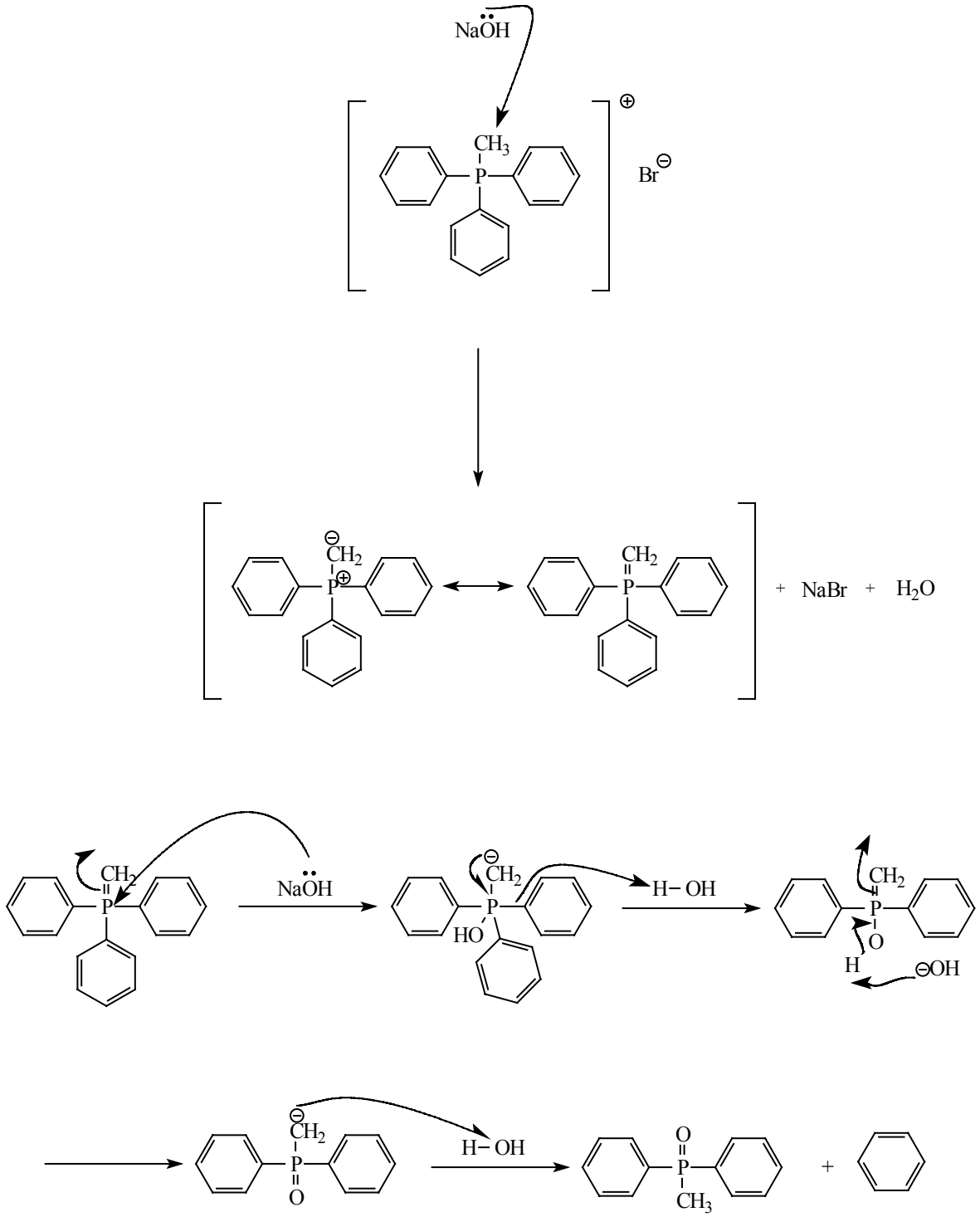

Scheme 2.3-2 A plausible mechanism for the oxidation of the phosphonium salt

The rate determining step is the formation of benzene,[17] which is understandable if we consider the high strength of of the phosphorus-carbon bond.

The use of water as solvent rather than acetone or toluene or even benzene, as has previously been done in similar reactions with other phosphonium salts is very impressive. The industrial implications of such solvent substitutions are countless, ranging from the reduction in the cost of production to decreasing harm to the environment. The purity of this intermediate was excellent as shown by TLC and phosphorus NMR. This could easily be explained from the suggested mechanism in which no other side products are expected beside the formation of benzene. The melting point of the white powder was 112^{o}C.

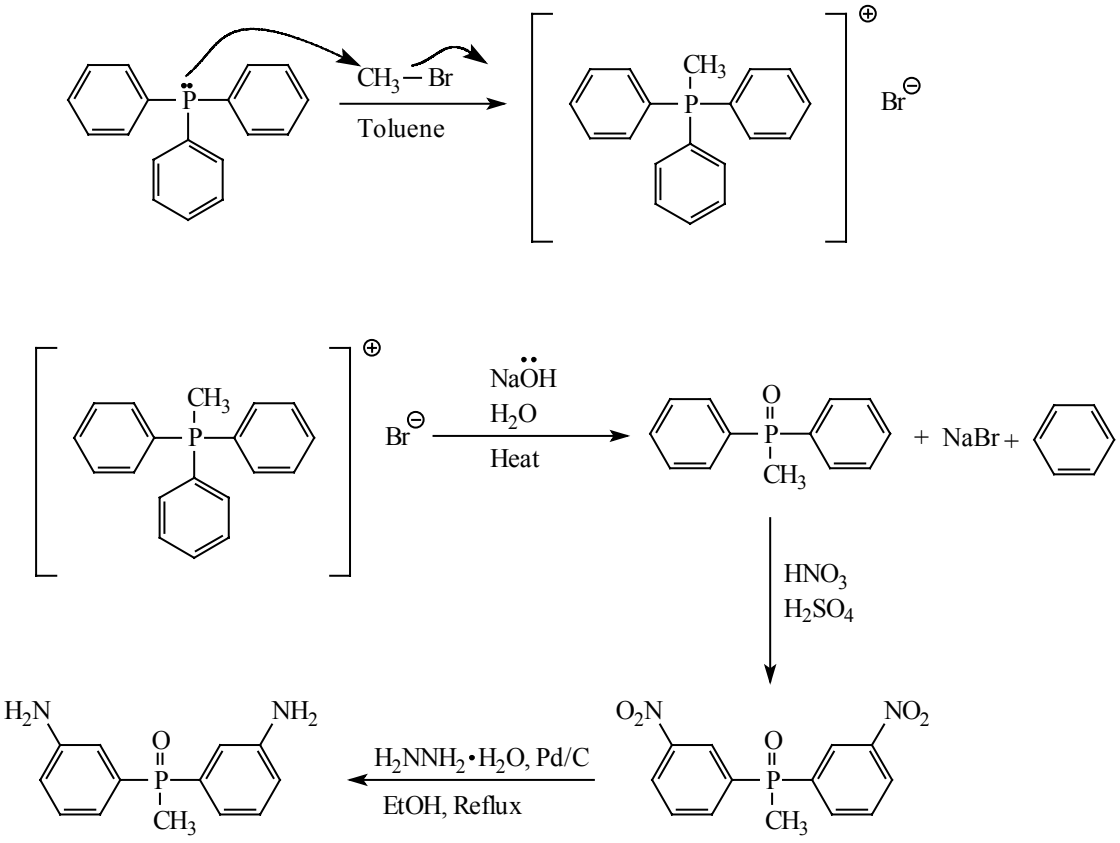

Scheme 2.3-3 Three step synthesis of *m*-DAMPO

2.3.5 Nitration of Methyl Diphenyl Phosphine Oxide

The nitration of this compound proceeded through a very familiar procedure but the nitro intermediate was subjected to a rigorous purification. Since no suitable method

could be found to purify the diamine obtained in the final stage, particular efforts were made to avoid any residual impurities in the nitro intermediate.

Methyl diphenyl phosphine oxide (255g, 1.18 mole) was charged into a 5L 3-necked round bottom flask fitted with an overhead stirrer, a reflux condenser, and an addition funnel. The flask was placed in an ice bath and concentrated sulfuric acid (723ml, 15 moles) was carefully added to the content of the flask. The mixture was stirred for about 30 minutes until the material completely dissolved.

In a separate ice bath, a 2 liter Erlenmeyer flask containing nitric acid (225g, 2.48 moles) was cooled and to it was slowly added 500ml (10.55 moles) of concentrated sulfuric acid. The amount of nitric acid was 5% in excess of the stochiometric amount and the total amount of sulfuric acid was 10 times that of nitric acid by weight. It should be pointed out that this operation (the mixture of the acids) is extremely exothermic and should be carried out cautiously.

The acid mixture was cooled to 0-5^{o}C and was transferred to the addition funnel of the reaction apparatus. The addition of the acid was dropwise and the reaction was allowed to continue for two hours at 0-5^{o}C and three hours at room temperature after the addition was completed. The reaction mixture was then precipitated into iced water. The precipitate was then filtered, washed with water until the filtrate turned neutral. During the washing period, the compound turned progressively yellowish green. The product was three times recrystallized from ethanol to yield light yellow crystals (m.p. 204 –205) with an overall yield of 85%.

2.3.6 Reduction of Bis(3-Nitrophenyl) Methyl Phosphine Oxide

The reduction of the dinitro intermediate was performed with hydrazine. This versatile and rarely used source of hydrogen allowed the reduction to proceed in less than five hours, which is a critical time beyond which *m*-DAMPO in solution would form redish impurities of undefined nature. This apparently simple detail could explain the fact that we obtained a product far purer (to the best of our knowledge) than that from any

other attempts to synthesize this molecule. Below is a plausible mechanism for the reductive amination of nitro compounds using hydrazine:

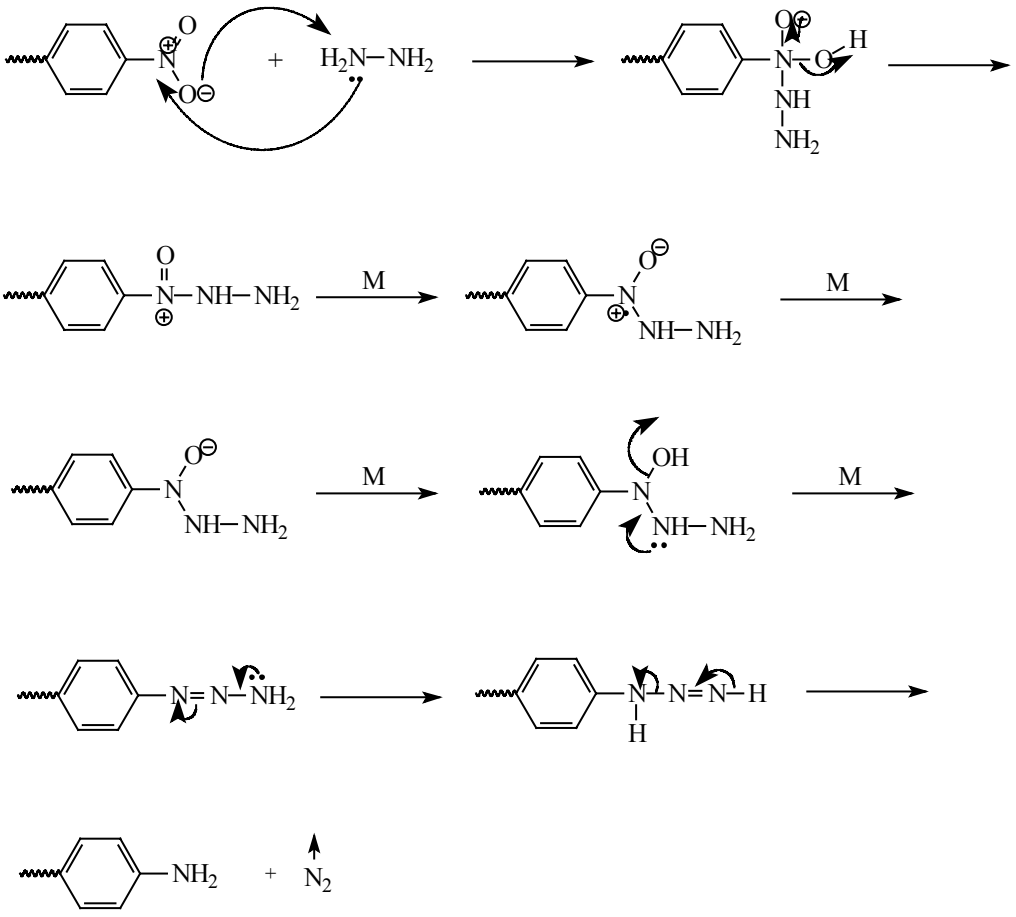

Scheme 2.3-4 Mechanism for the reductive amination of nitro compounds with hydrazine

Bis(3-nitrophenyl) methyl phosphine oxide (120g, 0.39 mole) and 1200mL of absolute ethanol were charged into a 5 liter 3 necked roune bottom flask fitted with an overhead

stirrer, an addition funnel and a reflux condenser. The mixture was purged with nitrogen and heated to about 50^{o}C. A small amount of catalyst Pd/C (~0.5g) was added and the hydrazine monohydrate (530g, 10.6 moles, 9 times the stoichiometric amount) was introduced dropwise from the addition funnel. A violent erruption of gas from this mixture denotes the occurrence of the reaction. No heating was needed at this stage, given that the reaction is exothermic. When the reaction slowed down as indicated by a decrease in the evolution gases, another portion of Pd/C was added and the reaction was heated to reflux for one hour. The completion of the reaction was ascertained by TLC (chloroform:methanol, 9:1). About 5g of decolorizing activated carbon was added to the reaction mixture and a gentle reflux was continued for an additional hour. The black solution was then cooled to room temperature under nitrogen and subsequently filtered through celite on a Buchner funnel to afford a clear light yellow solution. The solvent was immediately rotary evaporated. The product was washed with a combination of water and chloroform, then dried in a vacuum oven at 100^{o}C. The white crystalline product exhibited a melting point of 156^{o}C by capillary and no impurities were detected by HPLC (inverse phase, absolute methanol as mobile phase). ^{31}P NMR (*d*-DMSO) showed a single peak at 27.6 ppm (figure 2.3-2), suggesting that the diamine did not contain any phosphorylated impurities. Chemical shifts and integrations for ^{1}H NMR (*d*-DMSO) were consistent with the structure of the monomer (figure 2.3-3). ^{13}C NMR suggested the presence of seven different types of carbons (figure2.3-4), which is what could be expected from the structure of *m*-DAMPO. Elemental analysis results were also consistent with the structure of the monomer. The data are include here, with the theoretical values in parenthesis: C~63.55% (63.41); H~6.20% (6.14); N~11.52% (11.38); P~12.71% (12.58). Mass spectrometry (figure 2.3-5) gave a molecular ion of 246, corresponding to the molecular weight of DAMPO and both the molecular ion intensity and pattern were reminiscent of those of a compound containing a phosphorus atom. It was also noted from the mass spectrum that the methyl group attached to the phosphine oxide group was particularly labile; the (M^{+}-15) peak was particularly visible.

Infrared spectroscopy of the monomer and its synthetic intermediates (figure 2.3-6) was consistent with the assigned structures. The top spectrum (DPMPO) showed the P=O

strech at xx cm-1. In addition to the P=O strech, the bottom two spectra, DNMPO and DAMPO showed N=O strech and N-H strech, respectively.

X-ray diffraction data were consistent with the assigned structure of the molecule. The Laue symmetry and "systematic absences" were consistent with the monoclinic space group $C_{2h}^{5} - P2_1/c$. The final refinement involved an anisotropic model for all non-hydrogen atoms and a riding model for all hydrogen atoms. A pictorial representation of the molecular structure deduced from the X-ray diffraction data is shown in figure 2.3-7.

This monomer subsequently gave rise to high molecular weight polyimides and polyurethanes, which was the ultimate proof of its purity.[18, 19]

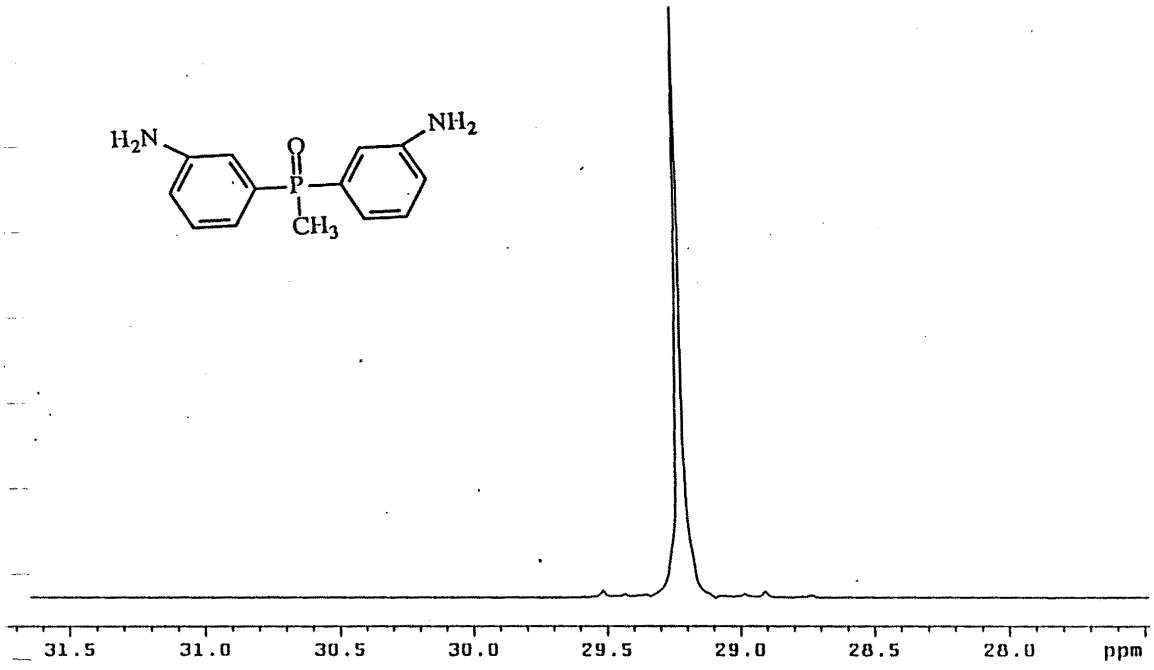

Figure 2.3-2 ^{31}P spectrum of bis(3-aminophenyl) methyl phosphine oxide

Figure 2.3-3 ^{1}H spectrum of bis(3-aminophenyl) methyl phosphine oxide

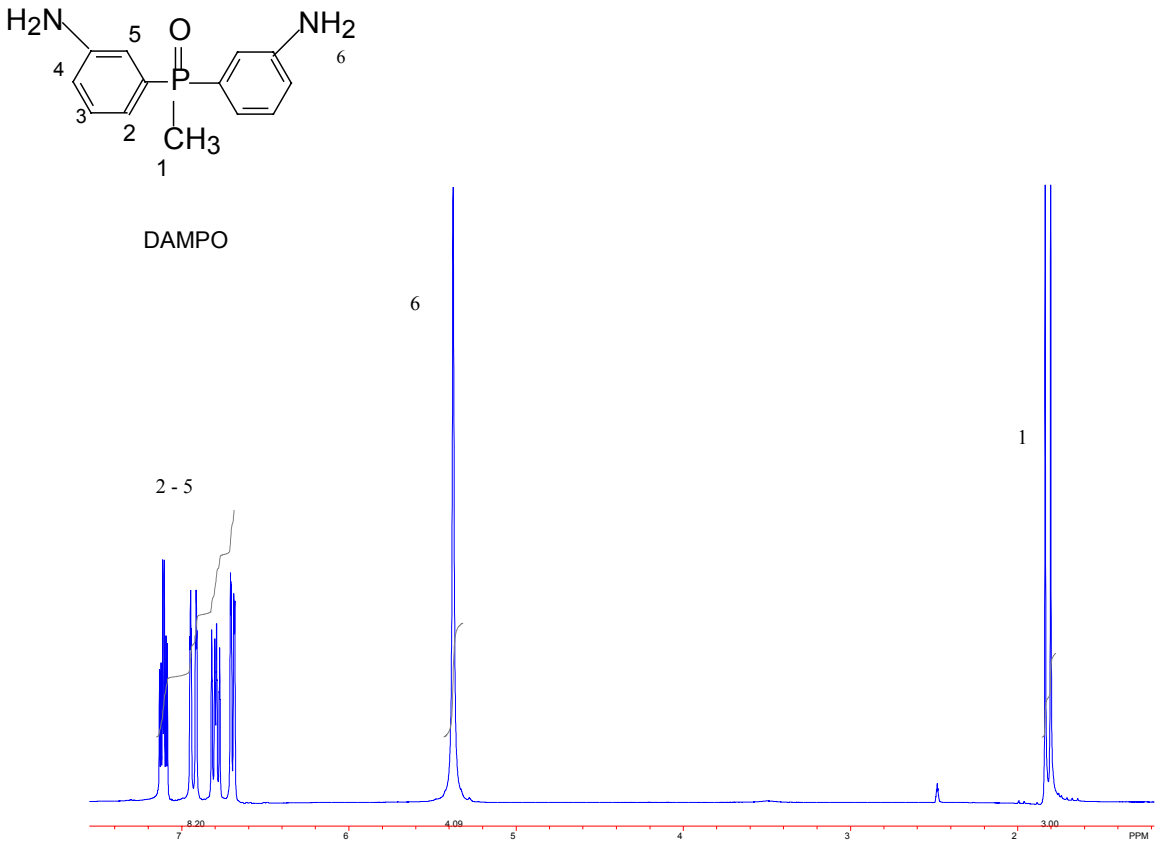

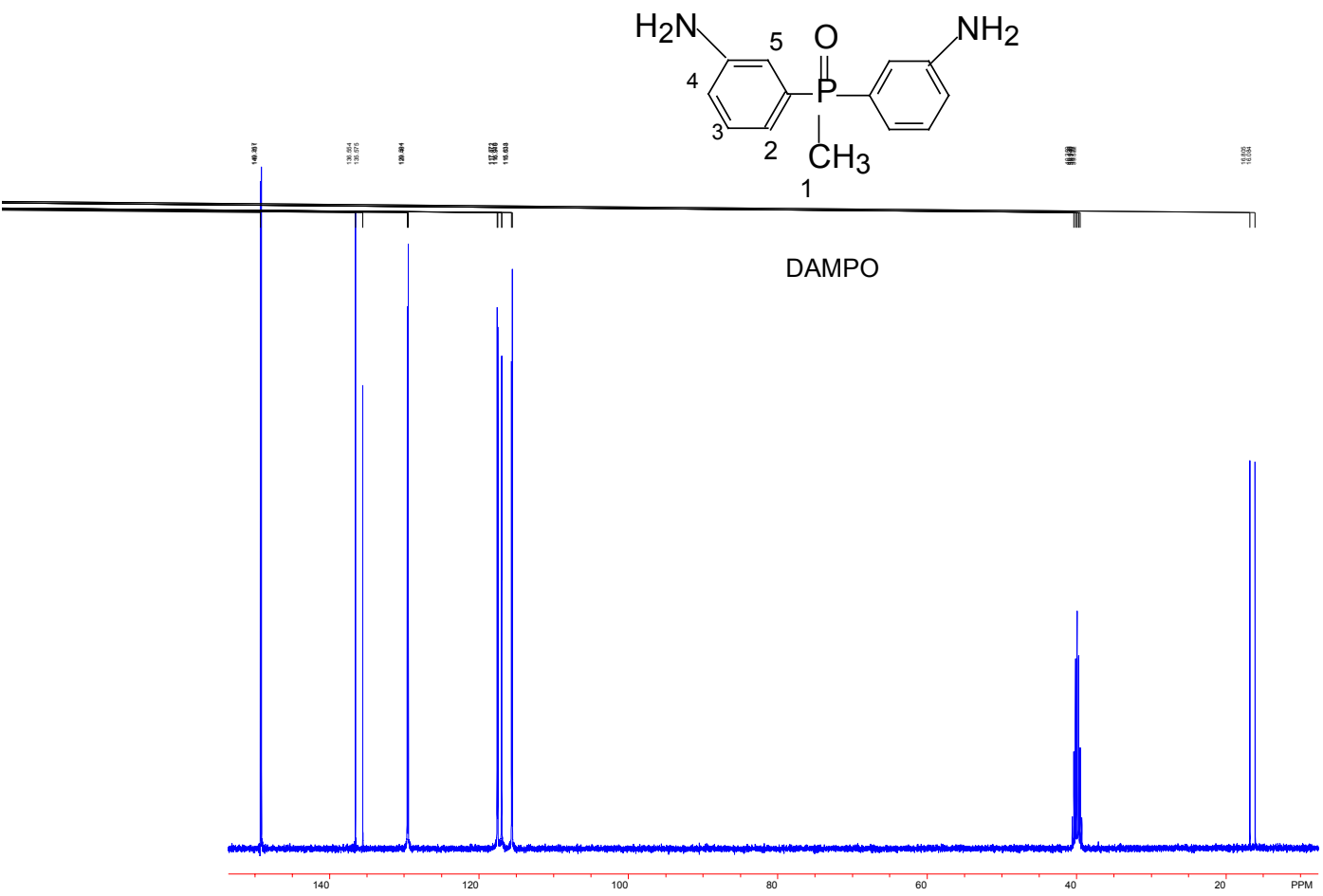

Figure 2.3-4 ^{13}C spectrum of bis(3-aminophenyl) methyl phosphine oxide.

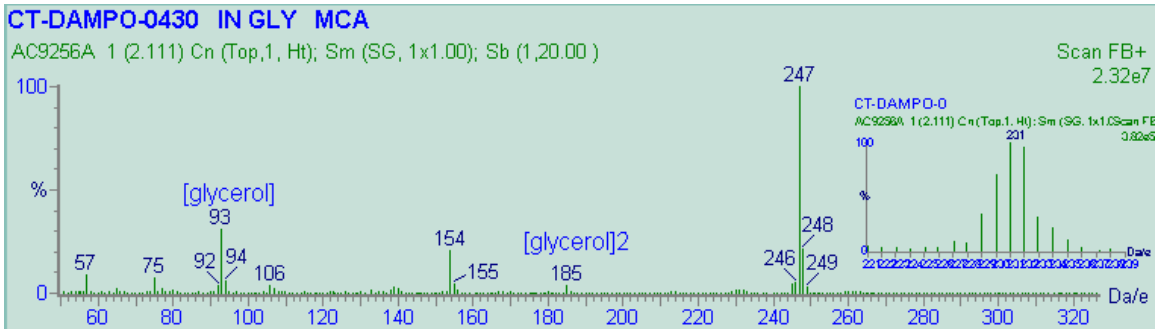

Figure 2.3-5 Mass spectrum of bis(3-aminophenyl) methyl phosphine oxide

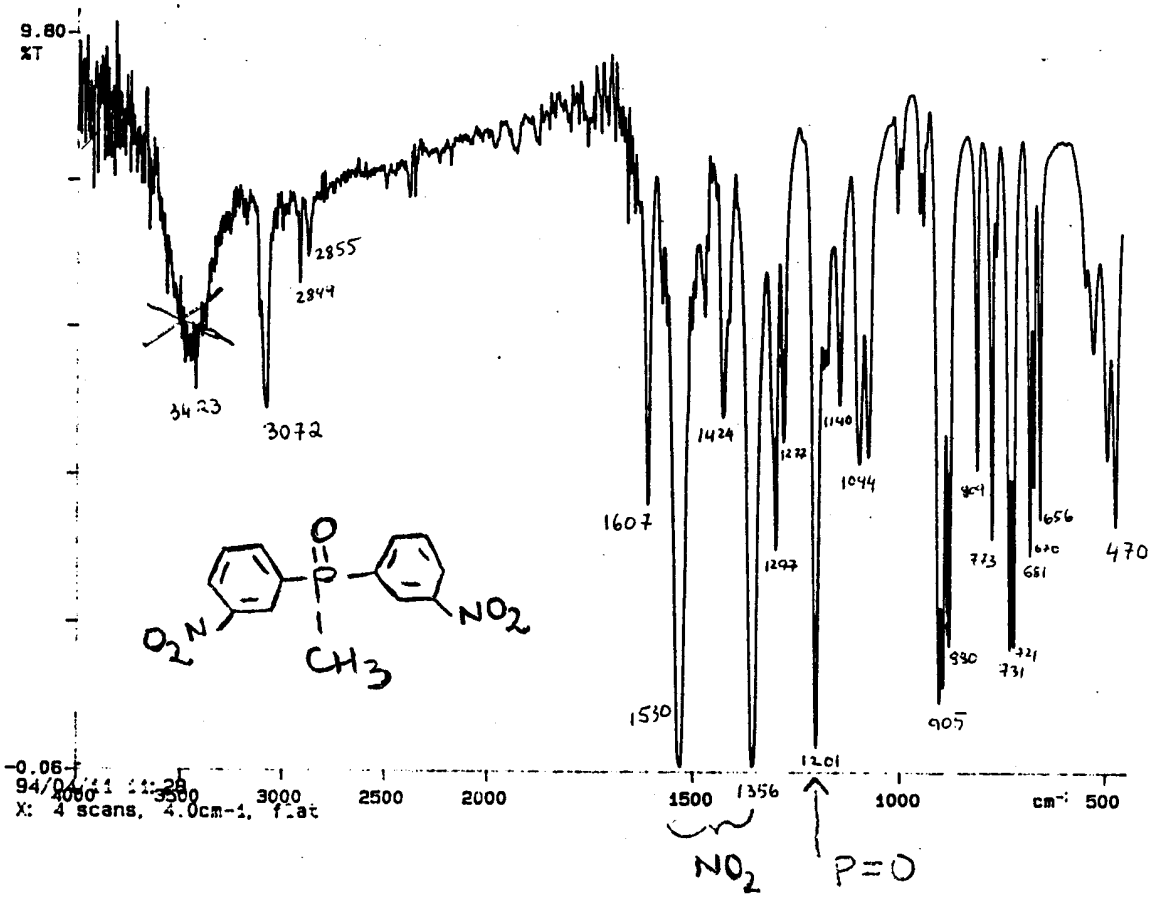

Figure 2.3-6 Infrared spectrum the nitrated intermediate of m-DAMPO.

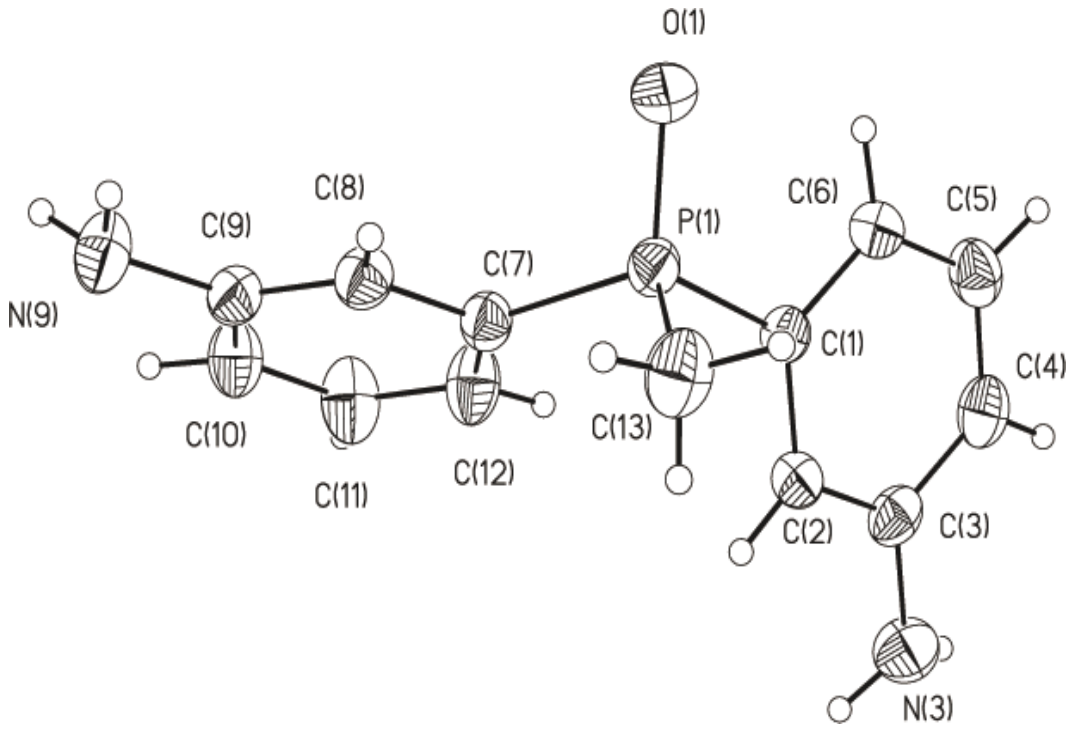

Figure 2.3-7 X-ray diffraction picture of bis(3-aminophenyl) methyl phosphine oxide

2.4 Bis(3-Aminophenyl) Phenyl Phosphine Oxide (DAPPO)

2.4.1 Modeling of DAPPO

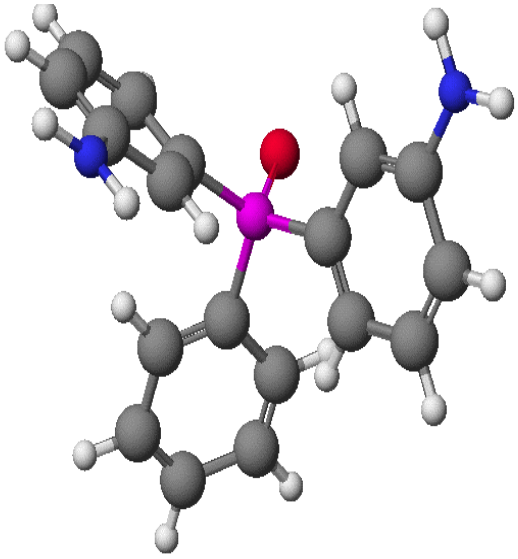

Figure 2.4-1 Lowest energy conformation of DAPPO by CAChe

2.4.2 Synthetic Strategy

The synthesis of this monomer starts with a three phenyl substituted phosphine oxide molecule (which is commercially available in large volume). Two of the phenyl groups are expected to undergo nitration. Since all three phenyl rings are identical its is necessary that the experimental conditions are selective enough to avoid the occurrence of trifunctional adducts in the final product.

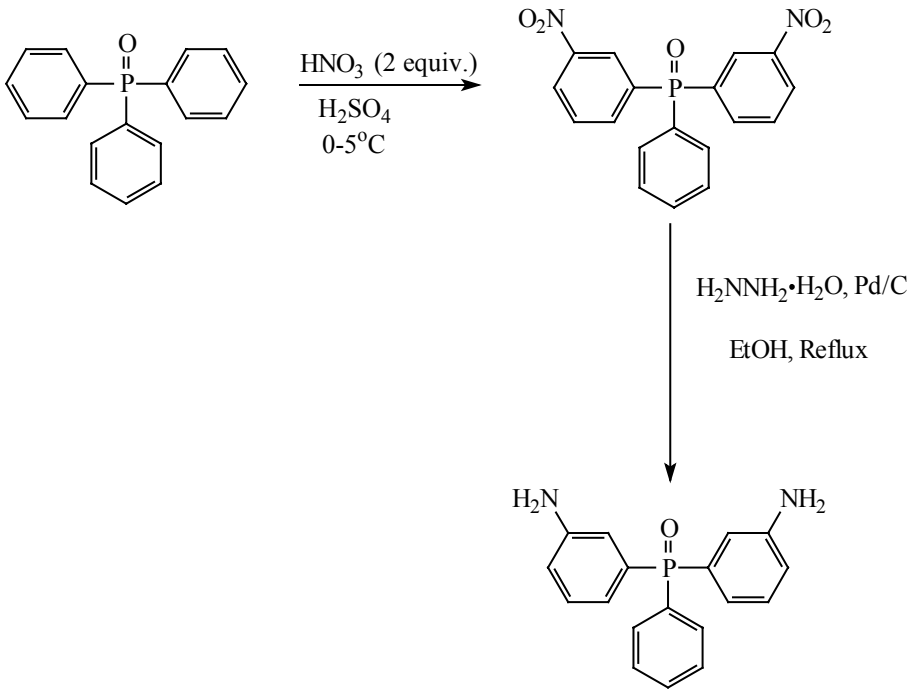

Scheme 2.4-1 Idealized synthesis of bis(3-aminophenyl) phenyl phosphine oxide

2.4.3 Nitration of Triphenyl Phosphine Oxide

The synthesis of a molecule such as tri(nitrophenyl) phenyl phosphine oxide can possibly proceed in three steps as depicted below:

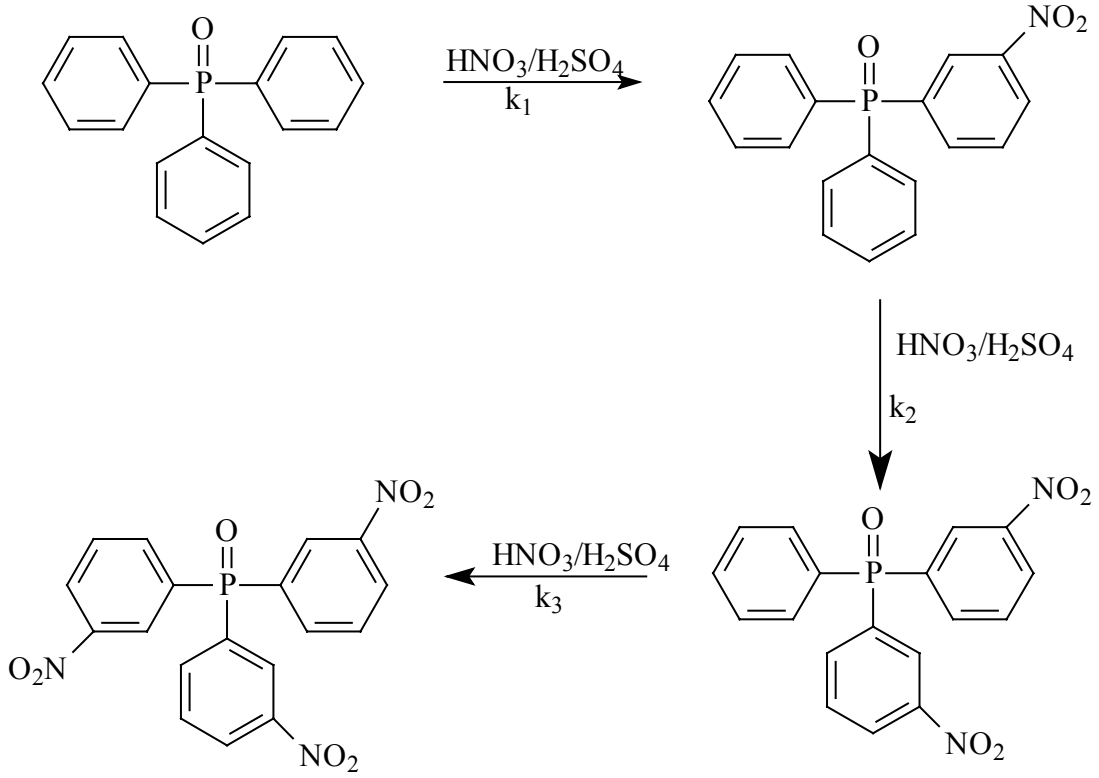

Scheme 2.4-2 Substitution possibilities during the synthesis of *m*-DAPPO

Given the relative hindrance of a nitro group for further nitration and some inductive effects, one can rationalize that $k_1 > k_2 > k_3$. The reaction was therefore performed at low temperature in order to maximize the dinitro adduct at the expense of the trinitro adduct. The stoichiometry was kept at 2:1 (nitric acid:triphenylphosphine) purely on a statistical basis.

Triphenyl phosphine oxide (500g, 1.8 mole) was charged into a 5L 3-necked round bottom flask equipped with an overhead mechanical stirrer, a reflux condenser and

an addition funnel. The flask was placed in an ice bath and concentrated (98%) sulfuric acid (1167mL) was carefully added to the content of the flask. The mixture was stirred for about 30 minutes until all of the starting material dissolved in the sulfuric acid.

In a separate ice bath, a 2 liter Erlenmeyer flask containing nitric acid (327g, 3.6moles) was cooled to 0^{o}C, and the concentrated sulfuric acid solution was slowly added to it. The number of moles of nitric acid was exactly two times that of the triphenyl phosphine oxide and the total amount of sulfuric acid was 10 times that of nitric acid (3.3L, 69moles) by weight. It should be emphasized that the mixture of sulfuric acid and nitric acid is very exothermic and must be performed with extreme caution.

The acid mixture was cooled to 0-5^{o}C and transferred to the addition funnel of the reaction apparatus. The acid was added dropwise and the ice bath temperature was maintained at –10 to -5^{o}C with sodium chloride, acetone and dry ice. After some period of time, it was allowed to rise to 0^{o}C for two hours and then to room temperture for three hours after the completion of the acid mixture addition. The reaction mixture was then slowly precipitated on ice. The precipitate was dissolved in chloroform (1L), washed with dilute sodium hydroxide to neutral pH and then with water, until the chloroform solution turned clear. The chloroform was removed by rotary evaporation and the resulting product was dissolved in methanol. The crude product contained 10% of the mononitro adduct as described in the above scheme, 10% of the trinitro adduct and about 80% of the desired dinitro adduct, as determined by ^{31}P NMR (figure 2.4-2).

In contrast to the nitration operation of the DAMPO synthesis, temperature control is extremely critical for the nitration of triphenyl phosphine oxide. The ice bath was made up of ice (as one might reasonably expect), sodium chloride and acetone. Dry ice was frequently added to maintain the temperature between -10 and -5^{o}C. The addition of the acid mixture was very slow, to prevent any unecessary heat build-up. The stoichiometry of nitric acid was important as mentioned ealier. The crude product was a viscous mass and could not be directly washed with water as was done in the synthesis of DAMPO. Rather, it was dissolved in chloroform and the impurities were then extracted with water.

2.4.4 Purification of Bis(3-Nitrophenyl) Phenyl Phosphine Oxide

The crude dinitro compound was purified by recrystallization from a mixture of water and ethanol. In order to achieve the ultimate purity (i.e. 100%) five to six recrystallizations were necessary. There was however a subtlety in this procedure that probably eluded earlier research on the synthesis of this molecule. The solubilities in ethanol vary in the order mono- > di- > trinitro adduct. Because of this, the ratio of water to ethanol was varied from 3:1 to 1:2 depending on the relative abundance of the phosphorylated side products as determined by ^{31}P NMR. The higher water:ethanol ratio was more efficient in eliminating the trinitro adduct (insoluble if the recrystallization solvent system is saturated) and the lower one was employed reduce the mononitro adduct content. The purified dinitro intermediate was a light yellow crystalline material with a melting point of 141-142^{o}C as determined by capillary. Reverse phase HPLC showed none of the "dreaded" impurities. ^{31}P NMR ($CDCl_3$) showed a single peak, in agreement with the absence of other phosphorylated side products. The chemical shifts from the NMR spectra, as well as the integrations, were consistent with the expected structure of this intermediate. The overall yield for the nitration experiment after the last recrystallization was 60%. One could note that for some applications such as thermosetting urethane synthesis or epoxy networks, the high purity achieved in this work would not be required, and the yield of useful product would be consequently higher.

2.4.5 Amination of Bis(3-Nitrophenyl) Phenyl Phosphine Oxide

The reductive amination of the dinitro intermediate proceeded according to the following scheme:

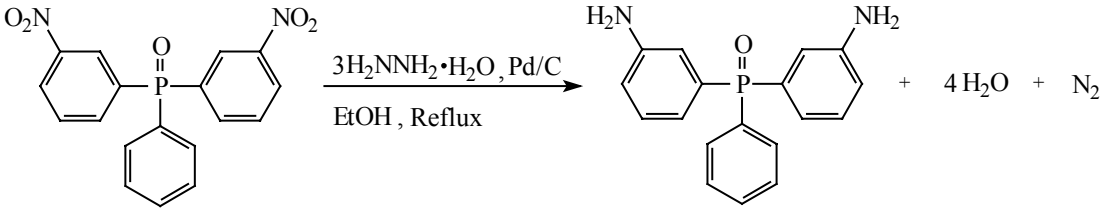

Bis(3-nitrophenyl) phenyl phosphine oxide (100g, 0.28 mole) was charged into a 5 liter three necked round bottom flask equipped with an overhead stirrer, an addition funnel and a reflux condenser. Absolute ethanol (1000ml) was added and heated to about 50^{o}C under a rapid flow of nitrogen. A small amount of catalyst, Pd/C (~0.5g) was introduced into the flask. Hydrazine monohydrate (367g, 7.3 moles, 9 times the stoichiometric amount) was introduced dropwise by means of the addition funnel. A rather intense nitrogen gas evolution denoted the occurrence of the reaction. No heat was needed at this stage because of the exothermic nature of the reaction. When the reaction decelerated as indicated by a reduction in the intensity of nitrogen evolution, more Pd/C (~0.5g) catalyst was added to the reaction mixture and the system was heated to reflux for about two hours. The completion of the reaction was indicated by thin layer chromatography (chloroform:methanol, 9:1). About 2g of decolorizing activated carbon was then added to the reaction and a gentle reflux was allowed to continue for one additional hour. The dark solution was then cooled down under nitrogen purge and subsequently filtered through celite with a Buchner funnel to afford a clear, light brown solution. The solvent was immediately removed by rotary evaporation. The product was washed with water and recrystallized in a mixture of ethanol and water (40/60 v/v) and subsequently dried in a vacuum oven at 100^{o}C for 48 hours. The product had a melting point of 212^{o}C as determined by DSC and no impurities were detected by HPLC (absolute methanol as mobile phase). Titration with HBr suggested that the purity of the diamine was higher than 99%. ^{31}P NMR (400MHz, d-DMSO) showed a singlet at 29.2 ppm (figure 2.4-3) suggesting that no other phosphorylated compounds were included in the diamine. This chemical shift is relatively higher than that of the DAMPO homologue, which was to be expected, considering the fact that the additional phenyl ring (which is the major difference between the two compounds) withdraws electron density from the phosphorus,

thus further deshielding it during NMR measurements. ^{1}H NMR (d-DMSO) data are shown in Figure 2.4-4. The chemical shifts and the integrations are consistent with those expected for a molecule with the expected structure. Elemental analysis of the purified monomer (Galbraith Laboratories, Inc.) are presented below, with the expected values included in parenthesis: C~69.71% (70.12); H~5.64% (5.56); N~8.91% (9.09); P~9.67% (10.05).

Compared to the reduction of DNMPO homologue, the reduction of the dinitrophenyl phenyl phosphine oxide (DNPPO) was much slower as monitored by thin layer chromatography. This can be partly ascribed to the steric hindrance of the additional phenyl ring or to the electron withdrawing nature of the ring as evidenced by the upfield shift of the phosphorus resonance in ^{31}P NMR spectroscopy.

Mass spectrum results (Figure 2.4-5) was consistent with the assined structure. The molecular ion (M^{+} =308) is visible, with a prominent (M^{+}+1) peak, as it could be expected from a molecule containing one or several P atoms.

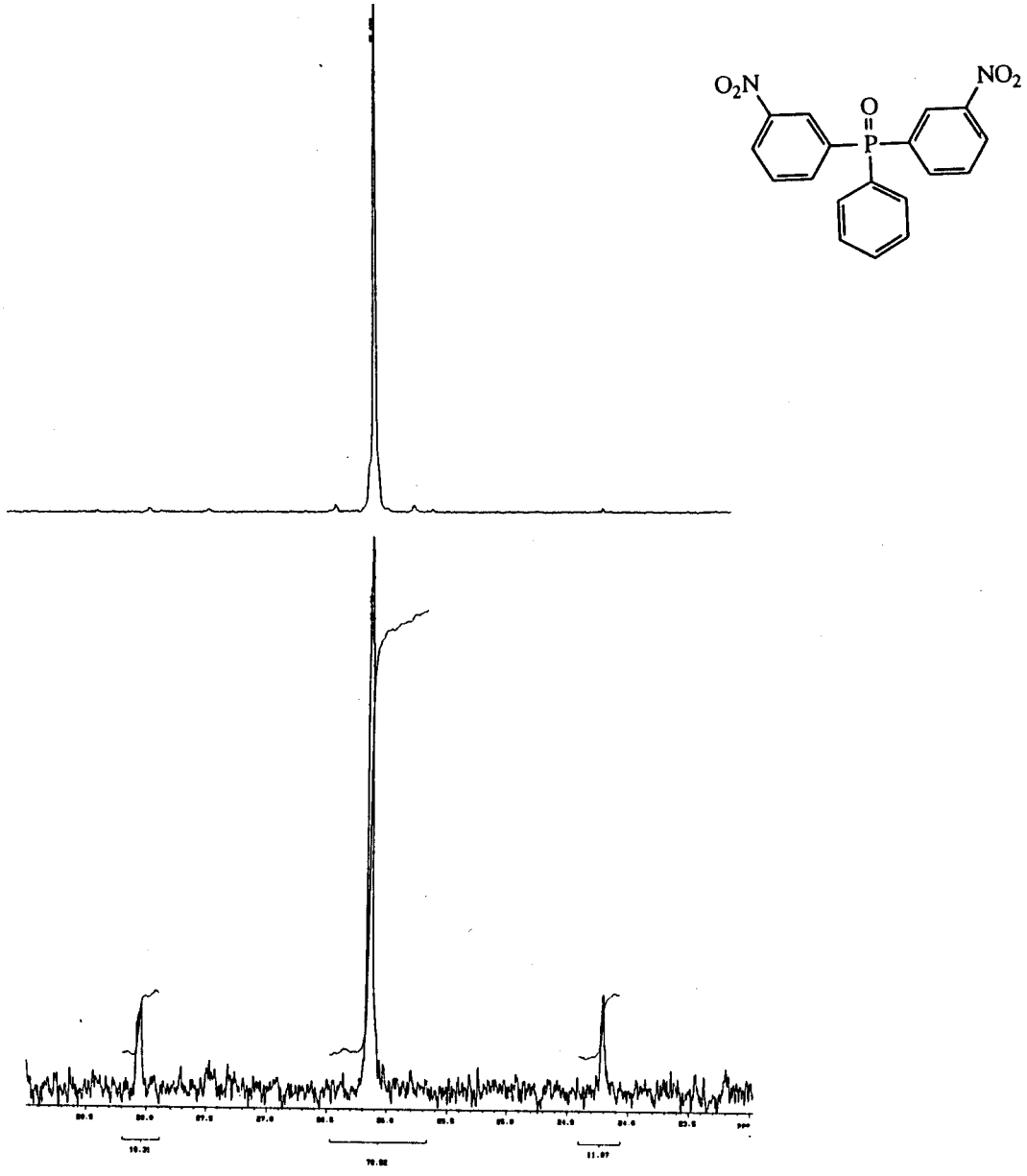

Figure 2.4-2 ^{31}P NMR Spectrum of Bis(3-dinitrophenyl) Phenyl Phosphine Oxide

(The bottom spectrum corresponds to the crude product and the upper spectrum to the product after purification)

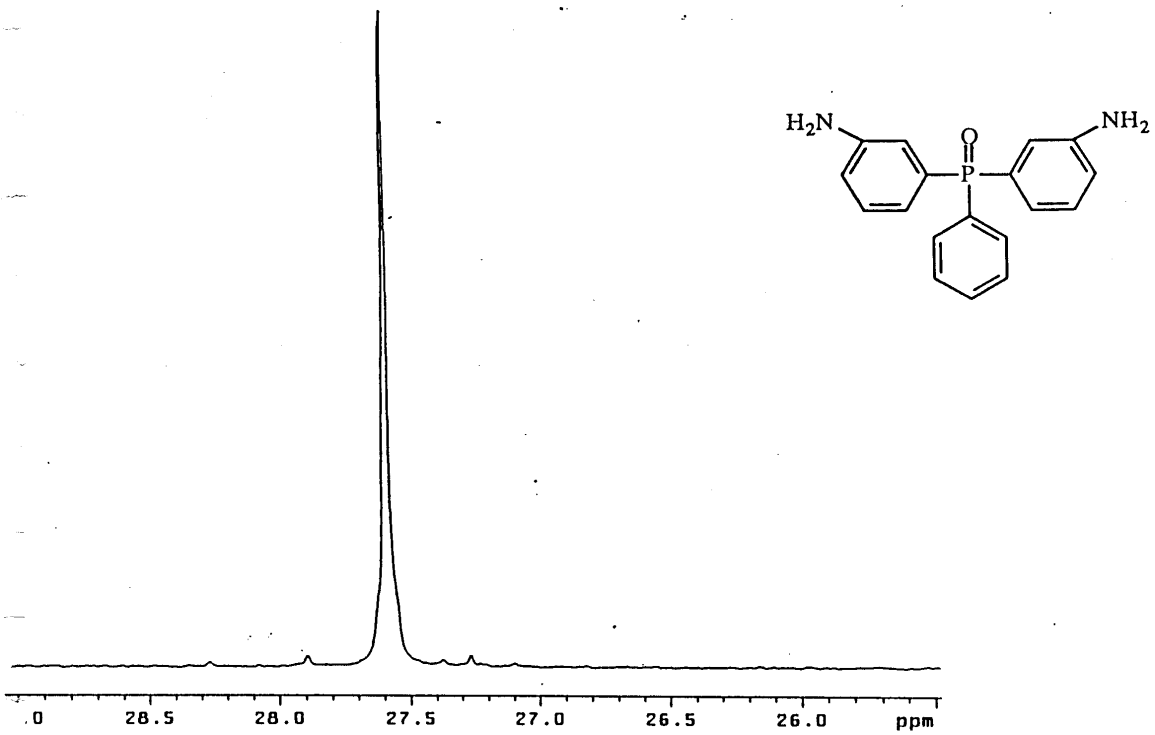

Figure 2.4-3 ^{31}P NMR specrum of DAPPO

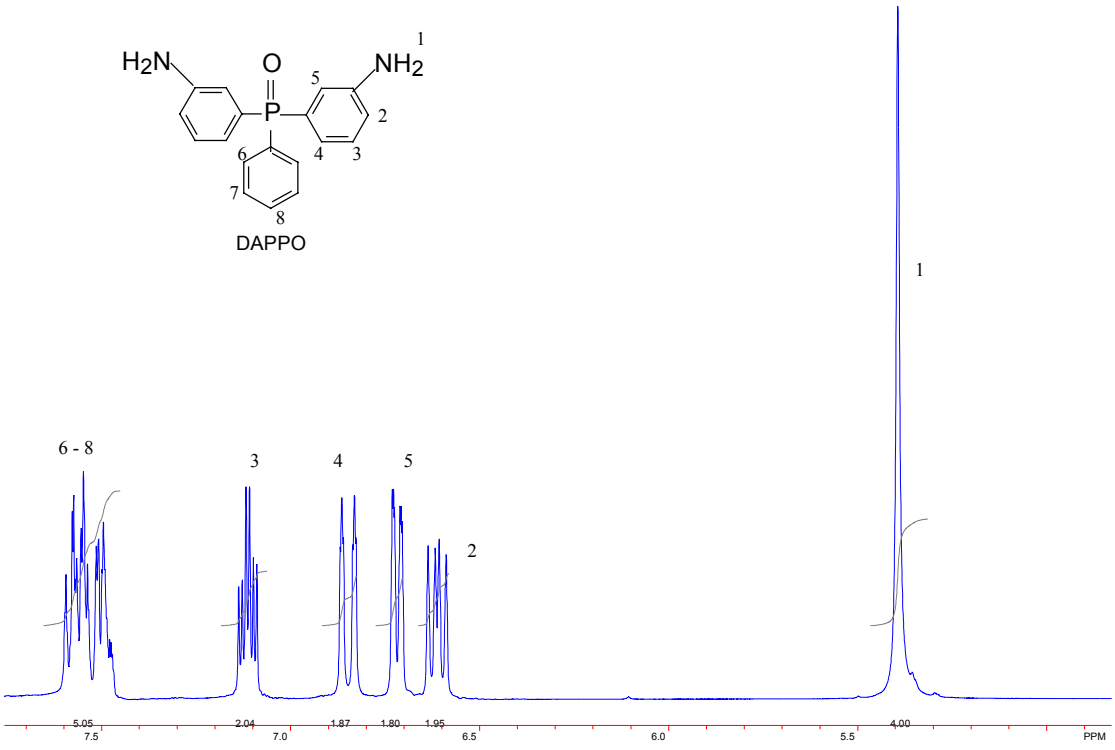

Figure 2.4-4 ^{1}H NMR Spectrum of Bis(3-aminophenyl) phenyl phosphine oxide.

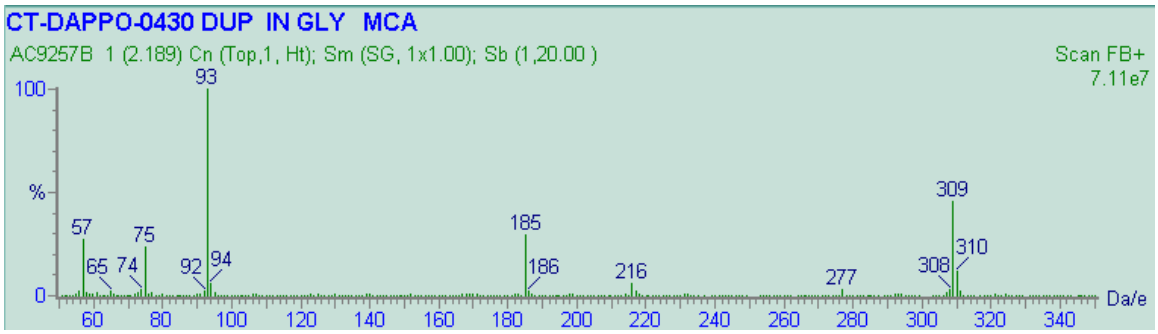

Figure 2.4-5 Mass spectrum of bis(3-aminophenyl) phenyl phosphine oxide

2.5 Bis(3-Aminophenoxyphenyl) Methyl Phosphine Oxide (*m*-BAMPO)

2.5.1 Synthesis of Methylphosphonic dichloride[20]

Thionyl chloride (1488g, 12.5 moles) was added to a 2 liter three necked round bottom flask fitted with a mechanical stirrer, a reflux condenser and a dropping funnel. The content of the flask was then heated to reflux with a heating mantle, under nitrogen purge. A mixture of dimethyl methyl phosphonate (620g, 5 moles) and N,N-dimethyl formamide (3.65g, 0.05mole) was added dropwise to the flask. The large excess of thionyl chloride controls traces of moisture in this reaction. The evolution of a sulfur dioxide denoted the reaction progress and the addition rate of the phosphonate was adjusted accordingly. After the end of the addition, the reaction was allowed to proceed for about two hours. The product mixture was twice distilled by microdistillation and the fraction collected at 162^{o}C was stored in a pre-tared 100 ml round bottom flask under nitrogen. The pure product crystallized from the melt over a period of 48 hours. The yield for this reaction after the purification procedure was approximately 80%. It should be pointed out that this product (methylphosphonic dichloride) reacts violently with water and one should exercise great care.

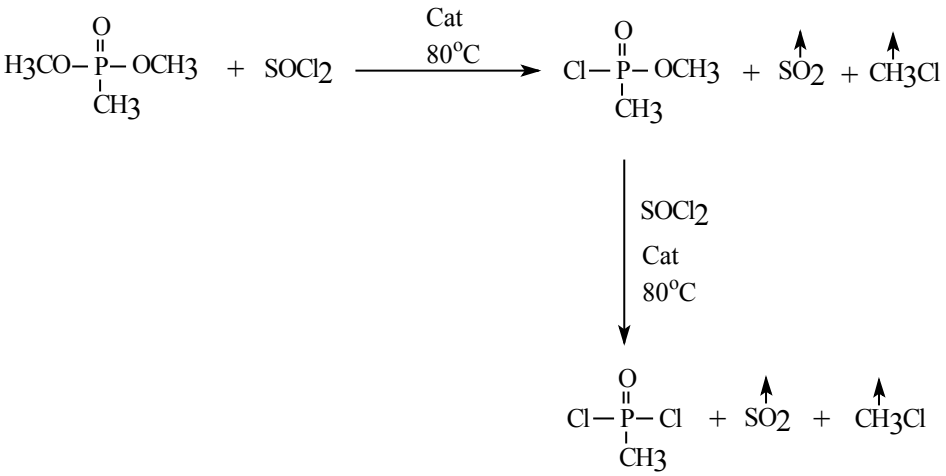

Scheme 2.5-1 Synthesis of methyl phosphonic dichloride.

Methanol was carefully slowly added to the reaction residues until no more exotherm was observed. Inactivation of the distillation flask residue proceeded in the same manner.

2.5.2 Synthesis of Bis(4,4'-fluorophenyl) Methyl Phosphine Oxide (BFMPO)

To a flame dried 5 liter 3-necked round bottom flask fitted with an overhead mechanical stirrer, an addition funnel and a nitrogen inlet were added 122g (5.01 moles) of magnesium turnings and 3.5 liters of dried tetrahydrofuran. An ice container was placed underneath the flask and the mixture was stirred. To this stirred solution was added dropwise at 5°C, 875g (5 moles) of 4-bromofluorobenzene over three hours. This solution was stirred for six hours to give a gray slightly cloudy solution. Methylphosphonic dichloride (300g, 2.25 moles) was then added dropwise at 5°C over a period of two hours. The solution was allowed to stir at room temperature for a period of 12 hours to afford a yellow clear solution. Sufficient 10% aqueous sulfuric acid was added to the mixture to make the solution acidic, followed by the addition of about 300

ml of water. Diethyl ether was added in order to separate the solution into an organic and an aqueous phase. The aqueous layer was several times washed with ether-THF solutions and all organic layers were combined. The ether solvents were stripped by rotary evaporation and the residual organic material was dissolved in chloroform. This organic layer was washed with water, 10% sodium bicarbonate, and then water again. The chloroform was stripped by rotary evaporation to afford an off white material which was purified by Kugelrohr distillation at 150^{o}C. The resulting product was further purified by recrystallization in a mixture (4/1) of hexane and methylene chloride (1g of monomer for 5 ml of solvent). The purified product was dried in a vacuum oven for 24 hours. The yield for this Grignard reaction was approximately 80%. ^{31}P NMR and ^{1}H nmr are shown in Figure 2.5-1 and Figure 2.5-2 respectively. The mass spectrum data for this compound are shown on Figure 2.5-3. The molecular ion M^{+} is visible and the M^{+}+1 is intense, as it is common for molecules containing P atoms.

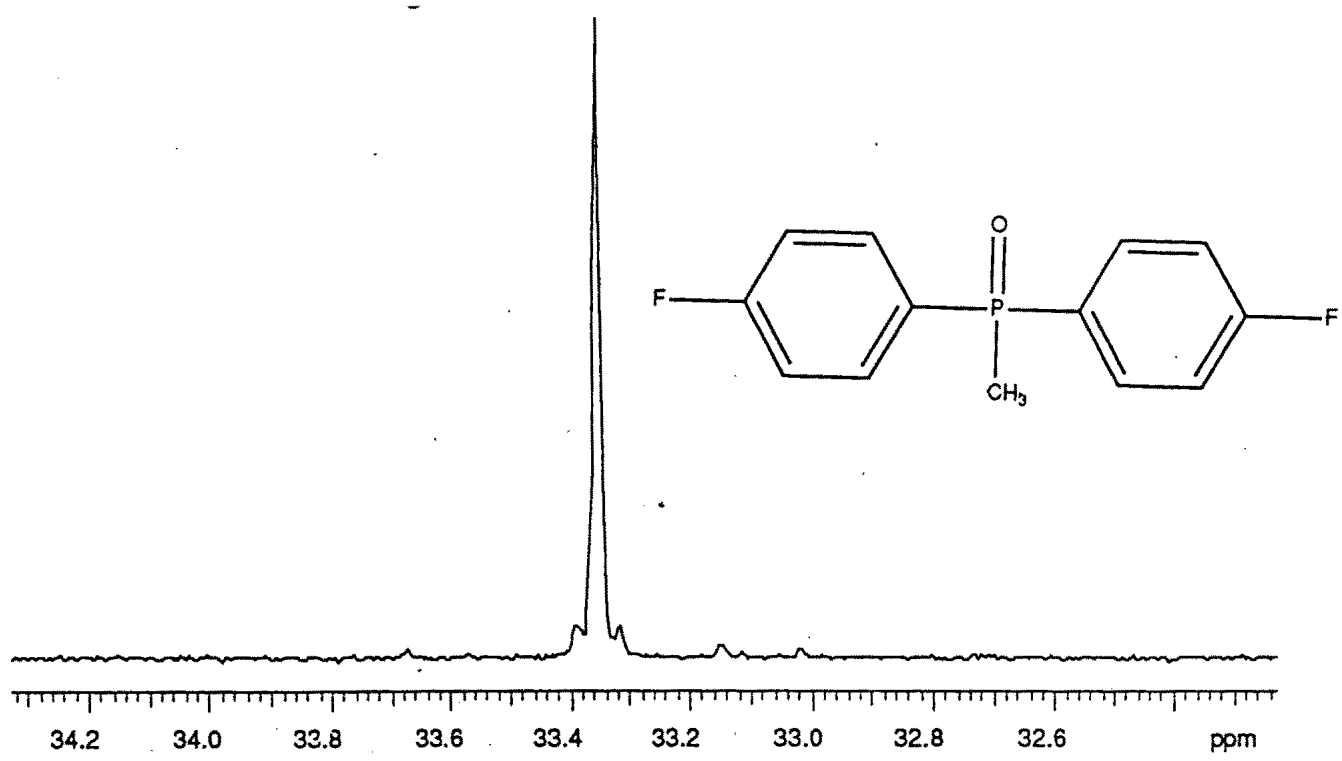

Figure 2.5-1 ^{31}P NMR of bis(4-fluorophenyl) methyl phosphine oxide (BFMPO).

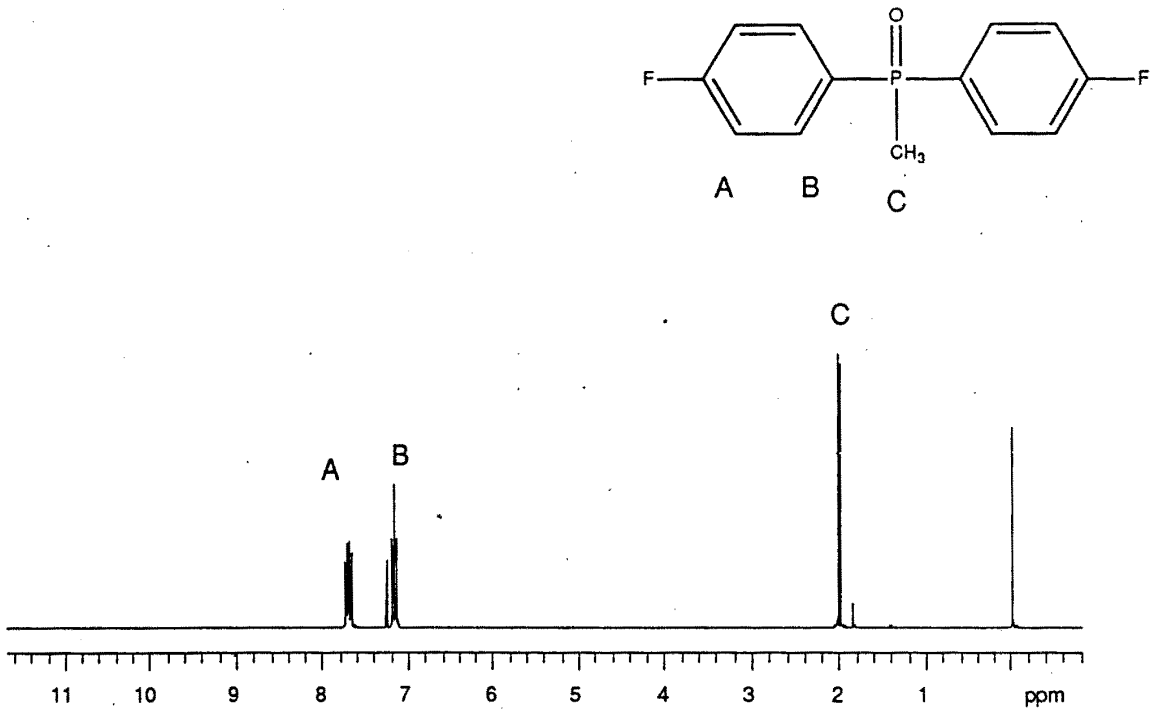

Figure 2.5-2 ^{1}H NMR Spectrum of Bis(4-fluorophenyl) methyl phosphine oxide (BFMPO).

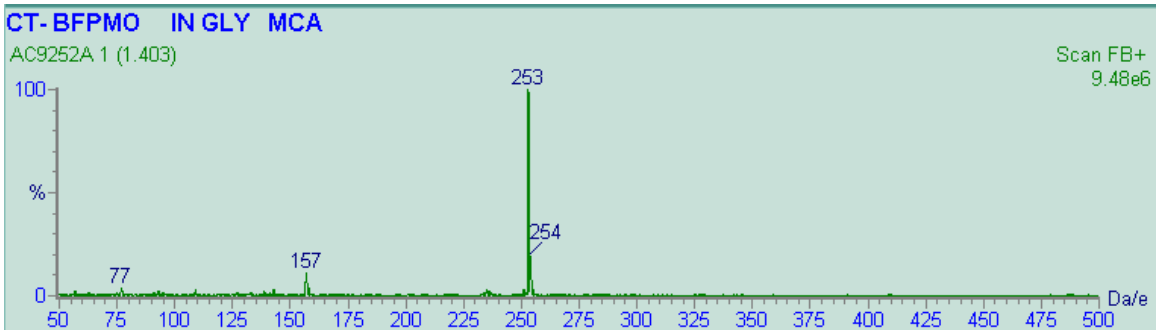

Figure 2.5-3 **Mass spectrum of bis(4-fluorophenyl) methyl phosphine oxide**

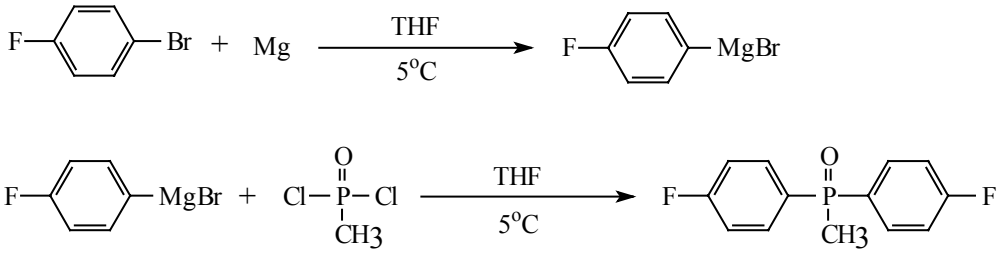

2.5.3 m-AminoPhenoxylation of Bis(4-fluorophenyl) Methyl Phospine Oxide

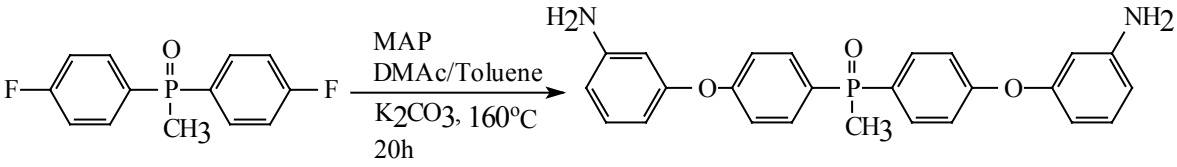

The synthesis of *m*-BAMPO was performed through a classic nucleophilic aromatic substitution where a phenoxide generated by the presence of a weak base (potassium carbonate) displaced an activated halogen. A slight excess of aminophenol (~3%) was used, given that it can easily be extracted from the organic phase with water.

To a flame dried 2 liter four necked round bottom flask fitted with a reflux condenser, a Dean-Stark trap and a nitrogen inlet, was added at room temperature *m*-aminophenol (133g, 1.215 mole), BFMPO (149g, 0.59 mole), potassium carbonate (180g, 1.3 mole), DMAC (1 liter) and 500 ml of toluene. The flask was heated with an oil bath whose temperature was adjusted to 170°C. Some toluene was removed through the Dean-Stark trap in order to maintain the reaction temperature at 150°C. The reaction was allowed to proceed for 16 hours, then all of the toluene was removed from the flask. The

complete removal of toluene was essential for the success of subsequent operations. Any remaining traces of toluene would results in a viscous product that does not precipitate into water. The solution was further concentrated, cooled to room temperature, then filtered through a Buchner funnel and precipitated into water. The off white precipitate was decanted, dissolved into chloroform and washed with water several of times. The chloroform was evaporated by rotary evaporation and the product was dissolved into ethanol and refluxed for one hour over activated decolorizing carbon. The solution was filtered through a Buchner funnel, concentrated by rotary evaporation then precipitated in water. This last precipitation assured the complete removal of DMAC from the product. The precipitate was filtered and recrystallized in a water/ethanol mixture. The crystals were collected, dried on a teflon dish in a vaccuum oven 100^{o}C for 48 hours, then crushed with a mortar and pestle to give a fine white powder. The yield for this reaction was 85% and the melting point was 81^{o}C as determined by capillary methods. ^{31}P NMR showed a singlet at 30.15 ppm (Figure 2.5-4). ^{1}H NMR and ^{13}C NMR are shown on Figure 2.5-5 and Figure 2.5-6 respectively. Elemental analysis of the monomer gave the following results (the theoretical values are indicated into parenthesis): C~xx% (69.76); H~xx% (5.39); N~xx% (6.51); P~xx% (7.20). The mass spectrum of the new monomer was consistent with its assisgned structure, particularly the molecular ion at 430, corresponding to the molecular weight of *m*-BAMPO and the molecular ion cluster clearly reminiscent of a phosphine oxide containing compound (Figure2.5-7).

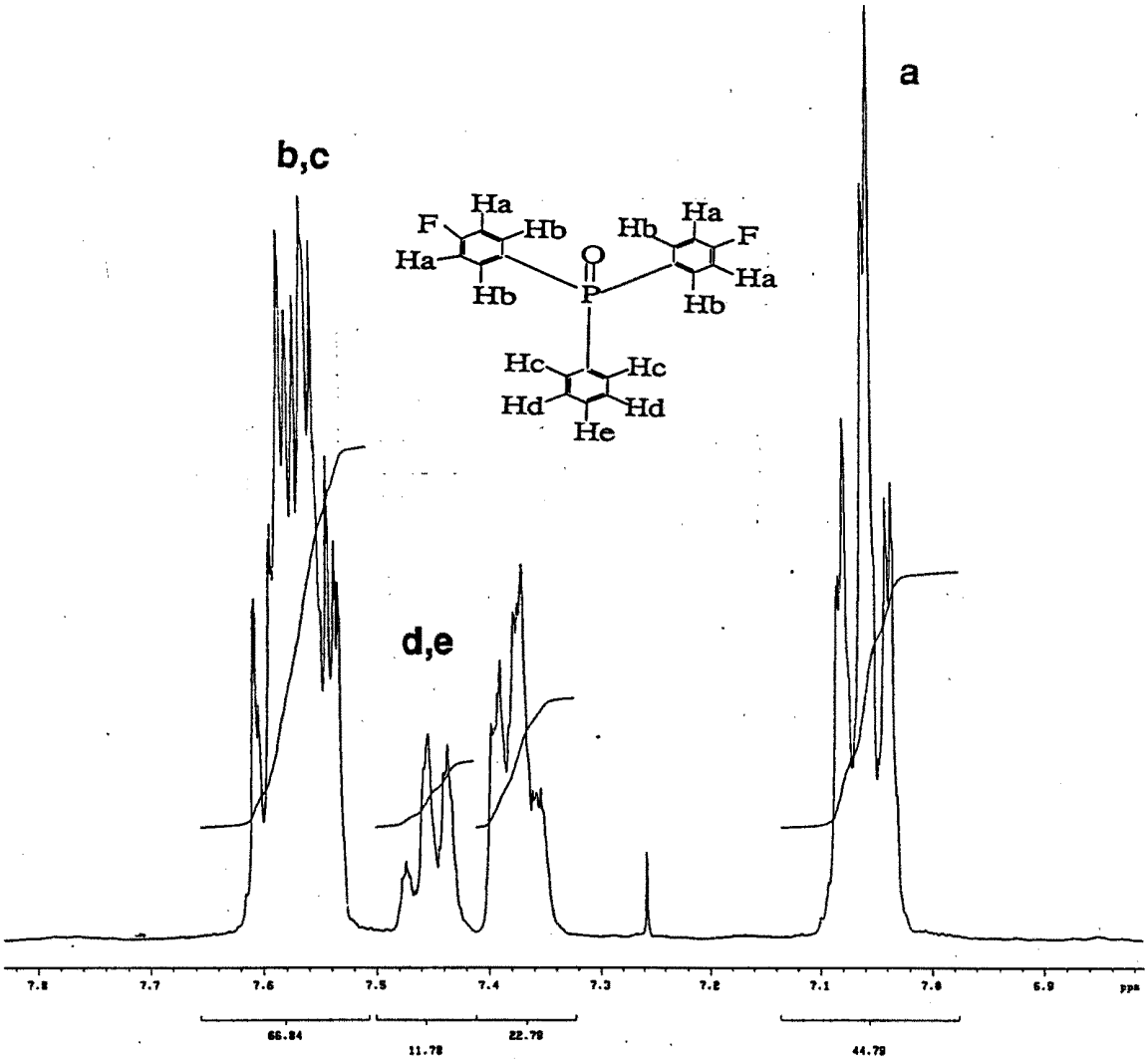

Figure 2.5-4 **^{31}P NMR spectrum of bis(3-aminophenoxyphenyl) methyl phosphine oxide (m BAMPO)**

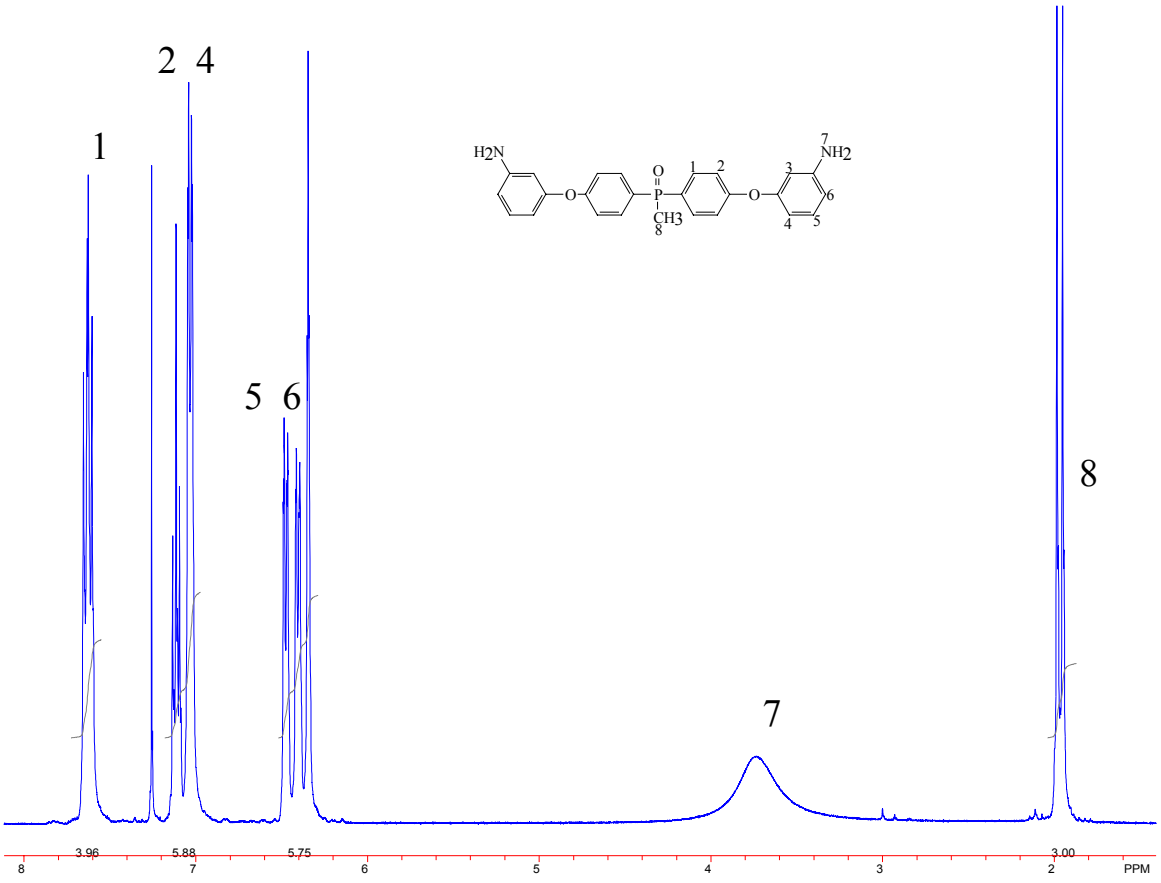

Figure 2.5-5 **Proton NMR spectrum of m-BAMPO**

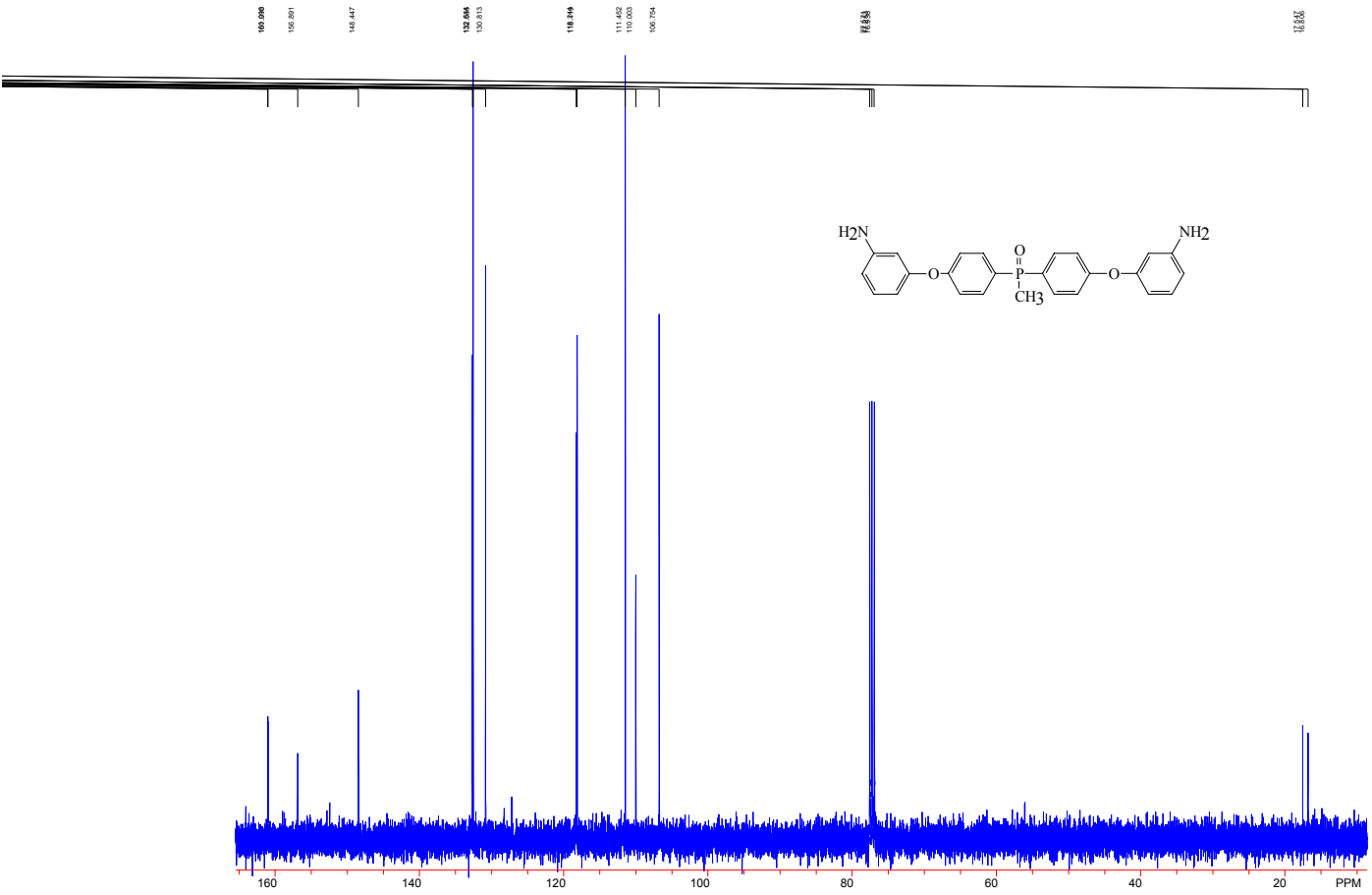

Figure 2.5-6 ^{13}C Spectrum of m-BAMPO

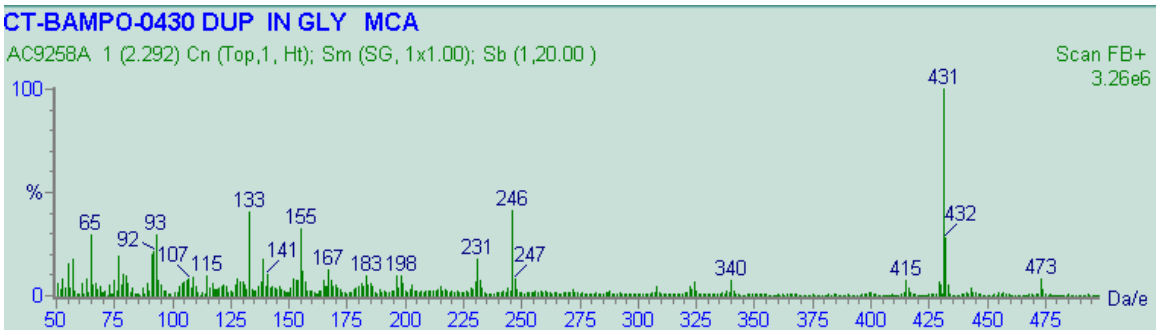

Figure 2.5-7 **Mass spectrum of m-BAMPO.**

2.6 Synthesis of Bis(3-aminophenoxyphenyl) Phenyl Phosphine Oxide (*m*-BAPPO)

2.6.1 Synthesis of Bis(4-fluorophenyl) Phenyl Phosphine Oxide

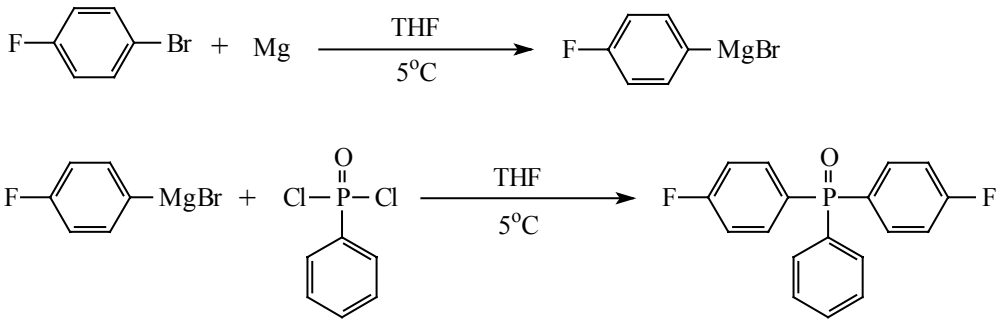

To a flame dried 5 liter three necked round bottom flask fitted with an overhead mechanical stirrer, a reflux condenser, an addition funnel and a nitrogen inlet were added magnesium turnings (85.1g, 3.5 moles) and 3.5 liters of previously purified and dried tetrahydrofuran. The content of the flask was stirred and cooled to approximately 5°C on an ice container. 4-Bromofluorobenzene (618.7g, 3.5 moles) was added dropwise to this flask by the mean of an addition funnel over a period of three hours. This solution was stirred for six hours to give a grayish appearance. Phenylphosphonic dichloride was then added dropwise at 5°C over three hours and this mixture was allowed to stir at room temperature for 12 hours. A clear yellow solution resulted. A 10% sulfuric acid solution was added to the flask until an acidic mixture resulted, followed by the addition of 500 ml of water. Diethyl ether was then added in order to allow a phase separation between the organic phase and the aqueous phase. The aqueous phase was further extracted with a tetrahydrofuran/diethyl ether mixture and all organic layers were combined. The ether

solvents were stripped by rotary evaporation and the residual organic material was dissolved into chloroform. This organic solution was washed with water, then 10% sodium carbonate solution and then water again. The chloroform solvent was then stripped by rotary evaporation to afford an off-white solid material that was further dried in a vacuum oven at 100^{o}C for 12 hours. This product was then purified by Kugelrohr distillation at 170^{o}C. The now bright white solid was recrystallized in a 1:4 methylene chloride-hexane mixture (1g of monomer for 5ml of solvent). The crystals were dried in a vacuum oven at 100^{o}C for 48 hours. ^{31}P NMR and ^{1}H NMR (in $CDCl_3$) were consistent with the assigned structure of this compound (figure xx and figure xx). The compound had a capillary melting point range of 125-126^{o}C.

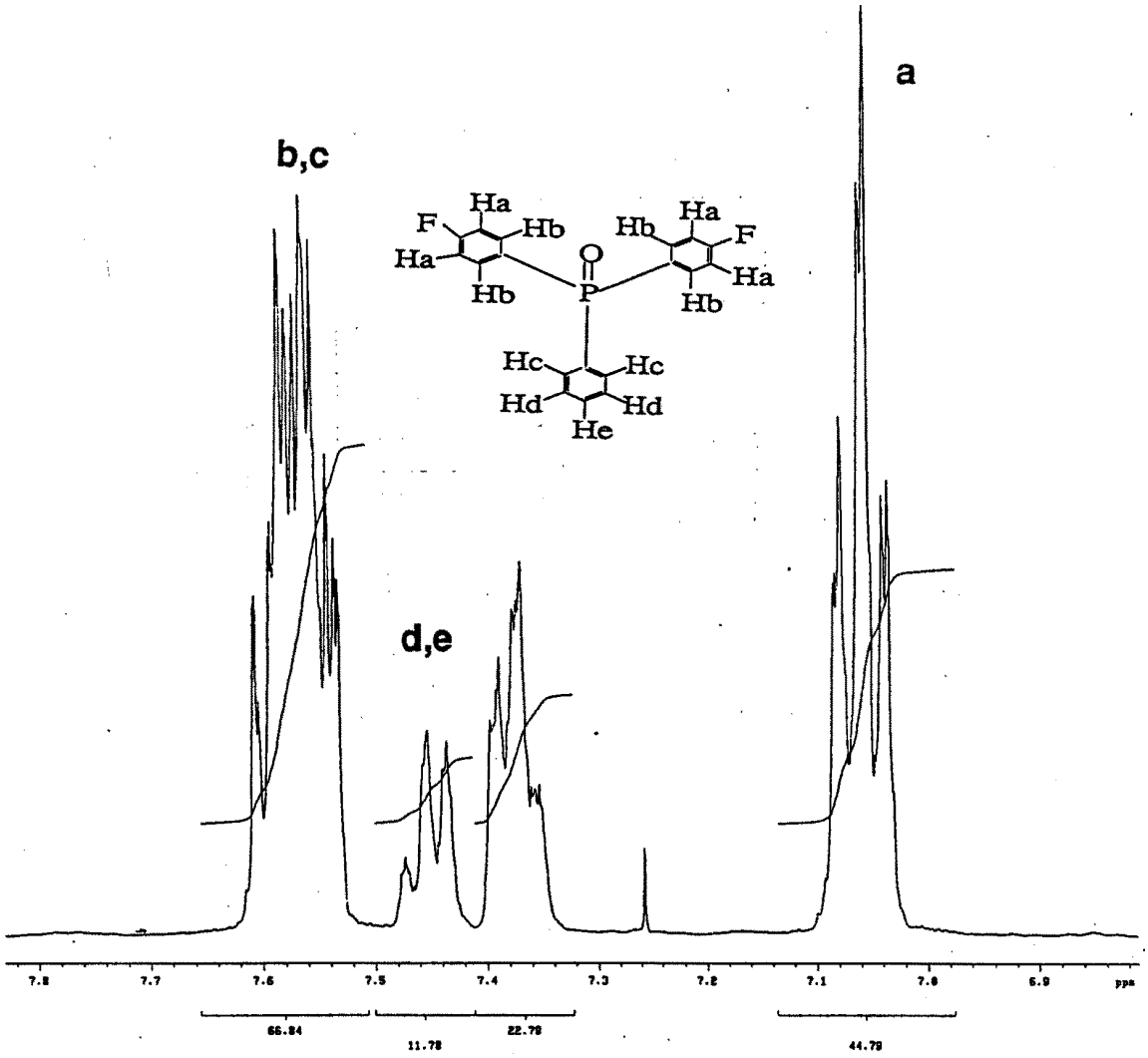

Figure 2.6-1 ^{1}H NMR spectrum of bis(4-fluorophenyl) phenyl phosphine oxide (BFPPO)

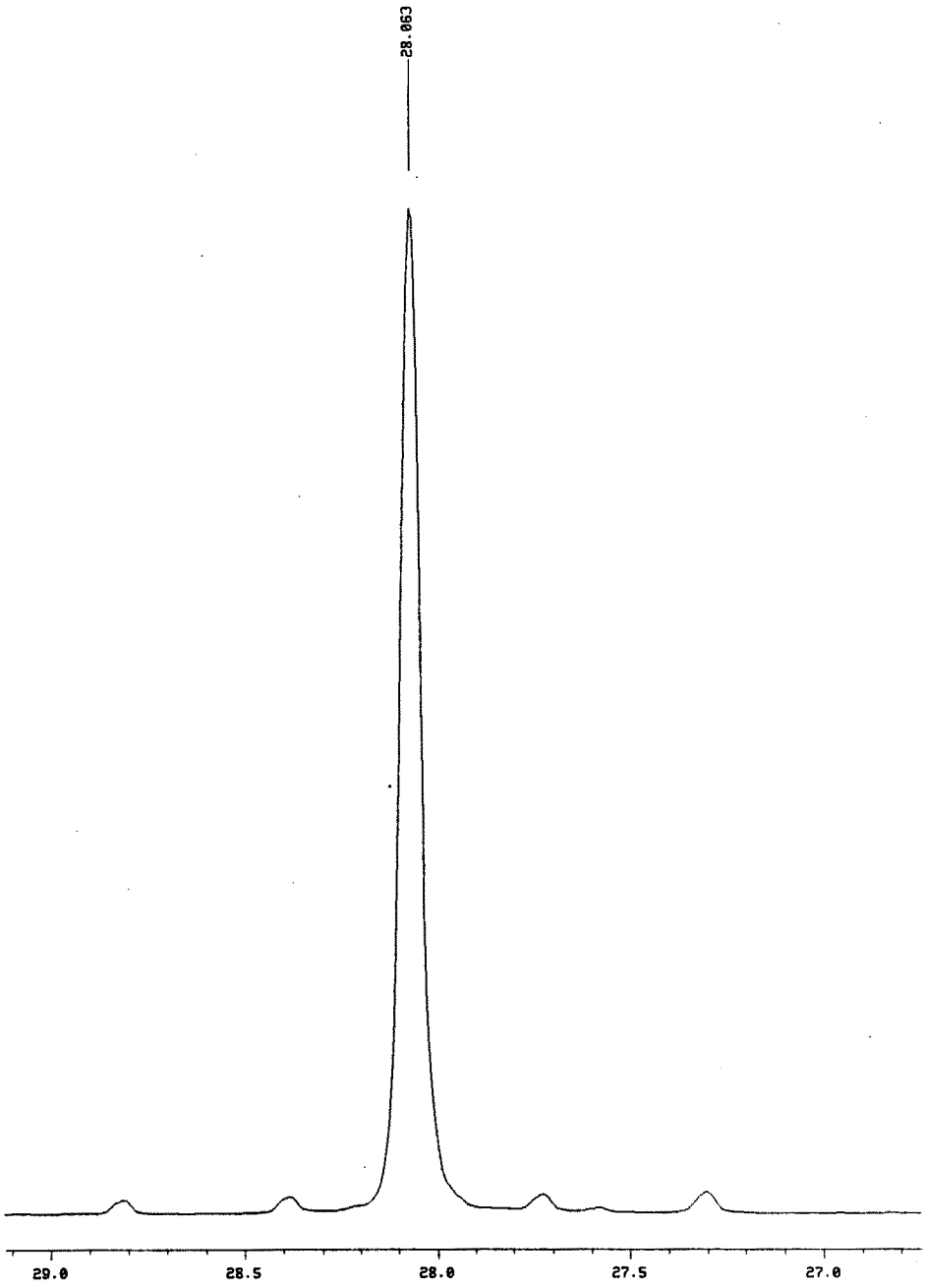

Figure 2.6-2 ^{31}P NMR spectrum of bis(4-fluorophenyl) phenyl phosphine oxide (BFPPO)

2.6.2 Amino Phenoxylation of Bis(4-fluorophenyl) Phenyl Phosphine Oxide (BFPPO)

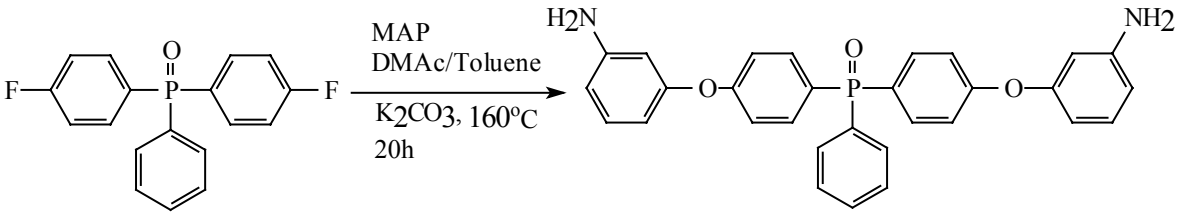

As in the case of BAMPO, The synthesis of BAPPO was performed by a nucleophilic aromatic substitution where the m-aminophenoxides generated by the potassium carbonate displace the activated fluorines. An excess of m-aminophenol (MAP) was used because of its solubility in water. During the purification of the monomer, the excess of m-aminophenol (MAP) can easily be extracted by water washing of the organic phase.

To a flame dried 2 liter four necked round bottom flask fitted with a reflux condenser, a Dean Stark trap, an overhead stirrer and a nitrogen inlet, was added at room temperature m-aminophenol (146g, 1.34 mole), BFPPO (200g, 0.64 mole), potassium carbonate (194g, 1.4 mole), DMAc (1liter) and 500 ml of toluene. The flask was heated with an oil bath whose temperature was adjusted to 170^{o}C. As soon as the mixture started to reflux some toluene was removed from the reaction mixture by opening the valve of the Dean-Stark trap in order to maintain the reaction temperature at 150^{o}C. The reaction was allowed to proceed for 16 hours, upon which all of the toluene was removed from the flask. The toluene removal for this type of reaction is crucial because any remaining traces of toluene would give rise to a viscous product during the precipitation operation and the recovery of the material would be complicated. The solution was further

concentrated, cooled to room temperature, filtered by vacuum filtration and precipitated into water by means of a blender. The white precipitate was dissolved in chloroform and washed ten times with water until no purplish colored substances appeared to migrate into the aqueous layer. After layer separation, the choroform was stripped by rotary evaporation, the product was dissolved into ethanol and refluxed for one hour over approximately 20g of activated decolorizing carbon. The charcoal treated solution was filtered through a Buchner funnel, concentrated by rotary evaporation, then precipitated into water. This last precipitation assured the complete removal of the reaction solvent (DMAc) from the product. The precipitate was filtered and recrystallized in an ethanol-water mixture (60:40). The crystals were filtered and dried on a teflon dish at 110^{o}C in a vacuum oven for 48 hours. The solid product (now liquid) was cooled to room temperature then crushed with a mortar and pestle to give a fine white powder. The yield for this reaction was approximately 80% and the capillary melting range was 90-92^{o}C. ^{31}P NMR showed a singlet at 29.40 ppm (Figure 2.6-3). ^{1}H NMR and ^{13}C NMR are shown on Figure 2.6-4 and Figure 2.6-5, respectively. Elemental analysis of the monomer gave the following results (the theoretical values are are shown in the parenthesis): C~% 72.63(73.16); H~% 5.14(5.12); N~% 5.65(5.69); P~% 6.05(6.29). The mass spectrum of m-BAPPO was consistent with its structure, particularly the molecular ion at m/e = 492, corresponding to the molecular weight of m-BAPPO and the molecular ion cluster clearly reminiscent of a phosphine oxide containing compound (Figure 2.6-6). The equivalent weight of this monomer was assessed by potentiometric titration with HBr. Its actual molecular weight is 492, and compared with 493 obtained by titration, it can be inferred that the purity of this diamine was higher than 99%.

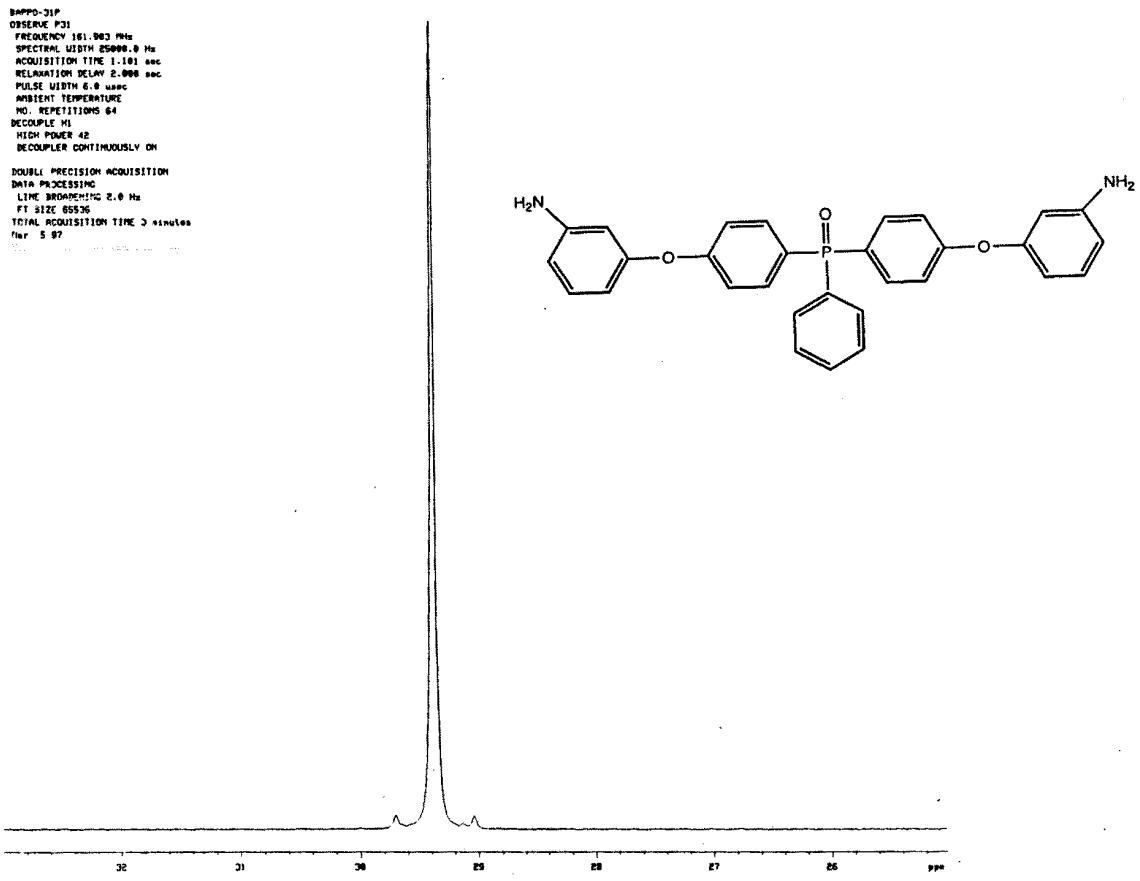

Figure 2.6-3 **^{31}P NMR spectrum of BAPPO**

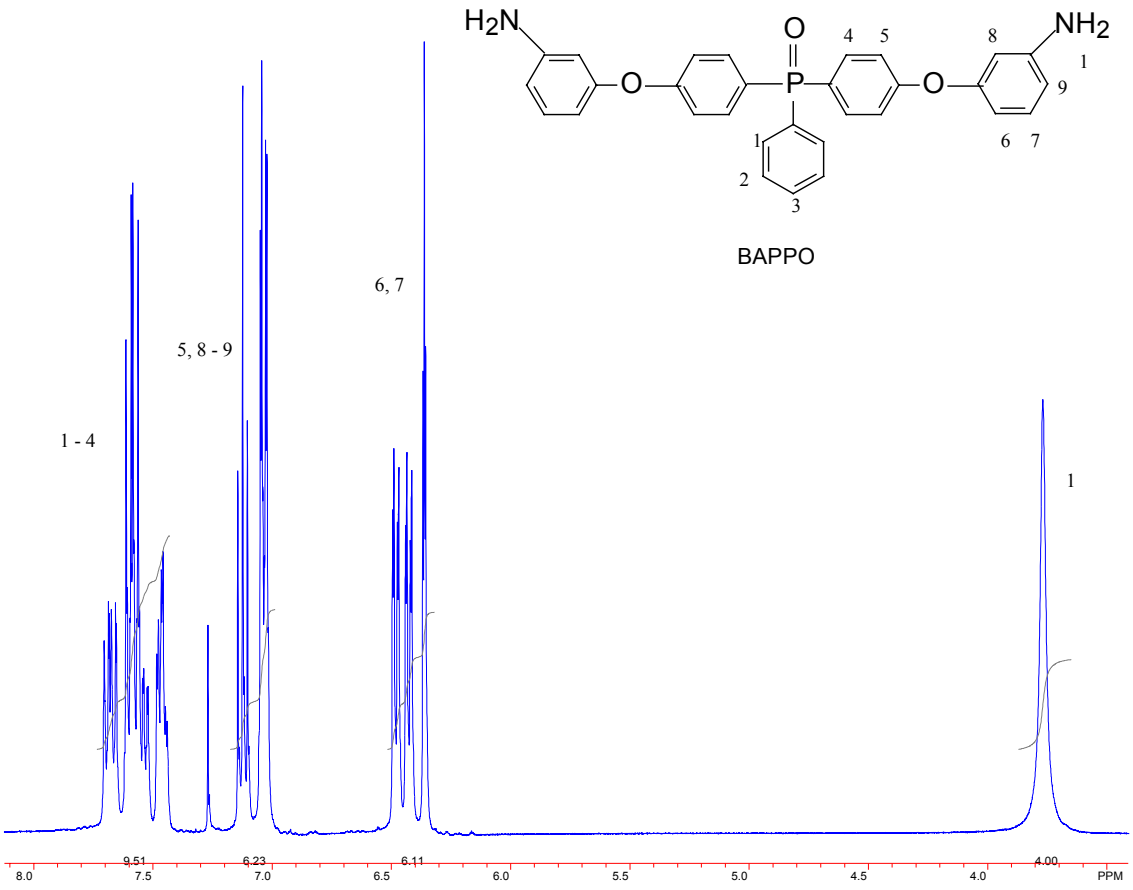

Figure 2.6-4 **^{1}H NMR spectrum of BAPPO**

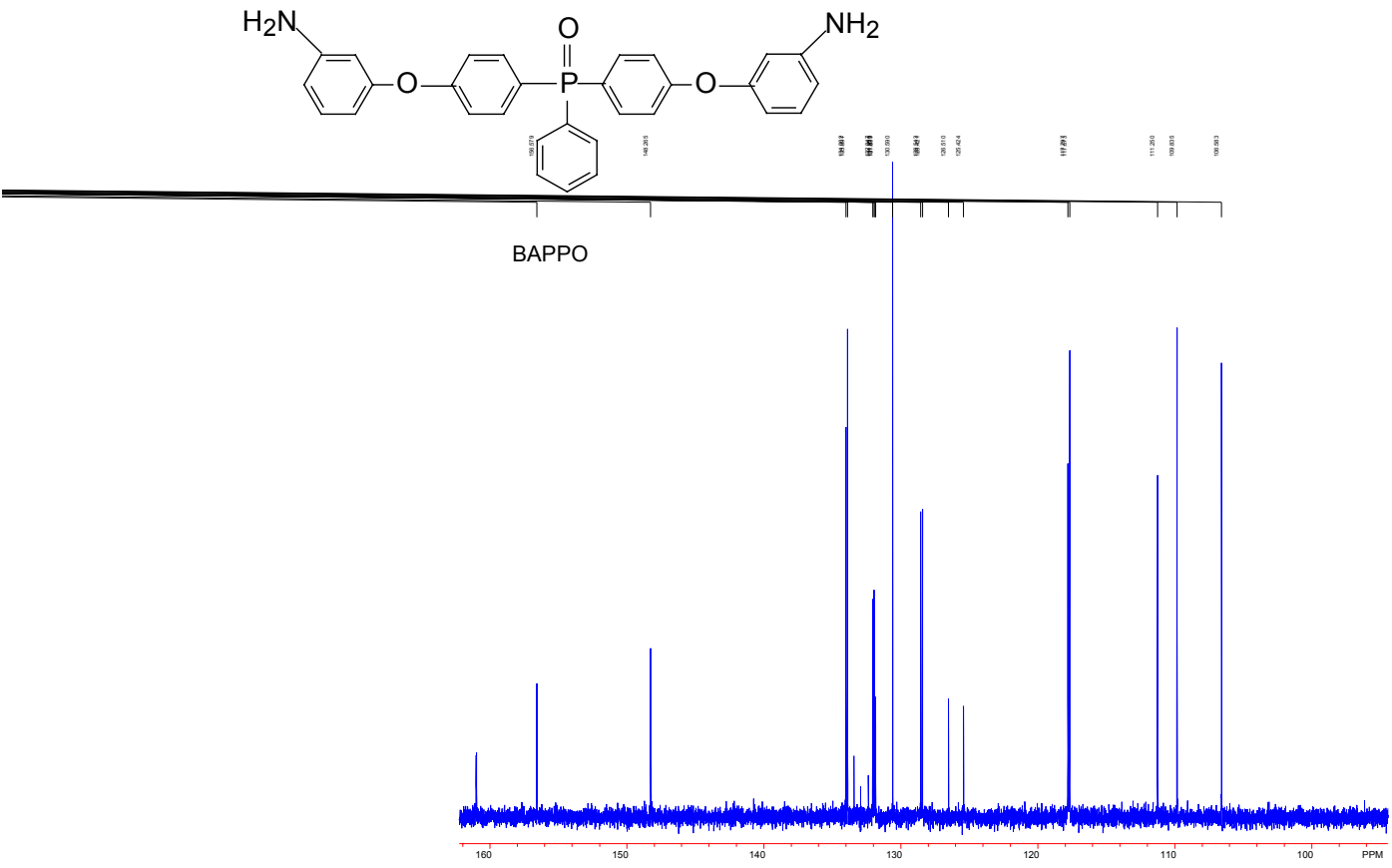

Figure 2.6-5 **^{13}C NMR spectrum of BAPPO**

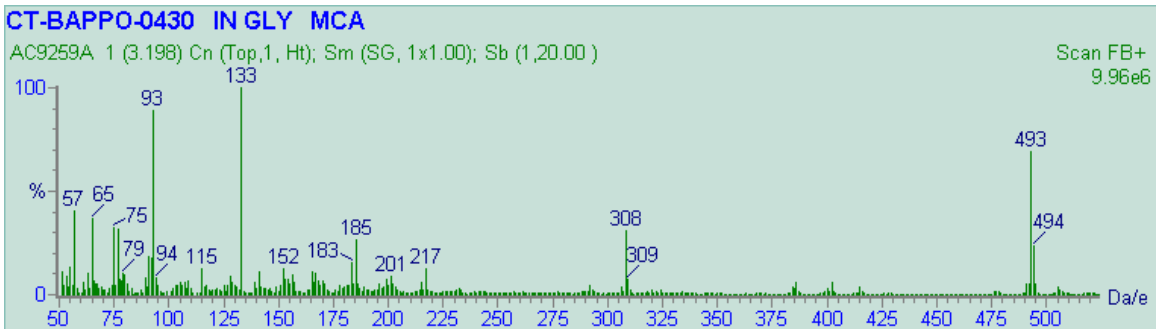

Figure 2.6-6 **Mass spectrum of BAPPO.**

2.7 Synthesis of the Tetraglycidyl Ether of Bis(3-aminophenyl) Methyl Phosphine Oxide (TGDAMPO)

2.7.1 Background

Epoxy resins are widely used as matrices for graphite fiber-reinforced composites. Higher functionality epoxies generate materials with high crosslinking density and high glass transitions, which are used in aerospace, machine and electronic applications. The cured materials have good mechanical and insulating properties, which are maintained briefly above 200^{o}C, and excellent resistance to many aggressive solvents. Epoxy resins of functionality higher than 2 would include the epoxy Novolacs, and the widely used tetraglycidyl ether of methylene dianiline (TGDDM). Even though several other high functionality epoxy resins have been reported, very few of them are commercially available. Our objective therefore was to synthesize a novel phosphine oxide containing epoxy resin of high functionality and evaluate the cured material for fire resistance. The properties of the novel networks were to be compared with those of the TGDDM.

2.7.2 Experiments

A well documented procedure for the epoxy derivatization of diamines was followed[21, 22, 23]. In a 1000 ml round bottom three-necked flask fitted with a mechanical stirrer, an addition funnel and a reflux condenser, DAMPO (20g, 0.08 mole) was dissolved in methanol (3.72g, 0.96 mol) and epichlorohydrin (125g, 1.35 moles). Water (4g, 0.22 mole) was added to the flask and the mixture was stirred at 80^{o}C for 4 hours. The mixture was then cooled to 60^{o}C and NaOH (260g, 6.5 moles) dissolved in water (260g, 14.4 moles) was added dropwise to the flask and the reaction was maintained at 60^{o}C for two additional hours. The greenish mixture was cooled to room temperature,

and extracted with 300ml of chloroform. The organic layer was washed several times with water and the chloroform solvent together with the excess epichlorohydrin reagent were stripped by rotary evaporation that lasted three hours at 80^{o}C. A brown and viscous resin was thereby obtained. The GC-mass spectrum of the novel resin (Figure 2.7-2) was consistent with its assigned structure, especially showing that the major product had a molecular ion cluster at m/e = 470 which corresponds to the molecular weight of the resin. The cluster pattern was reminiscent of those of other phosphine oxide containing molecules synthesized in our group. However a few side products with functionalities lower than 4 appeared to be present in the resin (Figure 2.7-3) and their structure determination relied on a previously published work[23]. Infrared spectroscopy (Figure 2.7-4) confirmed the presence of those lower functionality resins by clearly showing the presence of amine and hydroxy functionalities, which would not normally be present in the resin. The amine functionalities arise from unreacted amines in the starting material while the hydroxy groups come from incomplete ring closure of the epoxides, or from abnormal Friedel-Crafts ring closure of the halohydrin on a phenyl ring.

The relative abundance of the resins of lower functionalities was determined by titration (see section 2.2), ^{31}P and ^{1}H NMR spectroscopy (Figure 2.7-5 and Figure 2.7-6, respectively). The relative epoxy functionality of the novel resin was 3.4 (EEW = 99.8, for a theoretical value of 117.63) which is somewhat lower than that of the commercial resin (MY-721) of the same nature (3.6) but higher than those published by some other workers[19]. The lower epoxy equivalent weight than the theoretical value of 117.63 suggested that the product was a mixture of tri (or lower) functional and tetrafunctional resins with a ratio of 60/40. This result was confirmed by proton NMR since the ratio epoxy protons/aromatic protons was only 2 instead of the expected ratio of 2.5. this suggests that only 80% of the stoichiometric amount of epichlorohydrin reacted. Even though ^{13}C NMR (Figure 2.7-1) displayed the carbons that were expected, several of them were double peaks, which confirmed the presence of side products mentioned earlier in this section.

Scheme 2.7-1 Idealized synthesis of the Tetraglycidyl Ether of m-DAMPO

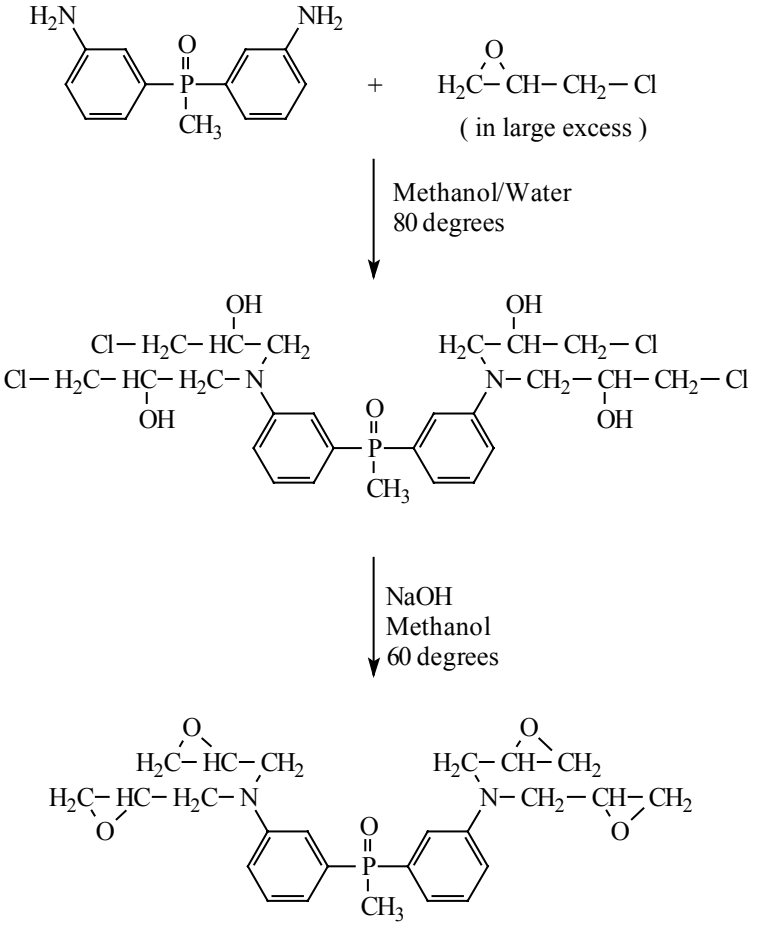

(TGDAMPO)

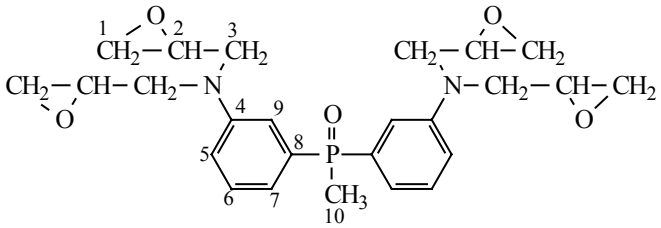

C_1 ~ 44.3 ppm (double peaks)

C_2 ~ 50.2 ppm (double peaks)

C_3 ~ 53.0 ppm

C_4 ~ 148.0 ppm

C_5 ~ 118.9 ppm (double peaks)

C_6 ~ 115.4 ppm (double peaks)

C_7 ~ 129.7 ppm

C_8 ~ 148.1 ppm

C_9 ~ 135 ppm

C_{10} ~ 76.8 ppm

Figure 2.7-1 ^{13}C NMR data of TGDAMPO

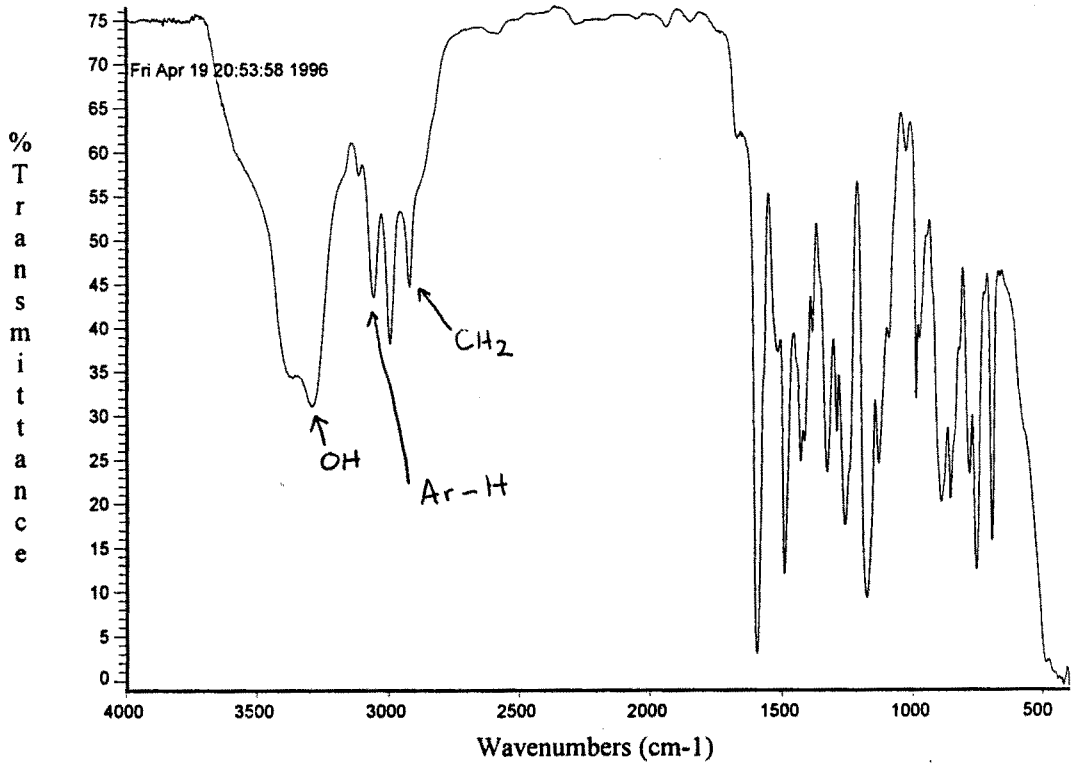

Figure 2.7-2 GC-Mass spectrum of the tetraglycidyl ether of DAMPO (TGDAMPO)

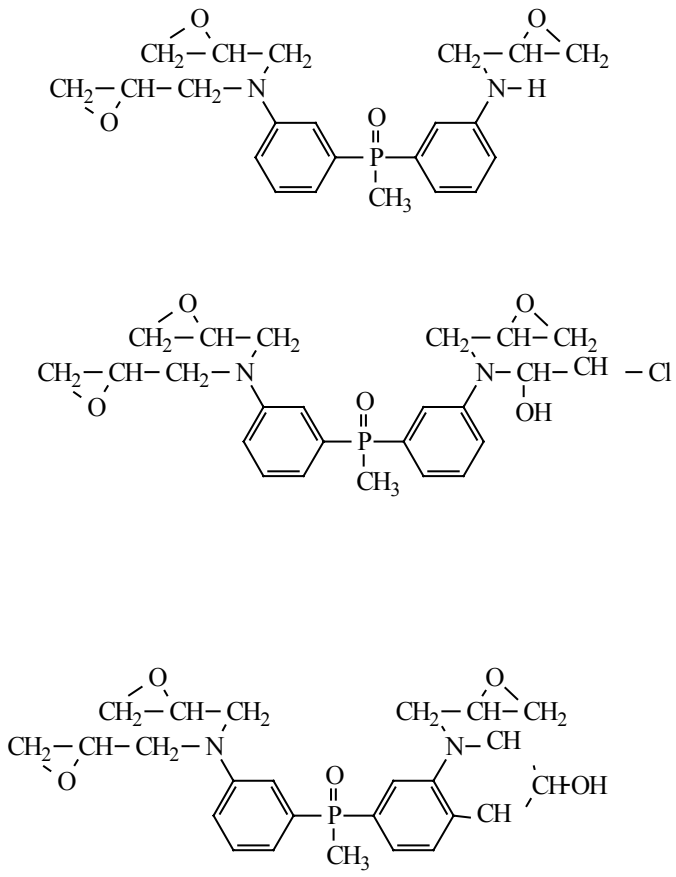

Figure 2.7-3 Side products identified during the synthesis of TGDAMPO

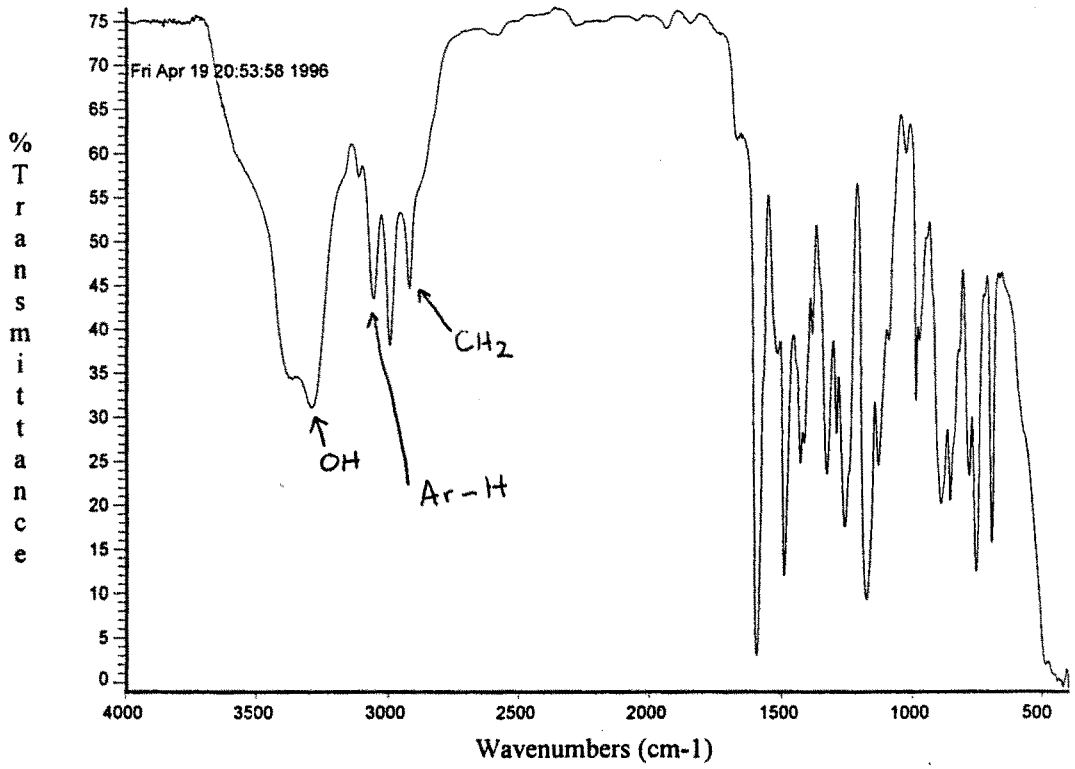

Figure 2.7-4 Infrared spectrum of the novel phosphine oxide containing resin (TGDAMPO)

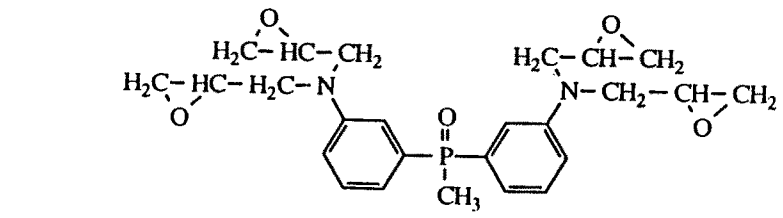

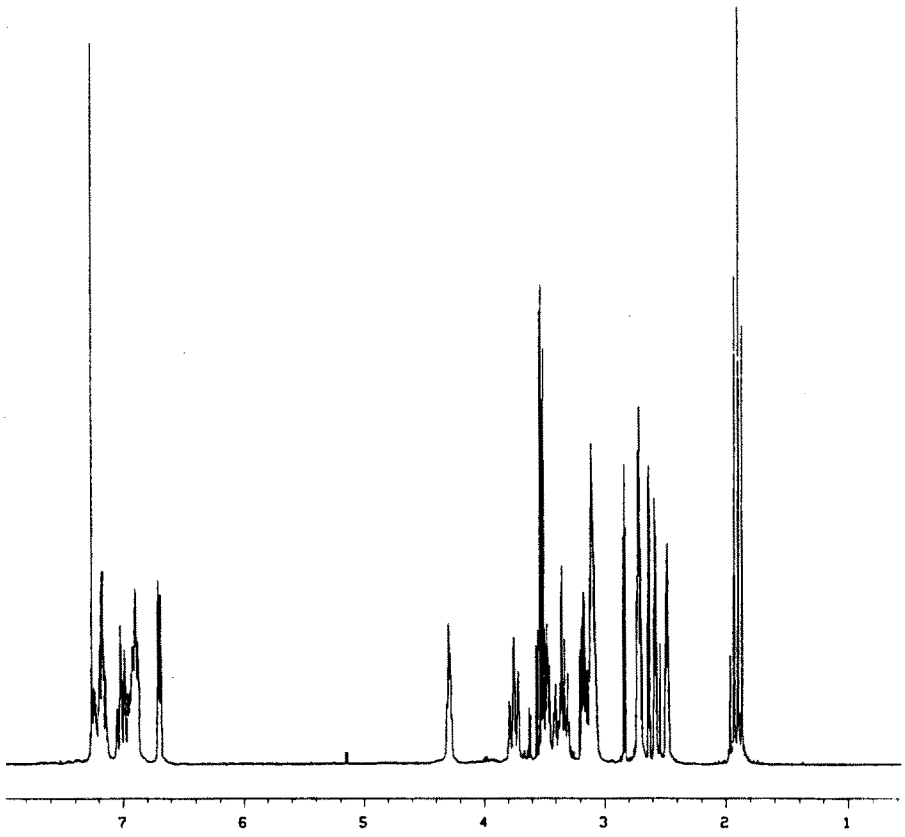

Figure 2.7-5 ^{1}H NMR of the tetraglycidyl ether of DAMPO (TGDAMPO)

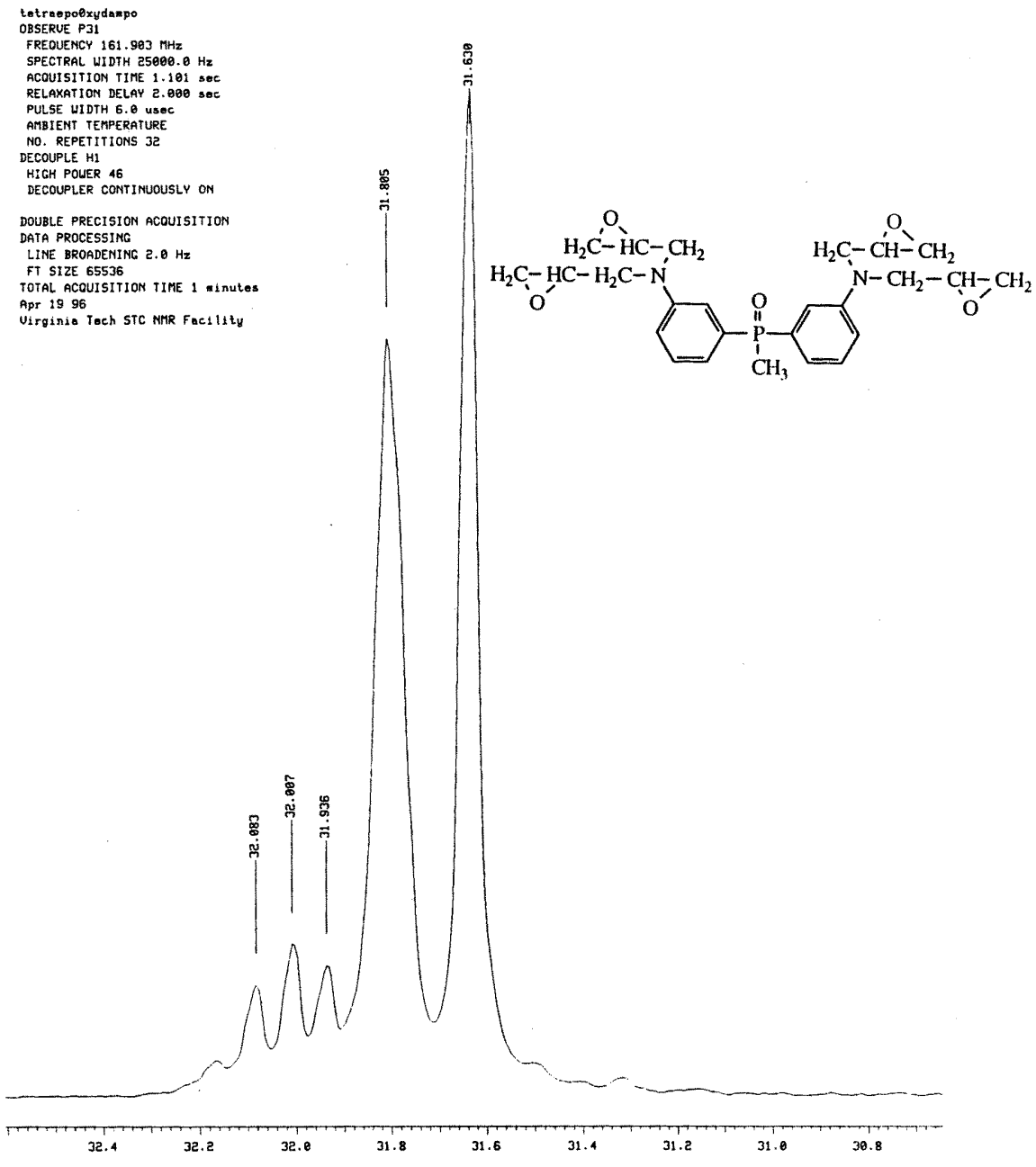

Figure 2.7-6 ^{31}P NMR spectrum of TGDAMPO

2.8 Synthesis of Bis(4-hydroxyphenyl) Phenyl Phosphine Oxide (BHPPO)

This synthesis used a variation of a procedure previously used in our laboratory.[24, 22]

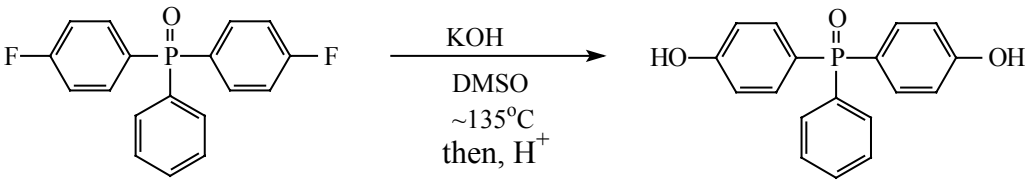

BFPPO BHPPO

To a four necked two liter round bottom flask equipped with a mechanical stirrer, a reflux condenser, a nitrogen inlet and a thermometer, bis(4-fluorophenyl) phenyl phosphine oxide (200g, 0.636 mole) and dimethyl sulfoxide (1000ml) were added. The mixture was stirred until a homogeneous solution was obtained after about 20 minutes at room temperature. Potassium hydroxide KOH (240g, 3.816 moles x 1.12-to account for the purity of the reagent) was dissolved in 260 ml of water to produce an approximately 15 N solution. The KOH solution was added to the mixture in the flask. The reaction temperature was maintained at 130°C with an oil bath for 24 hours, or until the reaction was completed as evidenced by thin layer chromatography using a mixture of methanol and chloroform (30:70, v/v). The reaction product was precipitated (drop wise) in a 1/3 (v/v) concentrated HCl/water solution. Large amounts of water were needed for the precipitation, which helped to reduce the amount of the residual DMSO in the product. The precipitate was filtered and washed several times with water affording a 90% yield. It was then dissolved in methanol, filtered to remove any glass particles (potassium hydroxide chews glassware) from the reaction of the glassware with the hot potassium hydroxide. The filtrate was concentrated and subsequently recrystallized in the same solvent. The recrystallized product had a capillary melting point of 242°C (literature

value 233-234°C)[25] and its structure was confirmed by ^{1}H and ^{31}P NMR spectroscopy (Figure 2.8-1 and 2.8-2). The mass spectrum of this compound is given in Figure 2.8-3

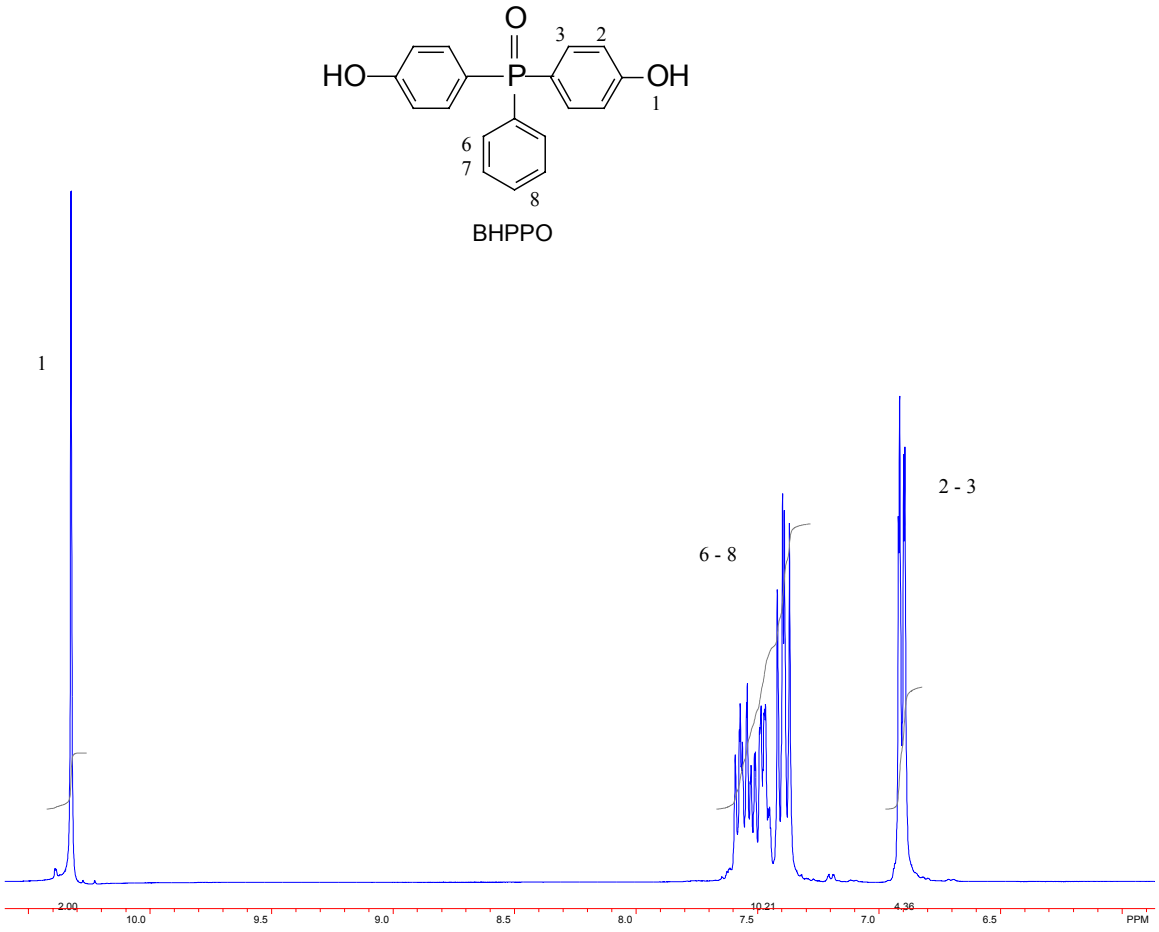

Figure 2.8-1 1H NMR of Bis(4-hydroxyphenyl) phenyl phosphine oxide (BHPPO)

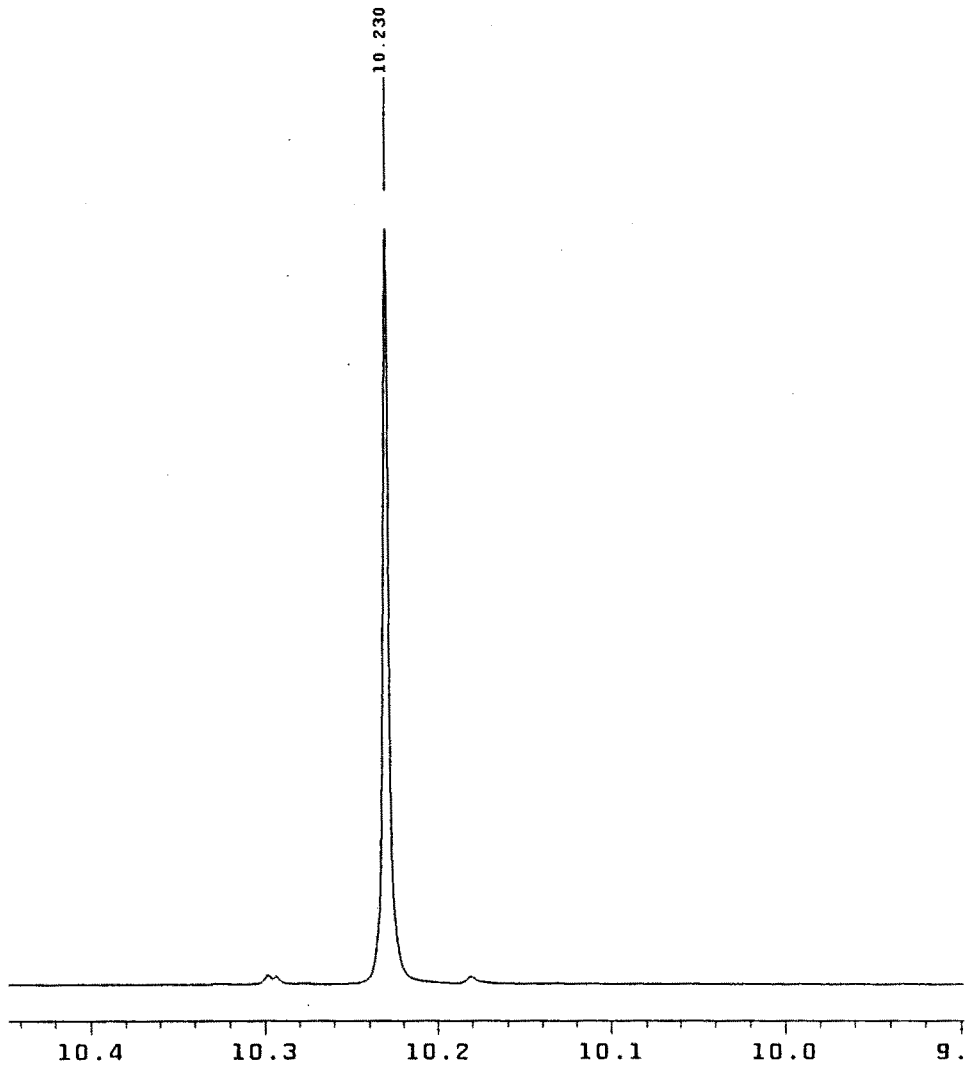

Figure 2.8-2 ^{31}P NMR spectrum of bis(4-hydroxyphenyl) phenyl phosphine oxide.

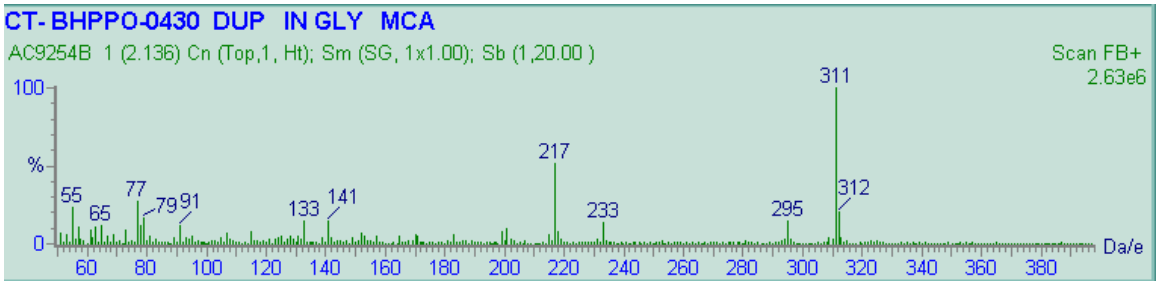

Figure 2.8-3 Mass Spectrum of bis(4-hydroxyphenyl) phenyl phosphine oxide

2.9 Synthesis of Bis 4-(2-hydroxyethyl 1-oxy)phenyl Phenyl Phosphine Oxide (Ethoxylated BHPPO).

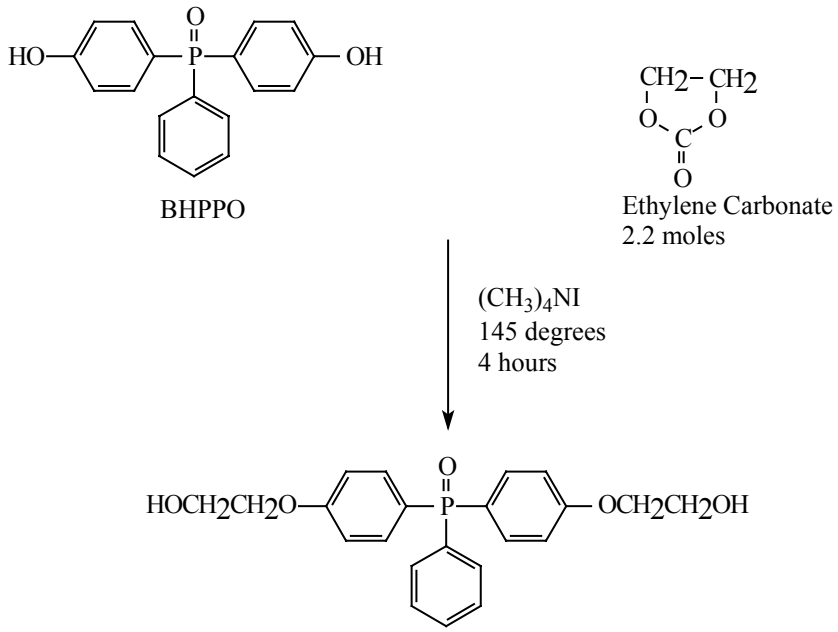

Scheme 2.9-1 Synthesis of ethoxylated BHPPO

Bis(4-hydroxyphenyl) phenyl phosphine oxide (60g, 0.19 mole) was added to a 500ml, three-necked round bottom flask fitted with an overhead stirrer, a reflux condenser and a nitrogen inlet. Ethylene carbonate (37g, 0.42 mole) and tetramethylammonium iodide catalyst (10.8g, 0.042 mole) were added to the flask and the mixture was stirred. The flask was immersed in an oil bath and the reaction temperature was maintained at 120^{o}C for 12 hours, or until no more carbon dioxide evolved. The reaction mixture was subsequently diluted with water and extracted with chloroform. The chloroform layer was washed three times with 5% sodium bicarbonate solutions. This organic layer was concentrated and precipitated dropwise into diethyl ether. This operation was necessary for the removal of the residual ethylene carbonate reagent. The product was again dissolved in chloroform, then washed several times with water and dried over anhydrous

magnesium sulfate. The chloroform was stripped by rotary evaporation to yield a viscous material, which eventually solidified. Attempts to recrystallyze this material failed. However its excellent purity was demonstrated by infrared and ^{1}H NMR spectroscopy (Figure 2.9-1 and Figure 2.9-2). Figure 2.9-3 Shows the ^{13}C NMR spectrum of this compound.

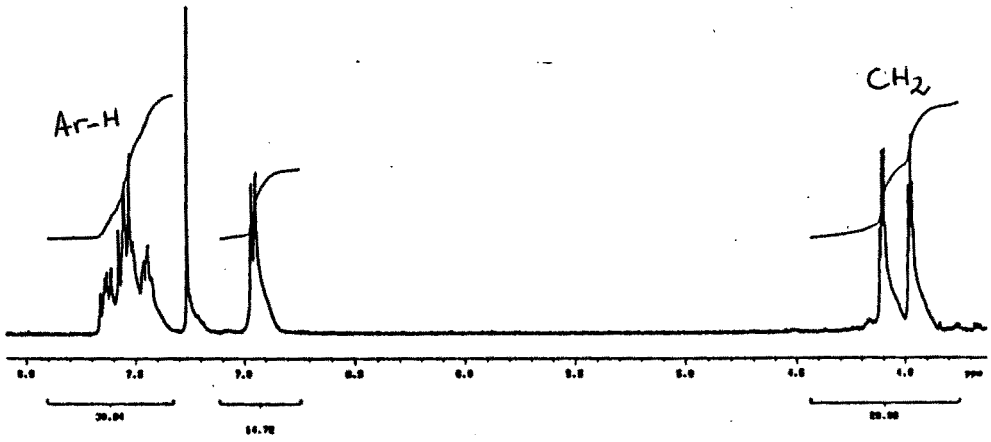

Figure 2.9-1 ^{1}H NMR spectrum of ethoxylated BHPPO (EBHPPO)

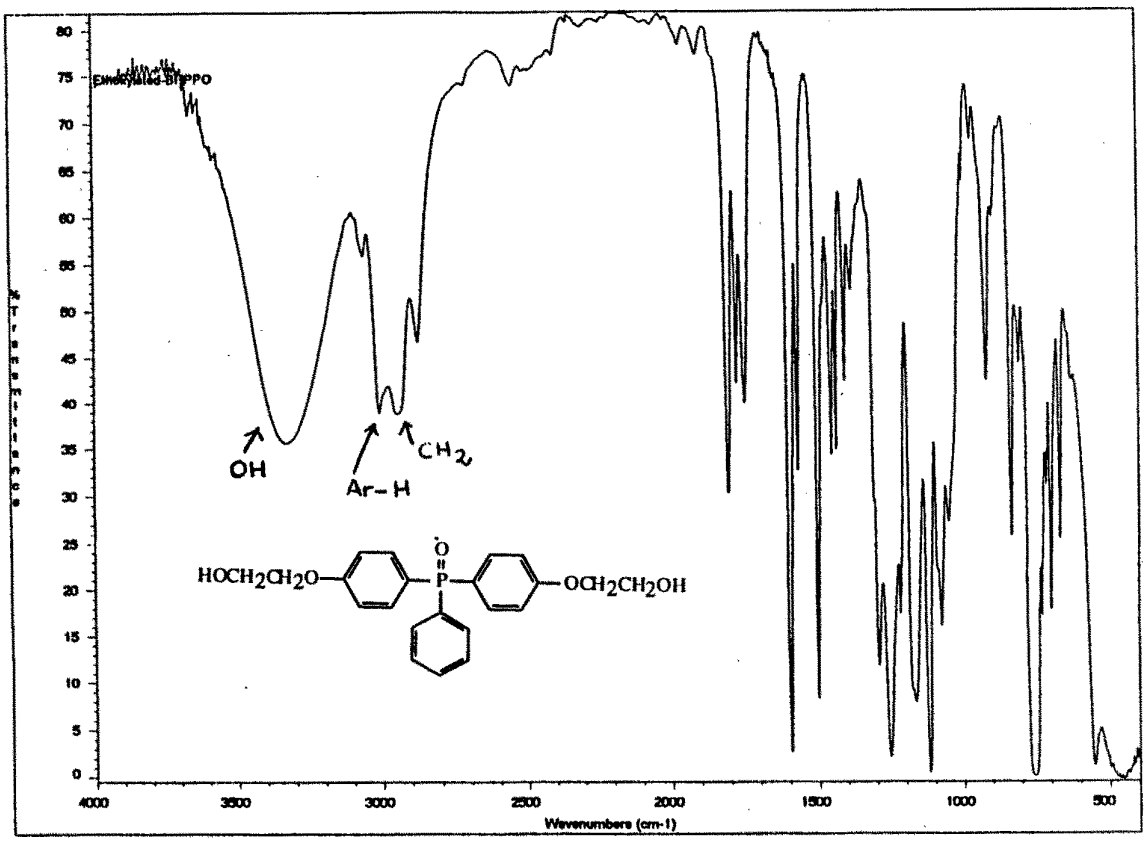

Figure 2.9-2 ^{31}P Infrared spectrum of ethoxylated BHPPO (EBHPPO)

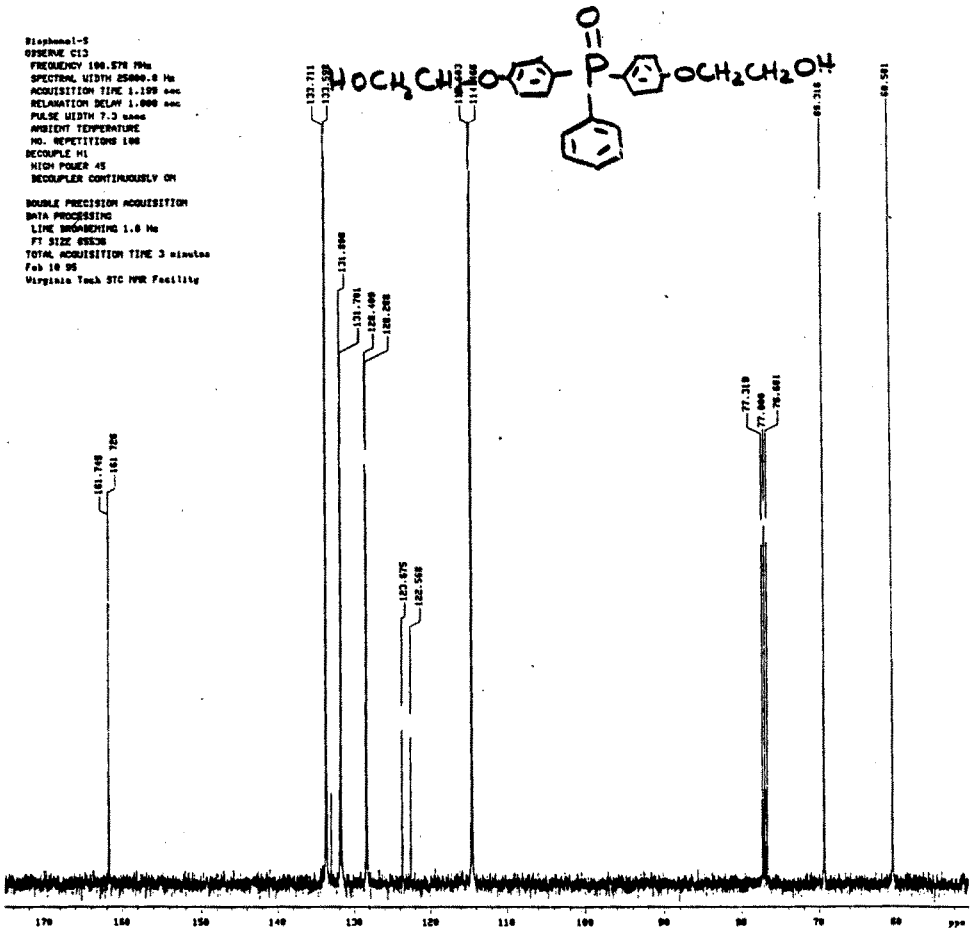

Figure 2.9-3 13C NMR spectrum of ethoxylated BHPPO (EBHPPO)

2.10 Bis(4-Phenoxyphenyl) Phenyl Phoshine Oxide (BPPPO)

2.10.1 Molecular Modeling

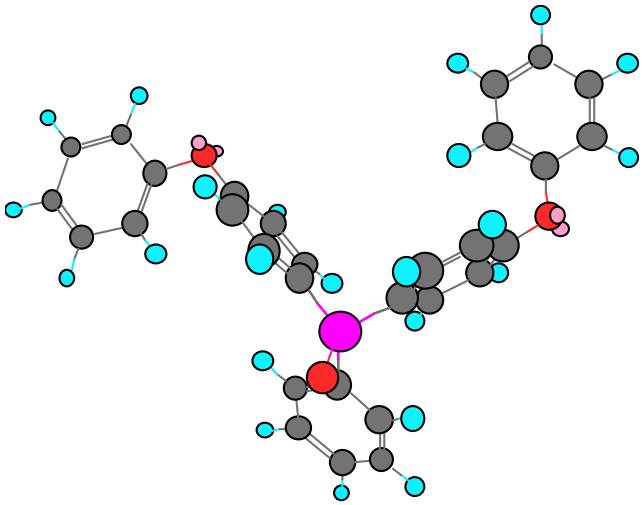

Molecular modeling data suggest that this molecule is not planar. This activated monomer, which is suitable for electrophilic substitution reactions was to be used to disrupt the stiffness in poly(ether ketones), thus allowing their synthesis and their processeability.

2.10.2 Synthetic Scheme

This monomer was to be used for electrophilic aromatic substitution (Friedel Crafts type) polymerzation. Its synthesis proceeded in a manner analogous to that of BAMPO previously described in this chapter, except that the nucleophile in this reaction was phenol rather than the *m*-aminophenol used in the former. Also, the product in this

sequence did not need to be recrystallized after its synthesis, because no impurties could be detected nor did it seem as if it could ever form crystals.

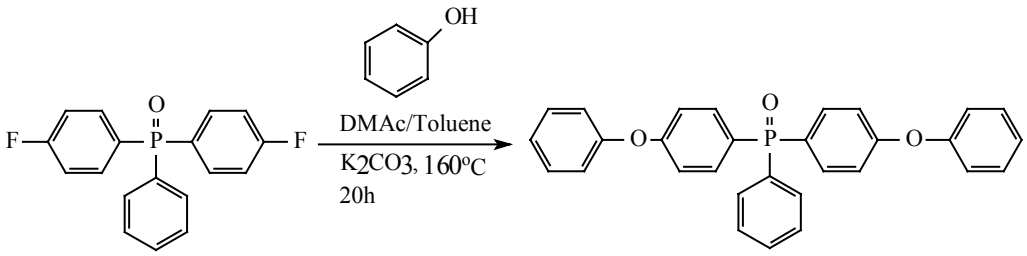

To a flame dried 2 liter four necked round bottom flask, fitted with an overhead stirrer, a reflux condenser, a Dean Stark trap and a nitrogen inlet was added at room temperature phenol (66.26g, 0.70 mole), BFPPO (100g, 0.32 mole), potassium carbonate (97g, 0.70 mole), DMAc (600ml) and 300ml of toluene. The flask was heated with an oil bath whose temperature was adjusted to 170^{o}C. The contents of the flask turned purple upon heating and remained that way throughout the reaction. As soon as the mixture started to reflux, some toluene was removed from the reaction flask by opening the valve of the Dean Stark trap. This operation allowed the temperature to rise to 150^{o}C. The reaction was allowed to proceed for 16 hours, after which all the remaining toluene was removed through the Dean Stark trap. Toluene removal in this step is very important, because without this, the precipitation step would be very tedious and only a viscous precipitate would be obtained. The solution was further concentrated until little solvent appeared to rise from the reaction, filtered through a Buchner funnel and precipitated dropwise into water in a blender. The semi-viscous precipitate was then dissolved in chloroform, and washed several times (a hundred times maybe) with a saturated sodium chloride solution until the purple color of the reaction mixture disappeared. The chloroform solution was stripped from the product by rotary evaporation. The product was dissolved in a minimum amount of ethanol, treated with activated charcoal and allowed to reflux for

one hour. It was then filtered through celite to remove the charcoal, precipitated in water, and dissolved again in chloroform. Chloroform allowed for rapid collection of the product and removal of water. The chloroform was stripped by rotary evaporation. The product was dissolved in a minmum amount of ethanol, then precipitated in water. This seemingly meaningless operation negotiated the total removal of DMAc, which would otherwise stay permanently in the product. It was then dissolved in chloroform, dried over magnesium sulfate and the chloroform was stripped by rotary evaporation. The product was dried in a vaccum oven to afford a very pure solid material which melted at 50-52^{o}C.

The yield was quantitative. ^{31}P NMR showed a beautiful singlet at 29 ppm, denoting the absence of any other phosphorylated material in the product (Figure 2.10-1). Proton NMR was consistent with the assigned structure of the monomer (Figure 2.10-2). Mass spectrometry data showed a molecular ion at m/e = 462, which is indeed the molecular weight of the assigned structure. The molecular ion cluster is reminscent of that of molecules containing a phosphorus atom (Figure 2.10-3).

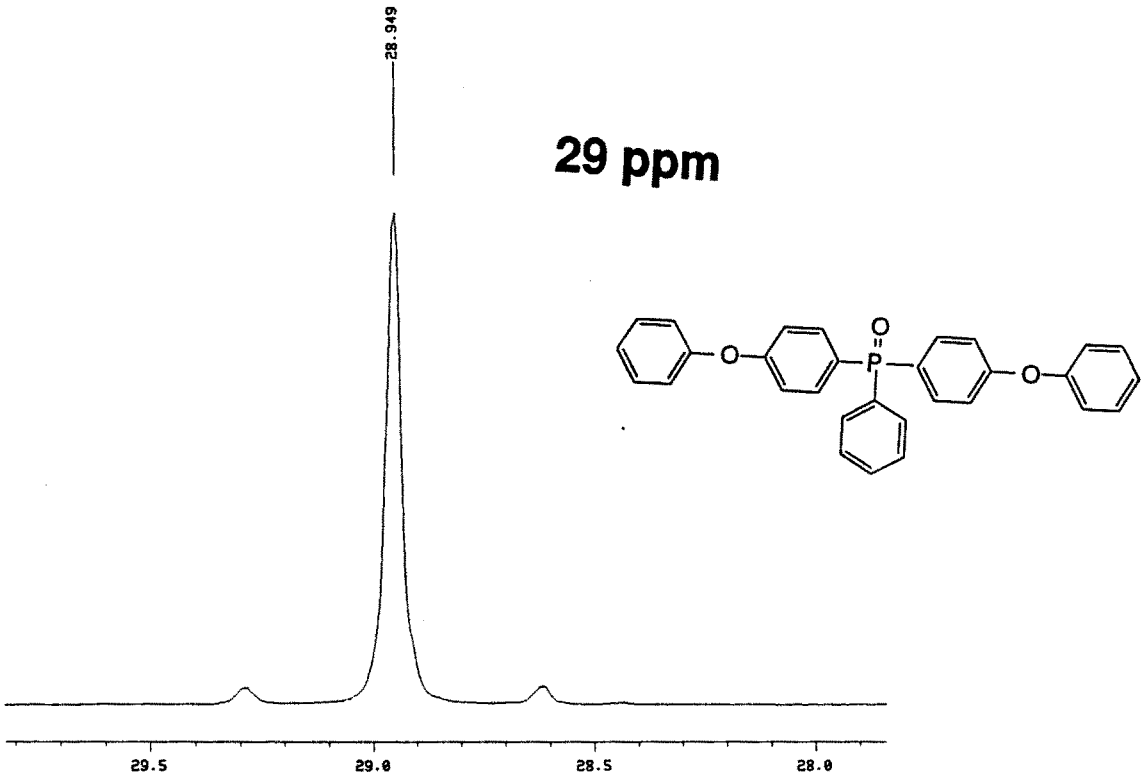

Figure 2.10-1 ^{31}P NMR spectrum of bis(4-phenoxyphenyl) phenyl phosphine oxide

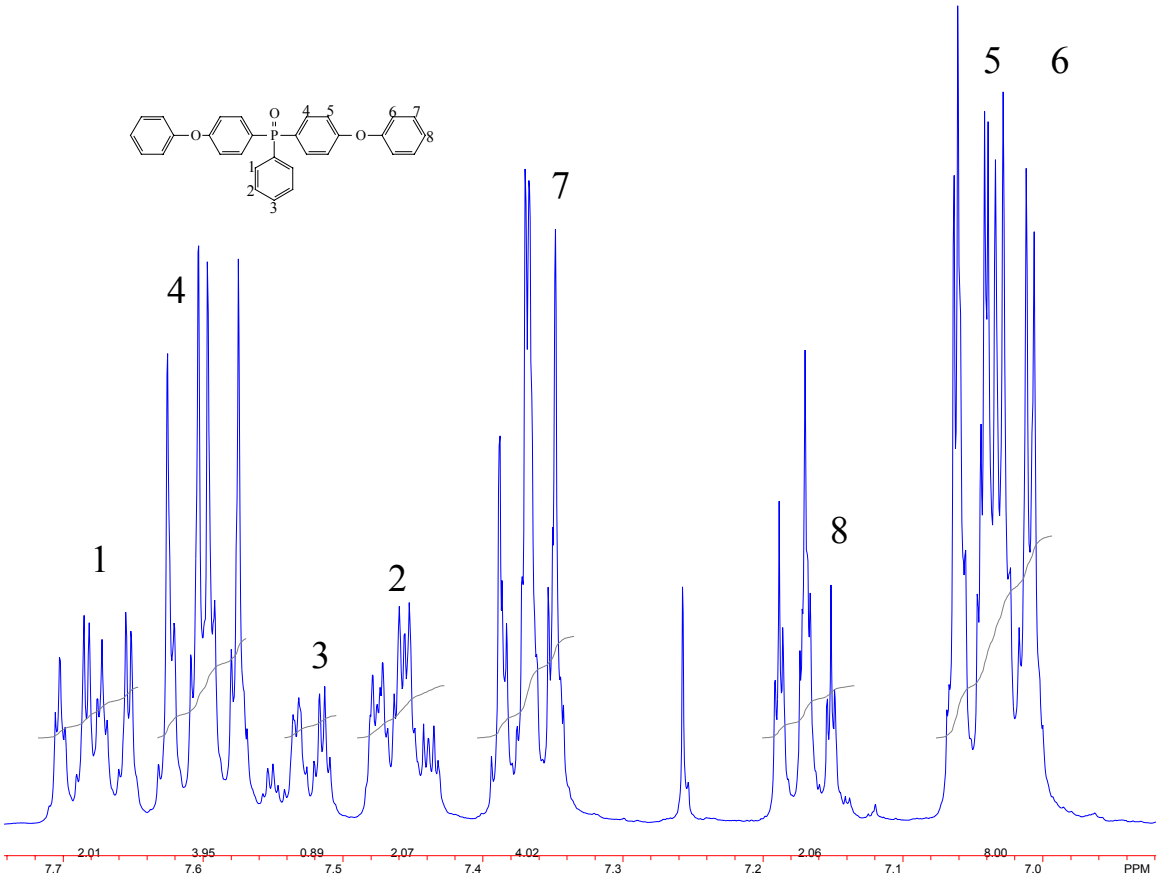

Figure 2.10-2 ^{1}H NMR spectrum of bis(4-phenoxyphenyl) phenyl phosphine oxide

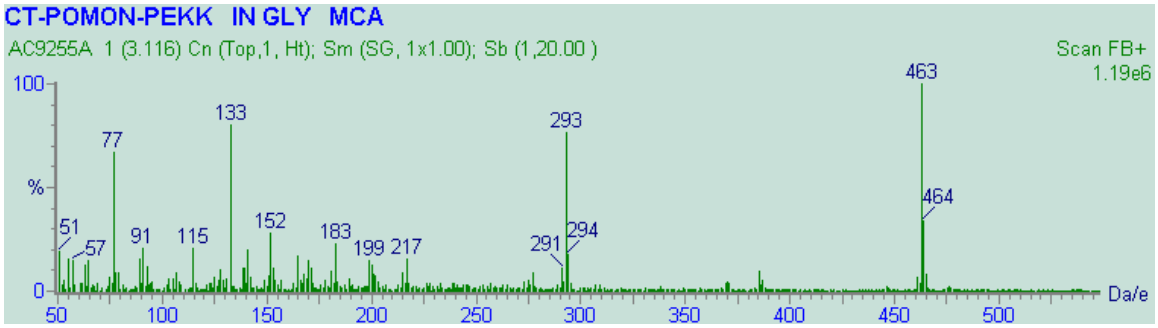

Figure 2.10-3 Mass spectrum of bis(4-phenoxyphenyl) phenyl phosphine oxide.

2.11 Discusion

It is very interesting to note that the purity of most of the monomers synthesized in this work was far higher than that in previous attempts. For example, DAMPO had a melting point of 156°C in this work,[18] which was more than 10 degrees higher than those in some earlier publications; (145-147°C),[9] (148°C).[26] For DAMPO, this can be partly ascribed to the rigorous recrystallization of the dinitro intermediate, which seemed to be an important factor in the purity of the final product. This was not emphasized in other published research. Also, this diamine seems to be very susceptible to oxidation, especially when left in solution for an extended period. Hydrazine, which is a particularly versatile agent for the reduction of nitri compounds was used in this work. This permitted a shorter duration of the reaction (3 hours) compared to 24 hours in other research.

The purification of the dinitro intermediate in the case of DAPPO was somewhat original. The two side products, mononitro and trinitro have different solubilities in the recrystallisation solvents as indicated earlier in this chapter. A change in the solvent composition at every stage of the recrystallization allowed for the relative ease in the purification of this intermediate.

The synthesis of BHPPO from the difluoro intermediate BFPPO, proceeds by the substitution of the fluorine by the hydroxide ion. There is an important side reaction that plagues the synthesis of this intermediate, that is the dimerization arising from the attack of the phenoxide ion (Scheme 2.11-1) as shown by NMR spectroscopy early in our research. The dimer impurity resulting from that reaction has been impossible to eliminate by recrystallization. We therefore chose a mild temperature, 135°C, at which the phenoxide ion, which is a weaker base than the hydroxide ion would not be likely to displace the fluorine. At temperatures above 145°C, this side product would likely occur. Once again the purity of our product (m.p.242°C) proved to be far higher that reported in the literature (233-234°C).[25]

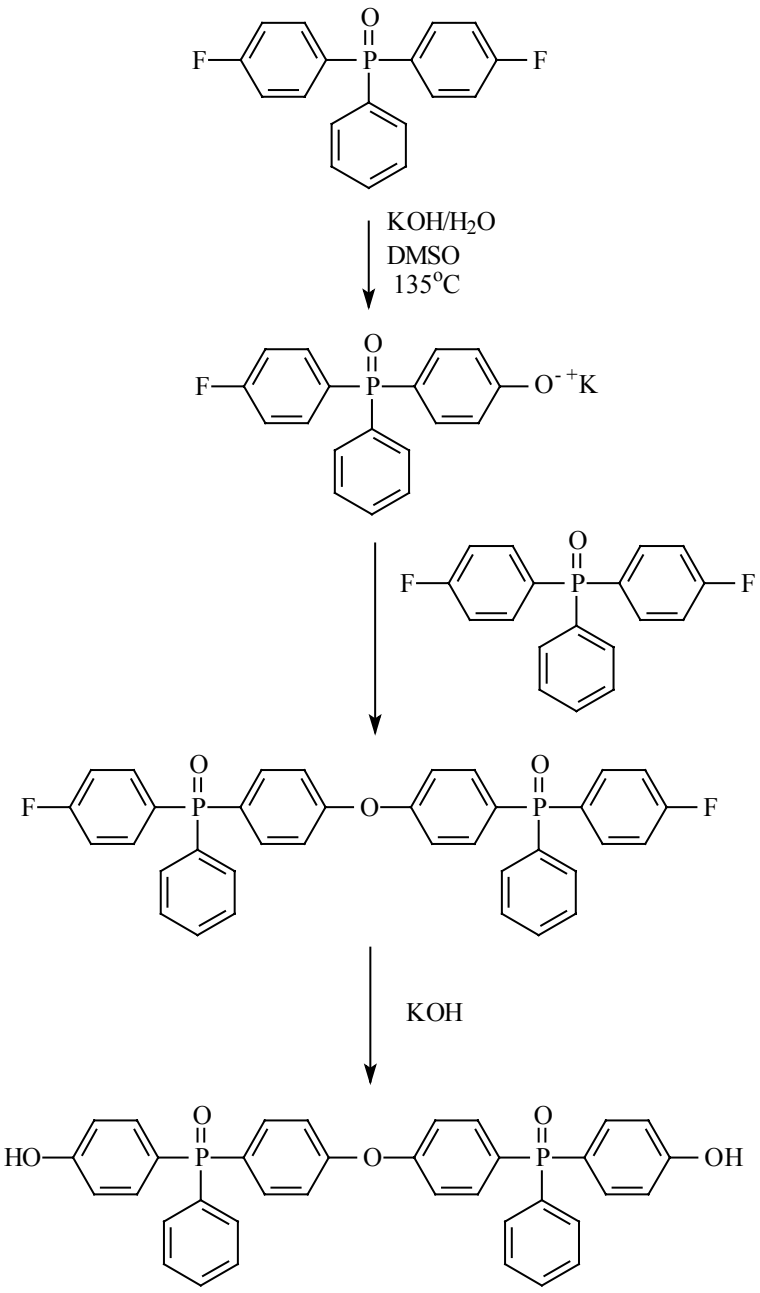

Scheme 2.11-1 Potential side products in the synthesis of p,p'(phenylphosphinylydene)bisphenol

In the syntheses of BAMPO, BAPPO, and BPPPO, the reactions proceed through a nucleophilic aromatic substitution as shown in scheme 2.11-2. The loss of the aromaticity in the phenyl ring is rate determining. The major side products for this type of reaction are potassium salts, which are easily filtered or eliminated through water wash.

The ethoxylation of the dihydroxy intermediates used a reagent, ethylene carbonate, which allows no phosphorylated residues after the completion of the reaction. the mechanism for this sequence is depicted in scheme 2.11-3.

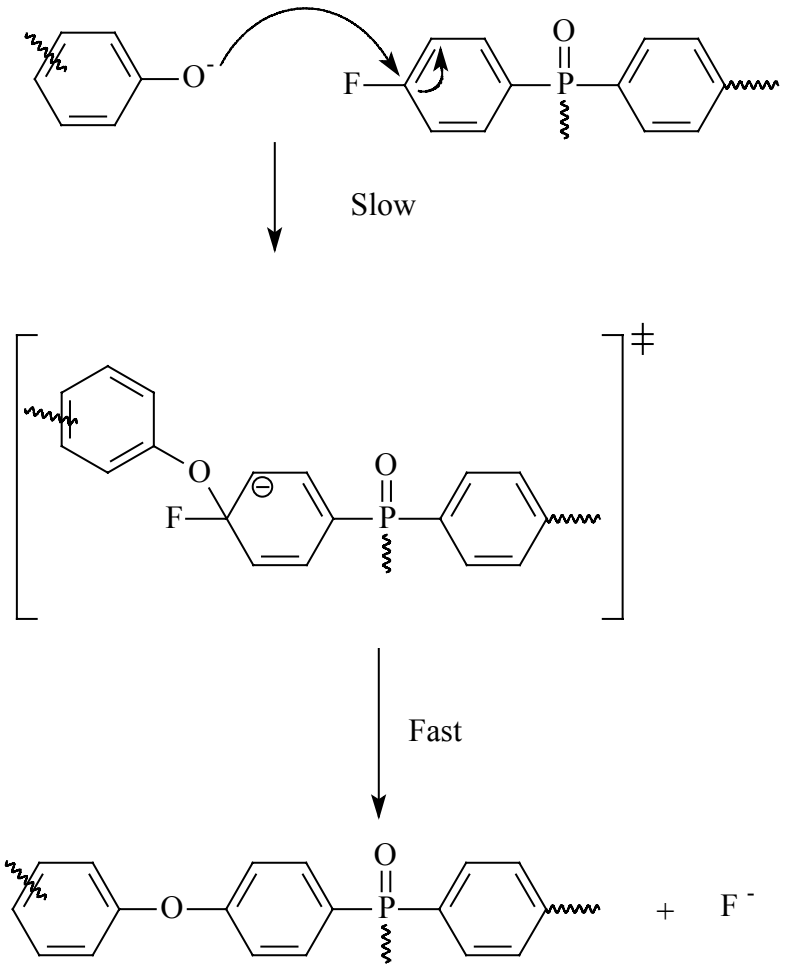

Scheme 2.11-2 Mechanism for phenoxylation on difluoro monomers

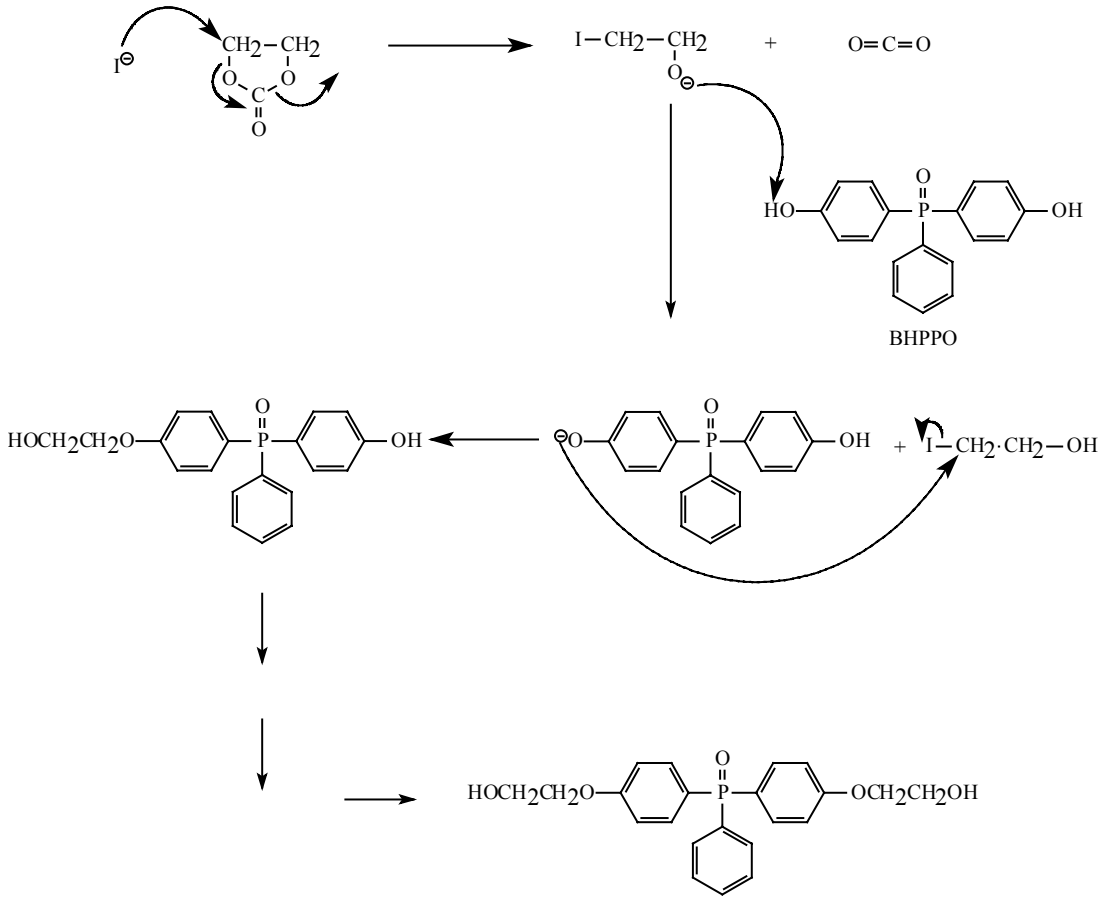

Scheme 2.11-3 Mechanism for the synthesis of ethoxylated BHPPO

2.12 Summary

Several phosphine oxide containing monomers have synthesised using organic reactions ranging from Grignard to Arbusov to nitration to nucleophilic substitution. The structure and the purity of the monomers were confimed by spectroscopic techniques, melting point, and high performance liquid chromatography (and X-ray crystallography for the case of DAMPO). The purity of the monomers as determined by melting points, was overall, higher than that achieved in previous attempts by other workers. The reason underlying this higher purity was the closer investigation of the organic chemistry of phosphorus in relation to the physical properties of the monomers that set we out to synthesize. The monomers will be incorporated in several types of linear polymers as well as epoxy networks.

2.13 References

1. Smith, C. (1991) Ph. D. Thesis, Virginia Polytechic Institute and State University.
2. Grubbs, H. J. (1993) Ph. D. Thesis, Virginia Polytechnic Institute and State University.
3. Gassemi, H (1994) Unpublished data
4. XSCANS v2.1 (1994) Siemens Analytical X-ray Instruments, Madison, WI.

5. Sheldrick, G. M. (1995) SHELXTL v5.03 (PC version). An Integrated System for Solving, Refining, and Displaying Crystal Structures from Diffraction Data; Siemens Analytical X-ray Instruments, Madison.
6. Stewart, J. J. P. (1989) *J. Comp. Chem*., **10**, 221-264.
7. Gallagher, D. (1996) *Scientific Computing & Automation,* June.
8. Cooper, C. F. (1995) *J. of Coating Technology*, August.
9. Korshak, V. V., T. M. Frunge, V.V. Kurasshev, T. Y. Medved, Y.M. Polykrpov, C. M. Hu and M. I. Kabachnik (1962) *Konf.po. Vysokomolekul. Soedin*, 63-6.
10. Asknes, G. and D. Asknes (1964) *Acta Chem. Scand*., **18**, 38.
11. Varma, I. K., G. M. Fohlen and J. A. Parker (1983) *J. Polym. Sci., Polym. Chem. Ed*. A., **21**, 2017.
12. Varma, I. K. (1989) *J. Macromol. Sci. A*., **26**, 937.
13. Gravalos, K. G. (1992) *J. Polym. Sci., Part A: Polym. Chem*., **30**, 2521.
14. Chin, W. K., M. D. Shau and W. C. Tsai (1995) *J. Polym. Sci., Part A: Polym. Chem*., **33**, 373.
15. Franciotti, M., A. Man and M. Taddei (1991) *Tetrahedron Lett*. 32, **46**, 6783.
16. Zanger, M., C. A. Van der Werf and W. E. McEwen (1959) *J. Amer. Chem. Soc*., **81**, 3806.
17. Hoffmann, H. (1960) *Annalen*, **634**, 1.
18. Tan, B., C. N. Tchatchoua, L. Dong and J. E. McGrath (1998) *Polym. Adv. Technol.* **9**. 83-93
19. Ji, Q., M. Muggli, C. Tchatchoua, S. Srinivasan, T. C. Ward and J. E. McGrath (1996) *Polym. Prep.* 37(1), 579.

20. Riley, D. J., A. Gungor, S. A. Srinivasan, M. Sankarapandian, C. Tchaatchoua, M. W. Muggli, T. C. Ward, T. Kashiwagi and J. E. McGrath (1997) *Polym. Eng. and Sci.* Vol 37, **9**, 1501.

21. Liu, W-L, E. M. Pearse and T. K. Kwei (1985) *J. Appl. Polym. Sci.*, **30**, 2907-2920.

22. Boutevin, B., J. J. Robin and C. Roume (1995) *Eur. Polym. J*. **31**, 313.

23. Podzimek, S. I. Dobas, S. Svestka and J. Horalek (1990) *J. Appl. Polym. Sci*., **41**, 1151-1160.

24. Riley D. J. (1997) Ph.D. Thesis Virginia Polytechnic Institute and State university.

25. Senear, A. E., W. Vailient and J. Wirth (1960) *J. Org. Chem.*, **25**, 2001-2005.

26. Societe des Usines Chimiques Rhone-Poulen (1961) Patent, FR 1288952. Chem Abstr., 58, 1963)1493a

2.14 Appendix

Table 2.14-1 Crystal data and structure refinement for DAMPO.

identification code	cs111
chemical formula	$C_{13}H_{15}N_2OP$
formula weight	246.24
color, habit	orange, wedge cut from trapezoidal rod
crystal size, mm	0.3 x 0.3 x 0.3
crystal system	Monoclinic
a, Å	7.2049(5)
b	14.6431(9)
c	11.8302(7)
beta, deg	93.874(5)
volume, Å^3	1245.26(14)
density (calc), g/cm^3	1.313
space group	$P2_1/c$
Z	4
mu, cm^{-1}	2.06
F(000)	520
diffractometer	Siemens P4
data collection software	Siemens XSCANS
radiation	MoK_α (0.71073 Å)
monochomator	graphite
T, K	293(2)
theta range, deg	2.22 to 27.00
scan type	$2\theta/\omega$ scans
standard reflections	5 measured every 95 reflections
index ranges	$0 \le h \le 9$, $-18 \le k \le 18$, $-15 \le l \le 15$
reflections collected	3348
independent reflections	2719 [R(int) = 0.0403]
observed reflections[a]	1928 [I >2σ(I)]
data reduction software	Siemens SHELXTL
absorption correction	Empirical
max. and min. transmission	0.8372 and 0.8187
structure solution	SHELXS-86 (Sheldrick, 1990)
refinement	SHELXL-93 (Sheldrick, 1993)
refinement method	Full-matrix least-squares
quantity minimized	Fsqd
data / restraints / parameters	2719 / 0 / 214
hydrogen atoms	refall
final *R*(F) [I>2σ(I)]	0.0392
final $R_w(F^2)$(all data)[b]	0.1038
goodness-of-fit on F^2	0.916
largest and mean shift/esd	0.002 and 0.000
largest difference peak, e$^-$/Å^3	0.341
largest difference hole	-0.304

[a] The criterions I>2σ(I) for reflections being observed was only used in calculating R(F); all data were used in the refinement.

[b] Least-squares weighting scheme: $w=1/[\sigma^2(F_o^2)+(0.0616P)^2+0.0000P]$ where $P=(F_o^2+2F_c^2)/3$

Table 2.14-2 Atomic coordinates (x 10^4) and equivalent isotropic displacement parameters (Å^2 x 10^3) for DAMPO. U(eq) is defined as one third of the trace of the orthogonalized U_{ij} tensor.

	x	y	z	U(eq)
P(1)	3577(1)	4691(1)	7890(1)	28(1)
O(1)	3001(2)	3986(1)	8714(1)	42(1)
N(3)	1211(3)	7956(1)	6616(2)	46(1)
N(9)	5564(3)	2214(1)	5124(2)	40(1)
C(1)	2101(3)	5686(1)	7918(1)	28(1)
C(2)	2254(3)	6445(1)	7215(2)	30(1)
C(3)	1089(3)	7198(1)	7310(2)	32(1)
C(4)	-179(3)	7191(1)	8159(2)	38(1)
C(5)	-324(3)	6446(1)	8856(2)	37(1)
C(6)	792(3)	5686(1)	8731(2)	33(1)
C(7)	3507(2)	4234(1)	6471(1)	28(1)
C(8)	4611(3)	3463(1)	6316(2)	31(1)
C(9)	4481(3)	2984(1)	5303(2)	31(1)
C(10)	3254(3)	3300(1)	4422(2)	39(1)
C(11)	2212(3)	4070(2)	4560(2)	46(1)
C(12)	2322(3)	4544(2)	5581(2)	41(1)
C(13)	5895(3)	5083(2)	8218(2)	43(1)

Table 2.14-3 Bond lengths [Å] and angles [deg] for DAMPO.

P(1)-O(1)	1.4969(13)
P(1)-C(13)	1.784(2)
P(1)-C(7)	1.805(2)
P(1)-C(1)	1.806(2)
N(3)-C(3)	1.386(2)
N(9)-C(9)	1.396(2)
C(1)-C(6)	1.392(3)
C(1)-C(2)	1.397(2)
C(2)-C(3)	1.395(3)
C(3)-C(4)	1.403(3)
C(4)-C(5)	1.376(3)
C(5)-C(6)	1.386(3)
C(7)-C(12)	1.386(3)
C(7)-C(8)	1.400(3)
C(8)-C(9)	1.386(3)
C(9)-C(10)	1.399(3)
C(10)-C(11)	1.370(3)
C(11)-C(12)	1.390(3)
O(1)-P(1)-C(13)	112.16(11)
O(1)-P(1)-C(7)	111.02(8)
C(13)-P(1)-C(7)	106.79(10)
O(1)-P(1)-C(1)	110.76(8)
C(13)-P(1)-C(1)	106.25(10)
C(7)-P(1)-C(1)	109.67(8)
C(6)-C(1)-C(2)	119.8(2)
C(6)-C(1)-P(1)	116.10(14)
C(2)-C(1)-P(1)	124.11(14)
C(3)-C(2)-C(1)	120.6(2)
N(3)-C(3)-C(2)	121.5(2)
N(3)-C(3)-C(4)	120.0(2)
C(2)-C(3)-C(4)	118.5(2)
C(5)-C(4)-C(3)	120.9(2)
C(4)-C(5)-C(6)	120.3(2)
C(5)-C(6)-C(1)	119.9(2)
C(12)-C(7)-C(8)	119.4(2)
C(12)-C(7)-P(1)	124.21(15)
C(8)-C(7)-P(1)	116.11(13)
C(9)-C(8)-C(7)	121.0(2)
C(8)-C(9)-N(9)	122.3(2)
C(8)-C(9)-C(10)	118.6(2)
N(9)-C(9)-C(10)	119.1(2)
C(11)-C(10)-C(9)	120.5(2)
C(10)-C(11)-C(12)	121.0(2)
C(7)-C(12)-C(11)	119.4(2)

Table 2.14-4 Anisotropic displacement parameters ($Å^2$ x 10^3) for DAMPO.

The anisotropic displacement factor exponent takes the form:
$-2\pi^2 [h^2 a^{*2} U_{11} + ... + 2 h k a^* b^* U_{12}]$

	U_{11}	U_{22}	U_{33}	U_{23}	U_{13}	U_{12}
P(1)	33(1)	24(1)	26(1)	0(1)	1(1)	1(1)
O(1)	58(1)	31(1)	38(1)	8(1)	10(1)	3(1)
N(3)	58(1)	34(1)	48(1)	11(1)	5(1)	10(1)
N(9)	48(1)	34(1)	38(1)	-6(1)	-4(1)	11(1)
C(1)	29(1)	26(1)	27(1)	-2(1)	1(1)	-2(1)
C(2)	30(1)	30(1)	29(1)	-1(1)	5(1)	-1(1)
C(3)	34(1)	28(1)	33(1)	-1(1)	-6(1)	-2(1)
C(4)	34(1)	36(1)	43(1)	-9(1)	-1(1)	7(1)
C(5)	31(1)	45(1)	37(1)	-8(1)	9(1)	-1(1)
C(6)	37(1)	32(1)	31(1)	0(1)	7(1)	-3(1)
C(7)	29(1)	27(1)	29(1)	-3(1)	2(1)	-1(1)
C(8)	34(1)	29(1)	29(1)	2(1)	-2(1)	2(1)
C(9)	31(1)	27(1)	33(1)	-1(1)	4(1)	-2(1)
C(10)	38(1)	43(1)	33(1)	-10(1)	-5(1)	4(1)
C(11)	45(1)	55(1)	36(1)	-8(1)	-12(1)	16(1)
C(12)	40(1)	41(1)	40(1)	-8(1)	-7(1)	15(1)
C(13)	37(1)	45(1)	48(1)	-10(1)	-5(1)	1(1)

Table 2.14-5 Hydrogen coordinates (x 10^4) and isotropic displacement parameters (Å^2 x 10^3) for DAMPO.

	x	y	z	U(eq)
H(2)	3111(28)	6470(13)	6698(16)	31(5)
H(3A)	1879(37)	7893(17)	6004(22)	58(8)
H(3B)	179(35)	8264(17)	6549(20)	51(7)
H(4)	-978(31)	7699(15)	8211(17)	44(6)
H(5)	-1199(32)	6488(15)	9406(19)	49(6)
H(6)	750(30)	5145(14)	9180(18)	41(6)
H(8)	5440(31)	3287(15)	6885(18)	45(6)
H(9A)	6071(35)	2011(16)	5706(21)	57(8)
H(9B)	4886(32)	1766(15)	4662(19)	48(6)
H(10)	3176(29)	2938(14)	3722(18)	42(6)
H(11)	1339(33)	4255(16)	3913(19)	55(7)
H(12)	1588(32)	5013(15)	5684(19)	46(6)
H(13A)	6805(41)	4650(19)	8146(24)	77(9)
H(13B)	6033(34)	5342(16)	9005(23)	60(7)
H(13C)	6280(35)	5518(17)	7787(21)	57(8)

Table 2.14-6 Torsion angles [deg] for DAMPO.

O(1)-P(1)-C(1)-C(6)	4.8(2)
C(13)-P(1)-C(1)-C(6)	-117.2(2)
C(7)-P(1)-C(1)-C(6)	127.68(14)
O(1)-P(1)-C(1)-C(2)	-177.64(15)
C(13)-P(1)-C(1)-C(2)	60.3(2)
C(7)-P(1)-C(1)-C(2)	-54.8(2)
C(6)-C(1)-C(2)-C(3)	-0.8(3)
P(1)-C(1)-C(2)-C(3)	-178.28(14)
C(1)-C(2)-C(3)-N(3)	-179.6(2)
C(1)-C(2)-C(3)-C(4)	2.7(3)
N(3)-C(3)-C(4)-C(5)	179.9(2)
C(2)-C(3)-C(4)-C(5)	-2.4(3)
C(3)-C(4)-C(5)-C(6)	0.1(3)
C(4)-C(5)-C(6)-C(1)	1.8(3)
C(2)-C(1)-C(6)-C(5)	-1.5(3)
P(1)-C(1)-C(6)-C(5)	176.21(15)
O(1)-P(1)-C(7)-C(12)	115.7(2)
C(13)-P(1)-C(7)-C(12)	-121.8(2)
C(1)-P(1)-C(7)-C(12)	-7.0(2)
O(1)-P(1)-C(7)-C(8)	-58.1(2)
C(13)-P(1)-C(7)-C(8)	64.4(2)
C(1)-P(1)-C(7)-C(8)	179.17(14)
C(12)-C(7)-C(8)-C(9)	-2.7(3)
P(1)-C(7)-C(8)-C(9)	171.39(15)
C(7)-C(8)-C(9)-N(9)	180.0(2)
C(7)-C(8)-C(9)-C(10)	1.7(3)
C(8)-C(9)-C(10)-C(11)	0.3(3)
N(9)-C(9)-C(10)-C(11)	-178.1(2)
C(9)-C(10)-C(11)-C(12)	-1.2(4)
C(8)-C(7)-C(12)-C(11)	1.8(3)
P(1)-C(7)-C(12)-C(11)	-171.8(2)
C(10)-C(11)-C(12)-C(7)	0.1(4)

3 CHAPTER 3 EPOXY NETWORKS: BACKGROUND

3.1 Introduction

Epoxy resins are a class of very interesting materials that are used in a wide variety of applications, which include coatings, adhesives, casting structural materials, matrix for composites, laminates and electrical insulation. More recently epoxy networks have found extensive use in the electronic industry in areas such as printed-circuit boards, microelectronic potting and encapsulation. Their interesting properties result from their excellent adhesion to a large variety of substrates, outstanding resistance to chemical and environment challenges, the absence of unecessary volatiles during their curing reaction, their heat resistance, low shrinkage during the curing reaction, their superior mechanical and electrical properties and their low moisture absorption.

3.1.1 Background Topics pertinent to the Present Work (Chapter 4)

In the following sections the nature of the oxirane ring and the syntheses of epoxy resins containing two or more oxirane rings will be reviewed. Network formation involving the reaction of epoxy resins with curing agents will then be described.

Following a brief presentation of gelation and network development theory, specific curing agent and their reaction mechanisms will be discussed. Thoughened epoxy network is examined within the framework of the time-temperature-transformation (TTT) concept, phase separation thermodynamics, and curing kinetics.

Various possible mechanisms for epoxy network toughening by the addition of rubbery or thermoplastic polymers are reviewed. Toughness is estimated by critical strain energy release for crack growth or by a critical stress intensity factor for the onset of fracture.

Finally, the application dielectric permittivity and loss monitoring to the study opf epoxy cure kinetics is briefly described.

3.1.2 Importance of Oxirane Rings

Epoxy resins are a class of versatile and widely used systems characterized by the presence of one or more epoxide or oxirane groups (Figure3.1-1). These groups contribute to the resin useful properties.

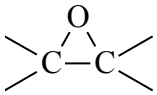

Figure 3.1-1 An oxirane ring

Epoxy resins are oligomeric chemical intermediates that must be further reacted (cured) to generate the desired products. The most important stoichiometric curing agents include aliphatic polyamines and their derivatives, aromatic amines, carboxylic acid, carboxylic acid anhydrides and phenol-formaldehyde resins. The properties of the material are of course dependent upon the nature of the resin, the curing agent and possible additives. Epoxy networks exhibit excellent resistance to chemicals and have outstanding resistance to corrosion. They also have very useful tensile, compressive, flexural and fatigue strength properties.

Electrical insulation properties of epoxy networks allow their use in microelectronics packaging.[1,2,3] The curing reactions generate no volatiles, and they ehibit excellent adhesion to a wide variety of substrates.

The above properties, together with good processing characteristics have resulted in the use of epoxies in transportation, packaging adhesives and coatings, appliances, electrical laminates, tooling, casting, molding, fiber reinforced composites, flooring, paving, and aggregates.[4]

3.2 Resin Synthesis

Organic reactions suitable for the synthesis of epoxides have been described previously.[5,6,7] They include oxidation of alkenes with a suitable reagent, cyclo-dehalogenation of halohydrins, condensation of α - halocarbonyl compounds and the ring closure of alkoxide ions. They are summarized in table 3.2-1. The currently most important route for the manufacture of epoxy resins is the reaction of a halohydrin with hydroxyl compounds.

The geometrical structure of the epoxy ring is planar and bond angles and lengths have been precisely determined.[6,8] The differences in C-O-C bond angle from that of dimethyl ether is considerable (60° versus 109°). This angular distortion gives epoxides a rather large ring strain, which translates into a large exothermic reaction enthalpy. The geometry of the epoxide ring is similar to that of cyclopropane, but because of the electronegativity of the heteroatom, the internal ring bond angles are not equal. Of course the bond angles of the atoms C and O are also naturally different because of their tetragonal and dihedral structures.

Industrial synthesis of Epoxy Resins

The most important routes for the synthesis of epoxy resins are dehydrohalogenation of halohydrins and epoxydation of alkenes. Details on the appropriate reaction conditions and the yields have been published.[9]

The compound 2,3-epoxypropyl chloride (epichlorohydrin) is a very important intermediate for the production of epoxy resins. It can readily react with aliphatic alcohols and epecially phenols to generate the desired epoxides.

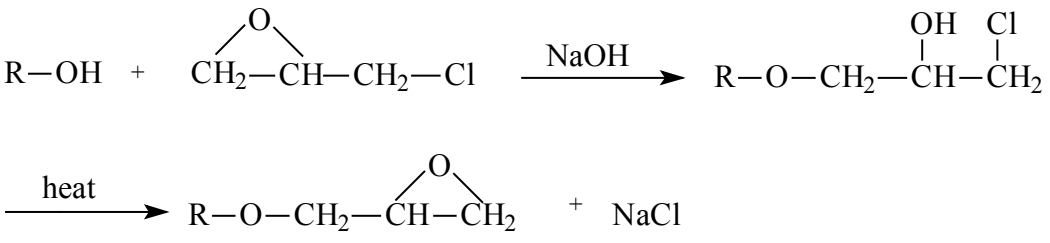

In the above reaction, the epoxy ring is formed upon cyclodehydrochlorination with a stoichiometric (or even less) amount of sodium hydroxide. Epichlorohydrin itself can be synthesized by a two-step reaction. The first step is the free radical chlorination of propylene to afford allyl chloride. The allyl chloride is subsequently converted to a dichlorohydrin with hypochlorous acid, and then dehydrochlorinated with lime to yield epichlorohydrin.[10,11]

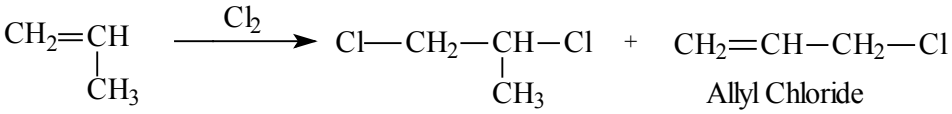

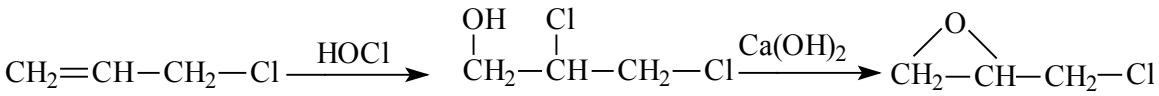

An alternative route for the synthesis of epichlorohydrin is the oxidation of propylene[11] to acrolein, which is then chlorinated to produce 2,3-dichloropropionaldehyde. This latter compound is in turn reduced to produce an α,β-dichlorohydrin. The α,β-dichlorohydrin (glycerol) can then be dechlorinated to produce the desired epichlorohydrin.

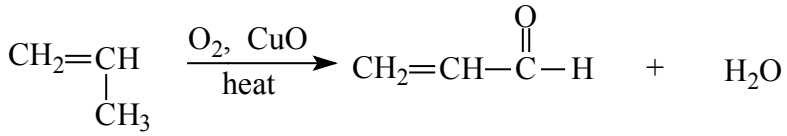

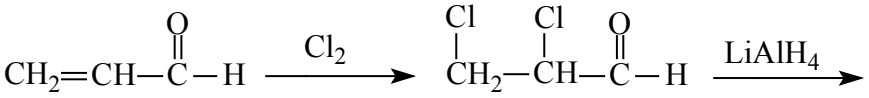

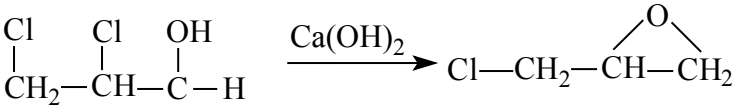

Epichlorohydrin is used to synthesize a wide range of epoxy resins (Table 3.2-2).

3.2.1 Epoxy Resins Derived From Bisphenol A

Bisphenol A, (2,2'-bis (p-hydroxyphenyl) propane is produced by the acid catalyzed reaction of acetone and phenol.

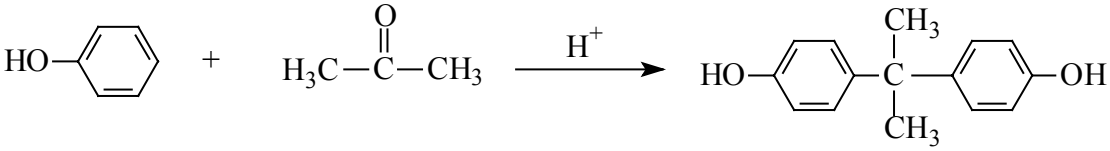

When a large excess of epichlorohydrin is reacted with bisphenol A and a stoichiometric amount of sodium hydroxide at about 65°C, the reaction produces approximately 50% of the diglycidyl ether of bisphenol A (DGEBA), 20% of higher molecular weight oligomers, and other side products.[12] The higher molecular weight resins result from the often unavoidable reaction of DGEBA with bisphenol A. Vacuum distillation can be used to provide a product of higher purity. Further purification by recrystallization techniques provides an essentially pure DGEBA.

Table 3.2-1 Reactions for the Synthesis of Oxiranes [5,6,7]

1. Oxidation of alkenes

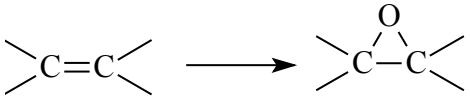

Hydrogen peroxide (H_2O_2), peroxy acids, or chromic acid are the common oxidizing agents.

2. Cyclodehalogenation of halohydrins

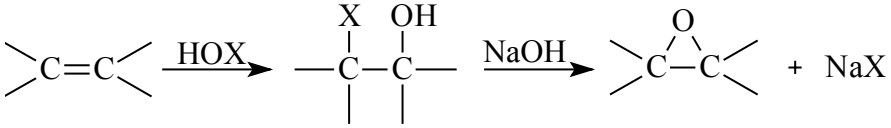

3. Darzen's condensation

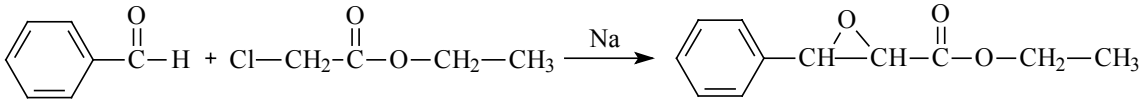

4. Reduction of α-halocarbonyl compounds

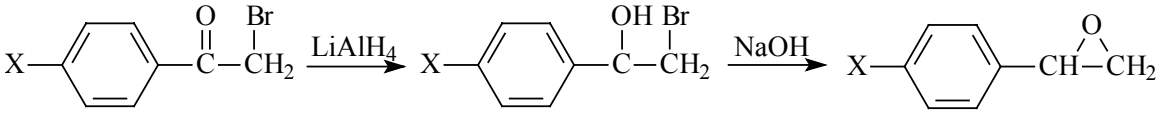

5. Addition of alkoxide ion to α-halocarbonyl compounds

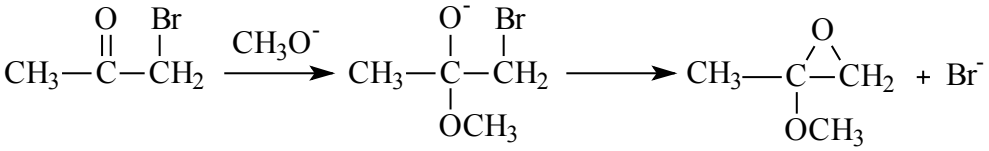

Table 3.2-2 Selected Epoxide Derivatives of Epichlorohydrin obtained from:

1. Phenols (e. g., bisphenol A)

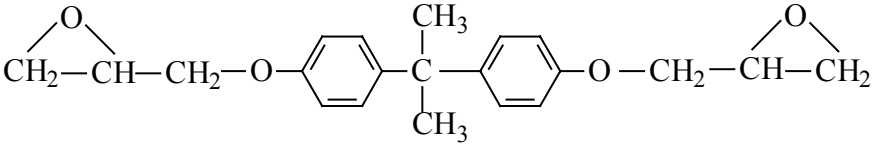

2. Aliphatic alcohols (example glycerol)

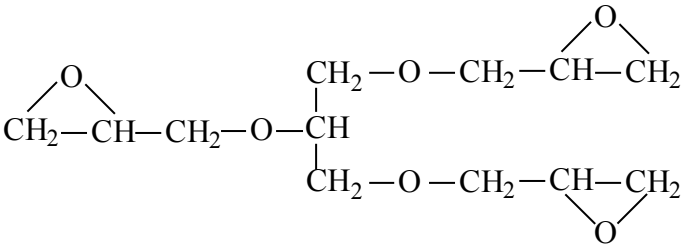

4. Carboxylic acid (example phthalic acid)

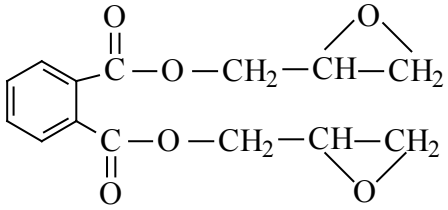

5. Phenolic formaldehyde resins, e.g.
Epoxy NOVOLACS

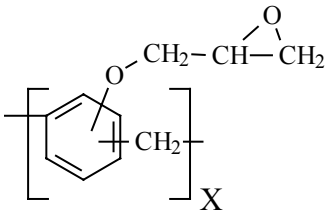

6. Amines (example bis anilines)

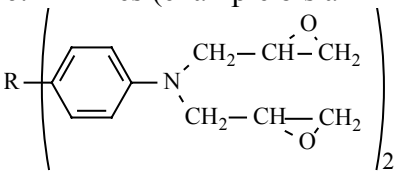

The Synthesis of the bisphenol A epoxy resin is depicted in Scheme 3.2-1. Commercially available biphenol A epoxy resins are prepared by using different molar ratios of epichlorohydrin to biphenol A, as shown in the table below.[12]

Epichloropydrin/bisphenol A ratio	Molecular Weight of the resin (g/mole)
1.4 : 1	791
2:1	450
10:1	370

Table 3.2-3 Molecular weight of bisphenol A epoxy resin as a function of reagent ratios. (pure diepoxide is 340 g/mole)

Oligomeric epoxy resins with controlled molecular weight, (e.g., n values ranging from 2 to 30) are usually prepared by two processes. Lower molecular weight liquid resins with n values up to 4 are prepared directly from epichlorohydrin, bisphenol A, and a stoichiometric amount of NaOH. This is the so-called "taffy" process. Side reactions are kept to a minimum by the careful control of pH, water concentration, and temperature.[13] Higher molecular weight solid resins are prepared by chain extension of liquid epoxy resins with bisphenol A, using inorganic reagents such as NaOH, KOH, Na_2CO_3 or LiOH as catalysts. This process is often referred to as the "advancement" or "fusion" process, and allows the manufacture of resins with degrees of polymerization ranging from 2 to 30, with n = 2 to 12 being the most common.[14]

3.2.2 Higher Functionality Resins

Most epoxy resins are diglycidyl ethers of bisphenol A, because high glass transition temperatures (well above 150° C) can be achieved and the products can be used in aggressive environments. Average functionalities around 2 and are suitable for a wide variety of applications, but there is an increasing demand for

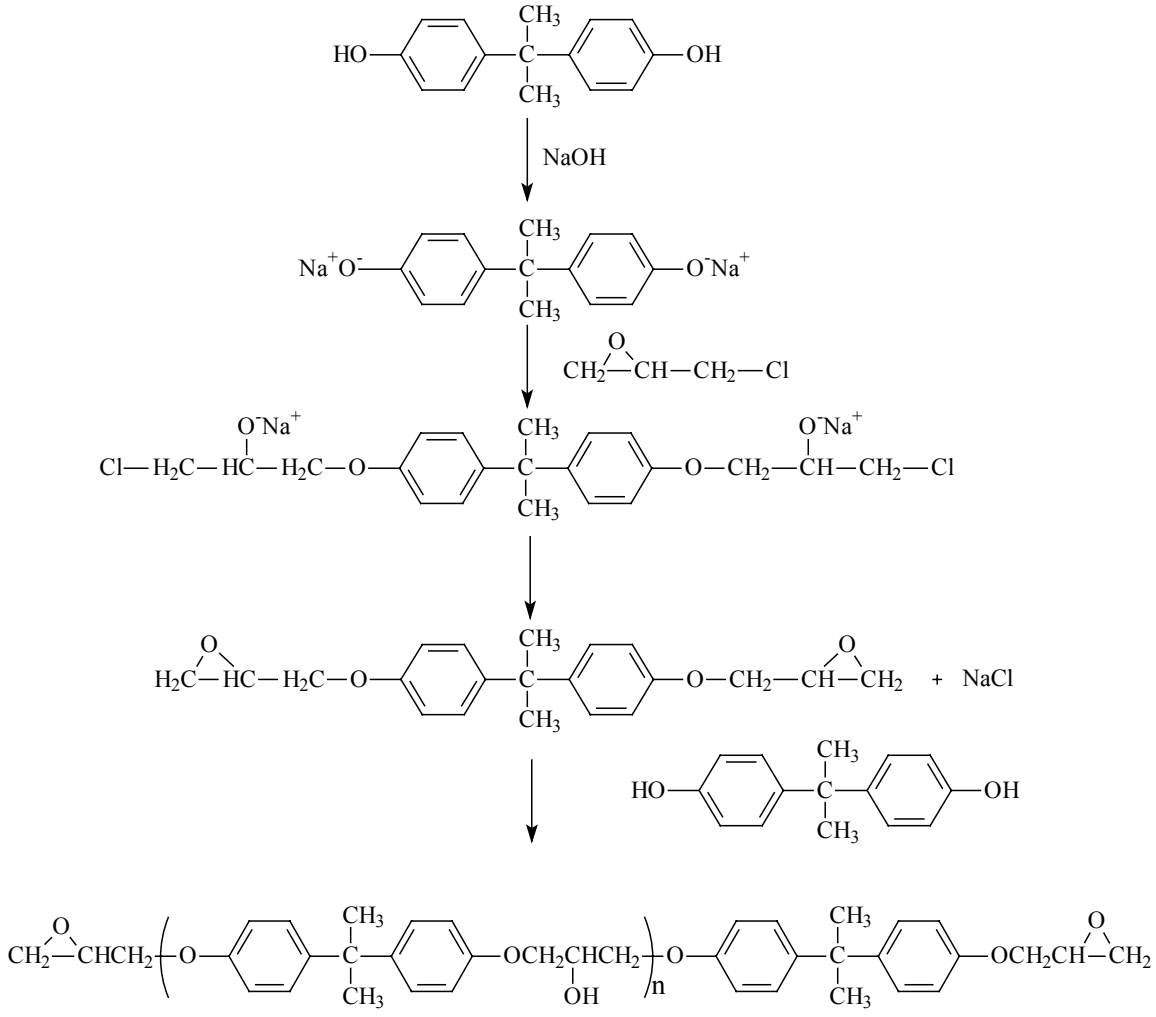

Scheme 3.2-1 **Synthesis of bisphenol A epoxy resin**

.

high performance materials, particularly with glass transition temperatures well above 200°C. The demand for such materials is particularly pressing in the aerospace industry. These applications require higher functionality resins with high aromatic ring content, which can generate high crosslink density upon curing. These resins include the epoxy novolacs and tetraglycidyl diaminodiphenylmethane (TGDDM). The latter is the most commonly used and can be synthesized by reacting diaminodiphenylmethane with epichlorohydrin in a process similar to the synthesis of DGEBA, except that the 4,4'-methylene dianiline (MDA) is reacted with epichlorohydrin in two steps.[15,16] The idealized two step method for preparing TGDDM from 4,4'-methylene dianiline (MDA) is shown in Schem 3.2-2. The reaction scheme for the MDA snthesis is depicted below.[17]

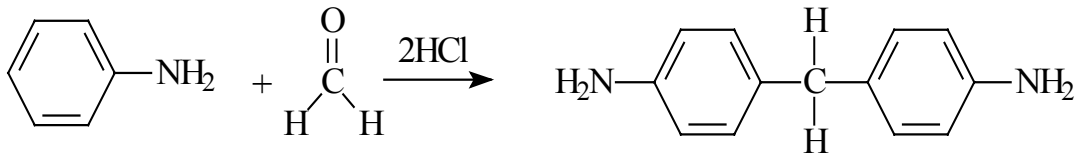

4,4'-Methylene Dianiline (MDA)

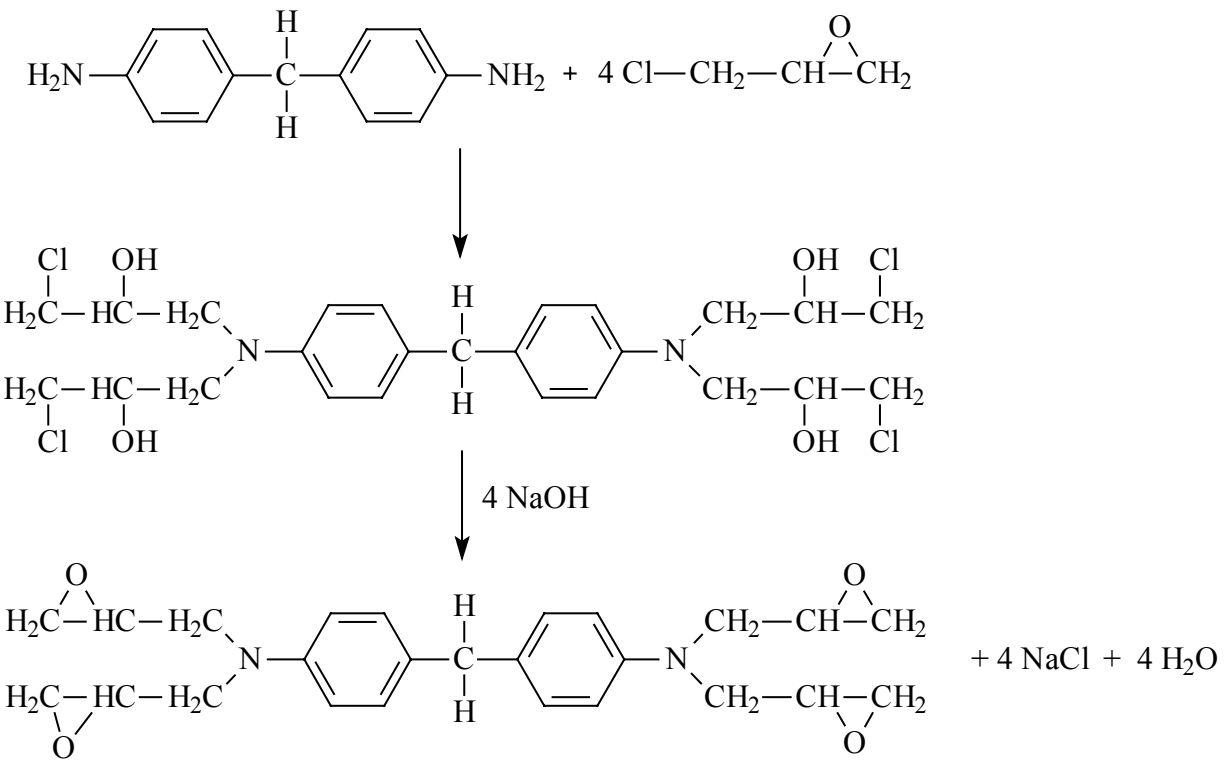

Scheme 3.2-2 **Idealized two step synthesis of TGDDM**[15]

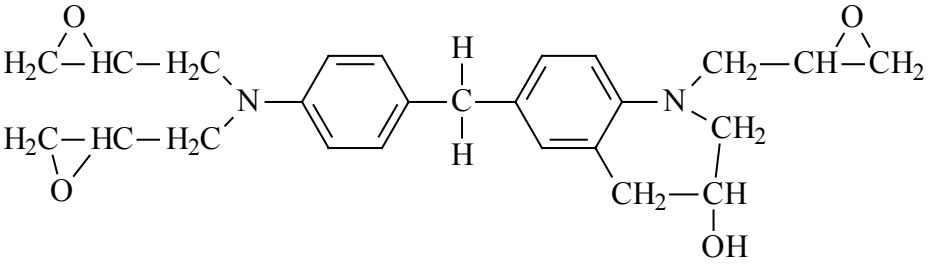

Second most prevalent side product

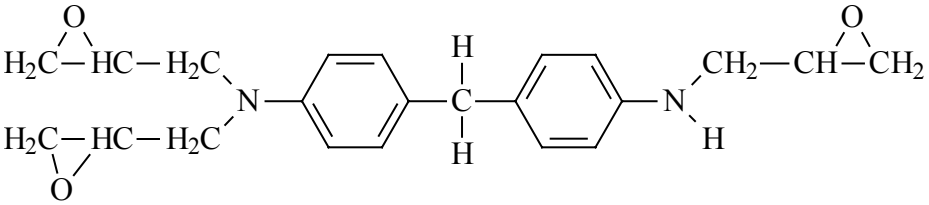

N,N,N'-triglycidyl-4,4'-diaminodiphenylmethane

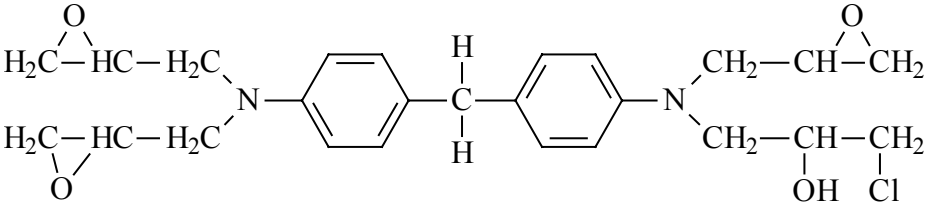

N,N,N'-triglycidyl-N'-(2-hydroxy-3-chloropopyl)-4,4'- diaminodiphenylmethane

Figure 3.2-1 **Secondary side products encountered in the synthesis of TGDDM** [15,17]

In the MDA synthesis, aniline reacts initially (after neutralization) with hydrochloric acid to give a quaternary ammonium salt which then reacts with formaldehyde to yield the 4,4′ -methylene dianiline (MDA).

During the synthesis of the TGDDM, several side reactions may occur as revealed by GPC, HPLC, NMR and UV analysis.[15,19] The most prevalent species is the dimer whose structure is shown below.

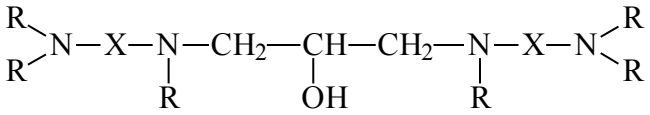

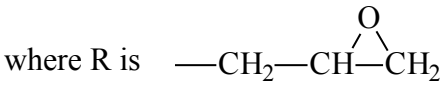

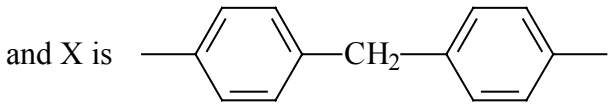

Other side products are depicted in Figure 3.2-1.

3.3 Curing Reactions.

3.3.1 Network Formation

Thermosets are insoluble and intractable three dimensional polymeric materials which do not flow or dissolve under any circumstances. These materials include synthetic rubbers, epoxy networks, phenol-formaldehydes, unsaturated polyesters/styrene, melamine-formaldehydes, bismaleimides, phenyl acetylenes, cyanate esters and others.

Crosslinking agents are used to convert oligomeric epoxy resins into hard, infusible thermoset networks. These crosslinking agents (often referred to as curing agents or hardeners) promote curing of the epoxy resin. Curing can occur either by stoichiometric reaction of the resin with a multifunctional curing agent or homopolymerization of the resin with a catalytic curing agent. Curing reactions generate insoluble and infusible macromolecules in which chains are joined together to form a 3-

dimensional network structure. Crosslinked macromolecules differ from their linear homologues in that they may swell in good solvents but cannot dissolve. They do not melt or flow under any circumstances, but they may soften at elevated temperatures.

In order to control the curing reaction to a technologically useful extent, it is important to understand the relationship between gelation, functionality, and the extent of reaction. The gel point is the extent of reaction at which an infinite molecular weight network begins to form. Chemical reactions may continue to take place beyond the gelation state and more chains may crosslink to contribute to the increase of the network density. The degree of crosslinking is a measure of the total number of links between the chains in a given volume of material. The number-average molecular weight of the chain between crosslinks is denoted as $<M_c>$. In a network, the amount of material which is soluble is referred to as the "sol fraction." The sol fraction consists of linear and highly branched molecules having finite molecular weights. The amount of insoluble material in a network is known as the "gel fraction." After gelation, the sol fraction, W_S decreases to essentially zero and the gel fraction W_g increases to approximately one.

Many of the physical and mechanical properties (e.g., Young's modulus Figure 3.3-1) of the cured resin depend on the details of the network structure. In the following development, it is assumed that the curing resin is homogeneous, that is, the property changes are uniform throughout the sample. However, this is not always true as some studies have shown.[19,20] It appears that some anomalus features observed in cured networks are due to poor mixing and dissolution of the hardener in the resin. In other cases there may be either phase separation, or the formation of microgel during the curing reaction. It is normally assumed that the inhomogeneities that may form during cure are unimportant.

There have been several approaches to the extent of reaction at which the gel point occurs.

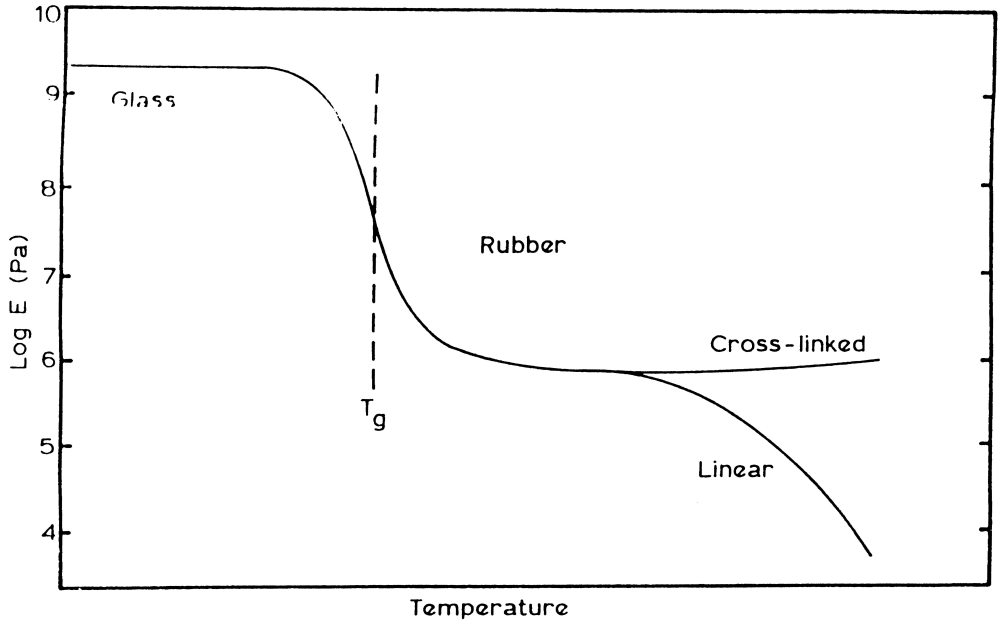

Figure 3.3-1 **Variation of Young's modulus (E) with temperature for a polymer, showing the effect of a low degree of crosslinking in the rubbery state.** [3]

3.3.1.1 Carother's Approach to the Theory of Gelation.[21]

This approach was developed for systems undergoing step growth polymerization. In this approach the critical extent of reaction for gelation is

$$p_{gel} = \frac{2}{f_{av}} \qquad \text{Equation 3.3-1}$$

where p_{gel} is the extent of reaction at the gel point and f_{av} is the average functionality. It can be shown that

$$f_{av} = \frac{N_i f_i}{N_i} \qquad \text{Equation 3.3-2}$$

where N_i is the number of molecules with a functionality f_i and the summation is over all monomers in the systems. Unfortunately this approach is only approximate and predicts higher extents of reaction at the gel point than observed experimentally.[22]

3.3.1.2 The Statistical Approach To The Theory Of Gelation [23,24,25]

In this approach an *f*-functional monomer RA_f (f>2) is allowed to react with difunctional monomers RA_2 and RB_2. A parameter α (or branching coefficient) is introduced and defined as the probability that an *f*-functional unit connects to another *f*-functional unit via a chain of difunctional units. α can also be defined as the probability of the existence of the chain shown below.

$$_{(f-1)}AR-AB-R-B[A-R-AB-R-B]A-R-A_{(f-1)}$$

The derivation of an expression for α requires the introduction of a term, γ, which is defined as the initial ratio of A groups from RA_f molecules to the total number of A groups. With γ defined in these terms, it is possible to find the probabilities for the existence of each of the linkages in the general sequence above. If the extent of reaction of the A groups is p_A and of the B groups is p_B then

the probability of $_{(f-1)}AR-\overrightarrow{AB}-R-B$ is p_A

the probability of $B-R-\overrightarrow{BA}-R-A$ is $p_B(1-\gamma)$

the probability of $A-R-\overrightarrow{AB}-R-B$ is p_A

the probability of $B-R-\overrightarrow{BA}-RA_{(f-1)}$ is $p_B\gamma$

where the arrows indicate the linkages under consideration and the direction in which the chain is extending. Thus the probability that the general sequence of linkages is formed is given by

$$p_A[p_B(1-\gamma)p_A]^i p_B\gamma$$

The branching coefficient, which is the probability that sequences with all values of *i* have formed is given by the expression below:

$$\alpha = p_A p_B \gamma \sum_{i=0}^{\infty} [p_A p_B (1-\gamma)]^i \qquad \text{Equation 3.3-3}$$

Noting that

$$\sum_{i=0}^{\infty} X^i = \frac{1}{(1-X)} \quad \text{for X<1}$$

The branching coefficient α is

$$\alpha = p_A p_B \gamma [1 - p_A p_B (1-\gamma)]^{-1} \qquad \text{Equation 3.3-4}$$

Networks are formed when n connecting chains lead to more than n chains through branching of some of them. The maximum number of chains that can arise from the end of a single chain, such as that analyzed above, is (*f*-l) and therefore the probable number of chains arising from the chain end is $\alpha(f\text{-}1)$. If this quantity equals or exceed unity, that is $\alpha(f-1) \geq 1$, network molecules will result. Thus, the critical branching coefficient, α_c, for gelation is given by

$$\alpha_c = \frac{1}{(f-1)} \qquad \text{Equation 3.3-5}$$

Substitution of equation 3.3-5 into equation 3.3-4, followed by rearrangement of the terms gives the following expression for the product of the critical extents of reaction at gelation:

$$(p_A p_B)_c = \frac{1}{1+\gamma(f-2)} \qquad \text{Equation 3.3-6}$$

If r is defined as the initial ratio of A groups to B groups, then $p_B = rp_A$ and

$$(p_A)_c = [r + r\gamma(f-2)]^{-1/2}$$
$$(p_B)_c = r^{1/2}[1+\gamma(f-2)]^{-1/2}$$

When RA_2 molecules are absent $\gamma = 1$ and $(p_A p_B) = \frac{1}{(f-1)}$, that is $(p_A p_B)_c = a_c$

3.3.1.3 Comparison of the Carother's and the Statistical Approaches to the Theory of Gelation.

The Carothers' approach is only approximate and predicts higher extents of reaction at the gel point than are observed experimentally.[22] The statistical treatment largely overcomes this error and predicts the extent of reaction at the gel point (for step condensation systems) based on the polymer size distribution, when it first extends into the region of infinite size. The simple statistical approach underestimates p_c because it does not take into account the effect of intramolecular reactions between end-groups. These give rise to loops in the polymer structure and the polymerization must proceed to higher extents of reaction in order to overcome this wastage of functional groups. When

the effects of intramolecular reactions are taken into account, the statistical approach gives accurate predictions of the gel point.[26]

3.3.2 Curing Agents

Many curing agents and catalysts are known for epoxy resins. The most common curing agents are amines, carboxylic acid anhydrides, phenol-formaldehydes and amino-formaldehyde resins.

- Amines

Aliphatic amines

Aliphatic amines may be simple systems, or amine functional polyamides, polyamidoamines, imidazolines, adducts with epoxy functional materials, Mannich bases, ketimines and acrylonitrile adducts, fatty diamines, polyetheramines, alicyclic amines, and polymeric amines. A plausible mechanism of epoxy curing with amines is depicted in Scheme 3.3-1.

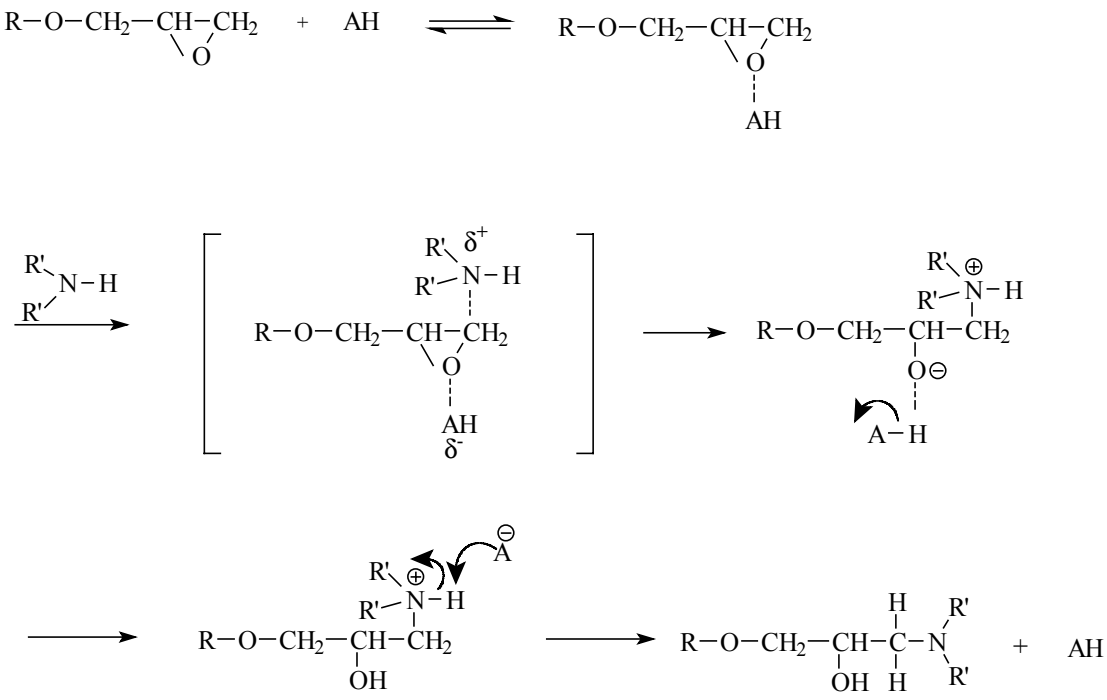

Scheme 3.3-1 **Mechanism of epoxy curing with amines**.[7]

(AH represents a hydroxyl group generated during the cure)

The reaction with aliphatic amines is faster than that with cycloaliphatic and aromatic amines, particularly at ambient temperatures. The initial step involves the amine active hydrogen adding to the epoxy group. This is followed by the resulting structure adding to another epoxy group.[27]

When the epoxy is a diepoxide (f = 2) and the amine is a primary diamine (f = 4) the resulting product is an infusible polymer. The reaction is accelerated by materials that stabilize the alkoxide ion intermediates. Therefore, hydroxyl groups are accelerators, including those generated during the curing reaction. They can also be added as accelerators and the more acidic they are, the more effective. Hydroxylic accelerators or hydrogen donors capable of catalyzing the amine epoxy reaction in decreasing order of efficiency are:

-OH (Ar >> $PhCH_2$ >RCH_2 >H); -CO_2H; -SO_3H; -$CONH_2$; -$SONH_2$.

Because of their unhindered polyfunctional nature, ethyleneamines are highly reactive and give tightly cross-linked networks, due to the short chain distances between the active sites. This results in cured resins with excellent solvent resistance and mechanical strength, but limited flexibility. Their low molecular weights imply that they have low viscosities; however, they may have high vapor pressures with the outcome that they are corrosive and irritating to the skin.[28] These amines are also high in odor, hygroscopic and may have poor compatibility with epoxy resins.

An alternative approach has been developed[29] to overcome the disadvantages of volatility, dermal irritation and hygroscopicity of the aliphatic amines. This involves reacting the amine with phenol and formaldehyde to form low molecular weight condensates or Mannich bases, as they are commonly referred to.

$$HO\text{-}Ar + CH_2O + H_2N(CH_2CH_2NH)_xH \longrightarrow HO\text{-}Ar\text{-}CH_2HN(CH_2CH_2NH)_xH + H_2O$$

These products cure rapidly at low temperature and in the presence of moisture, do not blush and are less susceptible to carbonation than other aliphatic amine modifications. They also have excellent chemical resistance.

Fatty amines are derived from C_{16} - C_{18} saturated and unsaturated fatty acids and are used as co-curing agents in epoxy applications. They are used primarily to provide flexibility and enhance water and corrosion resistance but are limited by their low reactivity.

Several polyetheramines have been used in the cure of epoxy resins; however, only polyoxypropylene derivatives have achieved prominence.[30] Most other polyglycol polyamines, notably ethylene oxide derivatives are too hygroscopic to be used extensively. By varying the functionality of the parent polyol and the molecular weight of the polyoxypropylene derivatives, several different molecular weight amine terminated curing agents can be made for use with epoxy resins. When cured, they show good film flexibility and thermal cycling properties due to the long chain distances between cross-link sites. Their flexible aliphatic nature does, however, limit their solvent and heat resistance.

Aromatic amines are less basic than their aliphatic or cycloaliphatic homologs and react only slowly with epoxy resins. They exhibit long pot lives and may require long periods at elevated temperatures to attain optimum properties. Aromatic amine cured epoxies are particularly notable for their high retention of mechanical properties at elevated temperatures. Most of the aromatic amines are solids at room temperature and are often liquefied for ease of mixing with liquid epoxy resins by the formation of eutectic mixtures or blending with cycloaliphatic polyamines for heat cure applications. Of all the aromatic amines ***m***-phenylene diamine provides the tightest crosslink density and hence exhibits the best solvent resistance. Methylene dianiline (MDA) which is prepared by condensation of aniline with formaldehyde exists in a number of forms ranging from pure solid MDA with a melting point around 90°C to low softening point mixtures with polyamines, which are easier to mix with epoxy resins.[31] The low polarity of the pure MDA curing agent which imparts excellent electrical insulation properties combined with high mechanical property retention, even under conditions of high humidity, make this the most suitable candidate for electrical casting, laminating and adhesive applications. Unfortunately, MDA is now classified as a potential human carcinogen and for most applications it has been replaced by other types of curing agents.

Diaminophenyl sulfone (4,4'-DDS) has a major advantage over other aromatic amines in providing the highest heat resistance. It has become the standard curing agent for specialized epoxy resins such as TGDDM in high performance and aerospace laminating applications. 3,3'-DDS, although giving reduced heat resistance (loer T_g) compared to the 4,4'-analog, is also of interest because of its high performance in honeycomb peel strength in aerospace laminating applications.

- Carboxylic acids and anhydrides

Carboxylic acid functional polyesters and anhydrides are the second most important family of curing agents for epoxy resins.[32] These can be combined together easily to give the necessary properties of correct softening point and reactivity for powder coatings applications. Reactions of carboxylic acid anhydrides with epoxy resins are characterized by low exotherms and although long times at elevated temperatures are required to achieve full cure, the resulting low shrinkage, stress-free systems provide excellent electrical insulation properties. These properties are retained even under moderate to high continuous operating temperatures due to the good thermal stability and have therefore helped their adoption in the heavy electrical industry.[32]

The mechanism of the reaction is more complex than that of amines, because of many competing reactions which can occur, especially when accelerators are added to enhance the curing rate. The mechanism of epoxy curing with carboxylic acid anhydrides in the absence of added accelerators is depicted in scheme 3.3-2. In the first step, the anhydride ring is opened by a hydroxyl group (e.g., a secondary hydroxyl found on the backbone of higher molecular weight epoxy resins) forming a half ester. The residual carboxylic acid group of this half ester may then react with the epoxide ring to form a hydroxy diester. The hydroxyl group of the diester can undergo reactions with anhydrides to form carboxyl groups, eventually yielding exclusively diesters.[14,33,34] These can then further react with epoxide groups, and continuation of this alternating sequence leads to the formation of a polyester. With respect to the above proposed mechanism, optimum properties are attained when stoichiometric equivalents of epoxy and anhydride are employed.

Tertiary amines can catalyze epoxy-anhydride reactions. The amine opens the anhydride ring to form a salt (a betaine), which then acts as an initiator for the cure. The resulting carboxylate group ion reacts with an epoxide group to give an alkoxide ester. In the final step, the anion undergoes a reaction with another anhydride, yielding an ester link. The continuation of this alternating sequence leads to the formation of a crosslinked network (scheme 3.3-3). Alternative mechanisms have been postulated, where the tertiary amine attacks an epoxy ring, giving rise to a zwitterion which contains a quaternary ammonium species and an alkoxide group. The alkoxide

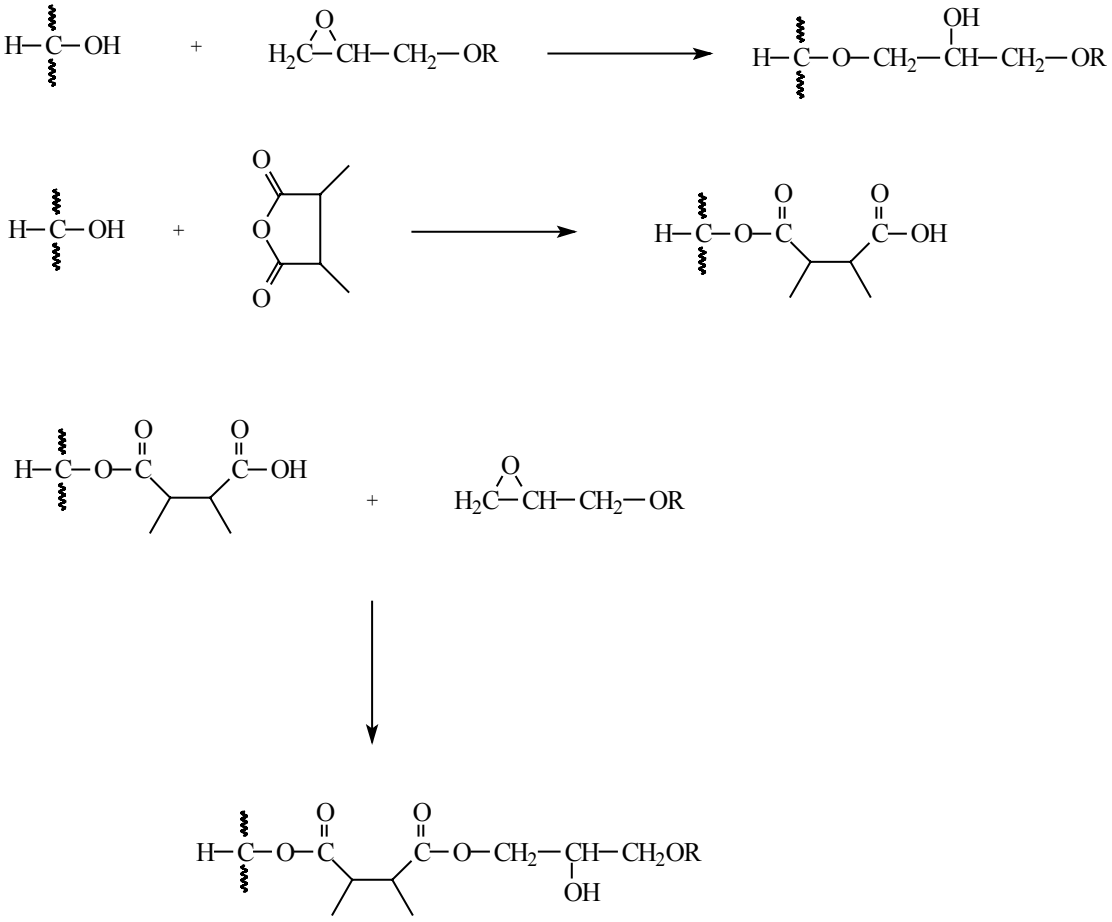

Scheme 3.3-2 **A Mechanism for epoxy curing with carboxylic acid anhydrides in the absence of accelerators**.[14]

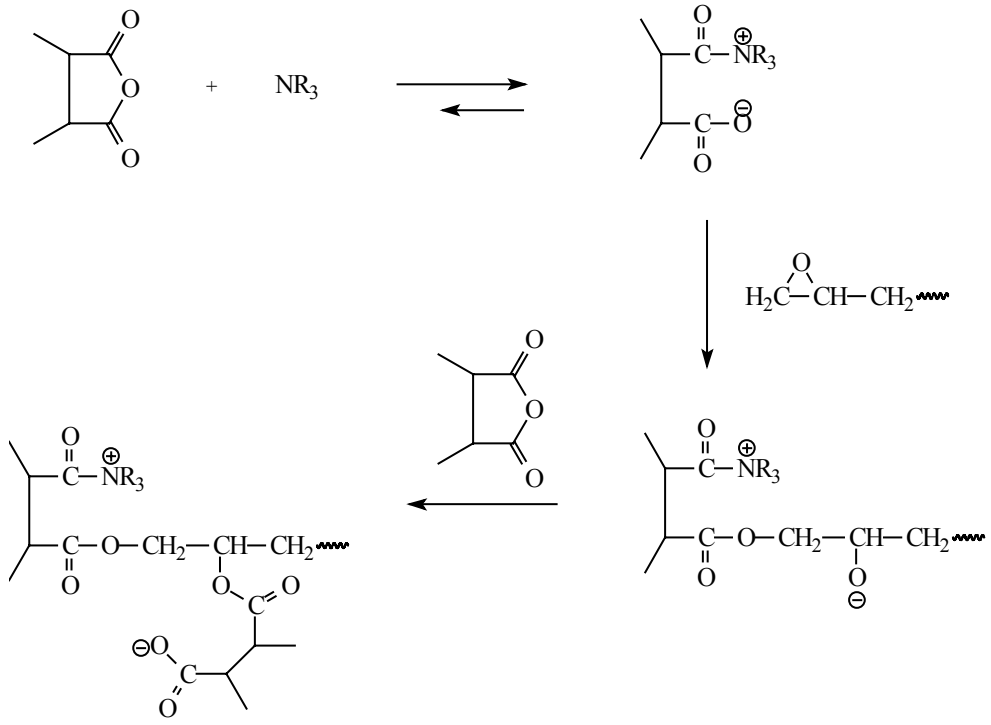

Scheme 3.3-3 **Mechanism of epoxy curing with carboxylic acid anhydrides in the Presence of a Lewis Base**.[14]

group then reacts with an anhydride to afford a quaternary salt.[35]

Lewis acids such as boron trifluoride-amine complexes and tetra-alkylammonium salts are known to catalyze the curing reaction of epoxy resins with anhydrides.[14] Although the mechanism of this reaction is not fully understood, it is thought that an etherification reaction takes place with as little as 0.55 equivalent of anhydride per epoxy equivalent to provide networks with optimum properties. A mechanism for the reaction is shown at Scheme 3.3-4. The epoxy resin is denoted R-OH (refer to Scheme 3.3-3).

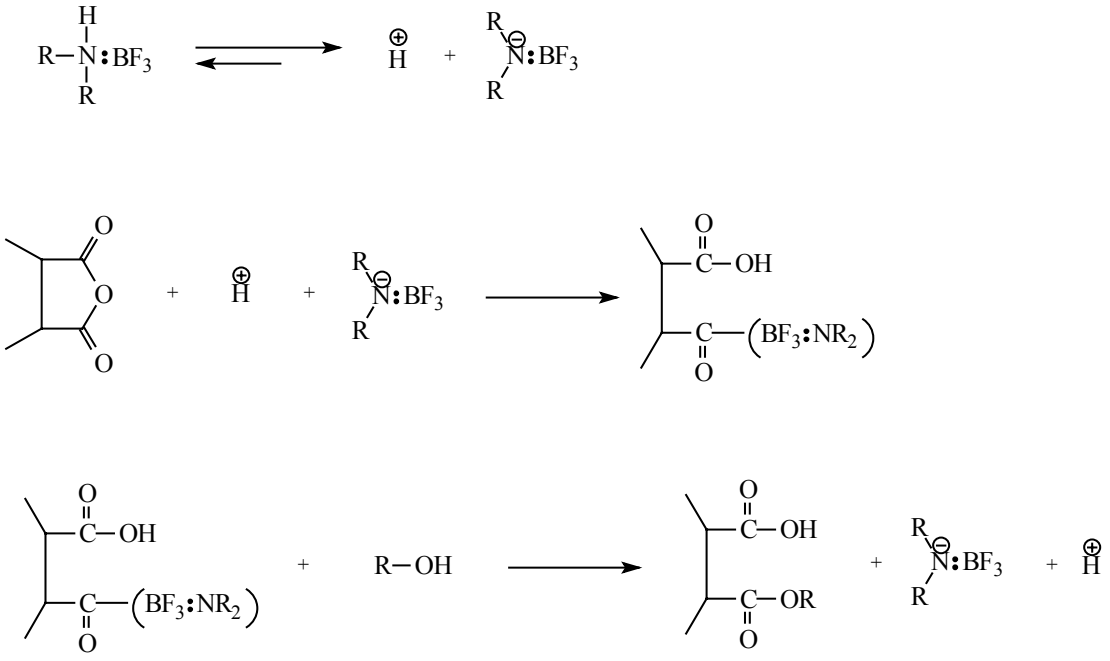

Scheme 3.3-4 **Acid catalyzed (BF_3 - amine complex) curing of epoxy resins with anhydrides**.[14]

Phthalic anhydride is the most common carboxylic acid anhydride used in the curing of epoxy resins. It is the least expensive and the most difficult to handle due to its strong tendency to sublime during use. Its hydrogenated derivatives, hexahydro phthalic anhydride and tetrahydro phthalic anhydride, are used chiefly for castings and laminates for electrical applications. They are darker in color, have lower melting points, and have less tendency to sublime during use. Pyromellitic dianhydride (PMDA) and

benzophenone tetracarboxylic acid dianhydride (BTDA) are aromatic dianhydrides which are used to achieve high cross-link density and high heat resistance. They are high melting solids and very reactive toward epoxy resins at high temperatures. They are therefore used in combination with other anhydrides such as maleic anhydride to make them easier to dissolve and more convenient to handle for a variety of electrical applications.

- Phenol formaldehyde resins

Novolac resins are the reaction products obtained from formaldehyde and excess phenol under acid catalysis. When reacted with high molecular weight solid bisphenol-A epoxy resins, they afford coatings with excellent adhesion, film strength, flexibility and chemical resistance. A reaction scheme is shown below.

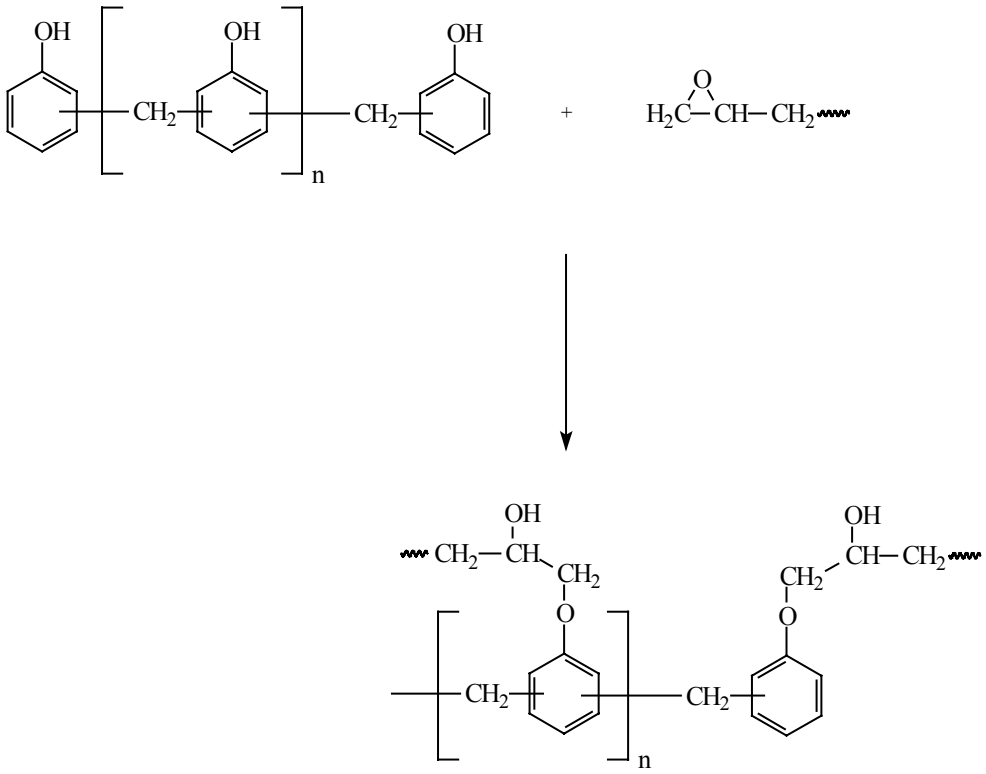

Scheme 3.3-5 **Curing Scheme for Novolac Resins and Epoxides**

Resole resins are produced by the reaction of formaldehyde in excess and phenol under basic conditions. When reacted with high molecular weight solid bisphenol-A epoxy resins, they produce a polyether. Because of secondary hydroxyls on the epoxy backbone, they give higher cross-link densities and higher chemical resistance than novolac resins. They are suitable for drum and pail coating applications where high curing temperatures easily drive off the water produced during the condensation curing reaction. The curing mechanism of the resole resins is depicted below.

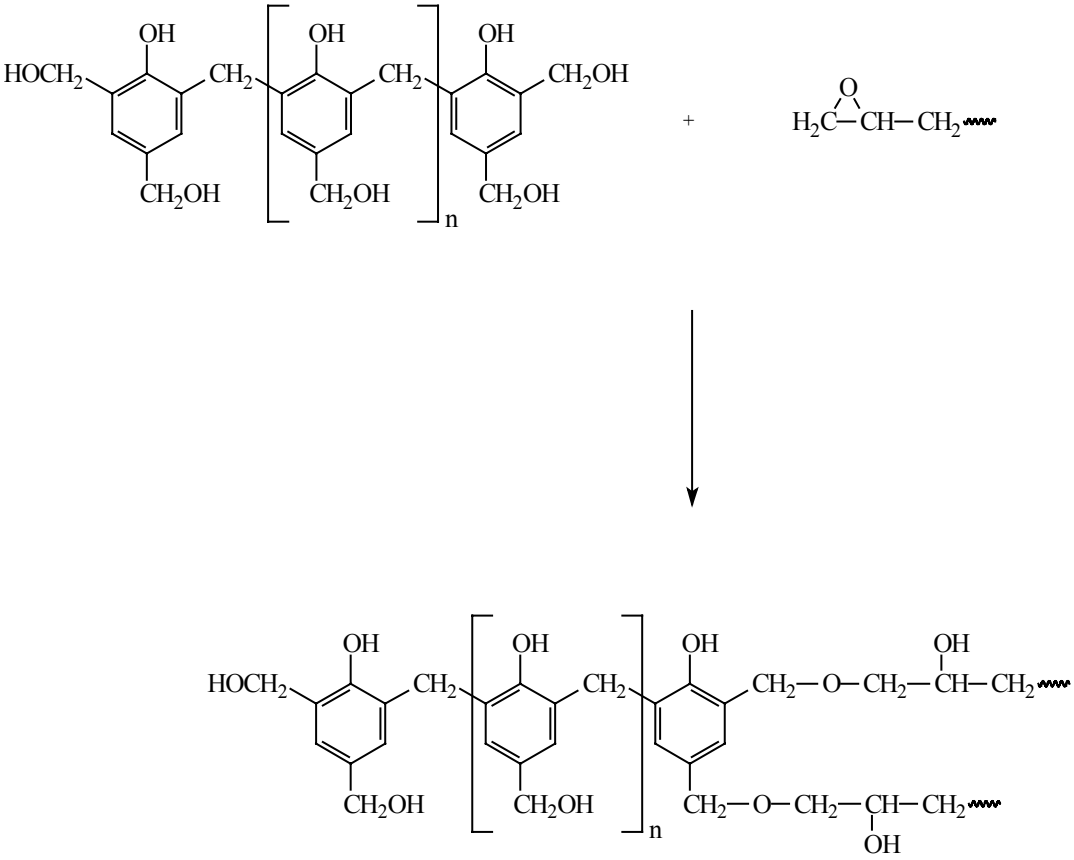

Scheme 3.3-6 **Curing scheme of epoxides with Resole Resins**.

■ Catalytic curing of epoxy resins.

Catalytic curing of epoxy resins refers to the homopolymerization of epoxy groups in the resin to provide the desired network. Both Lewis bases and Lewis acids can induce homopolymerization by initiating anionic and cationic reactions, respectively. The resultant network structures are, however, very similar and are essentially made up of ether linkages.

The reaction of tertiary amines with epoxy resins has been described in detail.[36,37] For most tertiary amines, the rate is low at room temperature. For this reason they are usually used as accelerators at elevated temperatures. They are seldom used as sole curing agents. In the absence of hydrogen donors, the polymerization results from the attack of the tertiary amine on the epoxide, with the alkoxide amine being the propagating species. The reaction mechanism is depicted below.

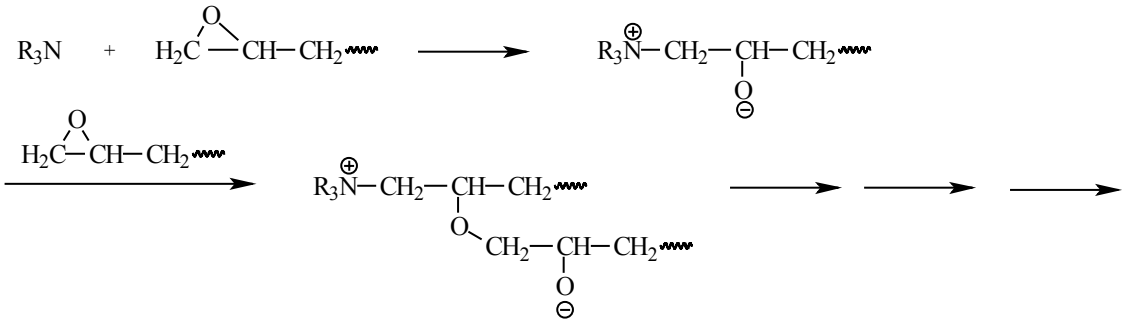

Scheme 3.3-7 **Catalytic Curing of Epoxy Resins with Tertiary Amine, in the Absence of a Proton Donor**. [7]

In the presence of alcohols or other proton donors the alkoxide amine can abstract a hydrogen atom to proceed through an anionic mechanism. The anionic homopolymerization mechanism is depicted below.[38,39,40]

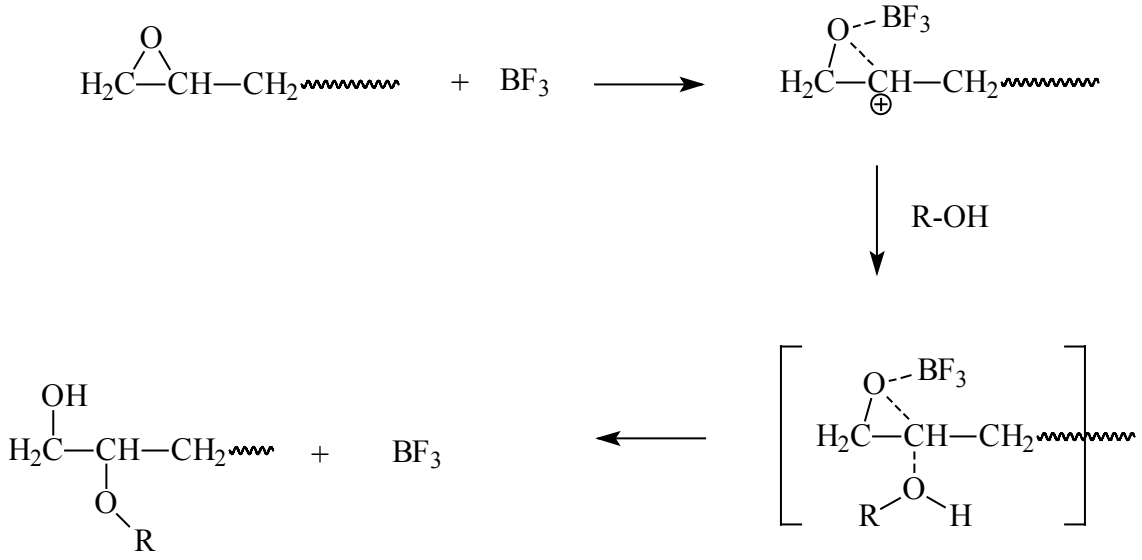

Scheme 3.3-8 **Catalytic curing of Epoxy Resins with Boron Trifluoride in the Presence of a Proton Donor**.[14]

Lewis acids can donate electrons to electron acceptors such as epoxide rings. Of all the many Lewis acids available, boron trifluoride and its complexes are the most suitable agents for epoxy curing. A polymerization mechanism for epoxy curing with boron trifluoride and a proton donor is depicted in Scheme 3.3-8. The curing mechanism of epoxy resins with boron trifluoride - amine complexes is depicted in Scheme 3.3-9. Other catalytic curing agents include the imidazoles and the urons (i.e., trisubstituted ureas).

Curing agents for epoxy resins and their characteristics are outlined in table 3.3-1.[41]

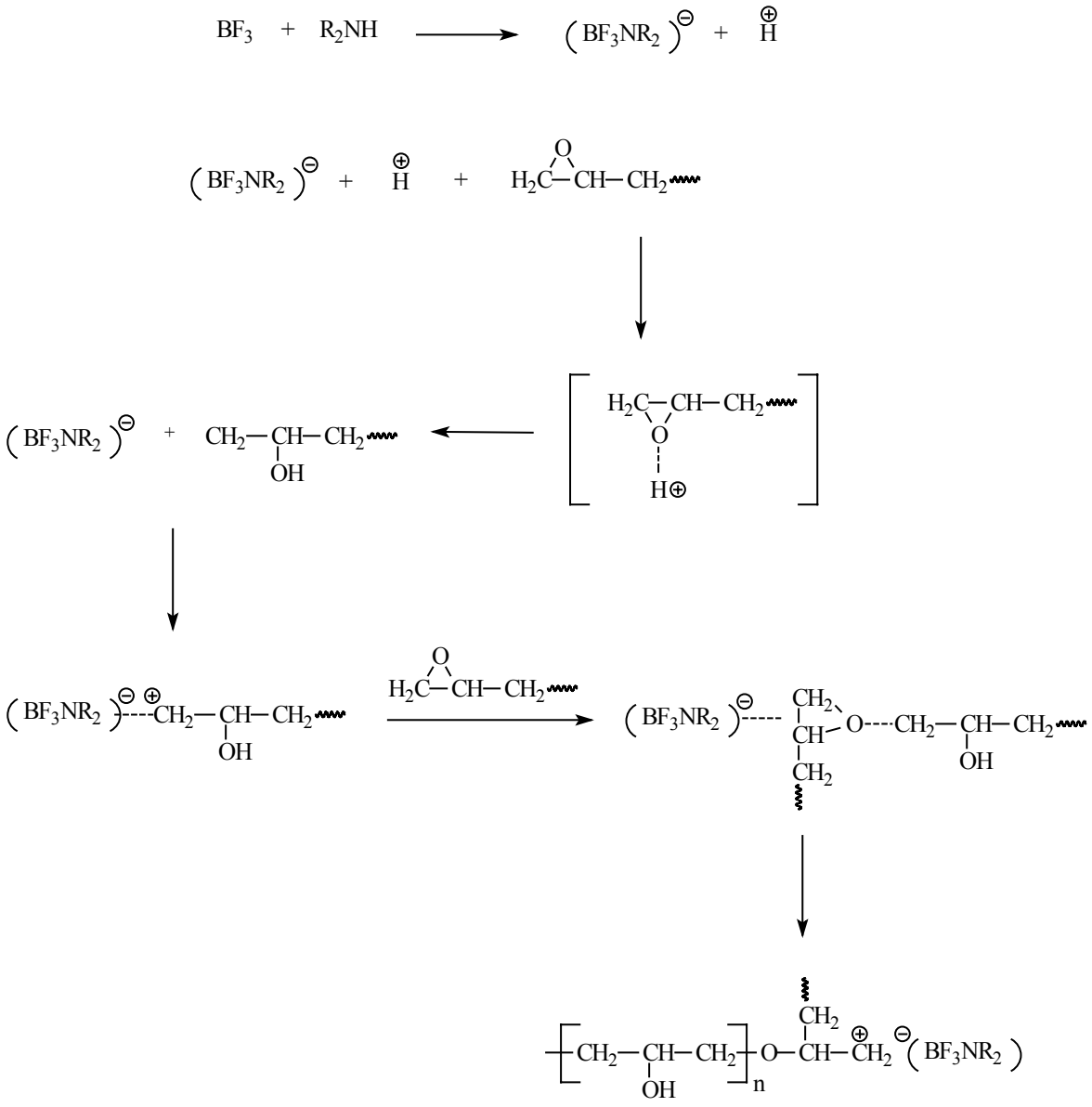

Scheme 3.3-9 **Catalytic Epoxy Curing with Boron Trifluoride-Amine Complexes**.[4]

Curing Agent	Advantages	Disadvantages	Applications
Aliphatic Amines	Convenience, room temp. cure, low viscosity, low formulation cost	Critical mix ratios, strong skin irritant, high vapor pressure, blushes	Civil engineering, adhesives grouts, casting and electrical encapsulation
Polyamides	Convenience, room temp. cure, low toxicity, flexibility or resilience, toughness, low vapor pressure	Higher formulation cost, high viscosity, low heat resistance	Civil engineering, grouts, castings, coatings
Amidoamines	Reduced volatility, convenient mix ratios, good toughness	Poor elevated temp. performance, some incompatibility with epoxy resins	Construct. Adhesives, concrete bonding, troweling compounds
Aromatic Amines	Moderate heat resistance, good chemical resistance	Solids at room temp. performance, some incompatibility with epoxy resins	Filament wound pipe, electrical encap-sulation, adhesives
Acid Anhydrides	Good heat resistance, good chemical resistance	Long, elevated temp. cure cycles, critical mix ratios	Filament wound pipe, electrical encap-sulation, adhesives
Catalytic	Extremely long pot life, high heat resistance	Long, elevated temp. cure cycles, poor moisture resistance	
Phenol/Formaldehyde	Good elevated temp. properties, good chem. resistance, good hardness, flexibility	solid, poor weatherability	Powder coatings, molding compounds
Dicyandiamide	Latent cure, good elevated temp. properties, good electrical properties	Long, elevated temp. cure cycles, insol. In resins adhesives	Powder coatings, electrical laminates, one component

Table 3.3-1 **Curing Agents for Epoxy Resins and their Characteristics**.[41]

3.3.3 Time-Temperature-Transformation (TTT) Diagrams

As the curing reaction proceeds, major changes in the properties of the resin occur. The molecular weight increases and highly branched structures form. Prior to gelation the sample is still soluble in suitable solvents, but after the gel point is reached the network will not dissolve, but will swell in suitable solvents. The glass transition temperature of the curing resin increases as the curing reaction proceeds, and these changes can be visualized in a time-temperature-transformation diagram.[42] The main features of the diagram are: gelation, vitrification, full cure, devitrification and phase separation (figure 3.3-2). The diagram displays the different states resulting from the curing reaction. These states include liquid, sol/gel rubber, gel-rubber (elastomer), ungelled sol glass, gelled glass and char. The gelled glass state is subdivided in two by the full cure line (in the absence of degradation, devitrification and char). The two regions are designated, as fully cured gel glass and undercured sol/gel glass.

Gelation corresponds to the formation of an infinite molecular weight network. After the gelation, the material consists of soluble and insoluble fractions; the insoluble fraction increases with increasing conversion.

The glass transition temperature, T_g, is one of the most important structural and technical characteristic of an amorphous solid. The correlation between T_g of linear polymers with their chemical composition, molecular weight, rigidity and symmetry of chains as well as some other characteristics of macromolecules have been well documented.[44,45] The information on networks is much poorer. When an isothermally cured system reaches the diffusion conversion limit α^{dif} corresponding to the chosen T_{cure}, all kinds of molecular motions responsible for the mobility of the reacting groups become frozen. In physical terms, this means that the free volume fraction of the formed bulk polymer drops below a critical value. Any increase in T_{cure} after reaching α^{dif} is followed by a resumption of the cure reaction. After this T_{cure} rise, some large scale molecular motions become again

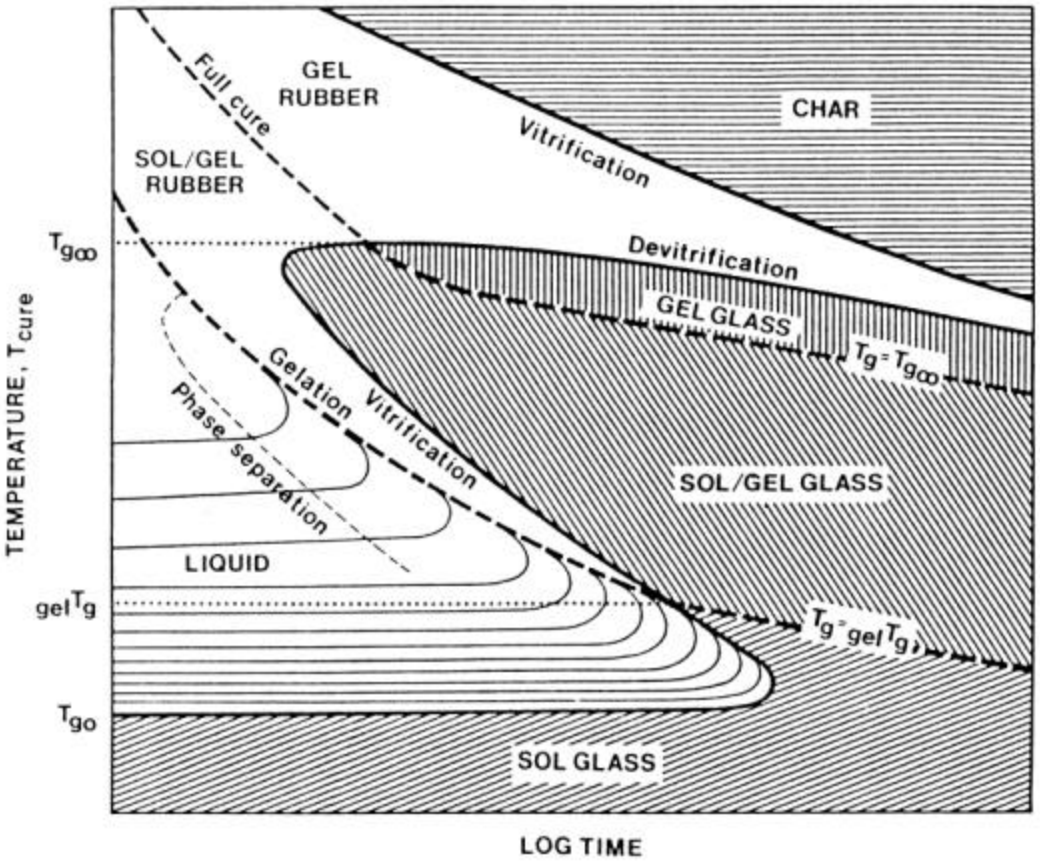

Figure 3.3-2 **Time-Temperature-Transformation (TTT) Isothermal Cure Diagram for a Thermosetting System**[43]

possible and allow the reacting groups to establish mutual contacts and react with each other. The motions, which the system needs for epoxy-amine curing reactions are segmental in nature. Thus the given T_{cure} must be close to the T_g of the polymer cured up to α^{dif} at this T_{cure}.

This glass transition temperature is called T_g^{exp} (experimental T_g) in contrast to T_g^{∞} (glass transition temperature of the polymer cured up to its topological limit α^{top}). The values of T_g^{∞} and T_g^{exp} may differ markedly. The following relations usually hold: $T_{cure} \approx T_g^{exp}$ for $T_{cure} \leq T_g^{\infty}$; $T_g^{exp} \leq T_g^{\infty}$; with increasing T_{cure}, lim $T_g^{exp} = T_g^{\infty}$ [46].

It is clear that T_g^{exp} is a function of curing conversion or molecular weight (for linear polymers) at α^{dif}. One can observe a noticeable difference between T_g^{exp} and T_g^{∞} for such processes as polyaddition or condensation reactions. It is especially important for a polymer with high T_g^{∞}. For many heat resistant polymers, T_g^{∞} is higher than the temperature limit for their chemical decompositon. The natural T_g^{∞} for those polymers can never be reached. For such polymers, one really only measures T_g^{exp}, the value of which depends on the reaction conditions. For networks, relationships between structure and glass transition temperature T_g^{∞} are the most important considerations.[47]

Vitrification of a curing network is a characteristic of the system. Usually the reaction will proceed with T_{cure} = const until vitrification appears as a result of molecular weight increase. Vitrification occurs when $T_{cure} < T_g^{\infty}$ where T_g^{∞} is the maximum glass transition temperature of the network. When $T_{cure} > T_g^{\infty}$ a "completely" cured network exists in its rubbery state. The most important feature of vitrification is that chemical reactions become diffusion-controlled and do not reach completion. Any rise of T_{cure} after the reacted mixture has reached α^{dif} leads to the continuation of a thermosetting process up to the next diffusion limit, which corresponds to the next T_{cure}. This stepwise curing stops only when T_{cure} becomes close to T_g^{∞} of the cured samples.[46,48]

Vitrification during cure leads not only to kinetic complexities but also to changes in the structure and properties of the cured polymers. Systematic decrease of T_{cure} finally gives polymers with very unusual properties of the glassy state. During cure, when vitrification

sets in, especially in the early stages of the reaction (low T_{cure}), phase separation processes can occur. Some workers reported that unreacted epoxy reactants can form small crystals which appear in a cured polymer and influence some of its properties.[49]

Devitrification occurs when T_g decreases below the isothermal cure temperature T_{cure} degradation for example. At high temperatures, other chemical reactions may result in degradation and consequently the T_g decreases owing to a decrease in the crosslink density and plasticization. Degradation can also result in vitrification due to char formation if an increase in crosslinking or volatilization of low molecular weight plasticizing material occurs.[50] In high T_g systems, cure and thermal degradation may effectively compete with each other.

Experimentally, the times for gelation and vitrification may be determined by techniques such as Torsional Braid Analysis (TBA), and melt rheology (parallel plate, cone & plate viscometer) in combination with techniques to monitor other parameters such as glass transition temperature (DSC), shear modulus (Torsional Pendulum), room temperature density and room temperature equilibrium water absorption.[51]

3.3.4 Phase Separation In Toughened Networks

The time-temperature-transformation diagram (figure 3.3-2) is often extended to include multiphase systems such as rubber or thermoplastic modified thermosets. Such modified systems involve changes from an initially homogeneous system to a heterogeneous multiphase separated morphology. The final morphologies are strongly influenced by the time-temperature cure history of the material and hence a knowledge of the TTT diagram is an essential prerequisite to achieve controlled phase separation.

Phase separation can be treated theoretically on the basis of the Flory-Huggins theory.[53,54,55] This theory permits the calculation of the combinatorial entropy, ΔS_m^{com}, of mixing molecules (1) having molar volume V_1 with molecules (2) having molar volume V_2 withing a volume equal to V_1.

$$\Delta S_m^{com} = -R\left(\phi_1 \ln \phi_1 + \frac{\phi_2}{x} \ln \phi_2 \right) \qquad \text{Equation 3.3-7}$$

Where ϕ_1 and ϕ_2 are the volume fraction of molecules (1) and (2), respectively. And x = V_2/V_1.

The Gibbs' free energy of mixing within the volume V_1, ΔG_m^* can be expressed by adding an interaction term, $RT\chi\phi_1\phi_2$ representing the change in enthalpy (heat) and local entropy (local order/disorder).

$$\Delta G_m^* = -T\Delta S_m^{com} + RT\chi\phi_1\phi_2 \quad \text{Equation 3.3-8}$$

If χ is zero or negative, ΔG_m^* is negative for all mixture compositions. The mixture are homogeneous, i.e., no phase separation occurs. If χ is positive, phase separation can occur at a critical value of χ and the composition of the equilibrating phases will become increasingly different as χ increases.

$$\Delta G_m^* = RT\left(\phi_1 \ln\phi_1 + \frac{\phi_2}{x}\ln\phi_2 + \chi\phi_1\phi_2\right) \quad \text{Equation 3.3-9}$$

Figure 3.3-3 is a schematic representation of ΔG_m^* as a function of ϕ_2 at two temperatures. At temperature T_1 the interaction parameter, χ, is negative or less than the critical positive value. The mixtures are all homogeneous since the slope of the curve (related to the chemical potentials of the components) is different for every value of the composition parameter, ϕ_2 . At temperature T_2 the interaction parameter is positive and exceeds its critical value. The inflexion points in the ΔG_m^* vs ϕ_2 curve correspond to the ϕ'_{2sp} and the ϕ''_{2sp} compositions lying on the spinodal curve (the loci of absolute instability for the mixtures). The inflextion point condition is

$$\left(\frac{\partial^2\Delta G_m^*}{\partial\phi_2^2}\right)' = \left(\frac{\partial^2\Delta G_m^*}{\partial\phi_2^2}\right)'' = 0 \quad \text{Equation 3.3-10}$$

The compositions ϕ'_{2sp} and ϕ''_{2sp} which lie on a common tangent to the ΔG_m^* vs ϕ_2 curve are the bimodal, equilibrated phase compositions.

Figure 3.3-4 illustrates the upper critical solution temperature (UCST) and lower critical solution temperature (LCST) phenomena, which may be observed in the binary mixture phase separations. A UCST occurs for endothermic (positive heat of mixing) mixtures. An LCST occurs for exothermic (negative heat of mixing) mixtures in which the positive χ value is the result of an unfavorable, negative local entropy of mixing.

Phase separation during an isothermal cure of a network forming matrix system containing a dissolved elastomer or thermoplstic yields a heterogeneous, toughened material. The phase separation occurs because of the positive value of χ increases as the molar weight (molar volume, V_1) of the matrix forming polymer increases during the cure.

$$\Delta G_m^* = RT[\phi_1 \ln \phi_1 + (\phi_2 / x)\ln \phi_2 + \chi \phi_1 \phi_2] \quad \text{Equation 3.3-11}$$

where ΔG_m^* is the Gibbs free energy of mixing per mole of segments, and χ is the Flory-Huggins polymer-solvent interaction parameter.

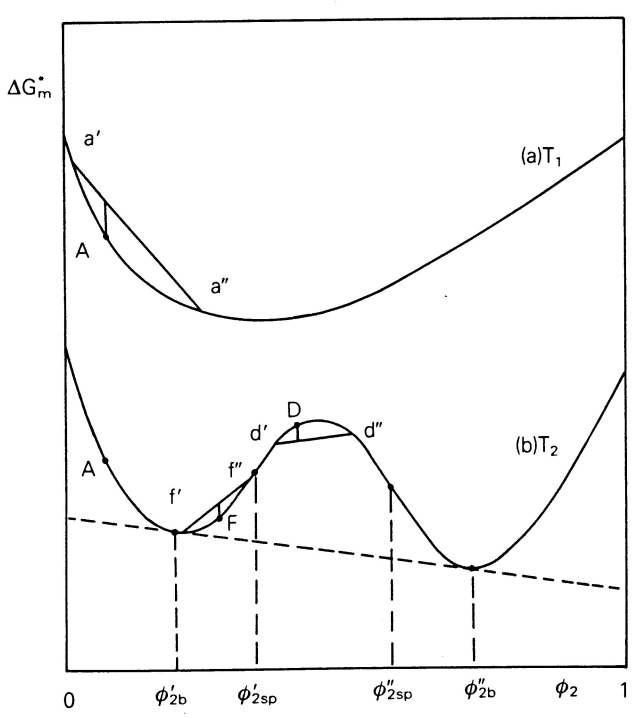

Figure 3.3-3 Schematic Illustration of the Variation of ΔG_m^* with ϕ_2 at two Different Temperatures (a) T_1 and (b) T_2 [55]

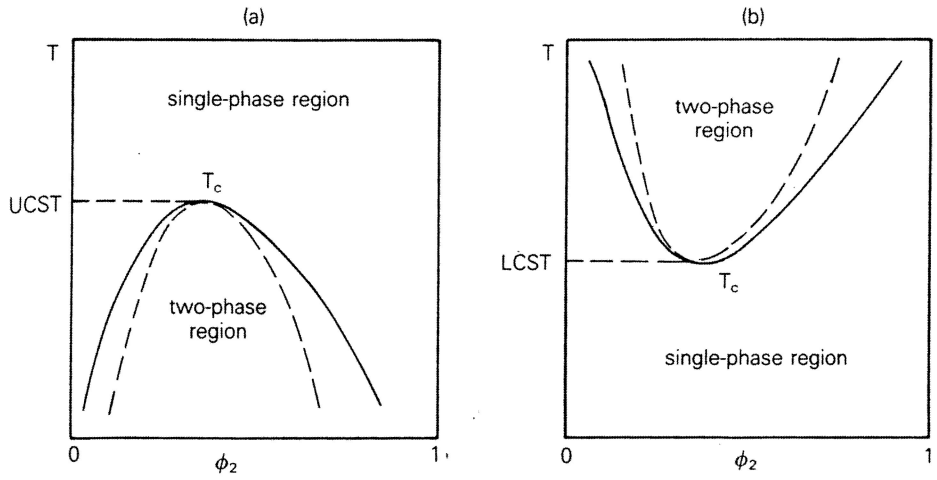

Figure 3.3-4 Illustration of Phase Diagrams for Polymer Solutions Showing Upper Critical Solution Temperature (top) and Lower Critical Solution Temperature (bottom). The Solid Lines are Binodals and the Dashed Lines are Spinodals.[55]

3.3.5 Kinetics Of The Cure [56]

The processing behavior of network systems is strongly determined by the kinetics of their polymerization reaction. High performance epoxy composites are generally produced by the autoclave lamination process. During the process, the consolidation of the preimpregnated ply is accompanied by polymerization reactions and rheological changes of the matrix that strongly influence the final properties and the quality of the laminates. The cure process is coupled with marked heat generation as a result of the exothermic nature of the thermosetting reactions. The relative rates of heat generation and transfer determine the values of the temperature and, therefore the values of the advancement of the reaction and the viscosity through the thickness of the composite. Isothermal and dynamic experiments conducted by differential scanning calorimetry (DSC) have been widely used for indirect determination of cure advancement in thermosetting systems.[57, 58]

Although the reactions occurring during the processing of thermoset-based composites are very complex, empirical kinetic equations have been successfully used to describe the general behavior of these systems. Considerable research activities have been reported in the field of epoxy resin and matrix cure. A complete review on the kinetic characterization of epoxy systems by differential scanning calorimetry (DSC) has been presented.[59]

Isothermal and dynamic experiments conducted by DSC are widely used for indirect determination of cure advancement in a thermosetting system. The analysis assumes that heat evolution during the polymerization reaction is proportional to the extent of reaction. DSC results are also used for the formulation and verification of theoretical and empirical kinetic models and for the calculation of the related parameters. To interpret DSC data, the degree of reaction (w) is defined as:

$$w = H(t) / H_T \qquad \text{Equation 3.3-12}$$

where H(t) is the heat developed during the reaction between the starting point and a given time t and H_T is the total heat developed during the cure and is calculated by integrating the total area under the DSC curve. The DSC thermogram gives the instantaneous generation of heat by the reactive system. The reaction rate is given by the expression

$$\frac{dw}{dt} = \frac{1}{H_T}\frac{dH}{dt} \qquad \text{Equation 3.3-13}$$

This information can be processed to construct a kinetic model that describes the degree of reaction as a function of time and temperature. When an overall kinetic process characterized by a generic degree of reaction (w) is assumed, the empirical kinetic equations for the cure process of thermosetting matrices are normally expressed in the form

$$\frac{dw}{dt} = Kf(w) \qquad \text{Equation 3.3-14}$$

Direct determination of the kinetic parameters are usually not attempted because of the complexity of the reaction mechanisms. A slightly more complex model was elaborated for the reactions of TGDDM+DDS systems:

$$\frac{dw}{dt} = (K_1 + K_2 w^m)(1-w)^n \qquad \text{Equation 3.3-15}$$

where K_1 and K_2 are the reaction constants and m and n are the reaction orders. The inclusion of a second kinetic constant allows consideration of the autocatalytic behavior observed in the polymerization reaction of TGDDM-DDS systems. The above equation can be considered a general empirical model for the description of the kinetic behavior of reactive matrices. It can be modified to account for the particular behavior of specific chemical systems. If the maximum reaction rate occurs at the starting point (time = 0)

then $K_2 = 0$ and the kinetic model corresponds to an n - order equation. Diffusion-control effects can be included in the kinetic model. In isothermal processes at low temperatures, the polymerization reactions are not completed. When the increasing glass-transition temperature (T_g) of the reactive system approaches the isothermal cure temperature, the mobility is strongly reduced and the reaction becomes diffusion-controlled and eventually stops.[62] A method to develop a kinetic model that includes the dependence between the final level of polymerization and the test temperature was described recently.[56] The final expression of the nth - order model is this case is

$$\frac{dw}{dt} = K(w_n - w)^n \qquad \text{Equation 3.3-16}$$

where w_n is the maximum degree of reaction reached by the reactive system at a given temperature. Equation 3.3-21 predicts that the reaction rate during an isothermal process will be zero when the degree of reaction becomes equal to w_m. The dependence of w_m on T can be obtained experimentally from isothermal DSC tests.

Equation 3.3-21 can be applied to interpret results of dynamic DSC tests performed at a constant heating rate because w_m is continuously growing with temperature and the rate constant (K) is a function of temperature. The value of the total heat (H_T) developed during the cure as assessed in the dynamic test is used as a reference value for the computation of w.

3.4 Toughening Of Network Systems.

3.4.1 Backcground

Highly crosslinked thermosets are an important class of high performance materials with good thermal, mechanical properties and excellent chemical resistance. Therefore, they are used for various applications such as matrix resins for composites, structural adhesives and electrical laminates. However it has long been recognized that as a result of their high crosslink density, thermosetting materials are often inherently very brittle and can fail prematurely when exposed to mechanical stress. At high strain rate or during high velocity impact, most conventional thermosets undergo brittle failure.

The development of a process called toughening of plastics, consisting of introducing small amounts of discrete rubber particles into rigid glassy thermoplastics such as PVC has made a significant contribution in the polymer industry.[63] When elastic domains are correctly dispersed in discrete forms throughout the matrix, the ductility, crack resistance and fracture energy or toughness can be greatly enhanced. Consequently, interest in using rubber to toughen crosslinked epoxy networks was developed consequently. Some of the research of this nature were reported as early as 1970.[64] During a toughening process, it is desirable to minimize the sacrifice in thermal properties and strength of the material.

Toughness may be defined as resistance to crack propagation under external mechanical stress. Fracture toughness or stress intensity factor (K_{1C}) and fracture energy or strain energy release rate (G_{1C}) can be used to assess toughness in polymeric materials. These terms will be discussed further in this section.

3.4.2 Toughening Mechanism

In order to improve toughness, the energy at a propagating crack tip must be dissipated effectively. Many different mechanisms have been suggested to explain the improved fracture toughness that may result from a multiphase microstructure of dispersed rubbery particles in a thermosetting system. The most important question is that to know whether the rubbery particle or the thermoset absorbs most of the energy and, if it is the matrix, whether the deformation mechanism involves the formation of crazes or plastic deformation. Figure 3.4-1 below shows a schematic representation of different toughening mechanisms involved in the fracture of multiphase rubber-toughened thermoset materials.

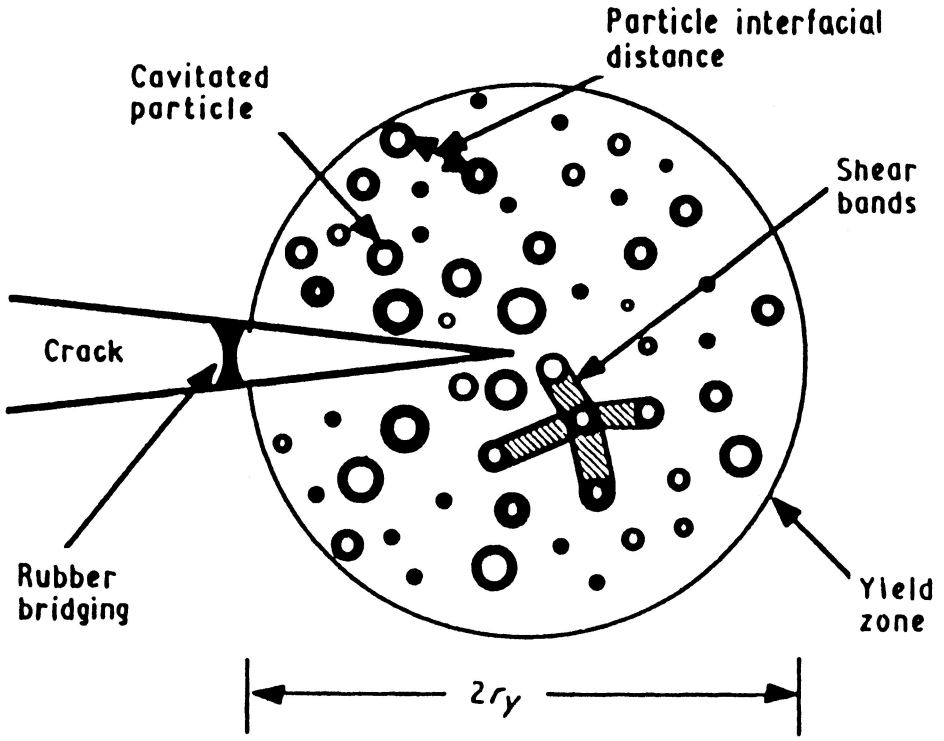

Figure 3.4-1 Schematic Representation of the Different Toughening Mechanisms Involved in the Fracture of Multiphase Rubber Toughened Epoxy polymers.[65]

After more than thirty years of investigations, two toughening mechanisms are widely accepted as providing the most important contributions. The first one is localized shear yielding, or shear banding, which occurs in the matrix around the rubber particles. The second mechanism is internal cavitation of the rubber particles or debond at the interface, which may then enable plastic void growth to occur in the matrix.[66] The relative importance of the toughening mechanisms may widely vary, depending upon the system involved[67] and the test rate and mode.[68]

3.4.2.1 Localized Shear Yielding

It has been suggested from finite-element stress analysis data that tensile stress concentrates in the matrix at equatorial areas of the rubber toughener (figure 3.4-2) for a rubber particle, which typically possesses a considerably lower shear modulus than the matrix, with a comparable bulk modulus.[66] Plastic deformation, particularly yielding, initiates from the point of maximum stress concentration. Then as the load is further increased, a band of shear-yielded material forms at an angle of approximately 45 degrees to the applied stress in the matrix. Crazing is difficult for systems of highly crosslinked structure. Because of the large number of particles involved the volume of thermoset matrix material that can undergo plastic yielding is effectively increased, compared with the single phase polymer. Consequently, far more irreversible energy dissipation is involved and the toughness of the material is improved.

3.4.2.2 Internal Cavitation.

The cavitation in rubber particles or at the rubber-matrix boundaries at the tip of the crack causes the redistribution of the stress and strain fields around the cavitated rubber particles. This in turn alters the stress that the surrounding matrix experiences. As a result of this, the fracture process is affected by the rubber particle cavitational event. The occurrence of cavitations in the rubber particles at the front of the crack serves to relieve the plane strain constraint to promote shear yielding of the matrix, and

acts as stress concentrators. The occurrence of these events depends largely upon the degree of interfacial adhesion at the rubber particle-matrix interface. There are two scenarios that relate to levels of interfacial adhesion. The use of a rubber with reactive end-groups resutls in a chemically bonded interface, i.e. high adhesion, and internal cavitation of the rubber particles is observed and can be shown by the increase of particle size

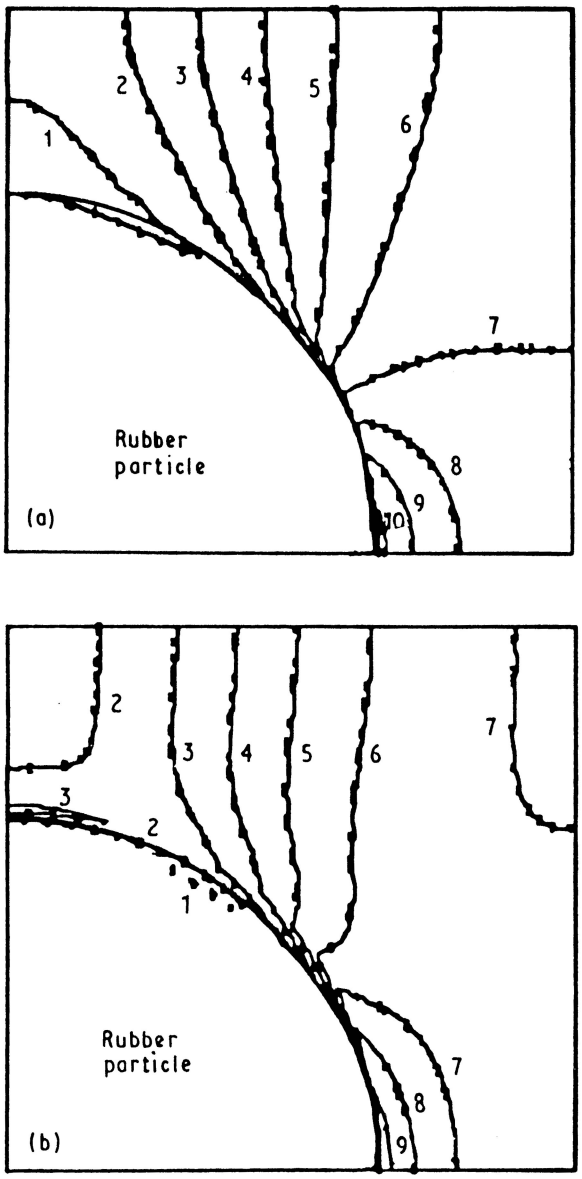

Figure 3.4-2 **(a) Distribution of Direct Stress σ_{YY}, at an Applied Strain of 0.001. (b) Distribution of the von Mises stress, σ_{vm}, at an Applied Strain of 0.001**.

Equivalent strain: 1/0.000; 2/0.56; 3/1.11; 4/1.66; 5/2.22; 6/2.77; 7/3.33; 8/3.88; 9/4/44; 10/5.00.

(Axisymmetric model; elastic analysis)[66]

after a fracture test.[69] On the other end, a rubber toughener that has non-reactive end-groups results in no chemical bonding at the interface and only a relatively weak adhesion, which arises solely from interfacial van der Waals forces or secondary interactions. Debonding of the particle from the matrix can be observed in this case. The importance of this type of cavitation mechanism is that the irreversible hole-growth process of the matrix can dissipate energy and contribute to the enhanced fracture toughness. This scenario has been studied, using holes instead of rubber particles for toughening polymer matrices. Some works have successfully studied the concept of microvoid toughening in polymers, either theoretically or experimentally.[70,71] The major difference between the pre-existing holes and the rubber particle cavitational event lies in the sudden buildup of an octahedral stress component upon the translucent rubber particles in the crack tip region.

3.4.3 Types of Toughening

Two strategies have been applied for toughening thermosetting materials: matrix flexibilization and dispersion of stress-concentrating microphase. Matrix flexibilization is achieved by introducing flexible segments with incident decrease in crosslink density. Because this approach may be associated with drastic softening of the matrix, it leads to improved toughness only at the expense of stiffness and thermal stability. As a consequence, the second approach represents the method of choice to promote toughness and to preserve high stiffness, strength and heat distortion temperature.

3.4.3.1 Rubber Toughened Systems

The incorporation of a second rubbery phase in a network system is usually accomplished through in situ phase separation during the cure process. The rubber is initially miscible with the resin and the curing agent. With the network formation, the

rubber phase separates from the thermosetting polymer and forms a multiple inclusion morphology.[72] The compatibility between the rubber and the matrix is very important. It has to be high enough for mixing at an initial stage and low enough for isolating out distinct rubber particles during the curing process. Typically, with a rubber volume fraction of 0.1 to 0.2, the fracture toughness may be increased by up to 10-20 times, in contrast with the lack of impact toughening observed for the direct blend of thermosets and rubbers. An important commercial illustration of this concept is the amine cured epoxies, toughened by carboxyl terminated butadiene-acrylonitrile (CTBN) copolymers.[73]

When a non-reactive rubber is used, the increase of fracture toughness is observed but not as high as an analogous toughener with reactive end groups. As previously mentioned, a good interfacial adhesion is important for effective toughening. The use of reactive rubbers or reactive elastomer prepolymers can achieve the greatest interfacial adhesion by chemically bonding with the matrix with the resulting improvement in the phase distribution. Traditional synthetic methods are used to prepare reactive rubbers.[74] The system of rubber materials often used include polybutadiene, carboxyl terminated butadiene-acrylonitrile (CTBN) and its epoxy or amine end capped adducts, silicone rubbers or their combinations.[75]

3.4.3.2 Thermoplastic Toughening

Using thermoplastics as dispersed toughening agents is a relatively recent approach, developed during the early 1980's. Two major reasons motivated the development of a new toughening system. The first reason arose from the consideration that rubber toughening adds soft inclusions into a stiff matrix, resulting in a reduction of standard mechanical properties. For example, both the tensile modulus and the yield strength are significantly reduced as it can be inferred from Figure 3.4-3. The second reason is that addition of soft inclusions into highly crosslinked systems does not provide significant improvements in toughness.[76] With thermoplastic toughening, a tough, ductile and thermally stable polymer such as polysulfone (PSF), polyether sulfone (PES),

polyether imide (PEI), polyether ketone (PEK), polycarbonate (PC) and some polycarbonate-polydimethyl siloxane (PC-PDMS) copolymers can be used to modify high performance thermosetting systems such as epoxy networks (especially tri- or tetra functional ones),[78,79] cyanate esters,[80] and bismaleimides.[81,82] In most of these cases, improvements in toughness along with retention of high modulus and thermal stability can be attained.

Similar to the case of rubber systems, thermoplastic systems are often obtained by dissolving the thermoplastic modifier in the matrix resin (sometimes a cosolvent may be needed) and then, finely dispersed thermoplastic particles phase-separate during the process of curing. The resulting microstructure consists of two phases: one phase which is predominantly the

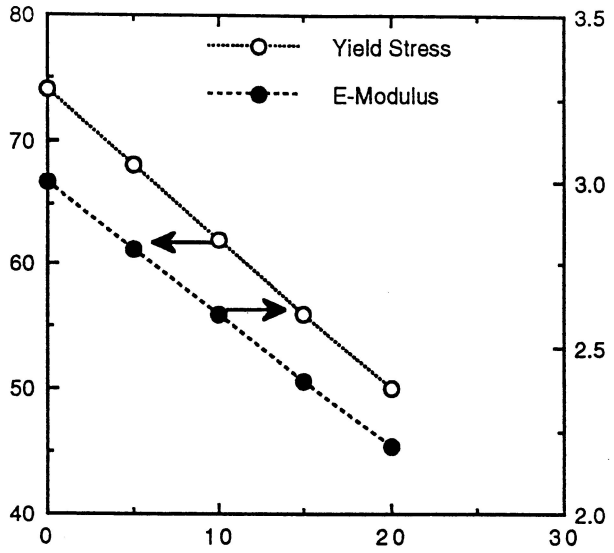

Figure 3.4-3 Mechanical Properties of a CTBN-modified Epoxy (DGEBA-piperidine).[77] Rubber Modification Reduced both the Yield Strength and the Modulus.

network matrix and the other phase which is rich in the thermoplastic polymer. Unlike the rubber toughening systems, the morphology of the thermoplastic modified networks can be particulate, continuous or even phase inverted. It has been reported that a co-continuous phase morphology, which is characteristic of spinodal decompostion[83] or a phase inverted morphology, where discrete thermoset particles are surrounded by a continuous phase of the thermoplastic polymer will provide optimum toughness.[80,81] The desired morphology can be obtained by systematically varying the modifier backbone structure or volume fraction. Co-continuous or inverted phases usually cause the loss of excellent chemical resistance of the crosslinked thermoset. However, in the case of reactive, chemically stable thermophastics, there is little reduction in the chemical resistance of the system.[81]

Toughening thermosetting polymers using commercial non-reactive thermoplastic modifiers has achieved a considerable success, but not always.[84,85] One of the reported successful works was that of modifying the network of tetraglycidyl-4,4'-diamino-diphenyl methane (TGDDM) cured with 4,4'-aminophenyl sulfone (DDS) with a commercially available poly (ether imide), Ultem 1000 (General Electic Company). The modified system resulted in a phase separated morphology with a dynamic loss modulus at 200-212°C corresponding to the glass transition temperature of the poly(eitherimide) phase. There was a linear increase in fracture toughness with the incorporation of the poly(ether imide), up to 25 percent by weight, as indicated by three point bending fracture tests.

The importance of introducing reactive functional groups on the structure of the thermoplastic modifier was suggested an demonstrated.[87] The reactive groups can exist at the ends of a polymer chain or as pendent groups[88]. For the same backbone and comparable molecular weights, thermoplastic modifiers with reactive end groups provide much better improvements in fracture toughness than do their non-reactive homologs. This is attributable to better interfacial adhesion in the former case, brought about by chemical bounding at the interface.[81,82] In some circumstances, the improvement in interfacial adhesion by the thermoplastic modifier's reactive end group can cause a change in the failure mechanism of the modified thermoset. In one study, it was shown that the topography of the fracture surface of the phase-inverted reactive thermoplastic

modified bis maleimide resins exhibited cleaved thermoset spheres (the thermoset was the limiting phase of the fracture), whereas the fracture surface of non-reactive phthalimide end capped polysulfones indicated that no thermoset spheres had been cleaved (the interphase between the separated domains was the fracture path).[81]

However, toughening networks with thermoplastic modifiers has not always been successful and the mechanisms and controlling parameters are still not well understood. The specific requirements for achieving optimum results, for example, the morphology type, the particle size, particle-matrix adhesion and the mechanical attributions, have not been clearly determined. There is still a considerable amount of work left to be done in this area.

3.4.4 Parameters that Determine Tougheness in Modified Networks.

Many interrelated parameters govern toughness in dispersed network systems. Those parameters can be grouped into two sets on the basis of the backbone architecture (molecular structure, spatial arrangement, compatibility) and processing or manufacturing factors.

The morphological parameters include:

- Phase structure
- Volume content of the particles
- Distance between the particles
- Shape and size of the particles
- Interfacial structure.

The micromechanical parameters include:

- Ductility of the matrix
- Crosslink density of the matrix
- Local stress concentration
- Stress between the matrix and the particles.

(This depends on the Young's modulus and the Poisson's ratio of the matrix and the particles).

The influence of the volume fraction of the modifying particles has been investigated.[89 90] Although the size and the particle morphology differed between studies, the toughness increased with increased rubber fraction and the most efficient toughening cases were observed for volume fractions between 25% and 40% of particles.

There was an optimum size for discrete toughener particles in each system. Some studies differentiated the effects of different toughening mechanisms.[66] If the toughening effect is based mainly on the formation of crazes, the particle diameter is of primary importance. Particles act as stress concentrators and directly initiate the craze. There are critical diameters, which depend only on the ability of the matrix to form crazes. The optimum particle diameter corresponds to the typical craze thickness in the matrix material. Relatively larger rubber particles are favored for toughening by the mechanism of microcavitation initiated inside the rubber. However, further increase of the modifier after a critical value showed little improvement in fracture toughness.[91]

For a thermosetting system which forms little craze, the particle size is relatively less important. The distance between the particles is of primary importance for shear deformation mechanisms. There is a critical minimum and a maximum interparticle distance for effective toughening. Yielding occurs only if the distance between the cavitated particles falls in this range. Particle cavitation enables a change in the stress from a triaxial situation to a more monoaxial one and in this case, a smaller distance between the cavitated particles is desirable.

Nearly all of the studies reported in the literature have been concerned with well bonded particles, a consequence of the chemical reactivity of the toughener. The intrinsic adhesion across the particle-matrix interface needs to be sufficiently high in order to provide effective stress transfer and decent toughening effect.

The effect of molecular weight between crosslinks (M_C) in the thermoset matrix has been investigated.[92,93] In summary, increasing the degree of crosslinking (i.e., decreasing M_C) significantly affects the matrix toughness by limiting the degrees of freedom for shear and plastic deformation. An increase in M_C produces an increase in the value of the fracture energy of the neat material and a more dramatic effect for the rubber toughened system. This is attributable to the large number of energy dissipating shear zones initiated by the rubber particles and the effect of increased ductility. It has been

suggested that only epoxies with a low crosslink density (i.e., large M_C) can be effectively toughened.[76]

3.4.5 Estimation Of Toughness

One approach for characterizing fracture resistance is by applying an energy argument balance to a linearly elastic cracked body of thickness B subjected to an applied load. It is then possible to determine the critical strain energy release rate G_C for fracture to occur

$$G_c = \frac{P_c^2}{2B}\frac{\partial C}{\partial a} \qquad \text{Equation 3.4-1}$$

where C is the compliance of the cracked body for a given crack length, P_C the critical load for the onset of crack propagation and a is the crack length. Equation 3.4-1 represents the basis for most G_C calculations with the basic requirement being a knowledge of the variation of specimen compliance with crack length. The compliance-crack length dependency can be determined either analytically or experimentally depending upon the complexity of the test specimen.

There are three basic modes of loading encountered in operational service, denoted I, II and III (figure 3.4-4). Mode I corresponds to simple cleavage or tensile opening, Mode II corresponds to inplane shear and Mode III corresponds to out-of-plane shear. The fracture energies associated with I, II and III modes of deformation are denoted G_{IC}, G_{IIC} and G_{IIIC} respectively. Mode I deformation is technically the most important of the three since it represents the most commonly encountered loading condition and generally has the lowest associated fracture energy. Mode I type loading is also much more readily simulated in laboratory conditions.

There are several varieties of fracture test specimen geometries, many of which were developed for specific applications. Two widely used configurations are the simple edge notch bend (SENB) and the compact-tension. The measurement procedures can be found in the American Society of Testing and Materials manual (ASTM D5045). The

dimensions of the samples are 3.2 mm X 6.5 mm X 38 mm. A notch of approximately 0.5 mm depth is made with a saw. An extremely sharp crack is initiated by first cooling a razor blade in liquid nitrogen and tapping the blade within the notch using an aluminum bar.[81]

Other methods used to estimate the fracture toughness include Mode II strain energy release rate G_{IIC}[94], tensile properties[95], (modulus, yield strength and percentage strain at break), storage and loss moduli measure by DMA[81] and dielectric relaxation measurements.[96]

Another approach frequently used to characterize the fracture resistance of materials is the critical stress intensity factor analysis. In this case, the stress field around a sharp crack in a linear elastic material can be defined by a stress intensity factor K_I (for Mode I loading).

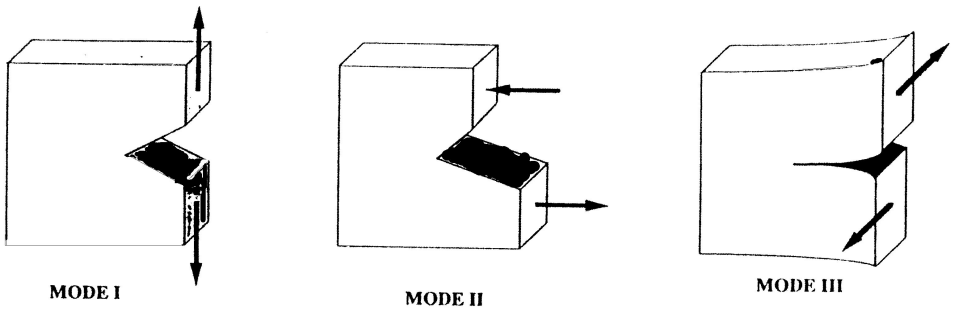

Figure 3.4-4 The three basic modes of loading.

The general form of the stress intensity factor is given by:

$$K_I = Y\sigma\sqrt{a} \quad \text{Equation 3.4-2}$$

where Y is a geometrical factor taking account of the specimen size, a is the crack length and σ the applied nominal stress. It is assumed that fracture occurs when K_1 reaches a critical value termed K_{IC}, a material property for a given test condition (temperature, rate…). K_{IC} for a finite plate is given by:

$$K_{Ic} = Y\sigma_c\sqrt{a} \quad \text{Equation 3.4-3}$$

where σ_c is the applied stress at the onset of fracture. In order to determine K_{IC} it is therefore necessary to know the geometrical factor Y for the particular geometry employed. Such factors have been established for a wide range of geometries containing cracks.[97]

3.5 Dielectric Monitoring Of The Cure

3.5.1 Background

The dielectric permittivity of a medium measures the polarization of the medium per unit applied electric field. The permitttivity of free space, ε_O has the value 8.85 X 10^{-}

^{14} Farads/cm. The dielectric properties of a medium are usually expressed in relation to ε_O. That is, the permittivity of a medium is written $\varepsilon'\varepsilon_0$, where ε' is the relative permittivity, also referred to as the dielectric constant of the medium. We must however bear in mind that the dielectric "constant" changes with the temperature and the progress of the curing reaction.[99]

The dielectric loss factor arises from two sources: energy loss associated with the time-dependent polarization, and bulk conduction. The loss factor is written $\varepsilon''\varepsilon_0$, where ε'' is the relative loss factor. The loss tangent of a medium, denoted by tan δ, is defined as the ratio $\varepsilon''/\varepsilon'$.

Dielectric measurements have been shown to be effective in monitoring curing of epoxy resins.[100, 101, 102] In those studies, changes in the electrical properties are related to the increase in the viscosity of the epoxy resin, thereby inferring that the increase in the glass transition temperature with time allows modeling of the isothermal curing process by the Vogel-Fulcher-Tamman equation that will be discussed later in this chapter. A somewhat different but more general treatment is based upon the premise that in all addition reactions the growth in the size of a macromolecular addition slows the rate of the very chemical reactions by which it grows, and that this continues until neither chemical reactions nor molecular diffusion occur at a perceptible rate.[103, 104] In this way the curing of an epoxy resin is pictured as a negative feedback process between chemical reactions and molecular diffusion, which ultimately irreversibly vitrifies or solidifies a liquid. Thermodynamic evidence for this vitrification has been provided from careful measurements of heat capacity.[105] There is an irreversible, abrupt decrease in the heat capacity of an epoxy resin over a narrow range of time, which remarkably resembles the (reversible) decrease in heat capacity observed on super cooling a liquid and a rubbery polymer through their glass transition temperature, T_g. The time at which this decrease occurs becomes less when the reaction occurs at higher temperature.

One problem that has plagued dielectric monitoring of epoxy curing has been the overwhelmingly empirical nature of the research, hampered by inadequate models with which to interpret the data. Furthermore, in only a few cases have the dielectric measurements been quantitatively coupled with measurements of other properties of interest, and often, experimental details that turn out to be important in hindsight, were

inadvertently overlooked during the original work. As a result, many well-intentioned experiments have somehow failed to provide that cumulative insight into fundamental issues that must ultimately accompany the successful scientific application of a measurement method.[99]

Dielectric measurements on curing systems are usually done with sinusoidal excitation at specific frequencies of interest. The frequency dependent dielectric response of a linear time-invariant sample can be obtained by applying a step-change in voltage, measuring the resulting current waveform at a series of time intervals following the step, then computing the frequency dependent dielectric properties from the Fourier transform of the current waveform.[106] The potential advantage of this approach is the use of digital signal processing methods to reduce the time needed to obtain data at ultra-low frequencies (to 10^{-4}Hz), but in practice, the duration of the step waveform must be short enough to keep the sample time-invariant throughout one measurement cycle. The total time for a measurement, in this case, is determined, first by the length of time one must hold the voltage at some initial voltage (e.g., zero) before applying the step (to assure zero initial polarization charge), and second, by the length of time one must hold the voltage at its non-zero value to obtain enough data for the lowest frequency of interest. For typical thermoset cures, reaction rates usually limit the lowest useful frequency to about 0.1 Hz..

3.5.2 Instrumentation

3.5.2.1 Capacitance And Impedance Bridges.

Whether using parallel plate or comb electrodes, the basic measurement involves determining the admittance between the electrodes under sinusoidal steady-state conditions (the only exception is the microdielectrometer). Many early studies were made with general purpose capacitance bridges designed for measurements of capacitors with small loss tangents. Because thermosetting resins become relatively conductive when they are heated, particularly early during the cure, such capacitance bridges could not be used without the addition of an insulating (or blocking) layer between at least one of the electrodes and the sample to lower the overall loss tangent of the sample to within the instrument range.

The effectiveness of these instruments for dielectric monitoring studies depends on sensitivity and accuracy. The sensitivity is related to the minimum resolvable phase angle which, for general cure studies, should ideally be less than 0.10. Unfortunately, actual sensitivity in use depends strongly on the measurement frequency, the admittance of the sample, the details of the cabling and shielding and the electrical noise level of the environment.

3.5.2.2 Microdielectrometry.

Microdielectrometry was introduced as a research method early in the last decade.[107 108] The microdielectrometry instrumentation combines the pair of field-effect transistor on the sensor chip with external electronics to measure the transfer function $H(\omega)$ that will be discussed later in this chapter. Because the transistors on the sensor chip function as the input amplifier to the meter, cable admittance and shielding problems are greatly reduced. In addition, the use of a charge measurement rather than the admittance measurement allows the measurements to be made at arbitrarily low frequencies.

Based on the accuracy of the amplitude and phase measurement electronics, the ε" sensitivity of the microdielectrometer is about 0.0l,[109] which for a medium having a dielectric permittivity of 4 corresponds to a $\tan\delta$ sensitivity of less than 0.03. At a frequency of 0.1 Hz, and ε" sensitivity of 0.01, this corresponds to a conductivity sensitivity of about 1×10^{-16} $(\Omega\text{-cm})^{-1}$. However the accuracy of the

microdielectrometry calibration at these conductivity levels has not been rigorously established.

3.5.3 Application Of Dielectric Monitoring To Our Research

In this work, we were interested in aquiring data on physical changes related to curing of epoxy resins. The time to vitrification could be determined directly from the the plots as we would show further in this section. Given that no electrical phenomena are associated with the gelation process,[99] the determination of the gel point relied on approximations, several of which are published elsewhere[110-113].

During the synthesis of epoxy resins such as TGDDM or the bisphenol A epoxy resin (DGEBA), epichlorohydrin and a strong base are needed. Not all of the base is consumed during the reaction and even after extensive purification, ions still remain in the resin, usually in the order of 10 ppm. These ions (Na^+ and Cl^- for example) are capable of of moving toward oppositely charged electrodes, and this is the origin of most of the dc conductivity in our system. Traces of ions, even in the order of 10 ppm are sufficient to produce dielectric signals that can be quantified. Figure 3.5-1 depicts the generation of a dc conductivity in the presence of an electric field. It can be inferred from this figure that ions migrate toward the electrode of opposite charge. As the system reacts and viscosity builds up, the mobility of the ions becomes restricted, which decreases the conductivity (Figure 3.5-2). The molecular dipoles also react to an applied electric field (Figure 3.5-3). When the system is going through its glass transition, a process which is the reverse of that in figure 3.5-2 occurs. The dipoles become very slow and do not respond to an electric field oscillating at any particular frequency, and thus they are essentially locked into a random orientation.

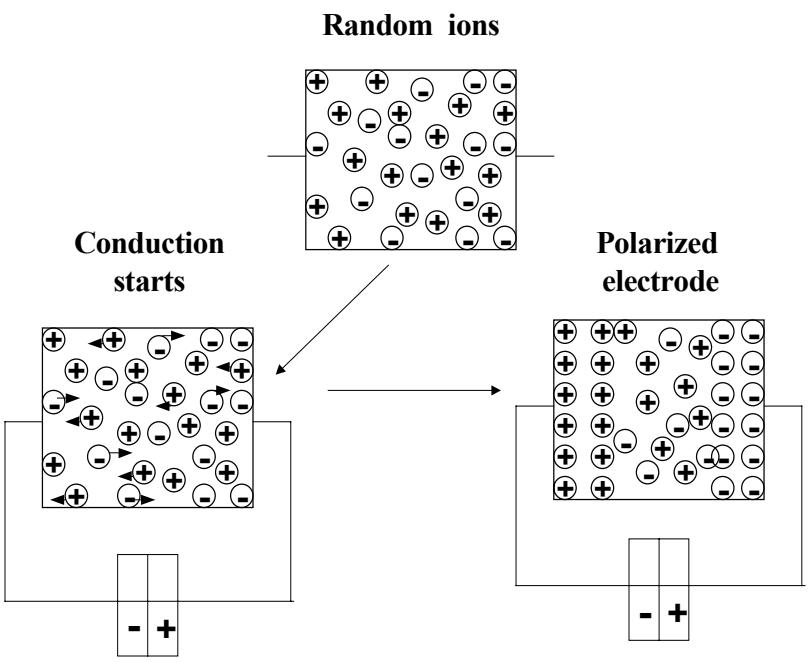

Figure 3.5-1 **After the Electric Field has Been Applied Conduction Begins and a Polarized Electrode is Formed**

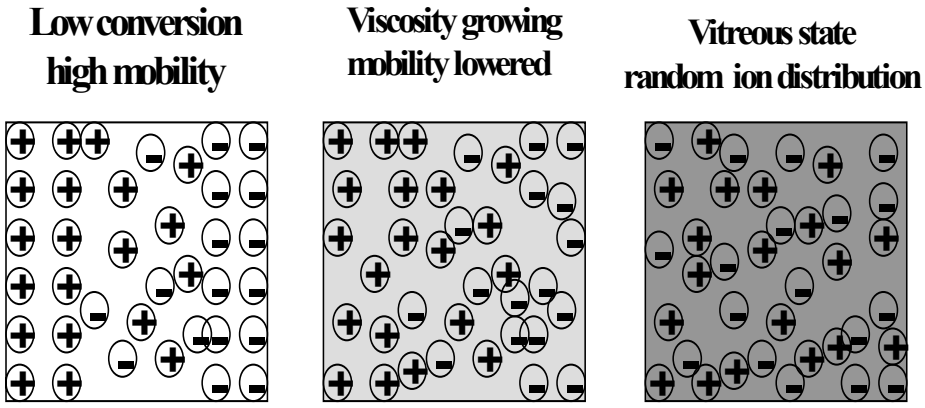

Figure 3.5-2 **Loss of Conductivity as a Function of Viscosity During Curing Process**

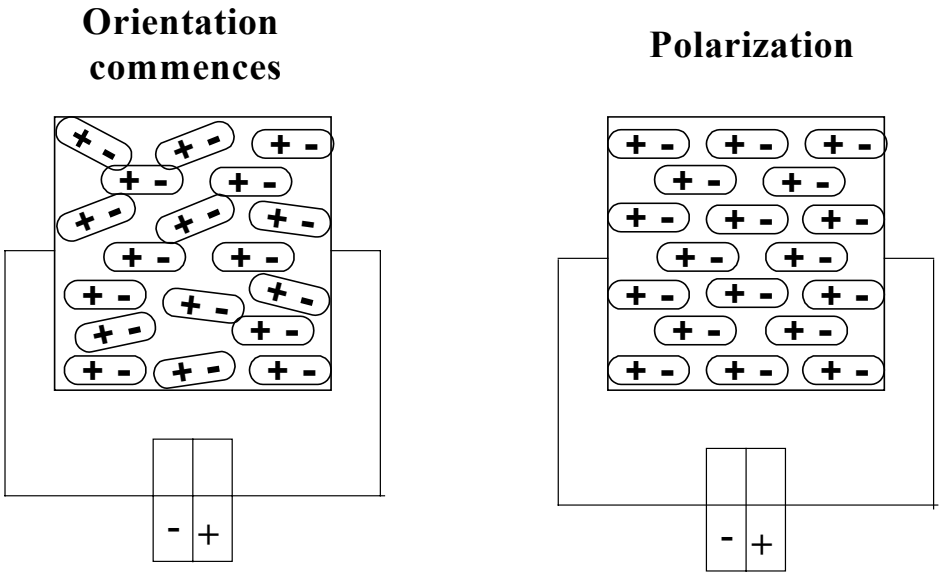

Figure 3.5-3 **Changes in Dipole Orientation as Electric Field is Applied:**

Relaxation Time Changes During Cure Process

In addition to phenomena that arise from dipolar relaxation, ions may also contribute to both the dielectric loss and the dielectric permittivity. Ions are ordinarily present in most epoxy resins. In the production of diglicidyl ether of bisphenol A as well as other epoxy resins NaCl and other ions occur as side products. Even after considerable purification efforts those ions remain present as impurity in the uncured resin. In addition to the resin ions, curing agents also produce ions, such as ammonium and hydroxyl ions in amines and anhydrides and hydrogen and hydroxyl ions in alcohols. Those ionic impurities altogether greatly contribute to the ionic conductivity according to the following equation:

$$\sigma = \sum_i n_i z_i \mu_i \qquad \text{Equation 3.5-1}$$

Where μ_i is the concentration of ions with ionic charge z_i and mobility μ_i. μ_i is related to the inverse of the viscosity according to Stokes' law[xx]. Assuming that n_i remain constant during the curing process, the dc conductivity σ is inversely proportional to the viscosity and decreases as the curing reaction proceeds[xx].

It seems however that this is an over simplification of dielectric phenomenons in curing networks[xx], because while the viscosity approaches an infinite value at gelation, measurable ionic and molecular motion still persist. It had been shown that the decrease in ionic conductivity is more related to the difference ($T-T_g$) which itself rapidly decreases as the curing reaction proceeds. Thus after approximately 40% conversion the conductivity becomes more sensitive to changes in Tg with time.

Several empirical expressions have been shown to relate ionic conductivity to curing parameters. One expression that is commonly used[xx,xx] is shown below:

$$\sigma_0(T,t_c) = \sigma_0(T,t_c \to 0)\left[\frac{t_{gel}(T) - t_c(T)}{t_{gel}(T)}\right]^{x(T)} \qquad \text{Equation 3.5-2}$$

It can be inferred from equation 3.5-2 that as x(T) increases the drop in conductivity becomes considerable. This expression can be used to determine of t_{gel} for difunctional

epoxy resins. Another expression that relates changes in conductivity to physical events during the cure cycle is the following[99]:

$$\sigma(T,t_c) = A(T)\exp\left\{\frac{-B(T)}{t_0(T)-t_c}\right\} \qquad \text{Equation 3.5-3}$$

A(T), B(T) and t_0 are empirical fitting parameters. This expression is the well known Vogel-Fulcher (VF) equation with times replacing temperatures. It basically describes the change in viscosity (conductance) as a point of singularity (t_0(T)) is approached. This equation leads to a "t_0" which is closer to a vitrification time than a gelation time, because the VF equation is usually applied to the glass transition phenomena. It can be inferred from this equation and experimental results that high conductance still persists after gelation and even shortly before vitrification (Figure 3.5-4). Given that equation 3.5-3 gives better approximation to to the gel point as compared to equation 3.5-2, the former will be used in calculating gelation time in this study. From the plots of dielecric loss versus curing time, vitrification time will be identified and used in creating time-temperature-transformation (TTT) diagrams in this work. Details for this inference are beyond the scope pf this work.

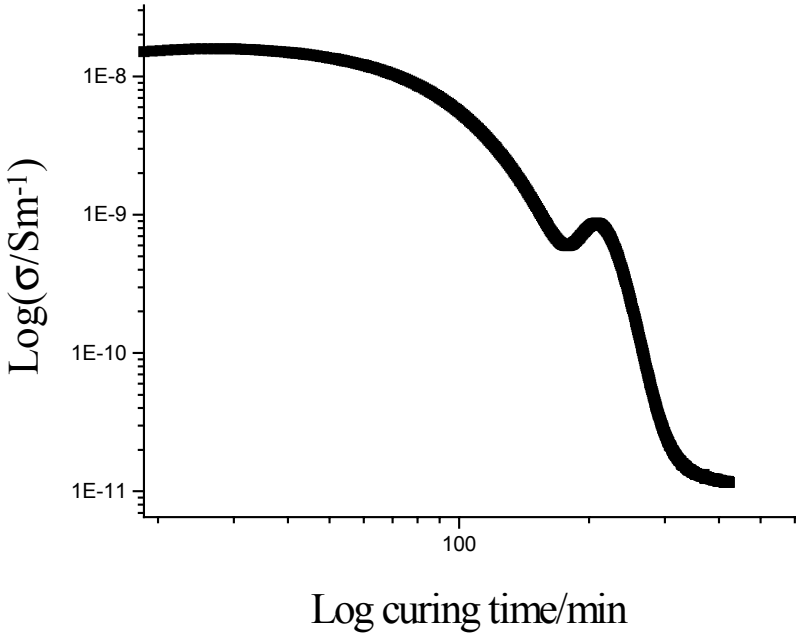

Figure 3.5-4 Conductivity Changes as Network is Formed.

(The peak on the right is the vitrification peak.)

3.6 References

1. Sherman, S., J. Gannon, G. Buchi and W. R. Howell, Encyclopedia of Chemical Technology (3rd Edit.), M. Grayson, Ed., John Wiley & Sons, New York, Vol. 9, 267-290, 1980.
2. Delides, C. G. , A. S. Vatalis, P. Pissisand R. A. Pethrich (1993) *J. Macromol. Sci. – Phys*., B32(3), 261-274.
3. Cowie, J. M., (1991) Polymers: Chemistry and Physics of Modern Materials, Blackie and Son Limited, Glasgow.
4. Bauer, R. S., 34th Int. *SAMPE* Symp., **34**, 1889 (1989).
5. Gritter, R. J. (1967), The Chemistry of the Ether Linkage, Ch. 9, Section II, ed. Patai, S. Interscience Publishers, pp. 381-390.
6. Lewars, E. G. (1984), Comprehensive Heterocyclic Chemistry, ed. Katritsky, A.R. and Rees, C. W. Vol 7, Section 5.0.5.4, ed. Lwowski, W. Pergamon Press, Oxford, pp. 114-118.
7. Tanka, Y. (1988), Epoxy Resins, Chemistry and Technology, 2nd edition, Ch. 2, ed. May, C. A. Marcel Dekker, New York, pp. 735-742.
8. Peters, D. (1967), The Chemistry of the Ether Linkage, Ch. 1, ed. Patai, S. WileyK-Interscience, New York.
9. Sandler, S. R. and W. Karo (1977), *Polymer Synthesis*, Vol. II, Ch. 3, pp. 75-113, Academic Press, New York.
10. Kilner, E. and D. M. Samuel (1960) *Applied Organic Chemistry*, p. 54, Macdonald and Evans.
11. Faith, W. L., D. B. Keyes and R. L. Clark (1965), Industrial Chemistry, 3rd edition,l p. 404, John Wiley, New York.
12. McAdams, L. V. and J. A. Gannon, (1986), Encyclopedia of Polymer Science and Engineering, J. I. Kroschwitz, Ed., John Wiley & Sons, New York, Vol. 6, pp. 322-382.

13. Oyanguren, P.A., and R.J.J.Williams (1992) *Polymer* 33(11), 2376.
14. Potter, W.G. (1970) Epoxide Resins, Chap. 2-4, Springre-Verlag, New York.
15. Podzimek, S., I. Dobas, S. Svestak and J.Horalek (1990) *J. Appl. Polym. Sci*., 41, 1161.
16. Liu, W., E. M. Pearce and T. K. Kwei (1985) *J. Appl. Polym. Sci.* 30, 2907.
17. Scanlan, J.T. (1935) *J. Amer. Chem. Soc.* 57(5).
18. Boutevin, B., J. J. Robin and C. Roume (1995) *Eur. Polym. J*. **31**, 313.
19. Ghaemy, M., N.C.Billingham and P.D.Calvert (1982) *J. Polym. Sci. Polym. Lett.*20, 439-443.
20. Dusek, K. (1986) *Adv. In Polym Sci.* 75, 9-12.
21. Carothers, W.H. (1936) *Trans. Far. Soc.* 32, 39-53.
22. Pinner, S. H. (1956) *J. Polym. Sci.* 21, 153-157.
23. Flory, P.J. (1941) *J. Am. Chem. Soc.* 63, 3091-96.
24. Stockmayer, W.H. (1953) *J. Polym. Sci.* 9, 69.
25. Stockmayer, J. W.H. (1955) *J. Polym. Sci.* 11, 424.
26. Macosko, C. W. and D. R. Miller (1976) *Macromolecules* **9**, 199-206.
27. Dannenberg, H. and C. A. May (1969) in Treatise on Adhesion and Adhesives, R. L. Patrich, Ed. Marcel Dekker, New York, Vol. 2, Chap. 2.
28. Ellis, B. (1993) Chemistry and Technology of Epoxy Resins, Blackie Academic & Professional, Chapman & Hall.
29. Halewood, P. (1962) British Patent 886, 767.
30. Lee, J. M. and J. C. Winfrey (1966) U. S. Patent 3, 236, 895.
31. Seeger, N.V. and E.E. Fauser (1954) U. S. Patent 2,683,730.
32. Husbands, M.J. (1987) in Resins for Surface Coatings, Ed. Oldring, P. and G. Haywood, SITA Technology III, 63-167.
33. Fish, W., W. Hofmann, J. Koskikallio, (1956*), J. Appl. Chem. (London)*, **6**, 429.
34. Fish, W. and W. Hofmann (1954) *J. Polym. Sci.*, **12**, 497.
35. Matejka, L., J. Lovy, S. Pokorny, K. Bouchal and K. Dusek (1983*) J. Polym. Sci.: Part A: Plym. Chem.*, **21**, 2983.
36. D. Schecter, L. and J. Wynstra (1956) *Ind. Eng. Chem.*, **48**, 86.
37. Narracott, E.S. (1953) *Brit. Plast.* **26**, 120.

38. Harris, J.J. and S.C. Temin (1966) *J. Appl. Polym. Sci.* **10**, 523.
39. Landua, A.J. (1964) *Org. Coat. Plast. Chem.* **24**(2), 299.
40. Arnold, R.J. (1964) *Mod. Plast.* **41**, 149.
41. Hickner, JR.A. and A.R. Meath (1992) in Reaction Polymers, W.F.Gum, W.Riese and H.Ulrich,Eds, Hanser (Oxford Univ. Press), New York, Chap II (Section 5).
42. Gillham, J.K. (1986) *Encyclopedia of Polymer Science and Engineering,* 2nd edition, John Wiley, New York, pp. 519-524..
43. Gillham, J.K. (1986) *Polym. Eng. And Sci.* **26**(20), 1429.
44. Boyer, R.F. (1963) *Rubber Chem. Tech.* **36**, 1303.
45. Boyer, R.F. (1977) *Encyclop. Polym. Sci., Techn.* **11**, 745.
46. Oleinik, E.F. (1981) *Pure Appl. Chem.,* **53**, p. 1567.
47. Oleinik, E.F. (1986) *Adv. In Polym. Sci., Resin and Composites IV, 73,* Springer-Verlag, New York.
48. Salamatina, O.B. (1983) *Vysokomol. Soedinl*, **25A**, 179.
49. Morgan, JR.J. and J.E. O'Neal (1977) in Chemisktry kand Properties of Crosslinked Polymers, Labama, S.S., Editor, 289 Academic Press, New York.
50. Chan, L.C. H.N. Nae and J.K. Gillaham (1984), *J. Appl. Polym. Sci.* **29**, 2831.
51. Enns, J.B. and J.K. Gillham (1983) *J. Appl. Polm. Sci.*, **28**, 2831.
52. Gillham, J.K. (1981) *Am. Chem. Soc. Prepr. Org. Coat. & Plast. Chem.* **44**, 185.
53. Flory, P.J. (1942) *J. Chem. Phys.,* **10**, 51.
54. Huggins, M.L. (1942) *J. Phys. Chem.***, 46**, 151.
55. Young, R.J. and P.A. Lovell (1991) Introduction to Polymers 2nd ed. p. 143, Chapma & Hall, London.
56. Kenny, J.M., A Trivisano and L. Nicolais (1993) Toughened Plastics I: Science and Engineering, C. Keith Riew and A. J. Kinloch, editors, American Chemical Society, Washington, D.C.
57. Kenny, J.M., A Maffezzoli, L. Nicolais (1990) *Comp. Sci. Tech.*, **38**, 339.
58. Kenny, J.M., A. Apicella and L. Nicolais (1989) *Polym. Eng. Sci.,* **29**, 972.
59. Barton, J.M. (1985) Epoxy Resins and CompositesI; Dusek, K., Ed., Advances in Polymer Science 72, Springer-Verlag, Berlin.
60. Stark, E.B., J. Seferis, A. Apicella and L. Nicolais (1983) *Thermochim. Acta,* **77**, 19.

61. Mijovic, J., J. Kim, and J. Slaby (1984) *J. Appl. Polym. Sci.* 29, 1449.
62. Enns, J.B. and J.K. Gillham (1983) *J. Appl. Polym. Sci.* **28**, 2567.
63. Seymour, R.B. (1993) Toughened Plastics I, p. 13. C.K. Riew and A.J. Kinloch, editors, American Chemical Society, Washington, D.C.
64. McGarry, F.J. (1993) Toughened Plastics I, p. 171. C.K. Riew and A.J. Kinloch, editors, Americal Chemical Society, Washington, D.C.
65. Huang, Y. and A. J. Kinloch (1992) *J. Mater. Sci.* **27**, 2763.
66. Huang, Y. and A. J. Kinloch (1992) *Polymer*, **33**, 1330.
67. Michler, G.H. and J.U. Starke 91996) Toughened Plastics II, p. 251. C.K. Riew and A.J. Kinloch, editors, American Chemical Society, Washington, D.C.
68. Julien, O., lP. Beguelin, L. Monnerie and H.H. Kausch (1996). Toughened Plastics II, p. 233, C.K. Riew and A.J. Kinloch, editors, American Chemical Society, Washington, D.C.
69. Huang, Y. and A.J. Kinloch (1992) *J. Mater. Sci. Lett.*, **11**, 484.
70. Bagheri, B. and R.A. Pearson (1995) *Polymer*, **36**, 4883.
71. Sue, H.J. and A.F. Yee (1996) *Polym. Eng. Sci.,***36**, 2320.
72. Lindsay, C.I., S.D. Jenkins, G.T. Emmerson and P.T. McGrail (1996) *Macromolecular Symposia,* **112**, 99.
73. Buckley, W.O. and K.J. Schroeder (1990) Engineered Materials Handbook, Vol. 3, p. 184-186, ASM International, Metals Park, Ohio.
74. Mulhaupt, R. (1996) Polymeric Materials Encyclopedia, p. 7370, J.C. Salamone, edutor, CRC Press, Boca Raton.
75. Mulhaupt, R. and U. Buchholz (1996) Toughened Plastics II, p. 75. C.K. Riew and A.J. Kinloch, editors, American Chemical Society, Washington, D.C.
76. Sue, J.H. (1993) *Polym. Mater. Sci. Eng.,* **70**, 256.
77. Pearson, R.A. (1993) Toughened Plastics I, p. 405, C.K. Riew and A.J. Kinloch, editors, American Chemical Society, Washington, D.C.
78. Yoon, T.H., S.C. Liptak, D.B. Priddy and J.E. McGrath (1994) *J. Adhesion*, **45**, 191.
79. Hedrick, J.L., I. Yilgor, G.L. Wilkes and J.E. McGrath (1985) *Polymer Bulletin,* **13**, 201.
80. Srinivasan, S.A. and J.E. McGrath (1993) *High Perform. Polym.*, **5**, 259.

81. Wilkinson, S.P. T.C. Ward and J.E. McGrath (1993) *Polymer*, **34**, 870.
82. Blair, M.T. and P.A. Steiner (1988) *Proc. 33rd Int. SAMPE Symp.*, 524.
83. Sefton, M.S., P.T. McGrail, S.P. Wilkinson, J.A. Peacock, M. Davies, P. Crick and G. Almen (1987) *Int. SAMPE Tech. Conf.,* **19**, 700.
84. Bucknall, C.B. and I.K. Partridge (1983) *Polymer*, **25**, 1017.
85. Raghava, R.S. (1983) *Natl. SAMPE Symp.* **28**, 367.
86. Bucknall, C.B. and A.H. Gilbert (1989) *Polymer*, **30**, 213.
87. Hedrick, J.L., I. Yilgor, G.L. Wilkes and J.E. McGrath (1985) *Polym. Bull.*, **13**, 201.
88. Di Pasquale, G., O. Motta, A. Recca, J. T. Carter, P. T. McGrail and D. Acierno (1997) *Polymer* **38**, 17, 4345.
89. Mauzac, O. and R.J. Schirrer (1987)*J. Mater. Sci*, **25**, 5125.
90. Wrotecki, C., P. Heim and P. Gaillard (1991) *Polym. Eng. Sci.,* **31**, 213.
91. Lovewll, P.A. (1996) *Trends in Polym. Sci.*, **4**, 264.
92. Peason, R.A. and A.F. Yee (1983) *Polym. Mat. Sci. Eng. Prep.*, **186**, 316.
93. Finch, C.A. S Hashemi and A.J. Kinloch (1987) *Polym. Commun.,* **28**, 322.
94. Russell, A.J. and K.N. Street (1985) *Moisture and Temperature Effects on the Mixed Mode Delamination and Fracture of Unidirectional Graphite Epoxy,* W.S.Johnson (ed.), ASTM STP ;876, p. 349, ASTM, Philadelphia.
95. Tjong, S.C. and Y.C. Ke (1996) *Polym. Eng. Sci.,* **36**, 2626.
96. Delides, C.G., A.S. Vatalis, P. Pissis and R. A. Pethraick (1993) *J. Macromol. Sci. (Physj),* **B32**, 261.
97. Rooke, D.P. and D.J. Cartwright (1976) *Compendum of Stress Intensity Factors,* HMSO, London.
98. Rada, H., P. Paris and G.R. Irwin (1973) The Stress Analysis of Cracks Handbook, Del Research Corp., Hellertown.
99. Senturia, S.D. and N.F. Sheppard, Jr. (1990) *Adv. Polym. Sci.* **80**, 1-47
100. Day, D.R. (1986) *Polym. Eng. Sci.* **26**, 362-366.
101. Lane, J.W. and J.C. Seferis (1986) *Appl. Polym. Sci.* **31**, 1155.
102. Alig. I. And G.P.Johari (1992) *Macromolecules*, **25**.
103. Johari, G.P. and M.B.M.Mangion (1991) *J. Noncryst. Solids,* **131**, 921.
104. Parthun, M.G. and G.P. Johari (1992) *J. Polym. Sci. B. Polym. Phys.* **30**, 655.

105. Cassettari, M., G. Salvetti, M. Tombari, S. Veronesi and G.P. Johari (1992) *IRNCOVO Cimento* **14D**, 763.

106. Mopsik, F.I. (1984) *Rev. Sci. Instr.* **55**, 79.

107. Sheppard, Jr., N.F., S.L. Garverick, D.R. Day, S.D. Senturia (1981) *Proc. 26th SAMPE Symp.* p. 65.

108. Micromet Instruments, Inc., Cambridge, MA j(1985) The Eumetric System II Microdielectrometer, Product Bulletin.

109. Coln, M.C.W. and S.D. Senturia (1985) *Proc. Transducers '85,* p.118.

110. Johari, G. P. (1993) Chemistry and Technology of Epoxy Resins, Ed. B. Ellis, Chapman & Hall, London, p. 175.

111. Maistros, G. M., H. Block, C. B. Bucknall, I. K. Partridge (1992) *Polymer*, **33**, 4470

Xx Seraphim, D. P., D. E. Barr, W. T. Chen, G. P. Schmitt, and R. R. Tummala (1997) Microelectronics Packaging Handbook, R. R. Tummala, E. J. Rymaszewsky and A. Klopfenstein Eds. Chapman & Hall, New York, part 3, p. 290.

Xx Bauer, R. S. (1993), Polymers for Electronic and Photonic Applications, C. P. Wong Ed. Academic Press, San Diego, p. 287.

4 CHAPTER 4 EPOXY NETWORKS

4.1 Introduction

The synthesis and the characterization of high performance epoxy networks based on the commercially available diglycidyl ether of bisphenol A (Epon-828) and the tetraglycidyl ether of diamino diphenyl methane (TGDDM) will be performed. These resins will be cured with, newly synthesized phosphine oxide diamines. Epon-828 is a difunctional resin and TGDDM contains four epoxy functional groups per molecule. The resulting networks will then be evaluated for flame resistance.

Another objective is to utilize suitable thermoplastic modifiers to improve the fracture toughness of the resulting networks. The oligomeric modifiers containing terminal amine functionalities will be compared with non-reactive controls.

Dielectric monotoring is also used to study and contrast the curing reactions of the epoxy resins with various diamines.

4.2 Materials and Methods

4.2.1 Chemicals

EPON 828

Supplier: Shell,

EEW: 189 (by titration) `

Melting Point, ^{o}C: Close to room temperature

Structure:

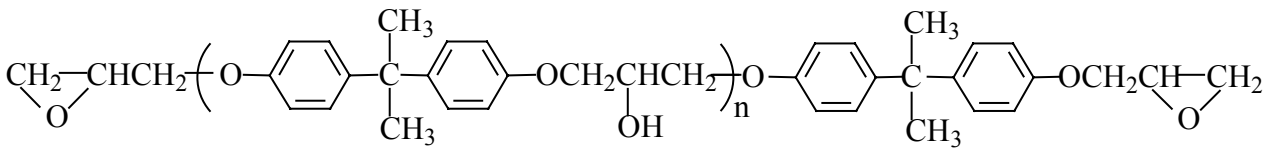

Purification: Used as received

TETRAEPOXY DAMPO

Supplier: Synthesized in our laboratory

Empirical Formula: $C_{25}H_{31}O_4N_2P$

Molecular Weight: 470.50

Structure:

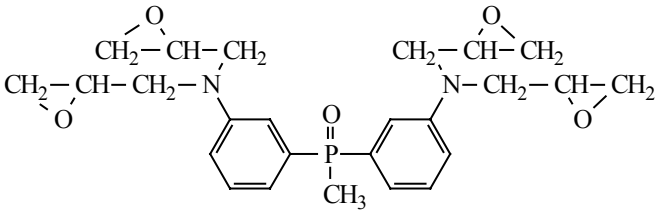

DAMPO

Supplier: Synthesized in our laboratory

Empirical Formula: $C_{13}H_{15}ON_2P$

Molecular Weight: 245.249

Melting Point, ^oC: 156

Structure:

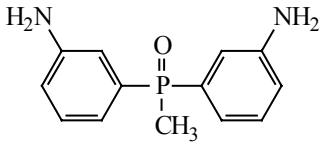

DAPPO

Supplier: Synthesized in our laboratory

Empirical Formula: $C_{18}H_{17}ON_2P$

Molecular Weight: 308.32

Melting Point, ^oC: 212

Structure:

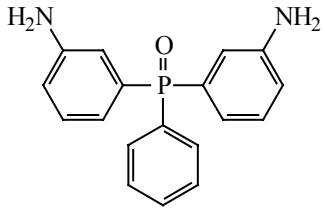

BAPPO

Supplier: Synthesized in our laboratory

Empirical Formula: $C_{30}H_{25}O_3N_2P$

Molecular Weight: 492.52

Melting Point, ^oC: 90-92

Structure:

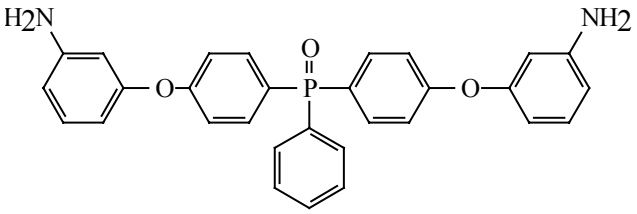

BAMPO

Supplier: Synthesized in our laboratory

Empirical Formula: $C_{25}H_{23}O_3N_2P$

Molecular Weight: 430.44

Melting Point, ^oC: 81

Structure:

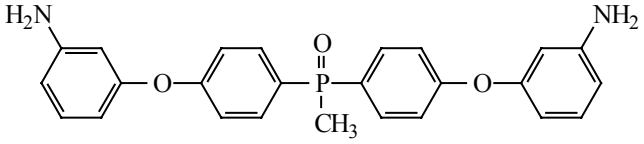

MY-721 (TGDDM):

Supplier: Ciba-Geigy

Empirical Formula: $C_{25}H_{30}O_4N_2$

Molecular Weight: 422.52

Structure:

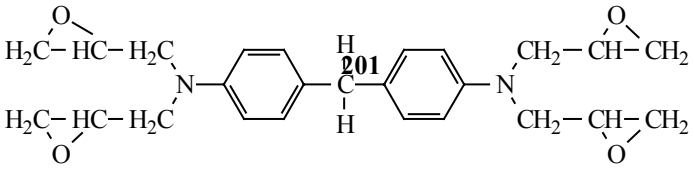

Purification: Used as received

The commercially available tetrafunctional epoxy resin used in this work, MY721, was generously provided by Ciba-Geigy. The epoxy was titrated to ascertain the average functionality per molecule. The Epoxy Equivalent Weight (EEW) was determined by titration of 0.3 g of MY-721 in 25 ml of hydrogen chloride-acetone (2.8 ml 36.5% HCl in 140 ml of acetone) by 0.1N sodium hydroxide solution and methyl red was used as the indicator. The Epoxy Equivalent Weights (EEW) of MY-721 determined by this procedure was 114 g/mole.

NMR analyses were also used to determine the Epoxy Equivalent Weight of MY-721. NMR spectra were recorded on a Varian Unity 400 MHz nuclear magnetic

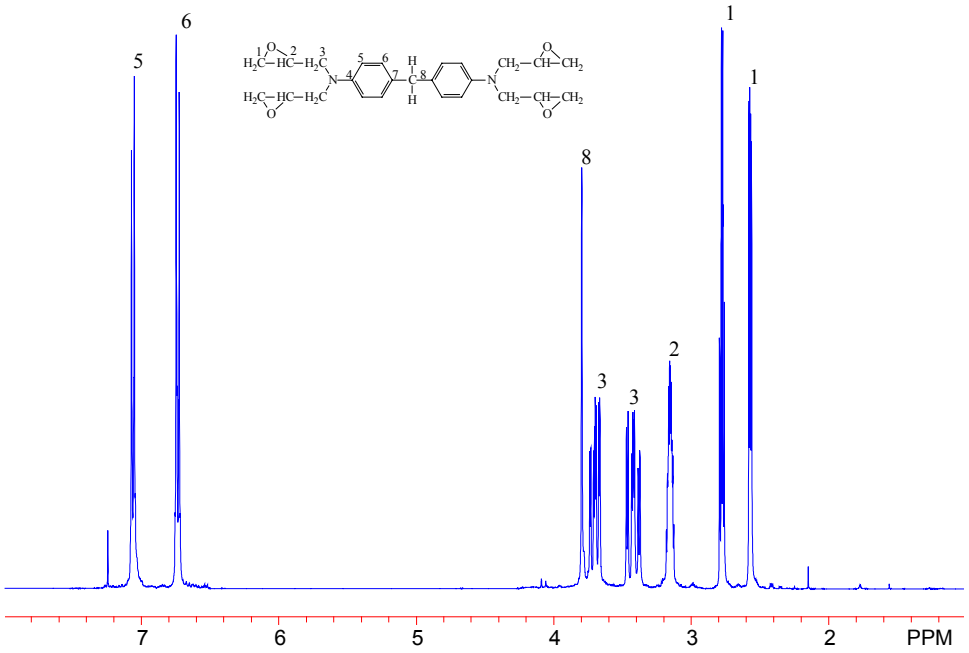

Figure 4.2-1 ^{1}H NMR spectrum of MY-721

resonance spectrometer in 5mm probes with deuterated chloroform as a solvent and tetramethylsilane as internal standard. The ratio between the epoxy protons and the aromatic protons were used to determine the epoxy content of the resin.[1] (See Figure 4.2-1).

4,4'-Diaminodiphenylsulfone (DDS)

Supplier: Acros, 97%

Empirical Formula: $C_{12}H_{12}N_2O_2S$

Molecular Weight: 248.30

Melting Point, ^{o}C: 175-177

Structure:

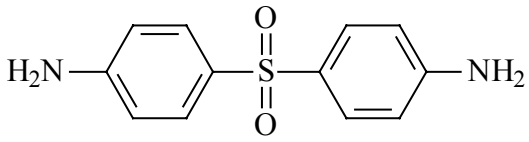

Purification:

The diaminophenyl sulfone (4,4'DDS) was purchased from Acros and was purified as follows:

Ethanol (3L of HPLC grade) was loaded in a 5L round bottom 3-necked flask. The flask was fitted with a reflux condenser, a nitrogen inlet and a mechanical stirrer. 500 g of DDS were added into the flask and stirred. The solution was heated to reflux

with a heating mantle and stirred under a nitrogen atmosphere until complete dissolution occurred. At this point 25g of activated charcoal was added to the mixture and the reflux was allowed to proceed for 30 additional minutes. The solution was filtered through celite, and stored in 2L Erlenmeyer flasks at room temperature until the formation clear needle-like crystals occurred. The crystals were quickly suction filtered and dried in a vacuum oven at 90°C for about 12 hours and stored in a sealed brown bottle (under nitrogen atmosphere) in a dessicator. The yield was 85% and the melting point was 176° C, which was consistent with the literature values.

The synthesis of DAMPO, DAPPO, BAPPO, BAMPO and the tetraepoxy DAMPO (TGDAMPO) were performed in this work and are detailed in Chapter 2.

4.2.2 Processing of the Tetrafunctional Epoxy Resins

The commercially available tetrafunctional epoxy MY721 was one of the multi-functional resins used in this work. It was generously provided by Ciba-Geigy. The other resin, tetraepoxy DAMPO (TGDAMPO) was synthesized in our work. The thermoplastic modifiers were Ultem, a trademark polyetherimide of GE Plastics, which is based on bisphenol A, and three analogs of Ultem, whose molecular weights were controlled by a moderate excess of the diamine co-monomer, *m*-phenylene diamine. Details for the synthesis of these modifiers will be provided in Chapter 5. The actual molecular weights (determined by titration) and the theoretical molecular weights (given in parentheses) of the synthesized toughenes were 11800 (10000), 14900 (15000) and 19300 (20000). The reactive end group function was an amine, which as one would expect, can allow the ether imide modifier to react with the epoxy resin. Even though the actual molecular weights as determined by titration did not exactly match the corresponding expected values, those values given in parentheses above were used to describe the toughenes. The loading percentage of the toughenes in the epoxy resins varied from 5 to 25 percent by weight for Ultem toughened materials and 5 to 20 percent by weight for the reactive toughenes.

In order to facilitate the quick dissolution of the polymers in the epoxy resins, a 10% polymer solution in chloroform was precipitated into methanol to get a finely dispersed powder. The powder was thoroughly dried in a vacuum oven at 100^{o}C to remove all traces of methanol and water. Before being charged into a round bottom flask with the epoxy resin, the polymer powder was ground in a mortar and pestle and sifted through a wire mesh with pores of 25 μm in diameter. The mesh permitted particles of 25 μm or less to pass through.

4.2.2.1 Resin Mixing.

The epoxy resin (approximately 40g) was weighed directly into a 250 ml two-necked round bottom flask (Figure 4.2-2). The flask was immersed in a preheated 140° C oil bath and stirred under vacuum until no apparent bubbles emerged from the resin. Then a determined amount of finely powdered modifier (the thermoplastic polymer) was added to the flask and the mixture was stirred under vacuum until the modifier appeared to have completely dissolved in the resin. A clear brown mixture resulted from this operation. The complete dissolution of the modifier in the resin was also verified by differential scanning calorimetry (DSC), where the transition temperatures of mixtures of known compositions were compared to those of the neat resins and the thermoplastic modifiers, using the well known Fox equation.[2] Details for these experiments will be pesented later. The diamine curing agent was then added to the mixture and vacuum was applied as the stirring proceeded. After the complete dissolution of the mixture was verified by the clarity of the solution, the viscous mixture was poured into a pre-heated silicone rubber mold, using a heat gun to prevent a premature solidification the system. The detailed preparation of the silicone mold will be presented in the following paragraph. The stoichiometric amount of the curing agent added, 4-aminopenyl sulfone (DDS) for example, was calculated using the following formula

$$grams(DDS) = \frac{grams(TGDDM)}{114} * 64$$

where 114 and 64 represent the equivalent molecular weight of TGDDM and DDS, respectively. The epoxy (now in the preheated mold) was degassed for 5 to 6 minutes at 150-160° C in a vacuum oven and was subsequently transferred to the curing oven at 160°C for 2 hous, then 220°C for 1 hour and 15 minutes at 240°C. The oven was programmed to cool at 4°C/min to ambient temperature.

4.2.2.2 Preparation Of The Mold.

A rectangular aluminum mold (inside dimensions 215 x 140 x 26 mm) was cleaned with acetone before use and stainless steel coupons for fracture toughness and/or flexural modulus (38 x 6 x 3 mm and/or 50 x 12 x 1.5 mm, respectively) were arranged as shown on Figure 4.2-3. The silicone resin (dark red) obtained from DOW was thoroughly mixed (5 - 10 minutes) in a 190 x 100 mm crystallizing dish. Approximately 37 grams of the catalyst (light blue) was weighed directly into the resin and mixed thoroughly for about 30 minutes. Vigorous stirring is not recommended as this will aerate the mixture, thereby resulting in a mold with many voids. A ratio of 8:1 (resin: catalyst) was used rather than the manufacturer recommended ratio of 10:1, resulting in a more flexible mold. The viscous, dark red mixture was poured slowly into the mold, in order to not disturb the coupons, covered with aluminum foil and left to cure at room temperature for 24 hours.

Before post-curing, the cured rubber mold was removed from the aluminum mold and the stainless steel coupons were removed from the rubber mold. Post curing at 260° C for 2 hours (that is 20°C above the expected use temperature of the mold) drastically reduced void formation in the epoxy samples, which often result from the silicone mold releasing gases into the samples. Large amounts of smoke and fumes could be generated, therefore this process should be performed in a well-ventilated area. Flanges surrounding the specimen were trimmed using a single edge razor.

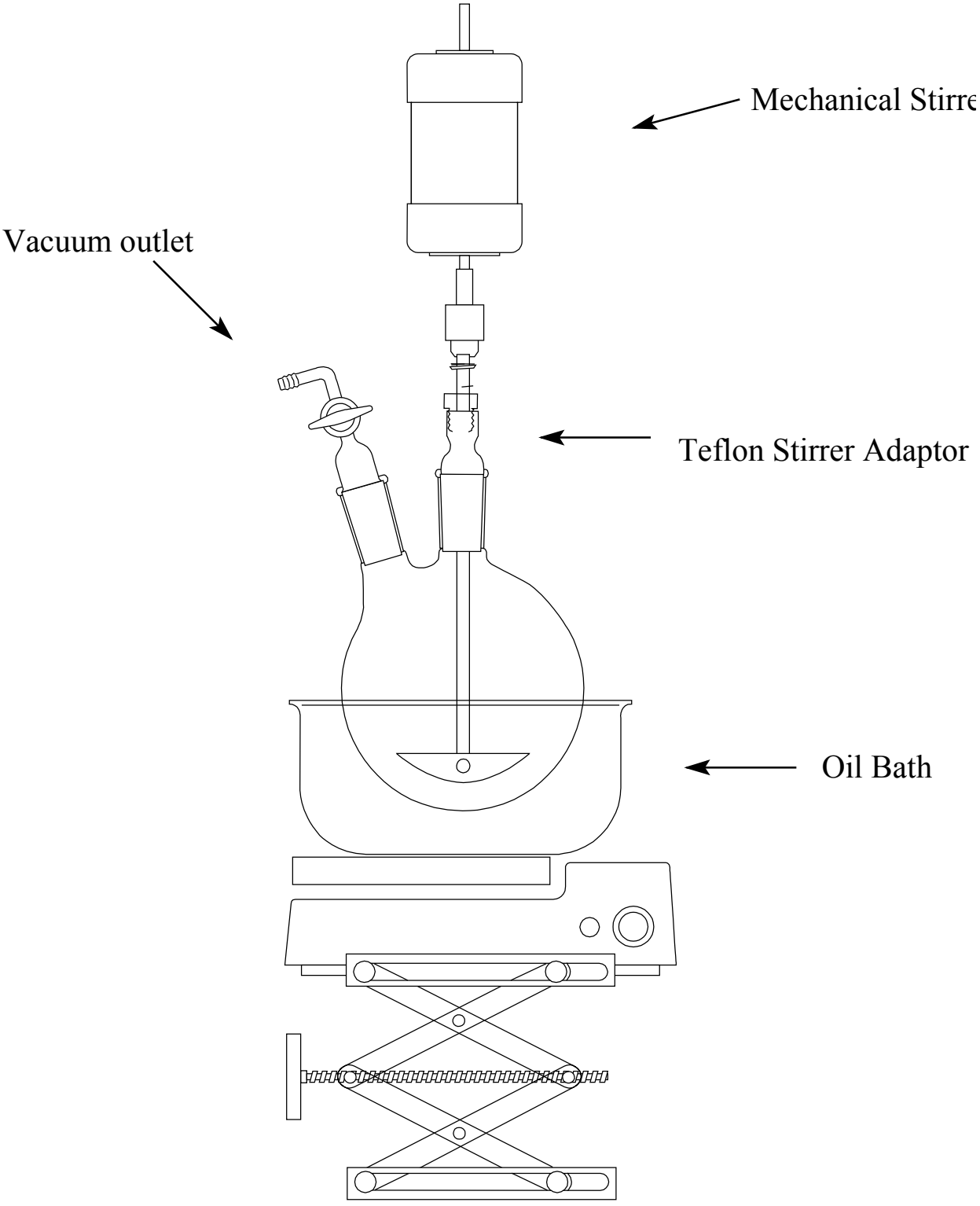

Figure 4.2-2 Apparatus Used in the Mixing and Degassing of Epoxy Resins

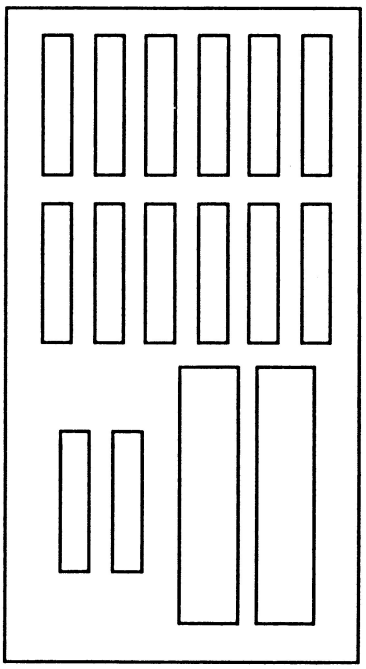

Figure 4.2-3 Assembly for Silicone Mold Preparation
(viewed from the top)

4.2.2.3 GEL FRACTION DETERMINATION

The soluble fraction of the cured epoxies was determined by Soxhlet extraction. Cellulose thimbles were soaked in chloroform for 12 hours and subsequently dried in a vacuum oven at 80° C for 24 hours, until the thimbles reached a stable weight. This procedure was performed to remove any soluble portion from the thimbles. Cured samples of approximately 0.5 gram were placed and weighed in the thimbles, then placed inside a Soxhlet extractor. The soluble portions of the samples were extracted by refluxing in chloroform for 4 days. The thimbles and samples were then dried at 100° C under vacuum for 3 days, until constant weights were obtained. The thimble were then collected in a dessicator and their weight was determined without delay. The gel fraction was determined from the following equation:

$$\text{Gel Fraction} = \frac{\text{Wt (extracted thimble) - Wt (pretreated thimble)}}{\text{Wt (sample)}} \text{ X } 100$$

4.2.2.4 Dynamic Mechanical Analysis

Dynamic mechanical analysis (DMA) was used to determine the glass transition temperature of the cured material. The tests were performed in a single cantilever

bending mode with a heating rate of 3° C/min on a Polymer Laboratories Mark II DMTA. A single frequency scan at 1 Hz was obtained.

4.2.2.5 Scanning Electron Microscopy

Scanning electron microscopy (SEM) was used to assess morphological features of the toughened epoxy systems. As would be anticipated, the materials phase separated into an epoxy rich and a thermoplastic modifier rich phase. SEM of the room temperature fractured surfaces helped in the determination of the morphology, because the toughener tended to undergo some ductile fracture and create a rough surface. The height differences helped in resolving phases. The samples were gold sputtered for three minutes to establish their surface conductivity. An ISI-SX SEM with an accelerating energy for the electron beam of 20 kV and a working distance of 15 mm was used.

4.2.2.6 SAMPLE ETCHING

In order to ascertain the chemical resistance superiority of the amine-terminated modifiers over their non-reactive commercial homologues, fractured samples were etched in chloroform for 10 days. The etched samples were dried at 80° C in a vacuum oven for two days and examined with scanning electron microscopic (SEM) techniques. Some of the samples could not stand a 10-day etching treatment without being completely destroyed. Those samples were simply etched for 7 hours before analyzing by SEM.

4.2.2.7 Mechanical Testing

The mechanical measurement geometry selected to assess the fracture toughness of the modified tetrafunctional epoxies was a single edge notch beam (SENB) sample. The geometry of this sample is shown in Figure 4.2-4 and follows ASTM standart D 5045-91. The samples were machined to achieve the dimensions specified in this standard. The jig used for testing the specimens was in compliance with the directions in

the standard. An Instron 1143 was used at a crosshead speed of 1 mm/min at ambient conditions. For the calculation of the fracture toughness, the maximum load was recorded, as well as the exact dimensions of the sample along with the initial crack length. The expression for the fracture toughness (K_{IC}) is shown in equation 4.1-1.

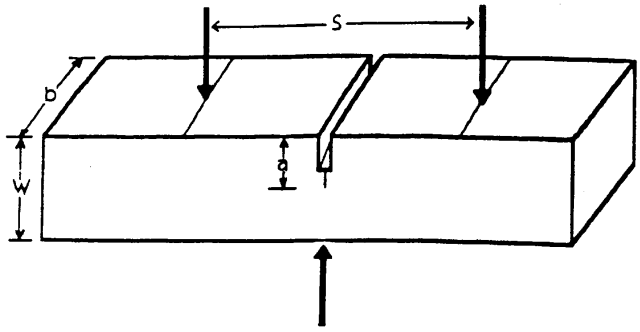

THREE POINT BEND

For Three Point Bend Specimen

FOR THREE POINT BEND SPECIMEN

$$K_{IC} = \frac{S * P}{b * w^{3/2}} \left(2.9\left(\frac{a}{w}\right)^{0.5} - 4.6\left(\frac{a}{w}\right)^{1.5} + 21.8\left(\frac{a}{w}\right)^{2.5} - 37.6\left(\frac{a}{w}\right)^{3.5} + 38.7\left(\frac{a}{w}\right)^{4.5} \right)$$

Equation 4.2-1

η = Geometry Factor
W = Width
a = Crack Length
b = thickeness
S = Span Length

Figure 4.2-4 SENB geometry with the parameters described above.

Flexural modulus was also determined from the initial slope of a stress-strain curve. The same instrument was used as for the SENB test with the same crosshead speed and environment. The bending jig was slightly modified from the previous test to accommodate ASTM D 5943 – 96. A slight modification of the specimens was necessary because of the sample quantity limitations. The length to thickness ratio (a/w) was smaller than specified, which makes the samples seem stiffer. However, for the purpose of this study, which was to compare among samples with a common geometry, this discrepancy was not viewed as critical for relative comparisons.

4.2.2.8 Thermogravimetric Analysis

Dynamic thermogravimetric analysis (TGA) was used to assess the relative thermal stabilities of the networks. TGA plots were obtained with a Perkin Elmer TGA 7 thermogravimetic analyser. Samples of approximately 10 mg were placed in a platinum pan connected to an electric micro balance. The samples were heated at a rate of 10^{o}C per minute in air. Weight loss of the samples was recorded as a function of the temperature.

4.2.3 Difunctional Epoxies

4.2.3.1 Titration

EPON 828 was generously provided by Shell Company. The epoxy equivalent weight was determined by titrating the resin with perchloric acid [$HClO_4$] of known normality. The $HClO_4$ solution in glacial acetic acid was standardized with a solution of potassium hydrogen phthalate [KHP] in glacial acetic acid. The function of the acetic acid is to enhance the basicity of the oxirane ring and to intensify the end points. Titrations were performed on an MCI GT-05 (COSA Instruments Corp.) automatic potentiometric titrator. The end points were defined as the maxima of the first derivative of the potential versus the volume of the titrant used. About 20-25 mg of epoxy resin

sample was accurately weighed in a 150 ml beaker and dissolved in 70 ml of glacial acetic acid. Tetraethylammonium bromide (1.5 g) was added to the solution as a phase transfer agent. Two or three such samples were prepared and titrated with the standardized $HClO_4$ solution to obtain the average equivalent weight.

4.2.3.2 Size Exclusion Chromatography

Chromatographs were obtained with a Waters 150C ALC/GPC instrument equipped with a differential refractive index detector and a Viscotek® Model 100 viscosity detector connected in parallel. The eluent was chloroform (HPLC grade). The stationary phase consisted of crosslinked polystyrene gel (Waters μstyragel HT 10^2 Å, 10^3 Å and 10^4 Å, mean particle diameter 10 μm) packed in three (7.8 mm I.D. X 30 cm) stainless steel columns. Resin samples of known concentrations (approximately 4 mg/ml) were dissolved in the mobile phase and filtered through 0.2 μm PTFE disposable filters prior to the analysis. The volume of the sample injected was 200 μl and the flow rate of the eluent was 1.0 ml/min. The column compartment, lines and detectors were kept at a temperature of 60° during the operation. The number average molecular weight ($\overline{M}_n$), the weight average molecular weight ($\overline{M}_w$) and the polydispersity ($\overline{M}_w/\overline{M}_n$) were determined by a standard technique called universal calibration, using narrow molecular weight distribution polystyrene standards.[3, 4] The chromatograph for EPON 828 will be shown in the next section. The number average molecular weight ($\overline{M}_n$) obtained by this method was compared with titration values in order to confirm the validity of the measurements.

4.2.3.3 Sample Preparation

Sample preparation was the same as that of the tetrafunctional resins described in the previous sections. EPON 828, donated by Shell Chemical was maintained under

vacuum (figure 4.2-2) while continuously stirring and the curing agent, 4.4′ DDS for example was added in a stoichiometric ratio. Stirring proceeded until all of the DDS dissolved. The mixture was poured into a pre-heated mold, then degassed in a vacuum oven at 100°C for 5-6 minutes. The samples were then transferred to a curing oven and cured at 130°C for 4 hours and were subsequently post-cured at 220°C for 2 hours (Scheme 4.2-1).

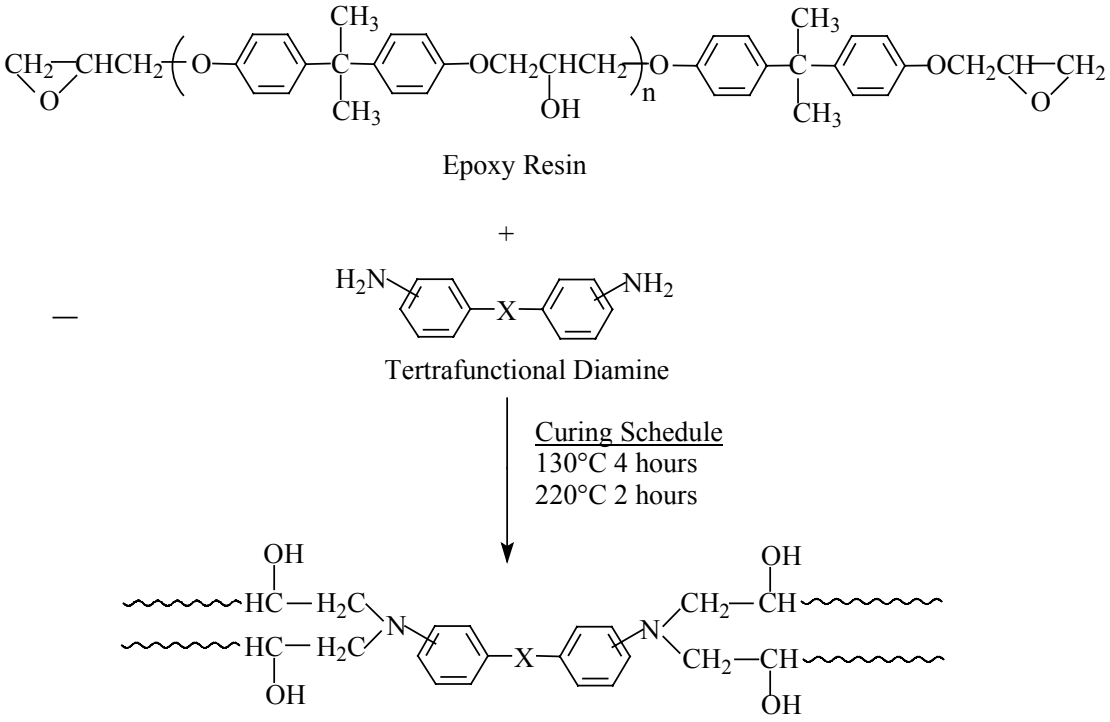

Scheme 4.2-1 Curing of the difunctional epoxy resin

4.2.3.4 Dielectric Monitoring of the Cure of Epon 828

Monitoring of the cure was performed by dielectric analysis using remote sensing probes from Micromet (See Figure 4.2-5). An external oven was operated to maintain isothermal control. The dielectric analyzer was an RLC Digibridge from GenRad, which was controlled through Polymer Laboratories System and Software. The isothermal cure was monitored at various temperatures ranging from 100°C to 190°C. The capacitance and dielectric dissipation were measured at four or five different frequencies between 100 Hz and 100 kHz. The data were then analyzed as a function of time. The analysis will be presented further in the discussion section.

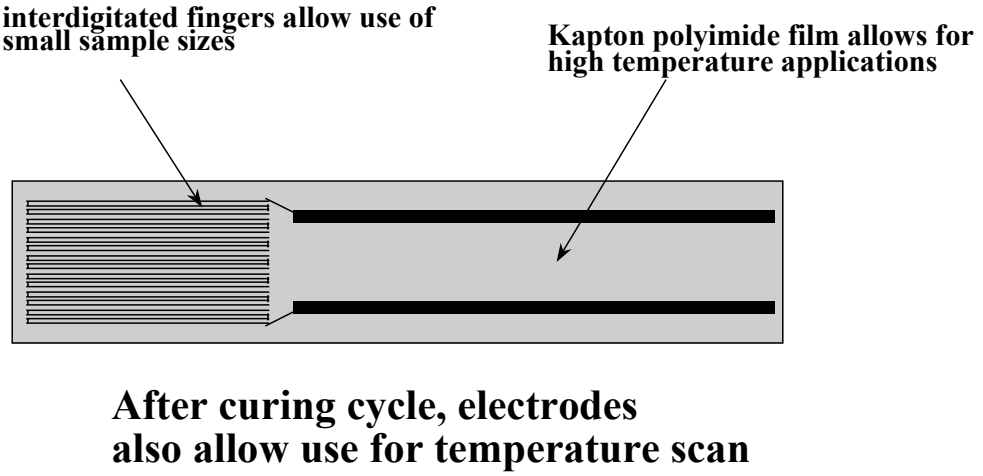

Figure 4.2-5 Dielectric probe for remote sensing

Dielectric monitoring of the cure proceeded in a manner similar to that described earlier in this chapter. The curing agents used were 4,4′ diaminodiphenylsulfone (DDS), bis(3-aminophenyl methyl phosphine oxide) (DAMPO), bis(3-aminophenoxy phenyl) phenyl phosphine oxide (BAPPO), and bis(3-aminophenoxy phenyl) methyl phosphine oxide (BAMPO). The syntheses of these phosphorus containing hardeners have been detailed in an earlier chapter. Plots showing dielectric loss as a funtion of time for four different frequencies at constant temperatures were recorded (Figure 4.2-6 for example). A temperature sweep of the cured network from 100 to 300^{o}C was perfomed on all of the systems investigated. The curves show transitions around 250^{o}C, which by all accounts correspond to the glass transition temperatures (Figure 4.2-7).

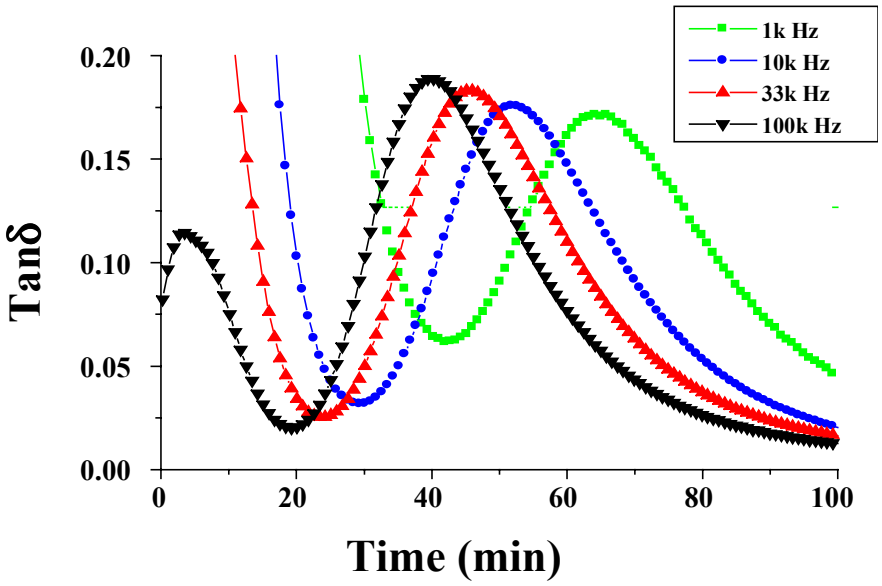

Figure 4.2-6 Influence of the Frequency on the Dielectric Monitoring of Epon 828 and 4,4' DDS Reaction at 177°C

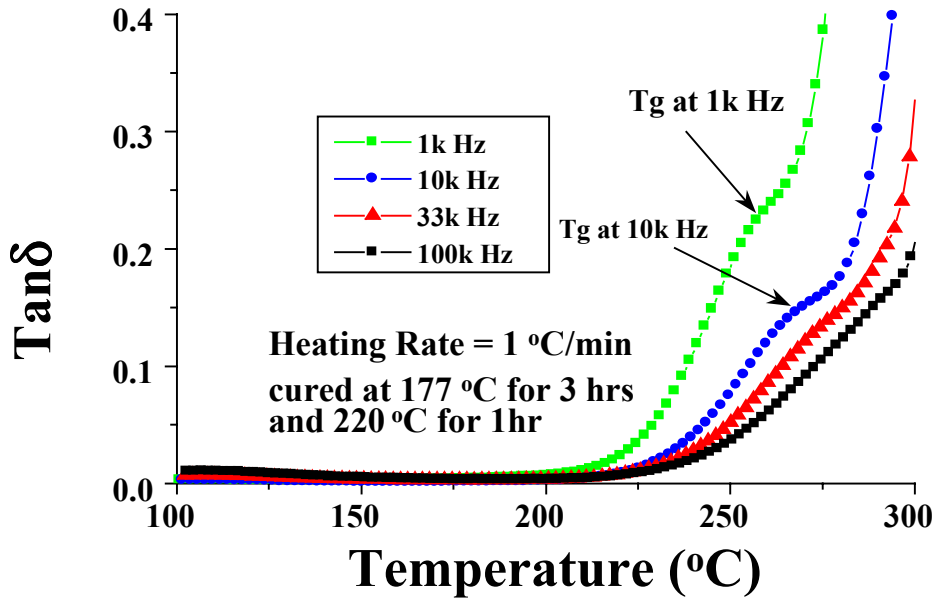

Figure 4.2-7 Behavior of a Cured Epon 828/DDS Network as a Function of Temperature and Frequency

4.2.3.5 Differential Scanning Calorimetry (DSC)

Glass transition temperatures were determined by differential scanning calorimetry. A Perkin-Elmer DSC 7 at a heating rate of 10°C/minute, (indium and lead as temperature calibrants) was used for that purpose. Flat samples of approximately 10 mg were used in order to obtain a good signal without causing thermal lag problems. The glass transition temperatures were detected through sudden increases in the heat flow.

4.2.3.6 Dynamic Mechanical Analysis (DMA)

Dynamic Mechanical Analysis plots were obtained on a Perkin-Elmer DMA 7 Dynamic Mechanical Analyzer. Samples were scanned in the three point bending mode at 5°C/minute. The glass transition temperatures were estimated from the maximum of the tan delta plot. The characterization results are presented in Table 4.3-1. The corresponding plots are shown in Figures 4.3-4 and 4.3-5.

4.2.3.7 Thermogravimetric Analysis (TGA)

Dynamic thermogravimetric analysis on the fully-cured specimens in air were performed on the TGA 7 Thermogravimetric Analyzer, and the graphs obtained were used to evaluate the relative thermooxidative stabilities of the samples. The samples were scanned from 30°C to 900°C at a rate of 10°C/minute. The graphs are presented in figures 4.2-2 and 4.2-4. The char yield represents the percentage of residual material at 650°C with respect to the original sample amount.

4.2.3.8 Flame Resistance Tests

Quantitative measures of flame resistance are often based on a technique known as Limiting Oxygen Index (LOI) where the amount of oxygen required to sustain a blue flame is measured. It has, however, been shown that LOI results are linearly related to char yields in thermogravimetric analyses.[5]

A qualitative "Bunsen Burner" method developed in our laboratory was used. The epoxy samples cured with diamines of various compositions (see Table 4.3-1) were exposed in a horizontal position to a blue flame for a few seconds until the sample apparently started to burn. Samples were ranked from flammable (if they continued to burn after removal of the flame) to self extinguishable (if the flame stopped). A picture describing the "Bunsen Burner" test is shown in Figure 4.2-8.

Another test used in assessing the flammability of the epoxy samples was done in conjunction with NIST laboratories. In this case, samples of dimensions 10cm X 10cm X 3.5cm were subjected to a cone calorimeter test and the peak heat release rates were determined. A cone calorimeter consists of a chamber in which a sample is introduced and ignited, while subjected to a high radiant heat flux, a hood where the emisson gases are collected, a gas analyser and a temperature monitor (see Figure 4.2-9).

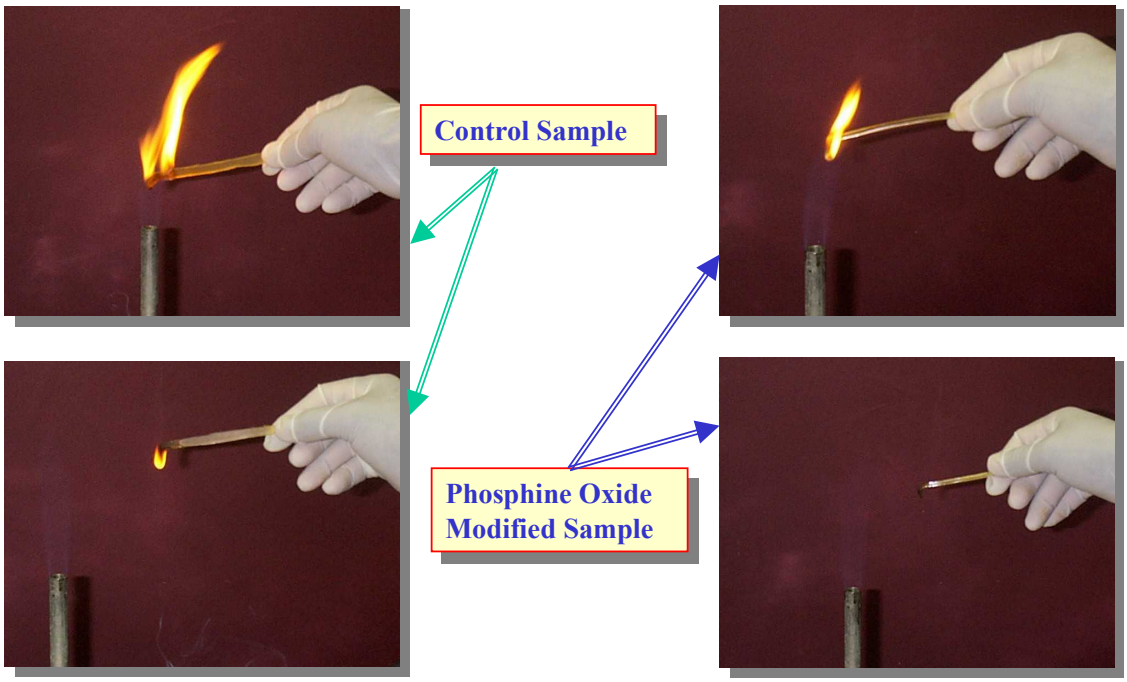

Figure 4.2-8 Qualitative Description of the "Bunsen Burner" test.
(The pictures to the left correspond to a flammable network and those to the right correspond to a self-extinguishable network).

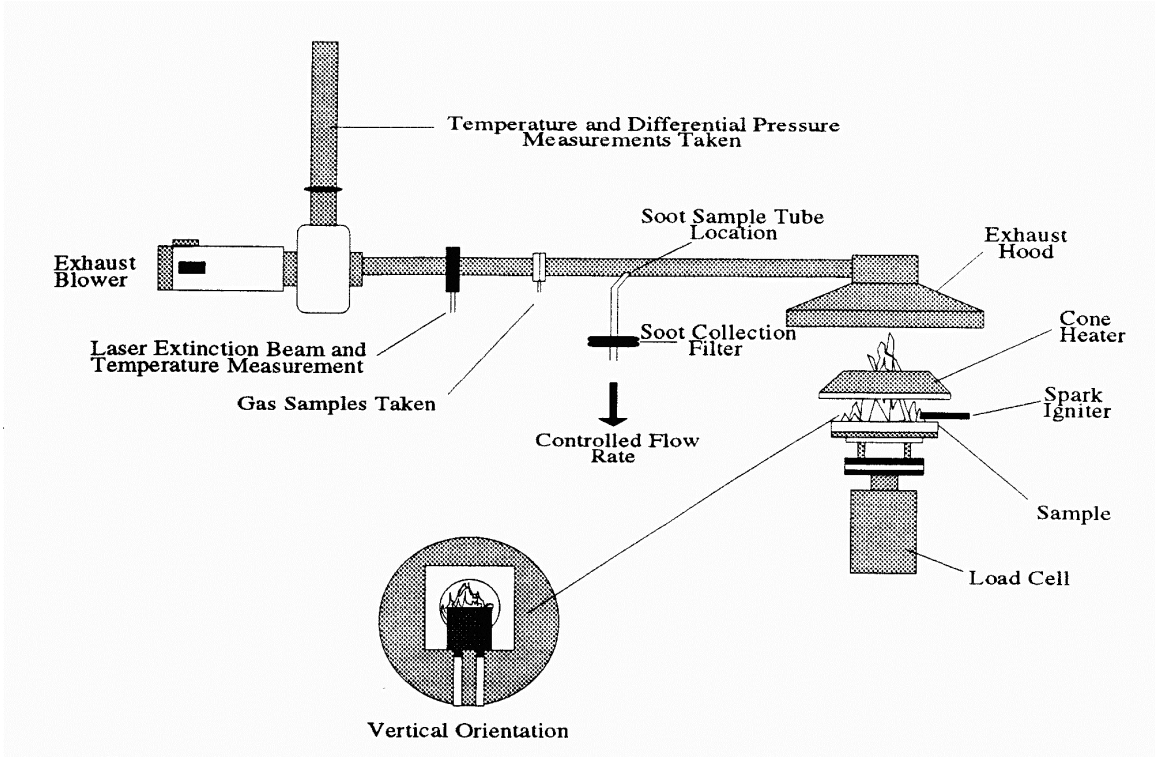

Figure 4.2-9 Cone calorimeter[6].

4.3 Results And Discussion

4.3.1 EPON 828 Based Networks

4.3.1.1 Characterization Of The Resin

The Epoxy Equivalent Weight determined by titration was 189g/mole. This figure was used throughout the experiments to assure a stoichiometric mixing of the epoxy with the amine curing agents. The number average molecular weight ($\overline{M}_n$) as determined by size exclusion chromatography was 388, which is comparable for all practical purpose to the value of 378 determined by titration. The modest difference in the estimates can be ascribed to the reduced sensitivity of the size exclusion apparatus in assessing the molecular weight of very small molecules, as in the case of monomeric bisphenol A epoxy resins.

Size exclusion chromatography fractionates macromolecules by size. The critical parameter is the hydrodynamic volume. The larger the hydrodynamic volume, the less likely are the polymer chains to reside in the column packing material. Adistribution of pore sizes in the packing material allows solute molecules of differing size to penetrate the packing to different degrees and to reside there until Brownian motion brings them out of the pores. Polymer chains that are too large will not permeate these void areas and hence will stay in the eluent stream. This action translates into an earlier elution of higher molecular weight macromolecules from the column. Consequently, one can conclude that the larger molecules exit the column sooner and the smaller ones elute later. All of the above observations are based on the assumption that

there are only steric effects[4] and no specific interactions of the polymer with the packing material.

The refractive index (detector) chromatogram (Figure 4.3-1) of Epon-828 showed three peaks corresponding to the major oligomers deriving from the industrial synthesis of the bisphenol A epoxy resin. In this synthesis, chain extension of the targeted molecule (n = 0) can occur, giving approximately 15% of the higher oligomer (n = 1 or 2). Since all the oligomers participate in the curing process, purification of the resin is not required. More over the liquid nature of the higher molecular weight oligomers improves the dissolution of the curing agent in the resin.

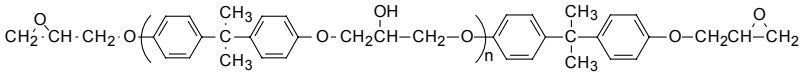

Mn = 340×85.3% + 624×12.9% + 908×1.79% = 388 (380)

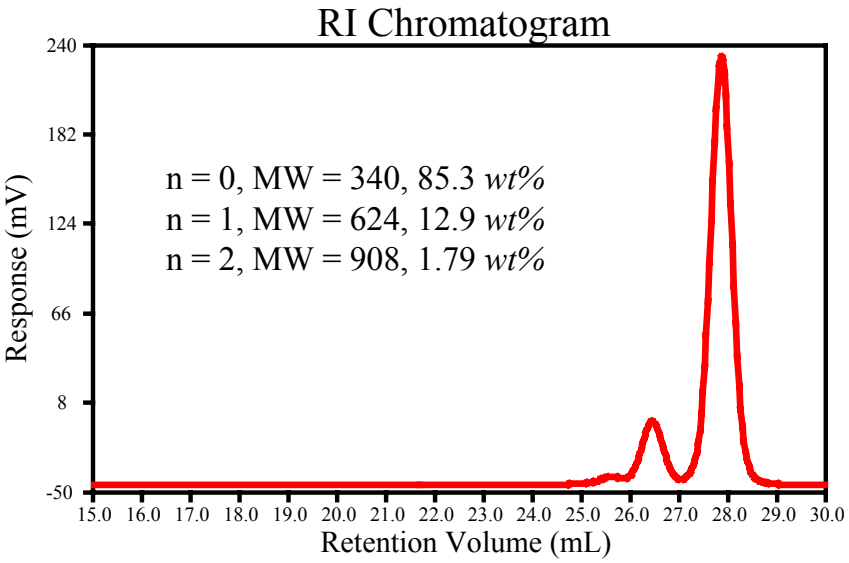

Figure 4.3-1 Gel Permeation Chromatography Determination of the Epoxy Equivalent Weight (EEW) of EPON 828.

4.3.1.2 Flame Resistance and Thermal Stability Evaluations

Epon-828 which is a difunctional epoxy resin was cured with the commercially available diamine 4,4'-DDS and phosphine oxide containing diamines synthesized during the course of this study. The diamine 4,4'-DDS, is by far the standard curing agent in both the industrial arena and academic laboratories, by virtue of its capability to generate networks with high thermal stability and high glass transition temperatures. For this reason, this commercial diamine was chosen as control in our experiments.

Dynamic thermogravimetric analysis data (Table 4.3-1) show that networks containing phosphine oxide units had higher char yields than those cured with the commercial curing agent, 4,4'-DDS. The char residue at 650^{o}C increased with the phosphorus content of the network from 0% of the initial weight for the control (cured with 4,4'-DDS) to 26% for networks where DAPPO was the only curing agent. High char yields in polymeric systems are often indicative of flame resistance, suggesting that networks with the novel phosphine oxide diamines should have higher flame resistance than the control networks. Temperatures at which the materials lost 5% of their weight was approximately the same for all the systems, around 375^{o}C; presented in other words, phosphine oxide units neither decreased, nor increased the thermal stability of Epon-828 based epoxy networks, if the criterion was suppression of initial volatiles production.

Furthermore, cone calorimetry data (Table 4.3-2) showed that phosphorus in the networks lowered the peak heat release rates. Cone calorimetry, simply explained, measures how rapidly heat is released when a sample is burned while exposed to a high radiant heat flux. For example, a flammable sample would release a lot of heat rapidly, while a sample which is less flammable releases heat more slowly during its combustion. In this work, a network with 75 mole % of the comercially available diamine had a maximum heat release rate of 740 KW/m^2 while a network cured only with the DAMPO diamine showed a maximum heat release rate of 400 KW/m^2. This indicates that the network cured entirely with DAMPO displayed a higher flame resistance. The decrease in the peak heat release rate however leveled after 50 mole % of the DAMPO curing

agent in the network. These findings suggest that there is an optimum phosphorus content of the network for maximum flame resistance, beyond which further increases in the phosphorus content of the network are not necessary.

The qualitative "Bunsen burner" flame tests (Figure 4.3-8) showed that networks

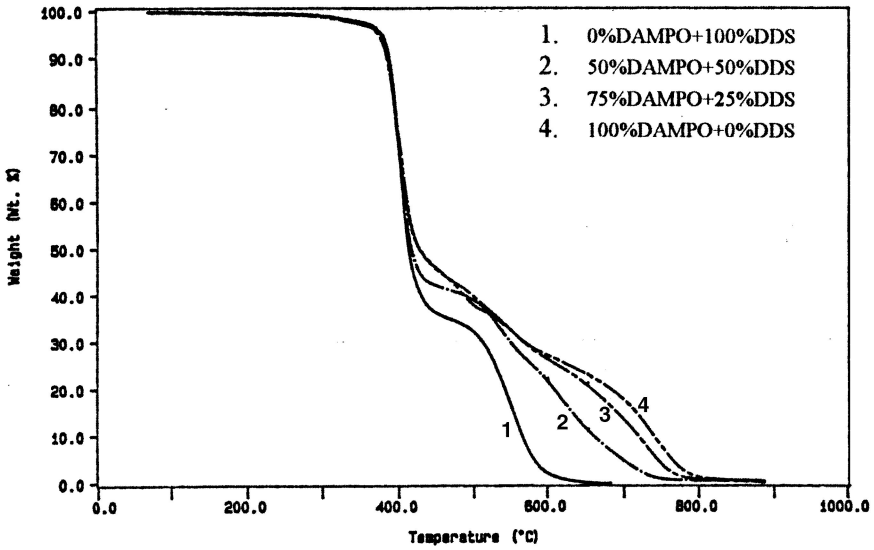

Figure 4.3-2 TGA plots of DAMPO based epoxy networks

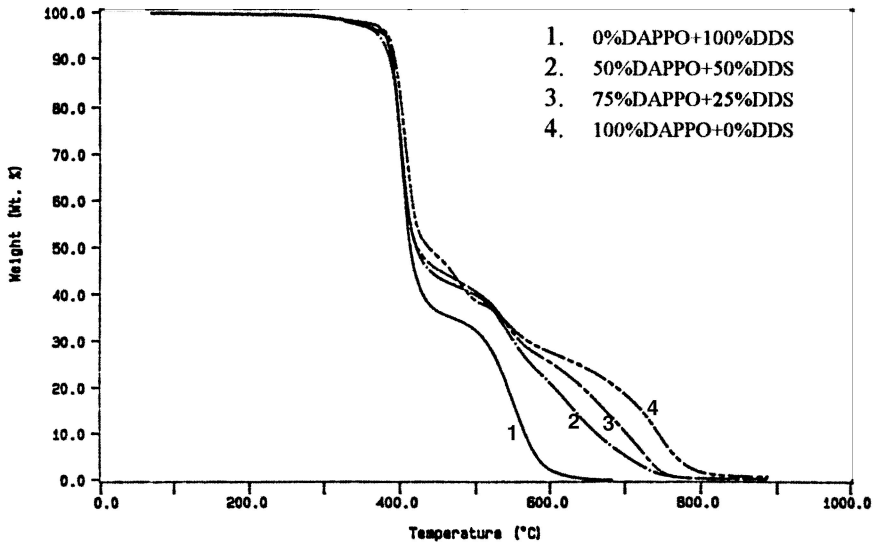

Figure 4.3-3 TGA plots of DAPPO based epoxy networks.

containing phosphine oxide units were self-extinguishing, while the control samples cured with the commercially available diamine 4,4'-DDS continued to burn indefinitly upon their removal from the flame, until sample was left. These findings are consistent with results from both dynamic themogravimetric analysis (TGA) and cone calorimetry investigations. It is remarkable however, that all of the phosphorus containing networks showed self-extinguishing properties during the qualitative test, at least within the limits of the phosphorus contents used in this work. This result is dramatic in that it suggests that only a few mole percent of the novel monomers would be necessary to impart flame resistance to a polymeric system. Futher investigations with either the epoxy systems or other classes of polymers will be necessary to determine the threshold phosphorus contents for flame resistance applications.

4.3.1.3 Dynamic Mechanical Analysis (DMA)

Dynamic mechanical analysis data showed that Epon-828 based networks had high glass transition temperatures, ranging from 160 to 215^{o}C. The novel phosphine oxide containing diamines gave rise to networks with lower glass transition temperatures than that of the control (T_g = 215^{o}C). The T_g decreased with increased content of the phosphine oxide monomer. The epoxies formed from the commercially available *p,p'*-diamine DDS are well established for high themperature applications. The drop in the glass transition temperatures could at least be partly ascribed to the *m,m'*- substitution of the the amine functionalities in the novel curing agents. In general, for polymers from similar monomers, the glass transition temperatures for those formed from monmers having meta substituted functionalities could be as much as 10^{o}C lower than those formed from their para homologues. Bearing these considerations in mind, one could conclude that decreases in the transition temperatures generated by the presence of the phosphine oxide units were not considerable.

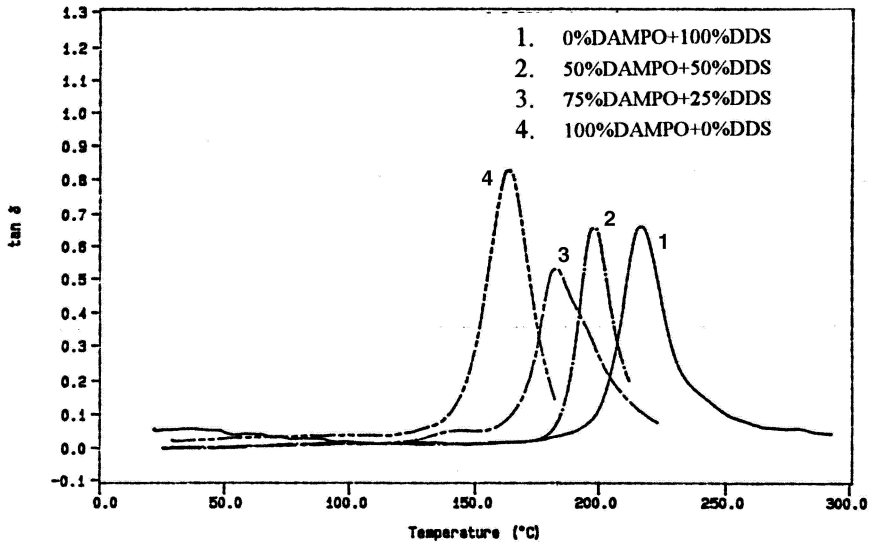

Figure 4.3-4 **DMA plots of DAMPO Based Epoxy Networks**

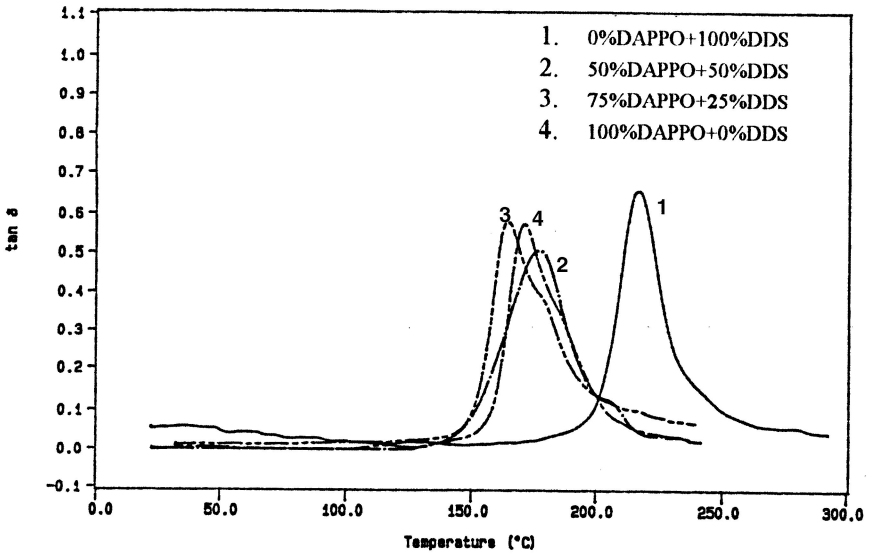

Figure 4.3-5 **DMA plots of DAPPO Based Epoxy Networks**

Diamine Curing Agent	5% Wt. Loss Temp. (°C)	% Char Yield @ 650°C	Tg(°C) DMA @ 1Hz
0% DAPPO + 100%DDS	375	0	215
50% DAPPO + 50% DDS	370	14	177
75% DAPPO + 25% DDS	380	22	170
100% DAPPO + 0% DDS	380	26	160
50% DAMPO + 50% DDS	375	10	198
75% DAMPO + 25% DDS	375	20	183
100% DAMPO + 0% DDS	375	24	170

DDS = 4,4′ - diaminodiphenyl sulfone

DAPPO = Bis(3-aminophenyl) phenyl phosphine oxide

DAMPO = Bis(3-aminophenyl) methyl phosphine oxide

Table 4.3-1 **Characterization Data of Epoxy Networks Cured with Various Diamines**.

Diamine Curing Agents	Peak Heat Release Rate (KW/m^2)
25% DAMPO + 75% DDS	740
50% DAMPO + 50% DDS	450
75% DAMPO + 25% DDS	400
100% DAMPO + 0% DDS	400

Table 4.3-2 **Cone Calorimetry data on Epoxy Networks Cured with various Amounts of DAMPO**

(the incident radiant heat flux was 40 kW/m^2)

4.3.1.4 Dielectric Plots Analysis

Plots of dielectric loss (tan δ) versus time at the constant temperature of 177°C showed two maxima for all four frequencies used in this work for the Epon-828/DDS systems (Figure 4.2-6). The same observations were made for the two other curing agents, precisely BAPPO and DAMPO, both of which were synthesised in this work. The first transition corresponds to the gelation and the second one can be logically interpreted as vitrification because gelation normally preceeds vitrification during a curing program.

The second point emanating from the dielectric plots was that gelation was frequency independent (all of the four frequencies showed the same gelation time) while the time to vitrification depended on a given frequency. This is explainable in these terms that gelation is a chemical event, which is equally detected by all four frequencies, while vitrification arises from relaxation phenomena and consequently its probing depends upon the frequency of interest. The lowest frequencies gave the longest vitrification times, for example at the frequency of 1k Hz , vitrification was observed in about 68 minutes trom the beginning of the cure for Epon-828/DDS (figure 4.2-6) while the 100k Hz frequency indicated vitrification at about 40 minutes for the same system at 170°C.

When all three Epon-828 systems (DDS, BAPPO and DAMPO) were compared, both gelation and vitrification occurred earlier in DAMPO than the two other systems, and latest in DDS. Explained in other terms, DAMPO cures a lot faster than the commercially available DDS (see figure 4.3-6). The rationale underlying these diferences revolves around the electron withdrawing character of the sulfonyl group in the commercial diamine, which deactivates the amine functionality, making it less prone to attack the oxirane ring.

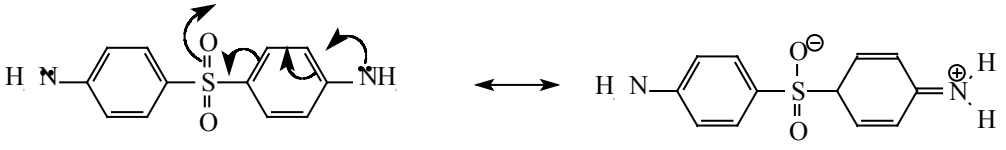

For the Epon-828/diamine systems cured for 3 hrs at 177^{o}C followed by ihr at 220^{o}C, the glass transtion temperatures were 270^{o}C for the DDS system, 240^{o}C for the DAMPO system and 235^{o}C for the BAPPO system (Figure 4.3-7). This trend is reminiscent of the trends found in our research group, using differential scanning calorimetry (DSC).

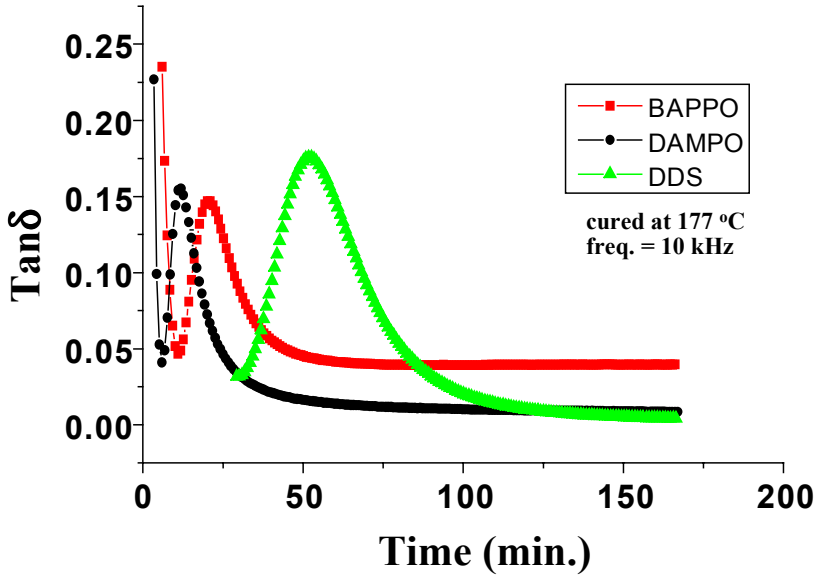

Figure 4.3-6 Dielectric Plots of Epon 828 Cured with Different Diamines

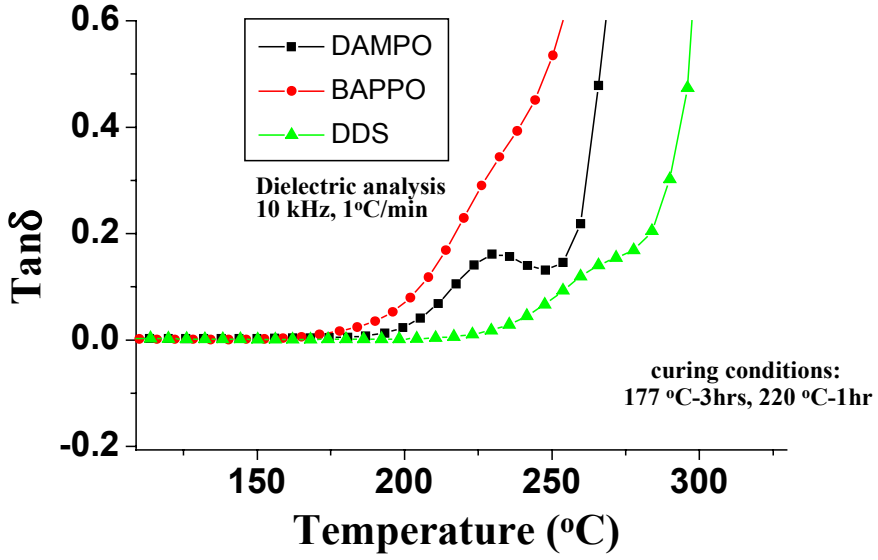

Figure 4.3-7 Glass Transition Temperatures of the Cured Networks (Epon-828 with Various Hardeners)

A TTT diagram was developed for the Epon-828 system using the techniques described in the previous sections. The gelation lines were created by using the conductance data analysis described in the previous chapter (Equation 3.5-6). When the times to gelation and the times to vitrification were recorded as a function of the curing isotherm, Figure 4.3-8 below was generated for the system Epon-828/DAMPO and Epon-828/4,4'-DDS.

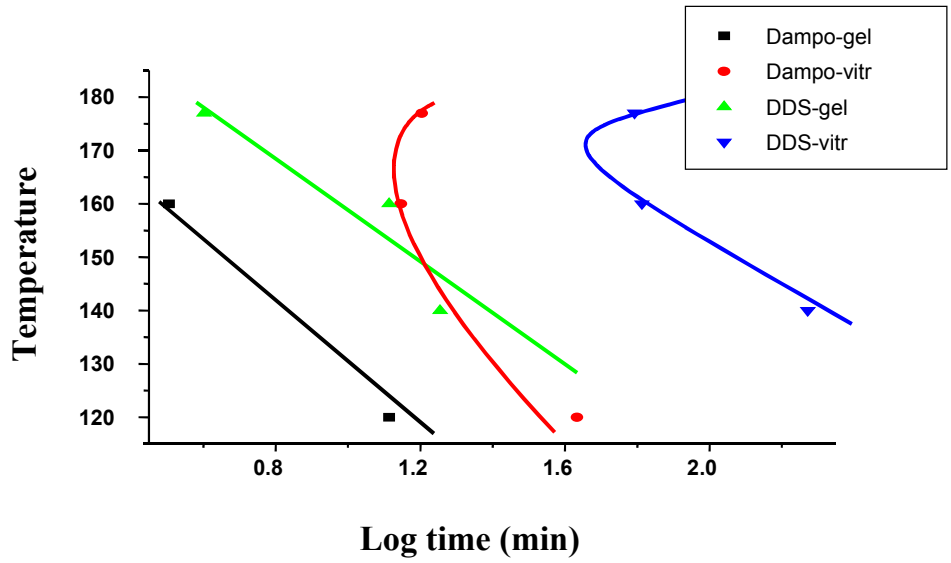

Figure 4.3-8 TTT diagram for the Systems Epon-828/DAMPO and Epon-828/DDS.

4.3.2 Tetrafunctional Networks

4.3.2.1 Tetraglycidyl Diamino Diphenyl Methane (TGDDM) Systems

Titration of MY-721 (TGDDM) showed an epoxy equivalent weight of 114g/mol, compared to a theoretical value of 105g/mol for an ideally pure resin; this is, by any account, a resin of high quality. NMR investigations gave a result of EEW = 108g/mol, which is somewhat closer to the ideal value of 105g/mol. However, epoxide protons from some other sources (such as residual epichlorohydrin) could have contributed to this value.

4.3.2.1.1 Dynamic Mechanical Analysis (DMA)

The storage and the loss moduli as functions of temperature for a network consisting of MY-721 and DDS are displayed in figure 4.3-9. On this graph, damping occurs at about 270^{o}C, which corresponds to the glass transition temperature. Similarly, Figure 4.3-10, the BAMPO and the DAPPO systems gave transition temperatures at 235 and 240^{o}C, respectively. The DDS system once again displayed higher thermal transitions when compared to the other systems used in this work (Figure 4.3-9). Transition temperatures were much higher for tetrafunctional systems as compared with Epon-828 networks. This result corroborates the idea that in highly crosslinked networks (which is the case for networks derived from MY-721), restriction in chain mobility requires higher temperatures to achieve transition temperatures.

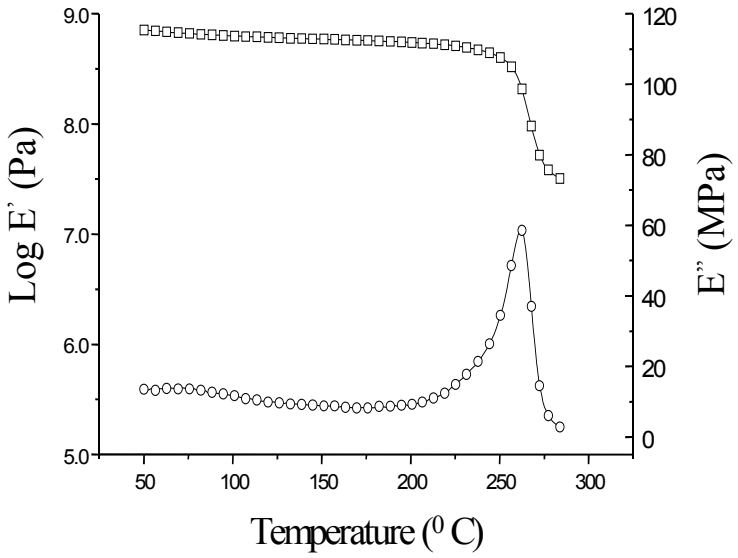

Figure 4.3-9 Storage and Loss Moduli for TGDDM/DDS (Frequency 1Hz)

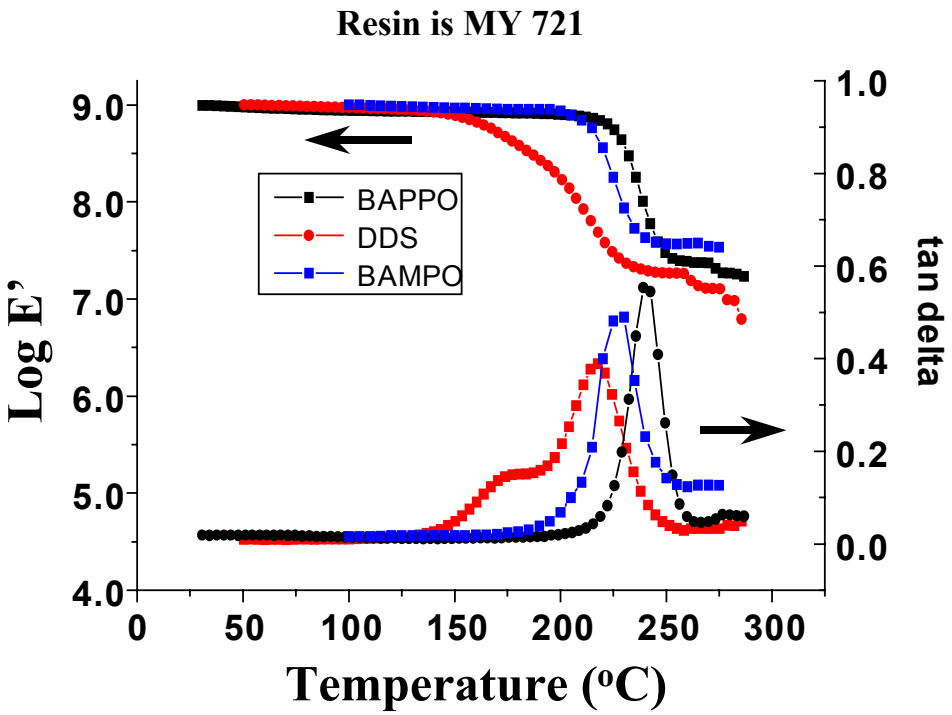

Figure 4.3-10 Storage and Loss Moduli for MY-721 (TGDDM) Cured with Various Diamines (Frequency 1Hz).

4.3.2.1.2 Dielectric Probing Results

Dielectric monitoring data are presented in Figure 4.3-11 for an isothermal cure of the tetrafunctional resin MY-721 with 4,4'-DDS as the curing agent. The dielectric loss as a function of time was recorded at four different frequencies, 1kHz, 10kHz, 33.3kHz and 100kKz. The first transition occurs at the same time for all four frequencies, while the second transition is frequency dependent. Gelation is the transition that appears at shorter times, and the latter peak can be interpreted as vitrification since gelation preceeds vitrification during curing. No other dielectric transitions were observed beyond the vitrification peak, at least within the time and temperature limits of our experiments. Gelation and vitrification both occurred at shorter times than those of the difunctional epoxy resin, Epon-828. The higher reactivity of the tetrafunctional resin can be ascribed to the greater number of oxirane rings, located on the resin.

When the gelation time and the vitrification time are recorded as functions of the cure isotherm , Figure 4.3-12 is generated for a TGDDM/DDS system. A time-temperature-transformation (TTT) diagram (Figure 4.3-13) was developed for this system (TGDDM/DDS), using relations described in the previous chapter. The gelation line was created by fitting conductance data to equation 3.5-6 (omitting data from the Cole arc in Figure 3.5-4).

The other curing agents used in this study, were bis(3,3'-aminophenyl) phenyl phosphine oxide (BAPPO) and bis(3,3'-aminophenyl) methyl phosphine oxide (BAMPO). They were synthesized in the course of this work and details for their synthesis have been presented in a previous chapter.

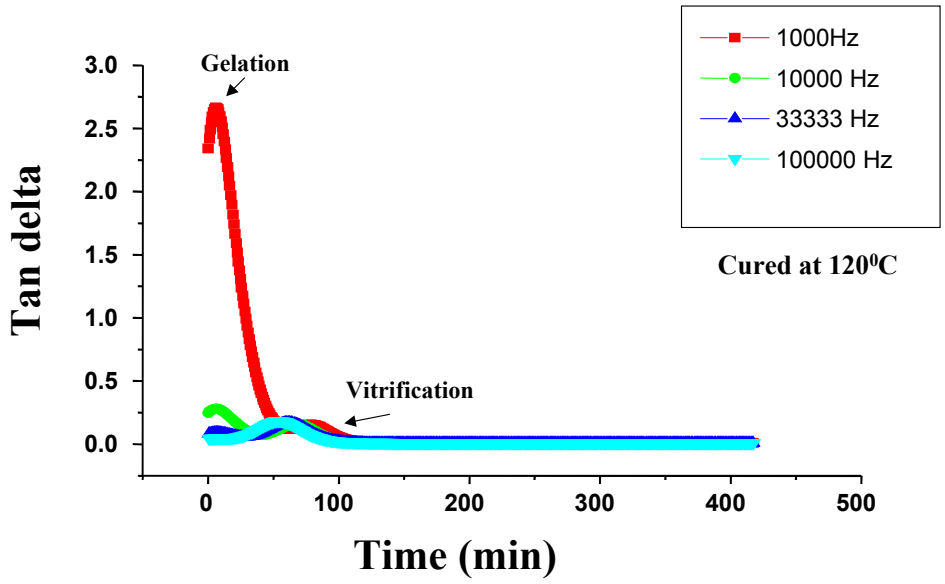

Figure 4.3-11 **Dielectic Monitoring of an Isothermal Cure of TGDDM-DDS**

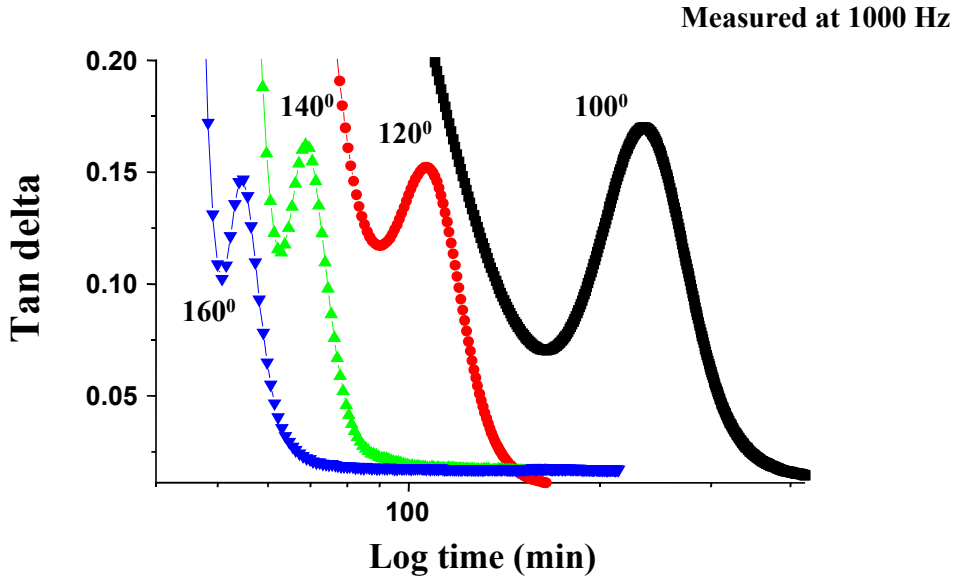

Figure 4.3-12 Curing Behavior (Vitrification peaks) of TGDDM-DDS as a Function of Temperature

The structures of BAMPO and BAPPO differ from that of DDS in that the amine functionality is para to a sulfonyl (electron withdrawing) group in the latter, while BAMPO and BAPPO have functional group in the meta position of an ether oxygen.

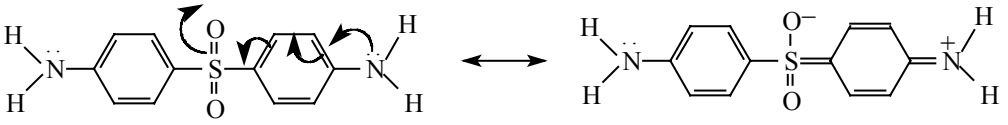

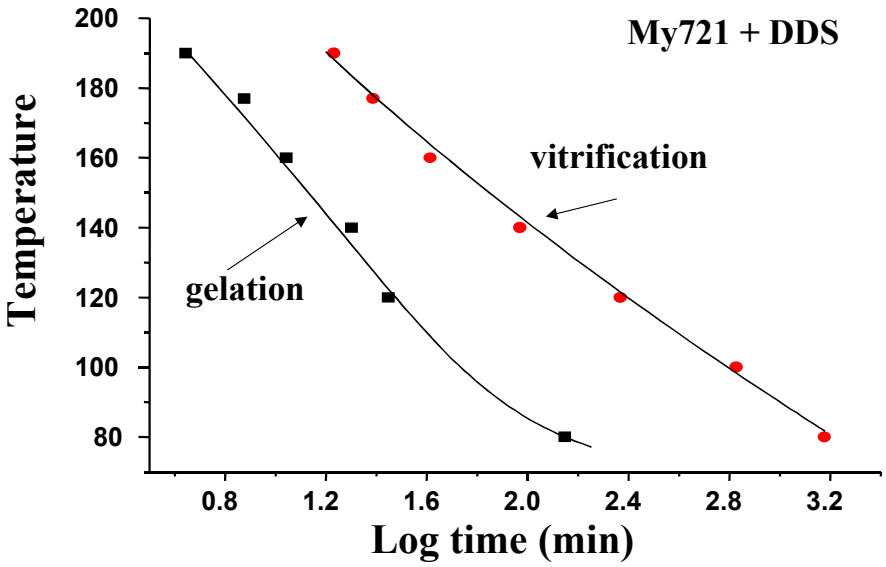

Figure 4.3-13 **TTT diagram for TGDDM/DDS @ 1000 Hz**

The sulfonyl group acts as an electron withdrawing group because of the difference in the electronegativity between sulfur and oxygen. The phosphine oxide moiety also has an electron withdrawing effect, with the negative charge similarly residing on the oxygen atom. The free electrons on the nitrogen in the para position are shared by the phenyl ring in resonance structures, indicating that they are less available for donation or for catalyzing the oxirane ring opening. Therefore, even though BAMPO and BAPPO are larger in size their reactivity is enhanced over that of 4,4' DDS. Using

this rationale it is not surprising to see that the two curing agents containing a phosphine oxide unit gel and vitrify quicker than those based on 4,4' DDS. Figure 4.3-14 and figure 4.3-15 demonstrate this behavior explicitly. A more subtle difference between the reactivity of BAMPO and BAPPO (the curing time of BAMPO is slightly shorter) could be explained by the fact that BAPPO's mobility is reduced by its large pendant phenyl group, compared to the methyl group in BAMPO. This difference is secondary with regards to the variations generated by resonance delocalization (meta or para substitutions).

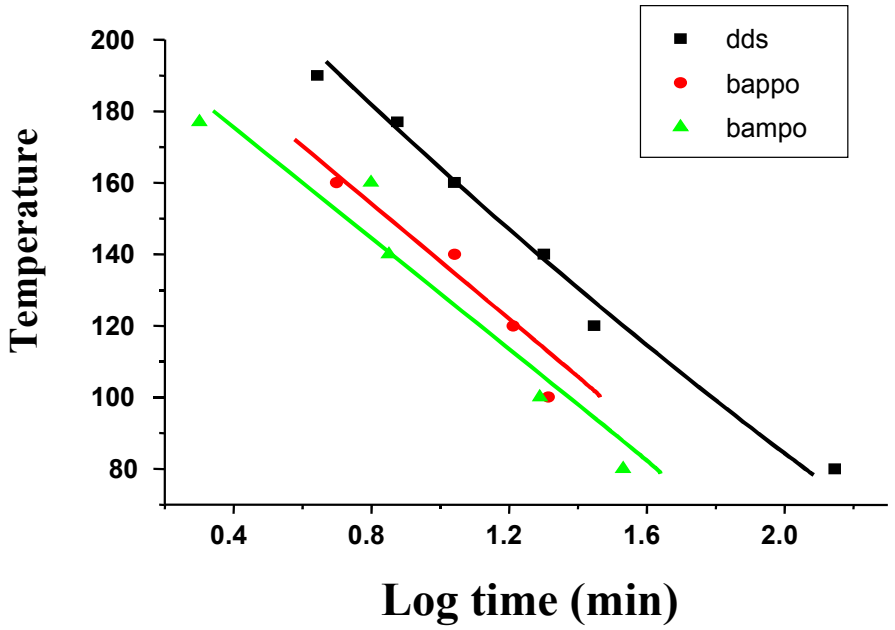

Figure 4.3-14 Gelation Times Measured by Dielectric Analysis for three Curing Agents (Frequency 1000 Hz)

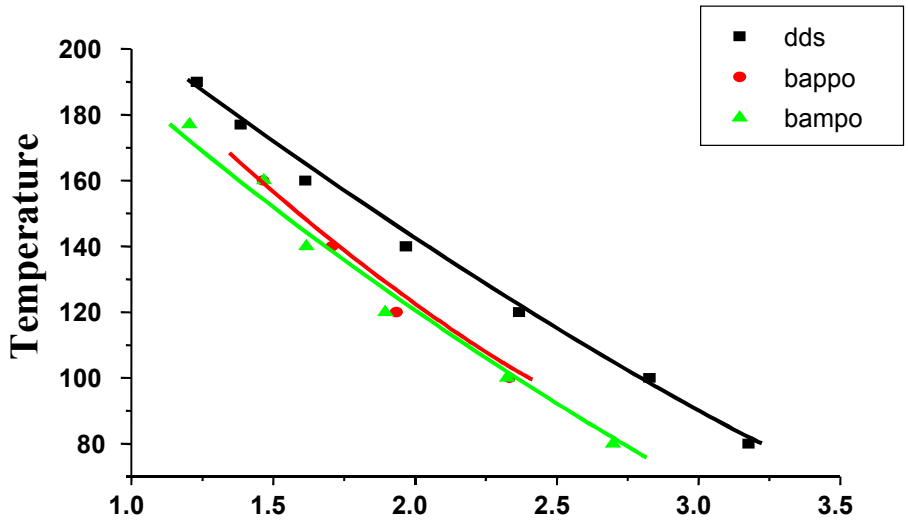

Figure 4.3-15 **Vitrification Curves from Dielectric Analysis for three Curing Agents (Frequency 1000 Hz)**

4.3.2.2 Tetraglycidyl Ether Of DAMPO (TGDAMPO)

Dynamic thermogravimetric analysis in air on the cured networks of TGDAMPO systems showed very high char residues, when compared to those of the commercially available TGDDM (Figure 4.3-16). This is attributable to the presence of phosphorus in both the resin and the curing agents synthesized in the course of this work. At 900^{o}C, the char residue was highest for the DAMPO curing agent and lowest for the control diamine 4,4'-DDS (Table 4.2-3). It is remakable however for any given system that there were any char residues at all at that temperature.

The glass transition temperatures as determined by dynamic mechanical analysis ranged from 230 to 242^{o}C. These relatively high values are to be expected from highly crosslinked systems. Even though the transitions were in the same range, systems with 4,4'-DDS proved to give the highest transition temperatures.

Diamine Curing Agent	**% Char Yield @ 800°C)**	**% Char Yield @ 900°C**	**Tg(°C) DMA @ 1Hz**
4,4'-DDS	7	5	242
DAMPO	28	18	220
DAPPO	35	10	230
BAPPO	25	12	

DDS = 4,4′ - diaminodiphenyl sulfone

DAMPO = Bis(3-aminophenyl) methyl phosphine oxide

DAPPO = Bis(3-aminophenyl) phenyl phosphine oxide

BAPPO = Bis(3-aminophenoxy phenyl) phenyl phosphine oxide

Table 4.3-3 **Characterization data of TGDAMPO Based Epoxy Networks Cured with Various Diamines**.

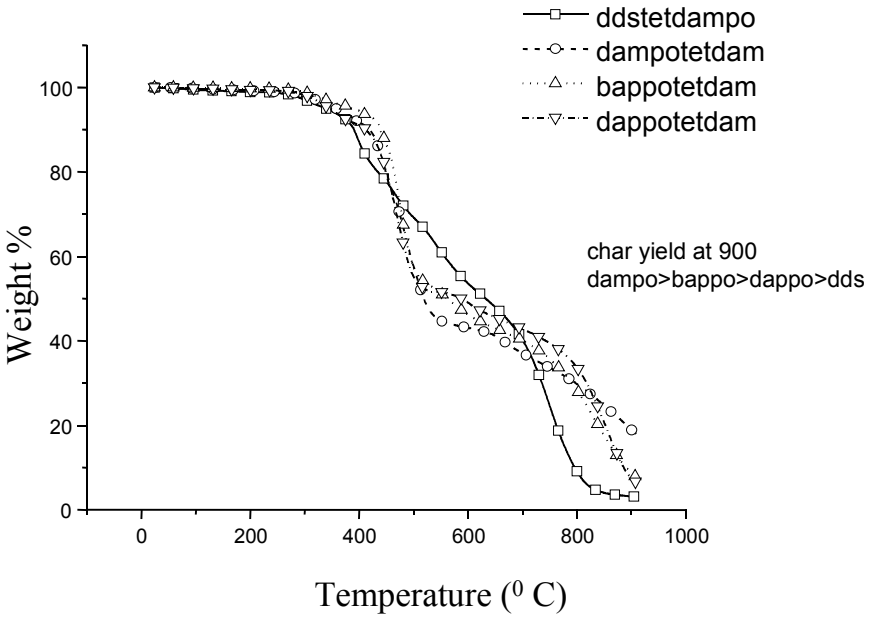

Figure 4.3-16 **Thermogravimetric Analysis (TGA) Data in Air on TGDAMPO Cured with Various Diamines** (the heating rate is 10/minute)

4.3.3 Toughened Networks

4.3.3.1 Resin Mixture Analysis

Differential scanning calorimetry (DSC) showed that the glass transition temperature (Tg) of the neat tetrafunctional resin (TGDDM) was –12.8^{o}C (Figure 4.3-17), for a second heating cycle at a heating rate of 10^{o}C per minute. The transition of the polyimide modifier had been shown to be about 217^{o}C[7]. Using the well known Fox equation[2] (Equation 4.3-1) as presented below, one would predict a single transition temperature around 21^{o}C, for a mixture having 25 weight percent of the modifier, if the mixture was indeed homogeneous.

$$\frac{1}{T_g} = \frac{W_A}{T_{g_A}} + \frac{W_B}{T_{g_B}} \qquad \text{Equation 4.3-1}$$

(where T_{gA} and T_{gB} represent the transition temperatures, and W_A and W_B represent the weight fractions of the resin and the modifier, respectively).

The experimental data (Figure 4.3-18) showed a single glass transition temperature (Tg), at 8.2^{o}C. This value departs from the calculated value (21^{o}C) derived from the Fox equation mentioned above. The reasons for this difference were not obvious, given that visual observations revealed a clear and transparent mixture. One might speculate however that the mixture was not as homogenous at the microscopic level as visual obsevations suggested.

4.3.3.2 Thermogravimetry (TGA) Results

Dynamic thermogravimetric analysis showed that even in the polyimide toughened

systems, phosphine oxide containing networks showed better fire resistance as evaluated by their higher char residues. For example, Figure 4.2-19 below depicts the TGA traces of two polyimide modified TGDDM systems, one cured with a phosphine oxide containing diamine and the other cured with the commercial diamine 4,4'-DDS. The phosphine oxide system displayed a char residue of 28% at 700^{o}C, while the control system had no char residue at the same temperature with a heating rate of 10^{o}C per minute. The same trend was observed in all of the systems that we studied.

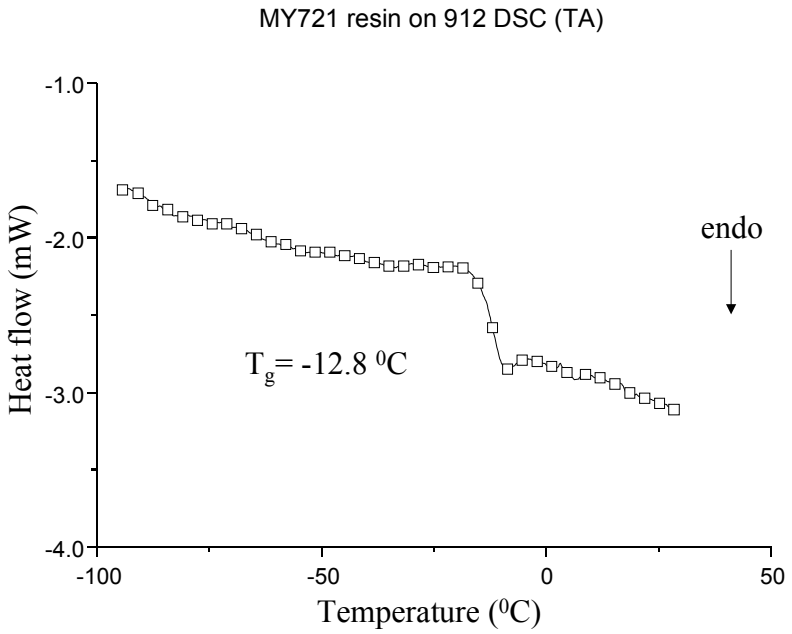

Figure 4.3-17 **Differential Scaning Calorimetry data of the Neat Resin (MY-721)**

(second heat, heating rate 10^{o}C/min)

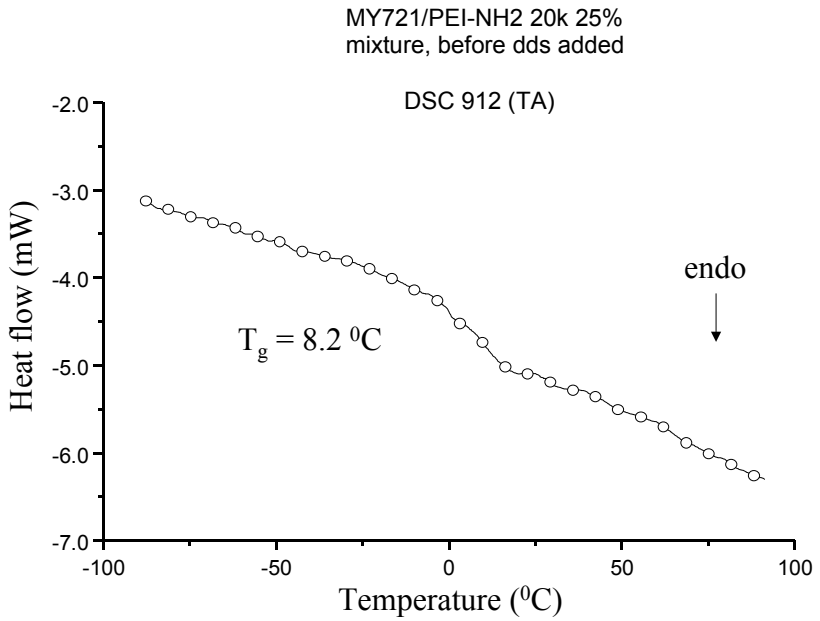

Figure 4.3-18 Differential Scaning Calorimetry of the Modified Resin (MY-721-PEI~NH_2/20K, 25%)

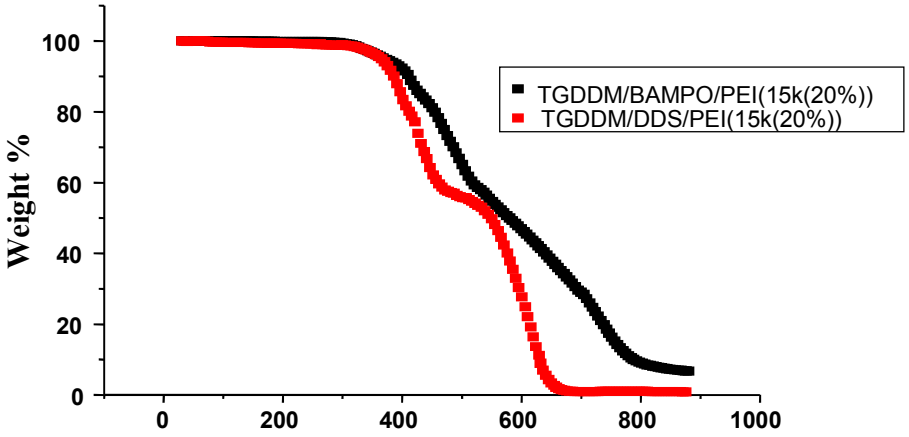

Figure 4.3-19 Thermogravimetric (TGA) Plots of Polyimide Toughened TGDDM Systems, Cured with Bampo and a Control Cured with DDS.

4.3.3.3 Dynamic Mechanical Analysis

Dynamic mechanical analysis (DMA) was relied upon to assess phase separation in the toughened epoxy networks and to determine the transition temperatures associated with each phase. Samples without any additional thermal treatment following the cure showed two transitions. One transition, whose peak ranged from 175-212^{o}C corresponding to the polyetherimide toughener, either reactive or non-reactive. The non-reactive polyetherimide phases always had lower glass transition temperatures than the corresponding reactive polyetherimide phases. This can be ascribed to the better interfacial adhesion of the reactive modifier with the epoxy matrix, or to the decreased mobility of the reactive modifier chains due to chemical attachment to the matrix.

The other thermal transition, which ranged from 260-270^{o}C corresponded to the epoxy phase glass transition temperature (T_g). The dynamic mechanical analyses (DMA) of these materials are illustrated in Figure 4.3-20 to Figure 4.3-22. The DMA behavior of the neat epoxy (without polyetherimide modifier) cured with DDS was shown earlier in Figure 4.3-9. It should be pointed out that the T_g of the epoxy phase in that neat system was approximately 270^{o}C. In the modified systems, it is noticeable that the glass transition temperature of the polyetherimide phase increased with its concentration. Also, the area underneath the transition seemed to increase with the concentration of the corresponding phase, even though the increase did not reflect any specific proportionality. Finally, the reactive polyetherimide modifiers all had higher transition temperatures than the non-reactive modifiers for the toughener rich phase at comparable compositions. Figures 4.3-23 and 24 summarize these observations.

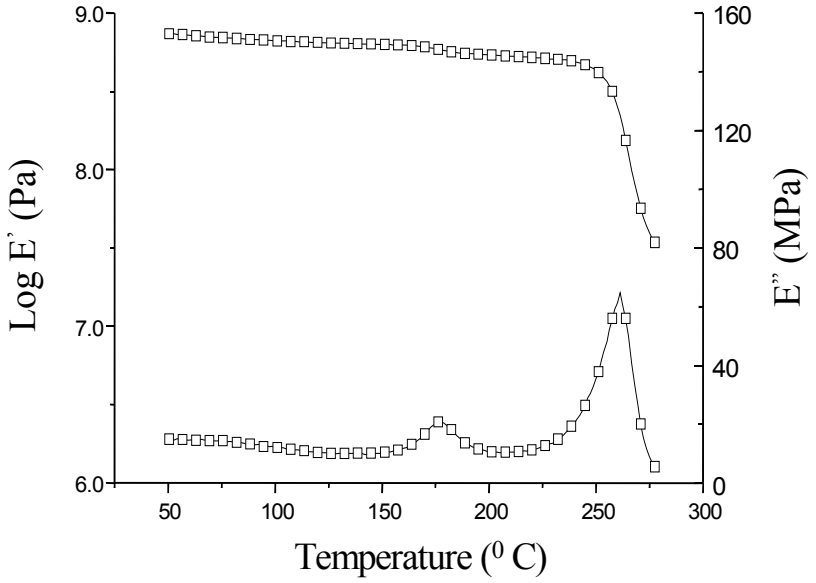

Figure 4.3-20 **DMA plot of a Modified Epoxy Network** (TGDDM-Ultem 10%/DDS)

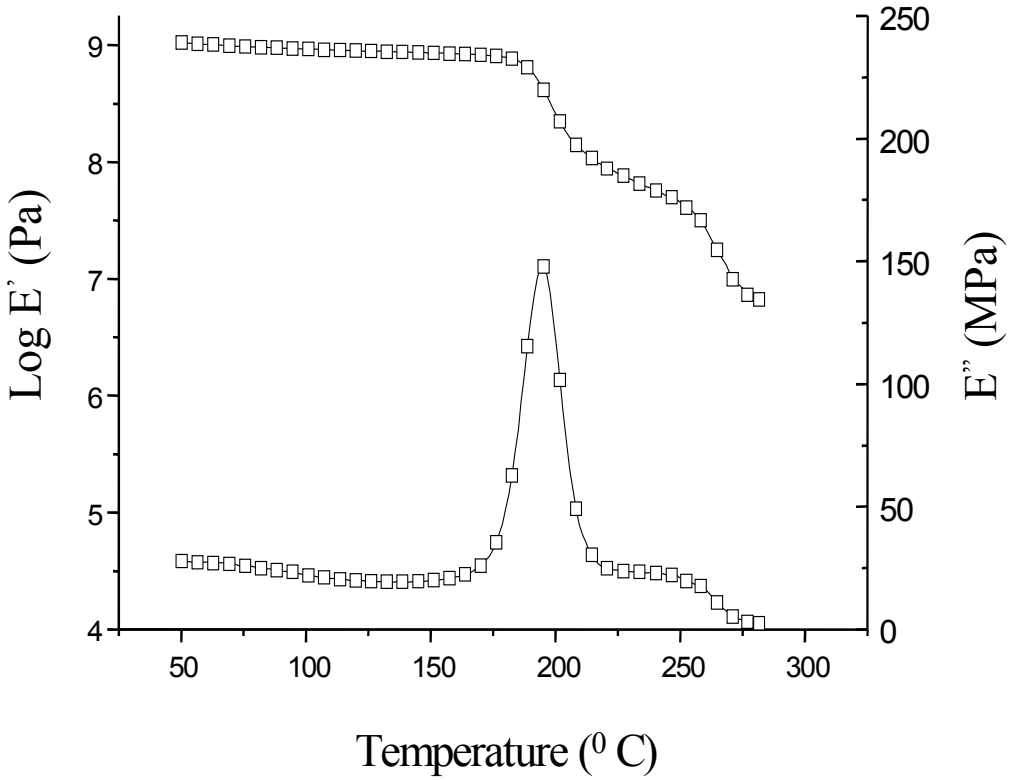

Figure 4.3-21 **DMA Plot of a Modified Epoxy Network** (TGDDM-Ultem 25%/DDS)

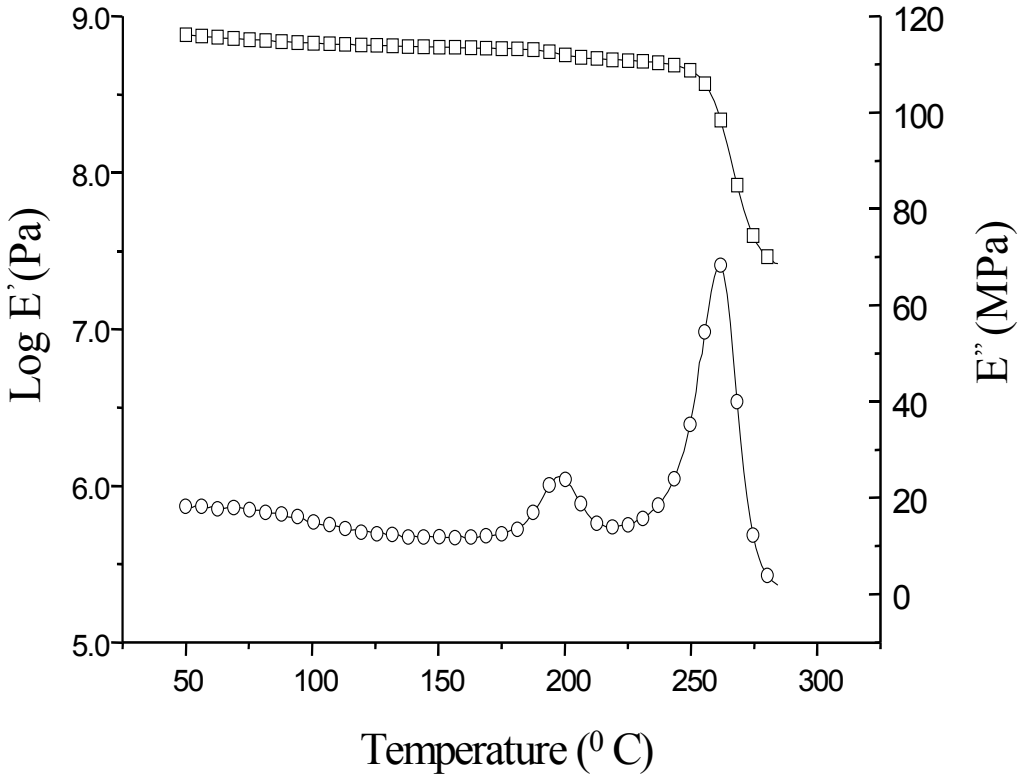

Figure 4.3-22 **DMA Plot of a Modified Epoxy Network** (TGDDM- PEI~NH_2 20k 10%/DDS)

As expected, the magnitude of the mechanical loss for the toughener also increased as its concentration increased in the modified systems. The epoxy T_g apparently remained constant in all systems, while the transitions for the tougheners T_g(toughener) increased with their concentrations. The thermoplastic modifier consisting of the 10k amine terminate (thus reactive) did not follow that trend. The reason for this discrepancy is not clear. It might possibly be explained if a more thorough interpretation of phase behavior phenomena were achieved.

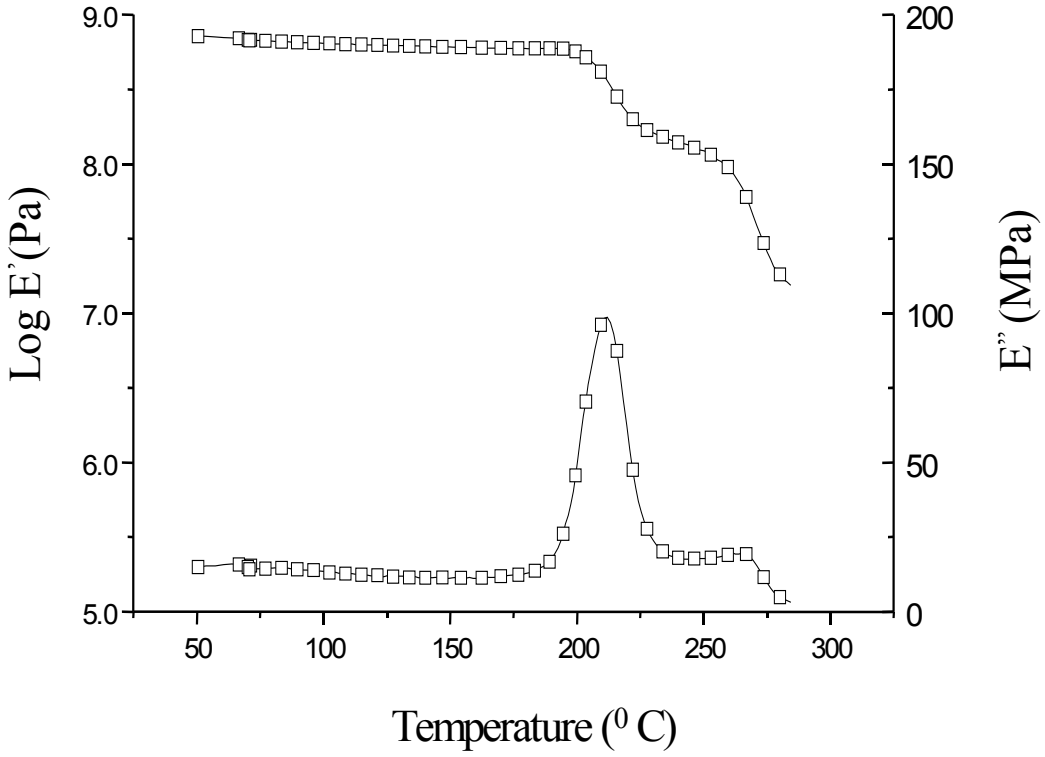

Figure 4.3-23 **DMA of a Modified Epoxy Network** (TGDDM-PEI~NH_2 20k 20%/DDS)

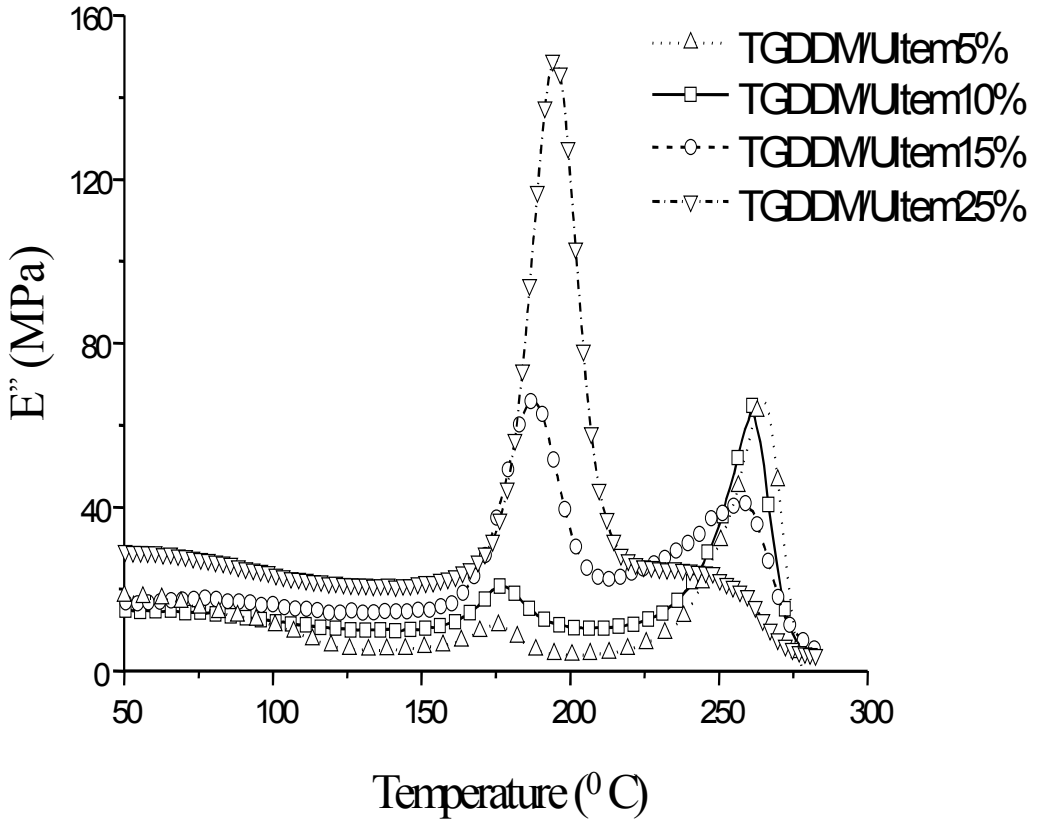

Figure 4.3-24 **DMA Summary Plots for Modified Epoxy Resins** (TGDDM-Ultem/DDS)

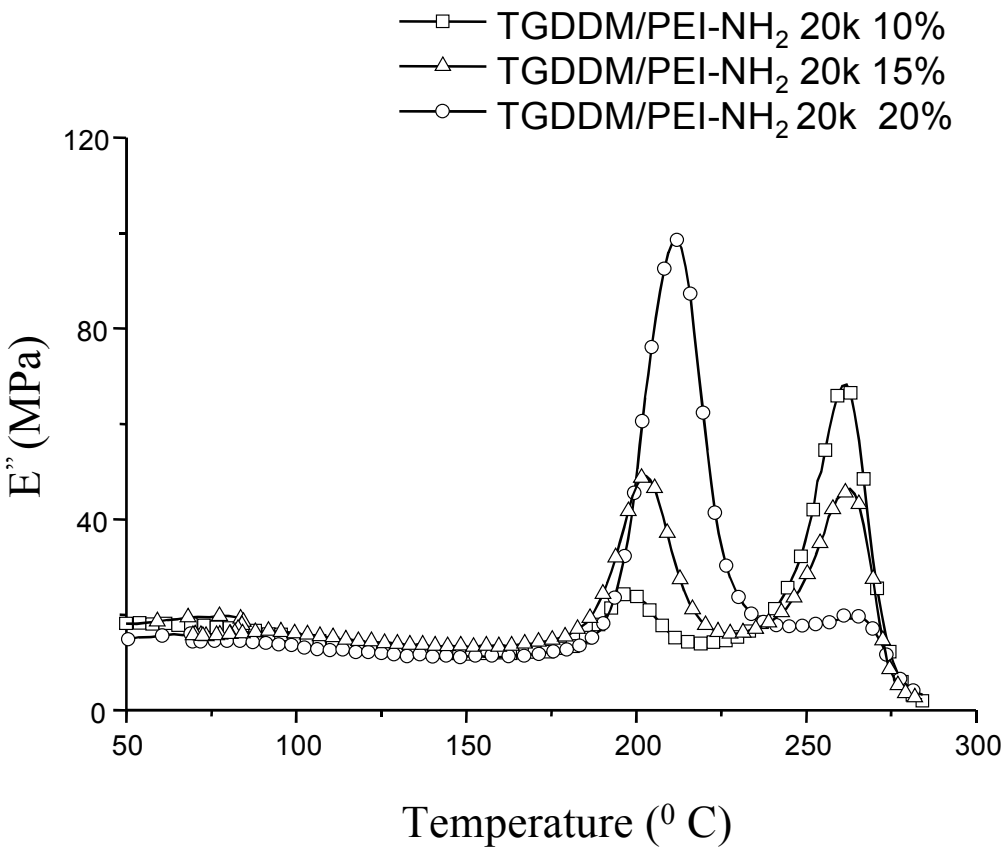

Figure 4.3-25 **DMA Summary Plots of Modified Epoxy Networks** (TGDDM-PEI~NH_2 20k modified /DDS)

4.3.3.4 Scanning Electron Microscopy

Besides giving information about the morphological features of the tetrafunctional epoxies, the scanning electron micrographs were used to complement the interpretation of the dynamic mechanical behavior of the networks. Polymer morphology is usually a function of the molecular weight and also, as we will verify later in this section, differences between the reactive and non reactive thermoplastic modifiers. As the molecular weight decreased the thermoplastic modifier contributed less to the continous phase. Even at 20% loading of the 10k PEI~NH_2 in the epoxy network, which is considerable, only discrete particles of the modifiers could be observed on the micrographs (figure 4.2-26). At 10% (a) and 15% (b) loadings this toughener distinctly shows only dispersed toughener particles. This behavior can be contrasted with figure 4.2-27 and figure 4.2-28 that show that higher molecular weights of the thermoplastic modifiers allowed them a greater contribution to the continuous phase (15k PEI~NH_2 modifiers for example), or even a phase inversion morphology as the 20K PEI~NH_2 modifier system at a 20% loading would suggest.

Phase inversion morphology was also observed for the ULTEM system (non-functional modifier) at 25% loading for example (Figure 4.3-32).

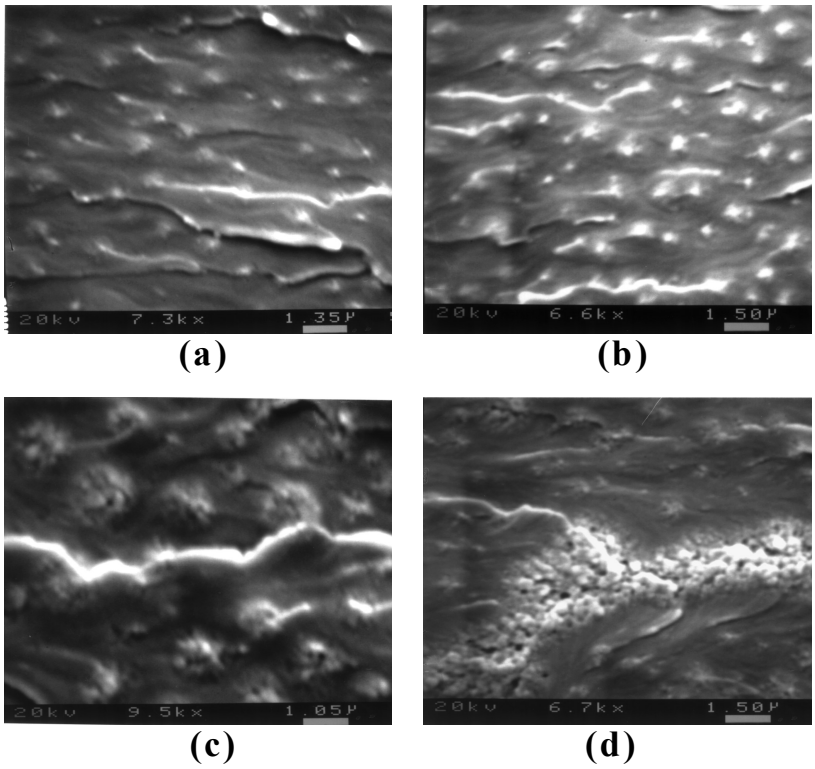

Figure 4.3-26 **Micrograph of theTGDDM/(PEI~NH_2 10k)-DDS Fracture Surface** (a) 10%;

(b) 15%; (c),(d) 20% PEI~NH_2

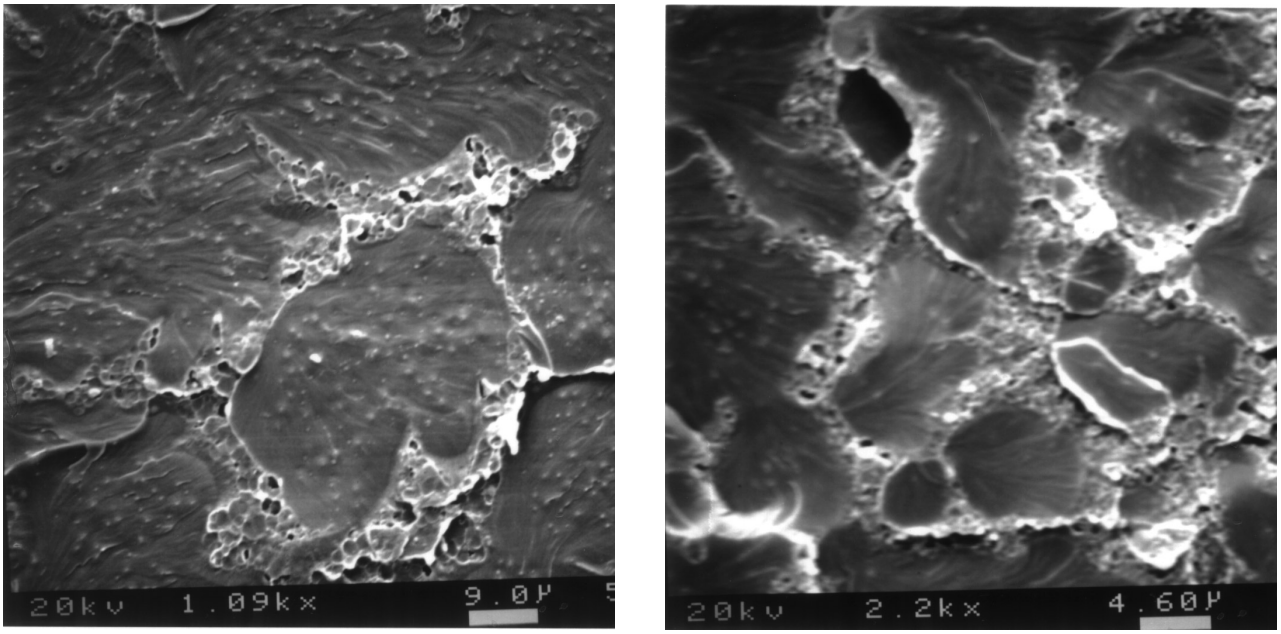

Figure 4.3-27 Micrograph of the TGDDM/(PEI~$NH_2$15k)-DDS Fracture Surface
(a)15%; (b)20% Toughener Content

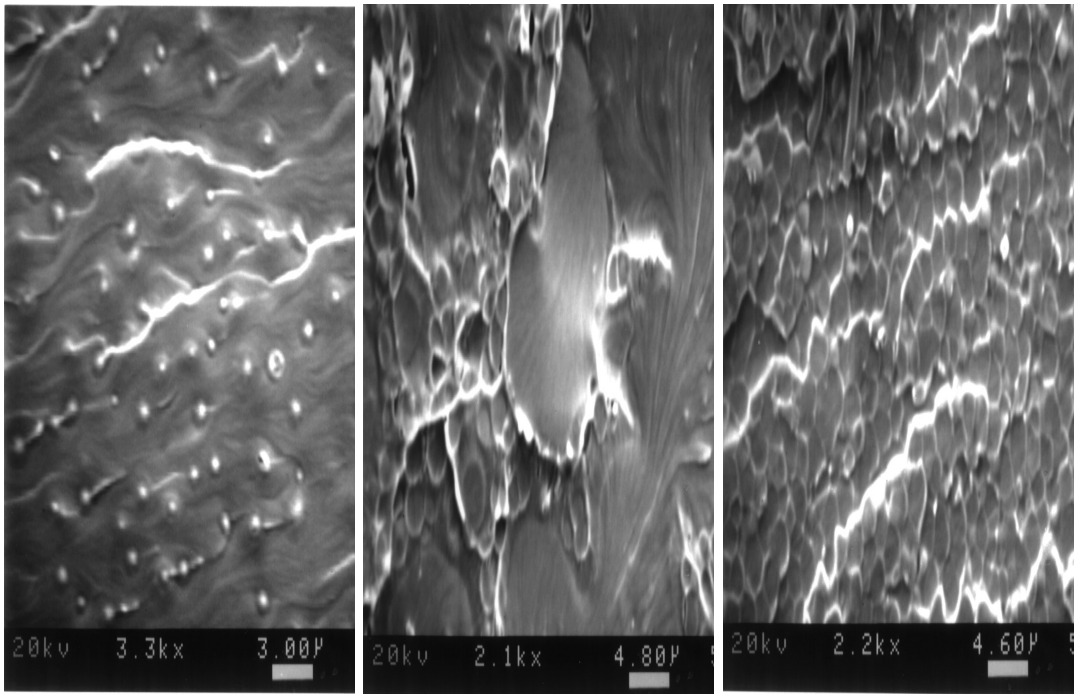

Figure 4.3-28 Micrograph of the TGDDM/(PEI~NH_2 20k)-DDS Fracture Surface (a)10%; (b)15%; (c)20% Weight of the Toughener.

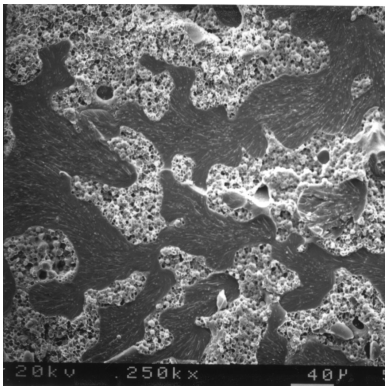

(a)

Figure 4.3-29Micrograph of the Fracture Surface for theTGDDM/(Ultem 15%)-DDS System

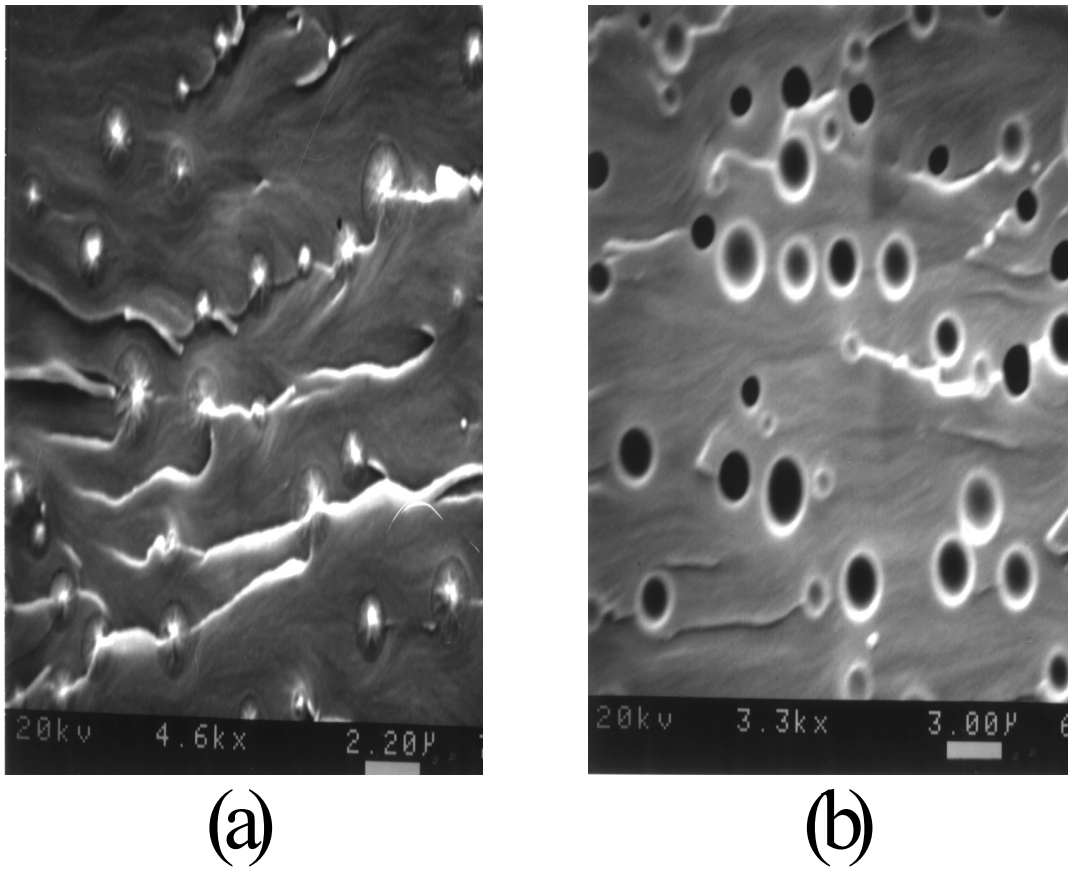

Figure 4.3-30 Micrograph of the TGDDM/(Ultem 10%)-DDS (a)Fracture Surface (b) Fracture Surface Etched in Chloroform

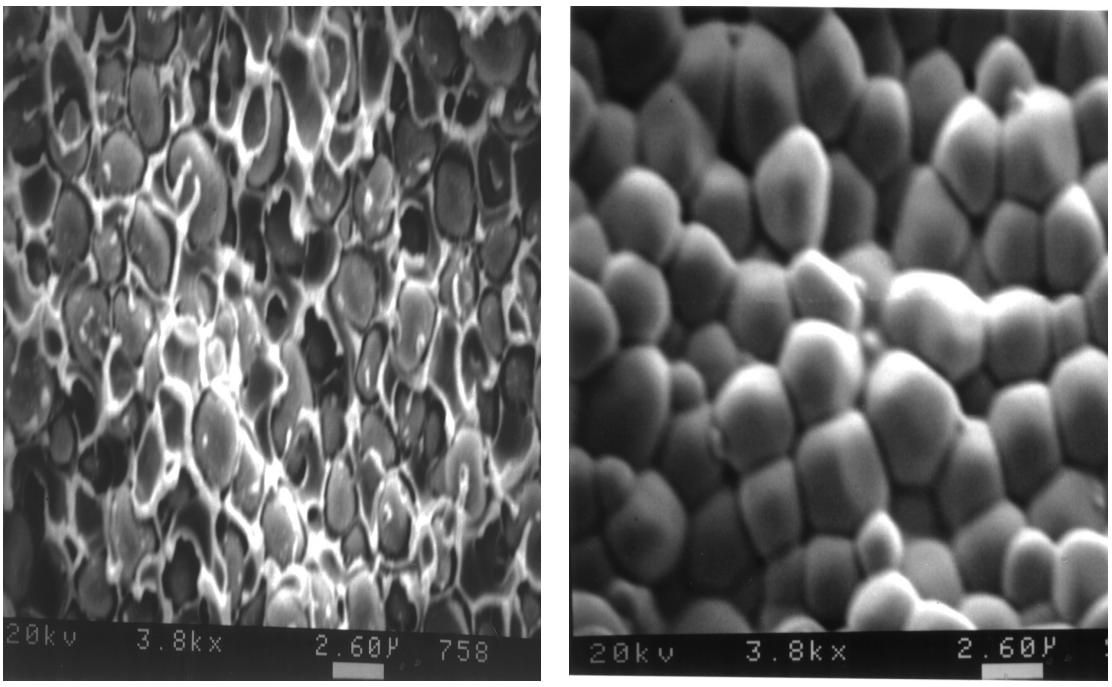

Figure 4.3-31 **Micrograph of the TGDDM/(Ultem 20%)-DDS System (a)Fracture Surface (b)Fracture Surface Etched in Chloroform**

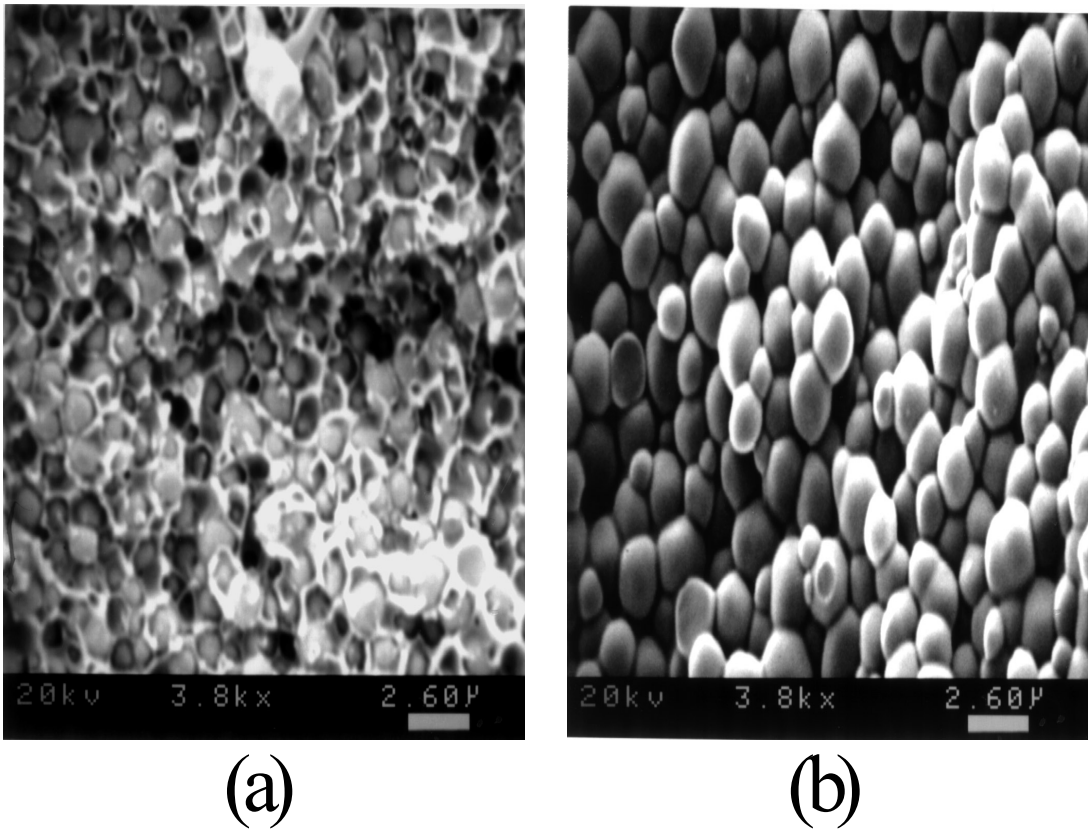

Figure 4.3-32 Micrograph of the TGDDM/(Ultem 25%)-DDS system (a)Fracture Surface (b)Fracture Surface Etched in Chloroform

All of the samples were etched in chloroform for 10 days unless they fell apart before then. The only samples that decomposed were the 15, 20 and 25% Ultem® toughened samples, which were only etched for 7 hours. The samples were vacuum dried and examined for dissolution of the toughener on the surface. The etched Ultem® samples are shown in (b) of figure 4.2-31 to figure 4.2-39 In all of these materials the Ultem® was removed from the surface to leave only epoxy on the surface. All of the

reactive PEI modified systems remained identical to their unetched state, and there was no evidence that the toughener was removed. This point gives credence to the idea that the amine terminal group does react with an epoxide group to achieve covalent interfacial interactions.

4.3.3.5 Mechanical Testing

Fracure toughness data showed that thermoplastic modification greatly improved the mechanical properties of the epoxy networks. The largest increase corresponded with 15% Ultem addition to the TGDDM. This result is consistent with what have previously been described by other workers.[8, 9] A large improvement in the fracture toughness was also observed with 20% PEI-NH_2 toughening of the epoxy network. These results are summarized in Figure 4.3-33 There was only a small enhancement of the fracture toughness at 10% loading for all of the thermoplastic modifiers. This is consistent with the hypothesis that a co-continuous morphology, which is characteristic of spinodal decomposition,[11]or a phase inverted morphology, where discrete thermoset particles are surrounded by a continous phase of the thermoplastic modifier will provide optimum toughness.[12, 13]

Thermoplatic modification generated only a moderate decrease in the flexural modulus.(Figure 4.3-34). This decrease did not appear to be significant.

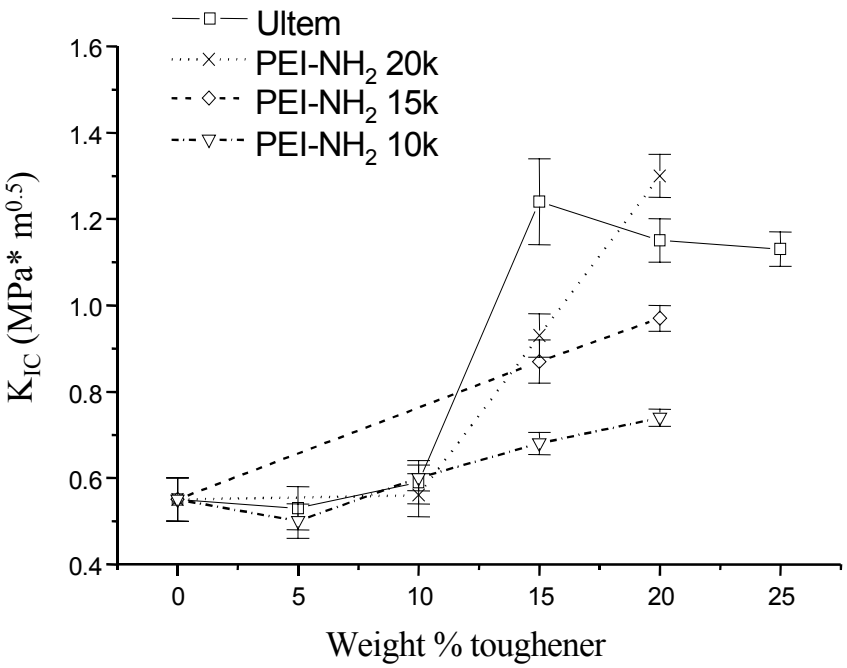

Figure 4.3-33 **Fracture Toughness of the Poly(etherimide) Modified Networks**

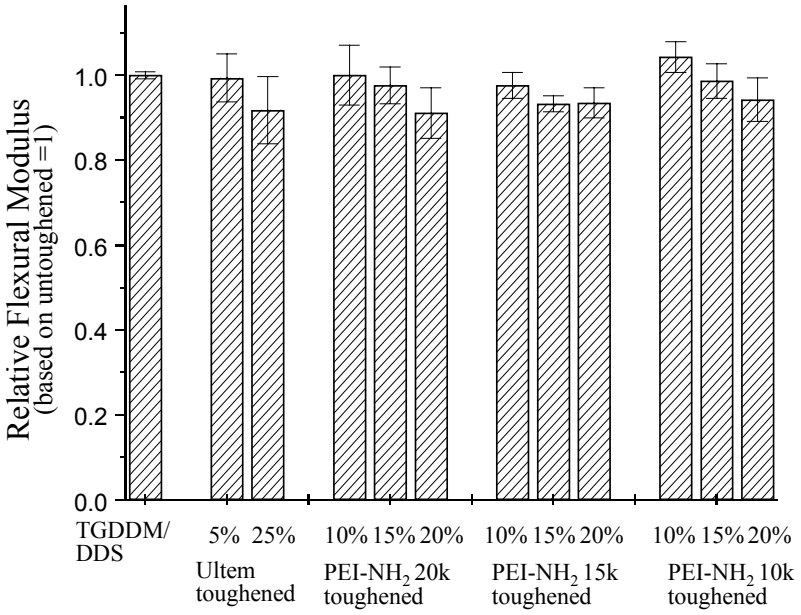

Figure 4.3-34 Flexural Modulus of the Touhghned Networks

4.3.3.6 Soxhlet Extaction

The extractable fraction of the toughened epoxy materials increased as the weight fraction of Ultem in the epoxy increased. This trend is shown in Figure 4.3-34. In the cases where the networks were modified with 15 - 25% Ultem (the continuous phase), the network structure collapsed. This collapse can be ascribed to the extraction of the thermoplastic modifier, given that in the cases where the modifiers were functionalized, there seemed to be little change in the structure of the net work during the extraction.

Solvent resistance of the amine terminated modifier systems was superior to that of the commercially available thermoplastic. In the former (PEI-NH2 toughened materials), no extractables were noticeable. This substantiates the chemical resistance of the amine terminated polyetherimides over Ultem.

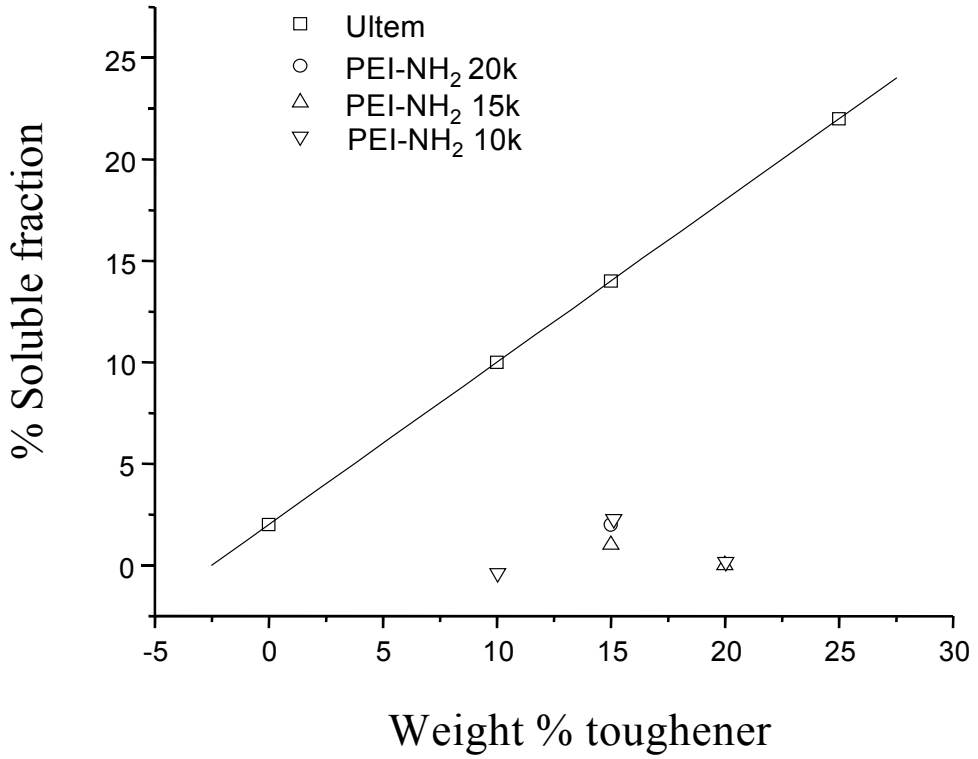

Figure 4.3-35 **Soxhlet Extractions of Toughened Tetrafunctional Epoxies**

4.4 SUMMARY

Epoxy netowrks containing phosphine oxide units showed higher flame resistance than the control, as assessed by thermogravimetric analyses, cone calorimetry, and qualitaive "Bunsen burner" tests.

Dramatic improvements of the fracture toughness of brittle epoxy networks were achieved through the means of poly(ether imides) thermoplastic modification, with only a moderate decrease in teir flexural modulus. Fracture properties were superior in the systems where the thermoplastic modifiers contained amine functional groups, when compared to their non functionalized comercial homologues.

Also, solvent resistance of the toughened networks was significantly higher when the thermoplastic modifiers were functionalized. These results were verified by scanning electron microscopy (SEM) and Soxhlet extraction.

Dielectric monitoring was an effective way to follow the curing process of epoxy resins. The time between the beginning of the cure and vitrification was longest for 4,4'-diaminophenyl sulfone at 177^{o}C when reacted with Epon-828 for example, and shortes for DAMPO. Also, tetrafunctional epoxy resins cured much faster than diffuctional resins.

Transition temperatures were significantly higher for tetrafunctional epoxy networks, when compared to networks generated with Epon-828.

4.5 REFERENCES

4. Boutevin
5. Fox, T. G. (1956) *Bull. Am. Soc*. **1**, 123.
6. Degoulet, C., J.P. Busnel and J.F. Tassin (1994) *Polymer,* **35**, 1957.
7. Konas, M., T.M. Moy, M.E. Rogers, A.R. Shultz, T.C. Ward and J.E. McGrath (1995) *J. Polym. Sci. Part B*, **33**, 1429.
8. Van Krevelen, D. W. 1974 Chimia 28, 504.
9. Cone Calorimeter?
10. Zhuang, H. (1998) Ph. D. Thesis, Virginia Polytechnic Institute and State University.
11. Bucknall, C.B. and I.K. Partridge (1983) *Polymer*, **25**, 1017.
12. Raghava, R.S. (1983) *Natl. SAMPE Symp.* **28**, 367.

13. Yoon, T.H., S.C. Liptak, D.B. Priddy and J.E. McGrath (1994) *J. Adhesion*, **45**, 191.

14. Sefton, M.S., P.T. McGrail, S.P. Wilkinson, J.A. Peacock, M. Davies, P. Crick and G. Almen (1987) *Int. SAMPE Tech. Conf.,* **19**, 700.

15. Srinivasan, S.A. and J.E. McGrath (1993) *High Perform. Polym.*, **5**, 259.

16. Wilkinson, S.P. T.C. Ward and J.E. McGrath (1993) *Polymer*, **34**, 870.

5 CHAPTER 5 POLYMER SYNTHESIS

5.1 OBJECTIVES

Monomers synthesized in this work (chapter 2) will be used to form different types of high molecular weight linear macromolecules. This is the ultimate proof of the very high degree of purity of those monomers. The polymers will include poly(urea-urethanes), polyimides and poly(arylene ether ketones). Their molecular weights and solubilities will be determined, and then the polymer samples will be evaluated for their flame resistance by dynamic thermogravimetric analysis.

Another objective of this chapter is to describe the synthesis of the thermoplastic modifiers that have been used to improve the physical properties of epoxy networks as shown in the previous chapter.

5.2 Materials and Methods

5.2.1 Chemicals

The monomers containing phosphine oxide units have been described in Chapter 2. Their structures are shown below simply as a reminder.

Bis(3-aminophenyl) methyl phosphine oxide (DAMPO)

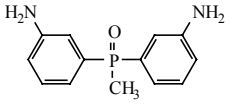

Bis(3-aminophenyl) phenyl phosphine oxide (DAPPO)

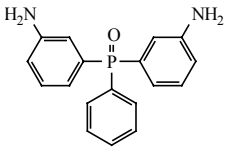

Bis(3-aminophenoxyphenyl) phenyl phosphine oxide (BAPPO)

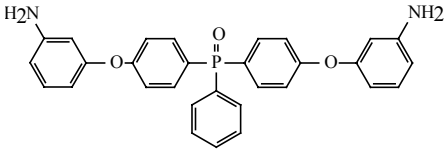

Bis(3-aminophenoxyphenyl) methyl phosphine oxide (BAMPO)

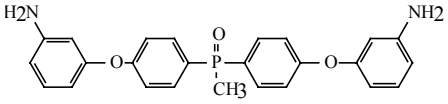

Bis[4-(2-hydroxyethyl 1-oxy)phenyl] phenyl phosphine oxide (EBHPPO)

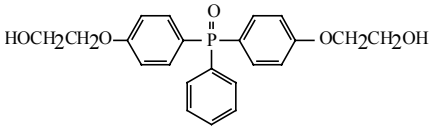

Bis(4-phenoxyphenyl) phenyl phosphine oxide (BPPPO)

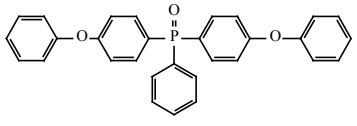

Methylene diisocyanate(MDI):

Supplier: Bayer Corporation

Empirical Formula: $C_{15}H_{10}N_2O_2$

Molecular Weight: 250.26

Boiling Point, ^oC: 194 (5mm)

Melting Point, ^oC: 37

Structure: 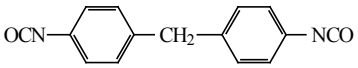

Purification: Used as received

Poly(tetramethylene glycol) (Poly THF):

Supplier: BASF

Empirical Formula: $C_4H_{10}O_2$

Molecular Weight: 650

Melting Point, ^oC: Liquid at room temperature

Structure: 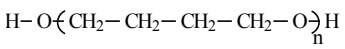

Purification: Used as received

1,4-Butanediol:

Supplier: Aldrich, 99+%

Empirical Formula: $C_4H_{10}O_2$

Molecular Weight: 90.12

Boiling Point, ^oC: 230

Melting Point, ^{o}C: 16

Structure: $HO-CH_2-CH_2-CH_2-CH_2-OH$

Purification: Used as received

Diphenyl Ether:

Supplier: Aldrich, 99%

Empirical Formula: $C_{12}H_{10}O$

Molecular Weight: 170.21

Boiling Point, ^{o}C: 259

Melting Point, ^{o}C: 26

Structure: 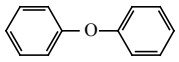

Purification: Used as received

Aluminum Chloride:

Supplier: Acros, 99%

Empirical Formula: $AlCl_3$

Molecular Weight: 133.34

Structure: $AlCl_3$

Purification: Used as received

1,2-Dichloroethane:

Supplier:	Acros, 99%
Empirical Formula:	$C_2H_4Cl_2$
Molecular Weight:	98.96
Boiling Point, ^oC:	83
Melting Point, ^oC:	-35
Structure:	$ClCH_2CH_2Cl$
Purification:	Distilled over calcium hydride

Terephthaloyl Chloride:

Supplier:	Acros, 99%
Empirical Formula:	$C_8H_4O_2Cl_2$
Molecular Weight:	203.2
Boiling Point, ^oC:	266
Melting Point, ^oC:	79
Structure:	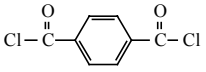
Purification:	Twice sublimed at 40^oC

2,2'-Bis[4-(3,4-dicarboxyphenoxy)phenyl]propane (Bisphenol-A dianhydride or BPADA):

Supplier: General Electric

Empirical Formula: $C_{31}H_{21}O_8$

Molecular Weight: 520.49

Melting Point, ^oC: 193

Structure: 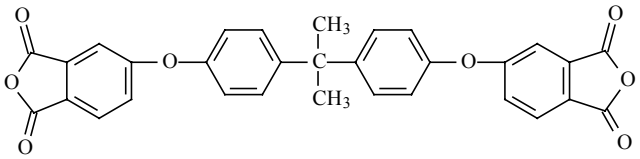

Purification: Recrystallyzed from a mixture of toluene and acetic acid (10:1, v/v)

1,3-Phenylene Diamine (*m*-PDA):

Supplier: Aldrich

Empirical Formula: $C_6H_8N_2$

Molecular Weight: 108.14

Melting Point, ^oC: 66

Structure: 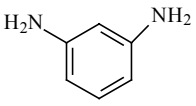

Purification: Sublimed at 80^oC

Triethylamine:

Supplier: Fisher Scientific

Empirical Formula: $C_6H_{15}N$

Molecular Weight: 101.19

Boiling point, ^oC: 88.8

Melting Point, ^oC: -115

Structure: 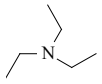

Purification: Dried on sodium and distilled

1-Methyl-2-Pyrrolidinone (NMP):

Supplier: Fisher Scientific

Empirical Formula: C_5H_9NO

Molecular Weight: 99.13

Boiling Point, ^oC: 202

Melting Point, ^oC: -24

Structure: 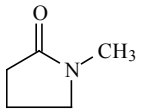

Purification: Dried over phosphorus pentoxide for 24 hours then vacuum distilled

o-Dichlorobenzene (*o*-DCB):

Supplier: Fisher Scientific

Empirical Formula:	$C_6H_4Cl_2$
Molecular Weight:	147.00
Boiling Point, ^oC:	180
Melting Point, ^oC:	-15
Structure:	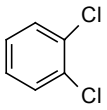
Purification:	Dried over calcium hydride for 24 hours then vacuum distilled

5.2.2 Instruments

The instruments used here are the same that were described in Section 2.2.1.

5.3 Poly(Urea-Urethanes)

5.3.1 Introduction

Segmented polyurethanes are a class of materials whose properties can be tailored by systematic variations in their synthetic components. They are derived from the reaction of diisocyanate monomers and diols or diamines, in which latter case they are referred to as polyureas. Their applications include adhesives, coatings, elastomers, fibers and foams (car seats). A typical segmented polyurethane consists of a soft segment which is an oligomeric diol (hydroxy terminated polytetrahydrofuran for example) and a hard segment deriving from the reaction of a diisocyanate (methylene-bis -4,4'-phenyl diisocyanate for example) and a diol monomer, more conveniently called chain extender (Scheme 5.3-1). Their unique properties derive from the thermodynamic incompatibility

between the segments. The possible variations of the length and the chemical nature of the segments place these materials among the most versatile polymers.

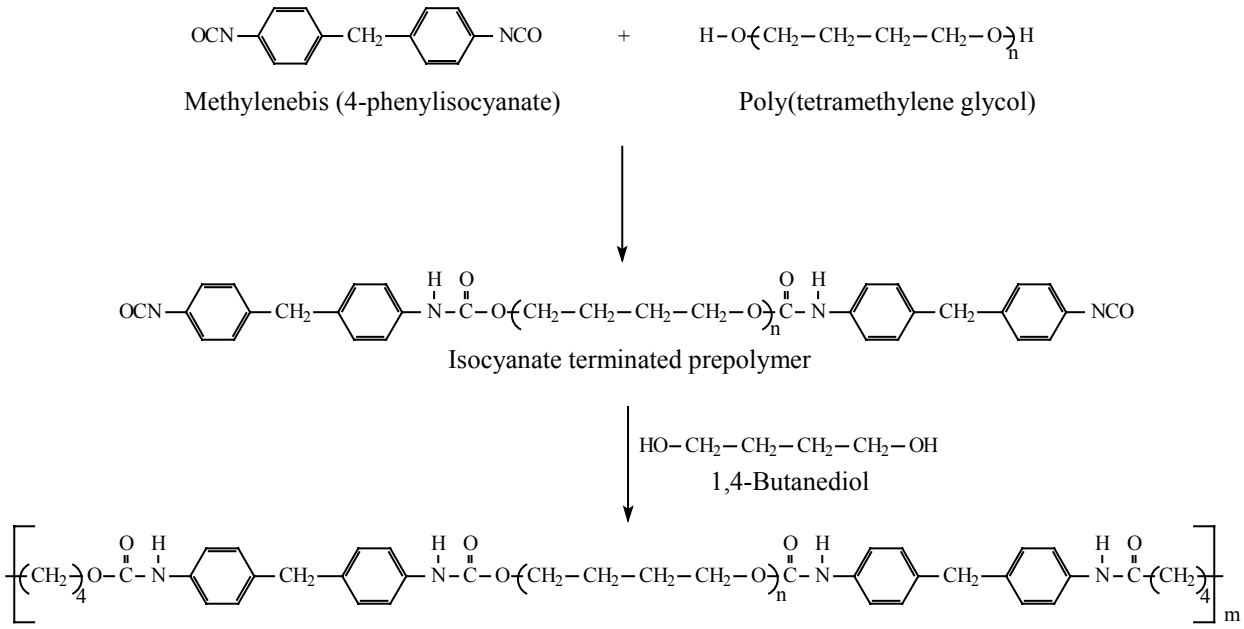

Scheme 5.3-1 Synthesis of a typical segmented polyurethane.

Polyurethanes have been used as thermoplastic elastomers and in some instances as substitutes for chemically crosslinked networks[1,2]. Thermoplastic elastomers can form three-dimensional networks, which differ markedly from thermosetting networks in this respect that their crosslinks are of physical nature. The advantages of these thermoplastic elastomers over chemically crosslinked systems include their processability and their solubility in some organic solvents, since no permanent crosslinks are formed. Thermoplastic polyurethanes give rise to microphase separation, resulting in hard and soft domains[3]. Below their glass transition temperatures (T_g), the hard segments act as physical junction points for soft segments. The domains would remain unmodified if the system were below the transition temperature for microphase separation.

Despite their wide range of applications, polyurethanes are flammable in nature. In this work we would show that chain extenders that contain phosphine oxide units could be used to improve some of the drawbacks of polyurethanes.

5.3.2 Experiments

A systematic series of phosphorus containing segmented polyurea-urethanes were prepared by a conventional two-step polymerization. To a 250 ml three-necked round bottom flask fitted with a mechanical stirrer, a nitrogen inlet and a nitrogen outlet were added in this order poly THF (13.00g, 0.02 mol) and MDI (10.01g 0.04 mol). The mixture was heated with an oil bath and was allowed to stir for about 1 hr at 80^{o}C. The temperature was then lowered to 60^{o}C and butanediol (1.80g 0.02 mol) was added to the flask. The viscosity of the mixture built up gradually. The reaction was discontinued after 1 hr or even before, if the viscosity of the mixture was becoming unmanageable. The viscous mixture was then poured into a Teflon dish and the clear polymer film was

subsequently characterized. Similar reactions with other chain extenders (diols or diamines) were performed and the results are summarized in Table 5.3-1.

Polymers Derived From	[η] dl/g 25° C in NMP	5% wt Loss Temp. (^{o}C) (TGA)*	% Char Yield at 600 °C (TGA)*	Tg (°C) (DSC)**
Butanediol (control)	0.38	300	5	-47
EBHPPO	0.59	320	18	-40
DAMPO	0.32	293	19	-32
BAPPO	0.60	305	20	-43
BAMPO	0.41	305	20	-39

- * Heating at 10^{o}C/min in air
- ** Heating at 10^{o}C/min under N_2, second heat scan data

Table 5.3-1 Characterization of the Phosphine Oxide Containing Poly(Urea-Urethanes)

5.3.3 Results and Discussion

The syntheses of segmented polyurea-urethanes were achieved, using monomers synthesized in this work and a control (butanediol). DSC thermograms of urethanes using butanediol (control) and DAMPO as chain extenders are shown in Figures 5.3-1 and 5.3-2, respectively. Dynamic thermogravimetric (TGA) traces of the urethanes with butanediol and EBHPPO as chain extenders are shown in Figures 5.3-3 and 5.3-4, respectively. The intrinsic viscosities, 5% weight loss temperatures, % char yields and glass transition temperatures of the polymers are summarized in Table 5.3-1.

The urethanes were of high molecular weight, since the intrinsic viscosities of all samples were greater than 0.3. DSC thermograms of the polymers showed single glass transition temperatures, around –40^{o}C, which correspond to the transition temperature of the soft segment. The glass transition temperatures of the hard segments were not detected.

The thermo oxidative stabilities (5% weight loss temperatures) of phosphine oxide containing polyurethanes were comparable to that of the control, 300^{o}C, with the exception of the urethane derived from DAMPO whose thermo oxidative stability was somewhat low (290^{o}C). This was readily interpreted as a result of the lower solubility of the monomer in the prepolymer (poly THF), yielding a less defined structure. This is corroborated by other work in our research group, were the DAMPO polyurethanes made with a solvent were comparable to those of control samples[4].

Urethanes containing phosphine oxide units had higher char yields than the control, which suggest their possible use in fire resistant applications. TGA traces of the urethanes showed a two-stage degradation, one at approximately 300^{o}C and the other at 500^{o}C. This is often observed in segmented polymers. Further studies could determine which segment degrades first.

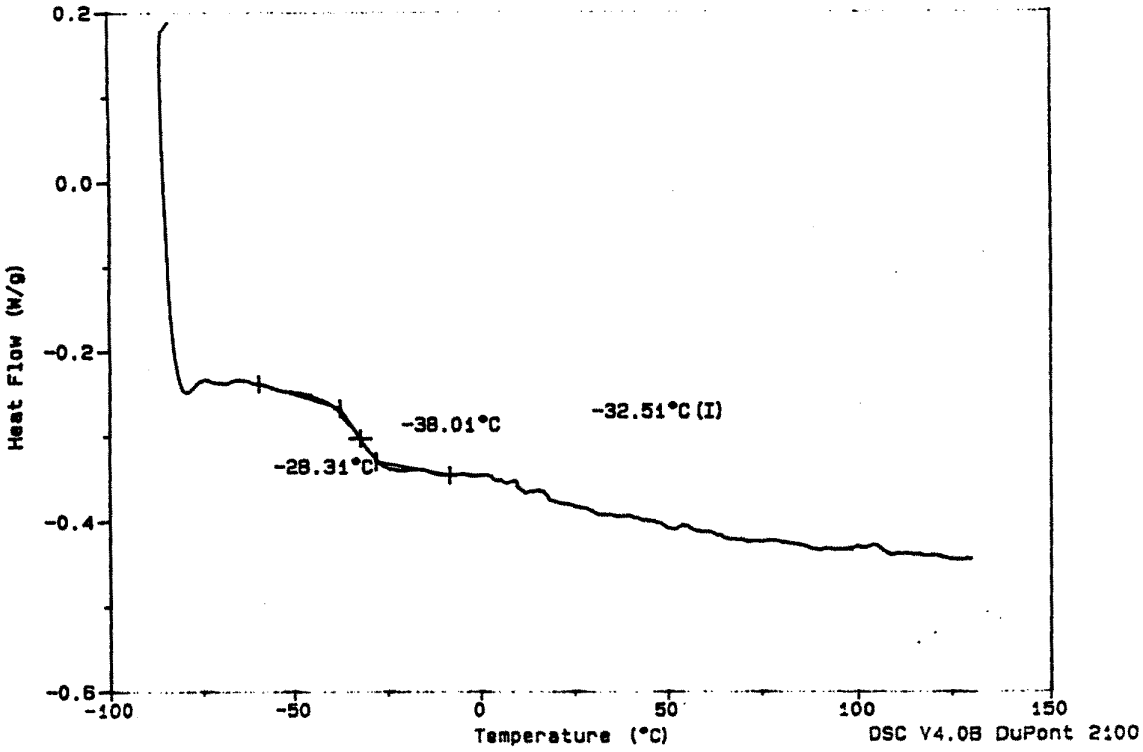

Figure 5.3-1 DSC Thermogram of a Segmented Polyurethane with Butanediol as Chain Extender

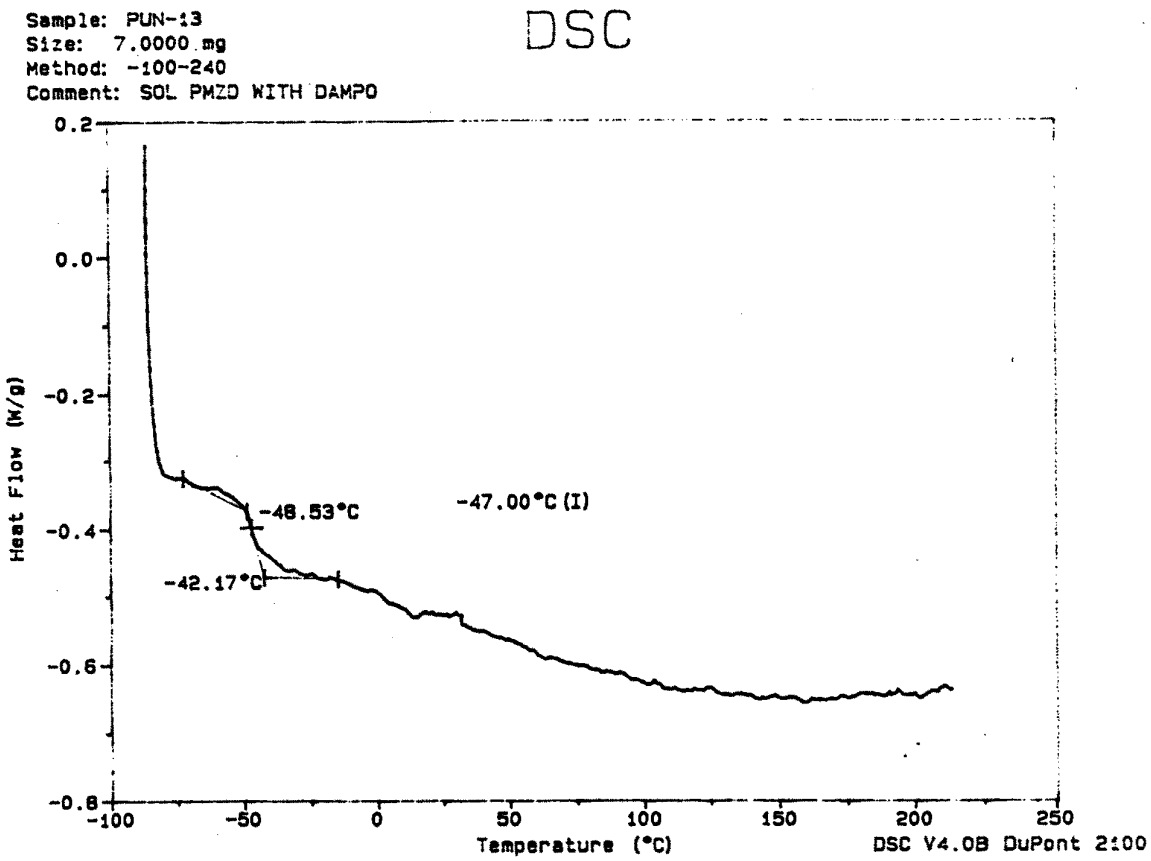

Figure 5.3-2 DSC Thermogram of a Segmented Polyurethane with DAMPO as Chain Extender (Control)

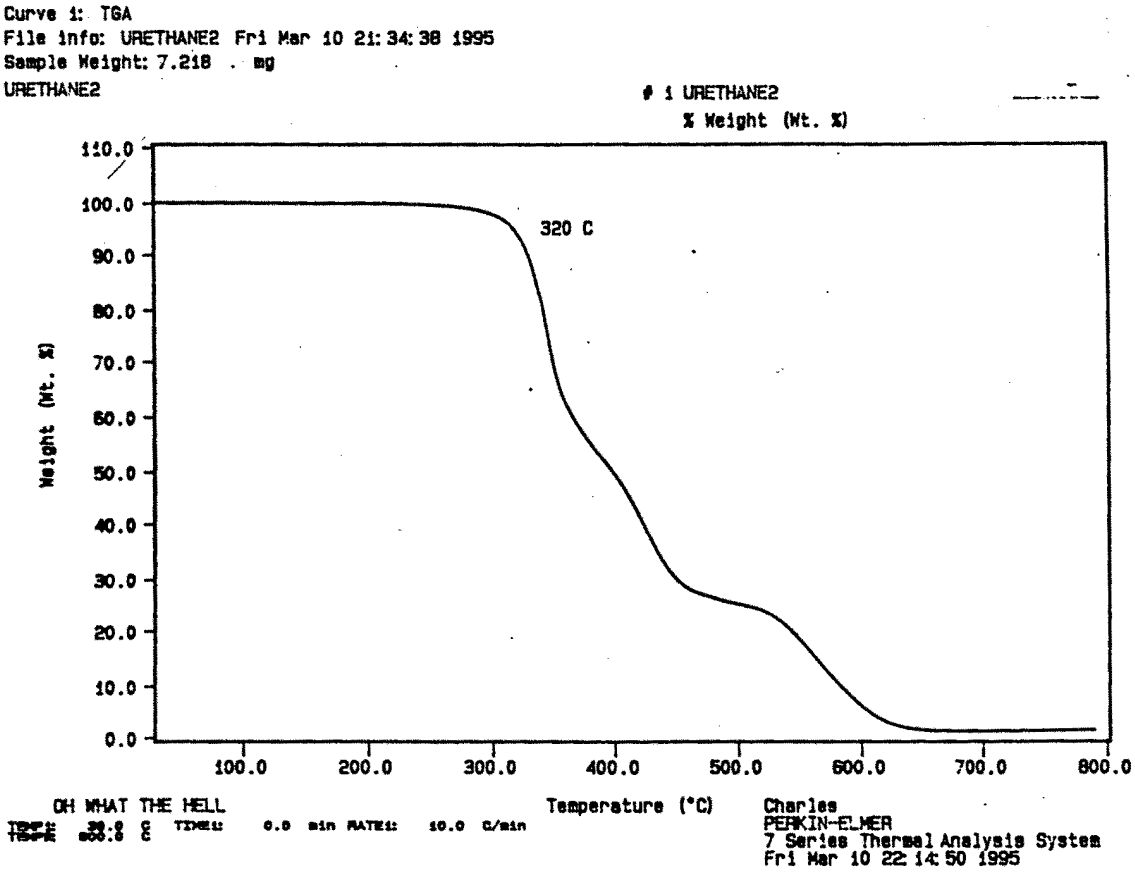

Figure 5.3-3 TGA traces of a Segmented Polyurethane with Butanediol as Chain Extender (Control)

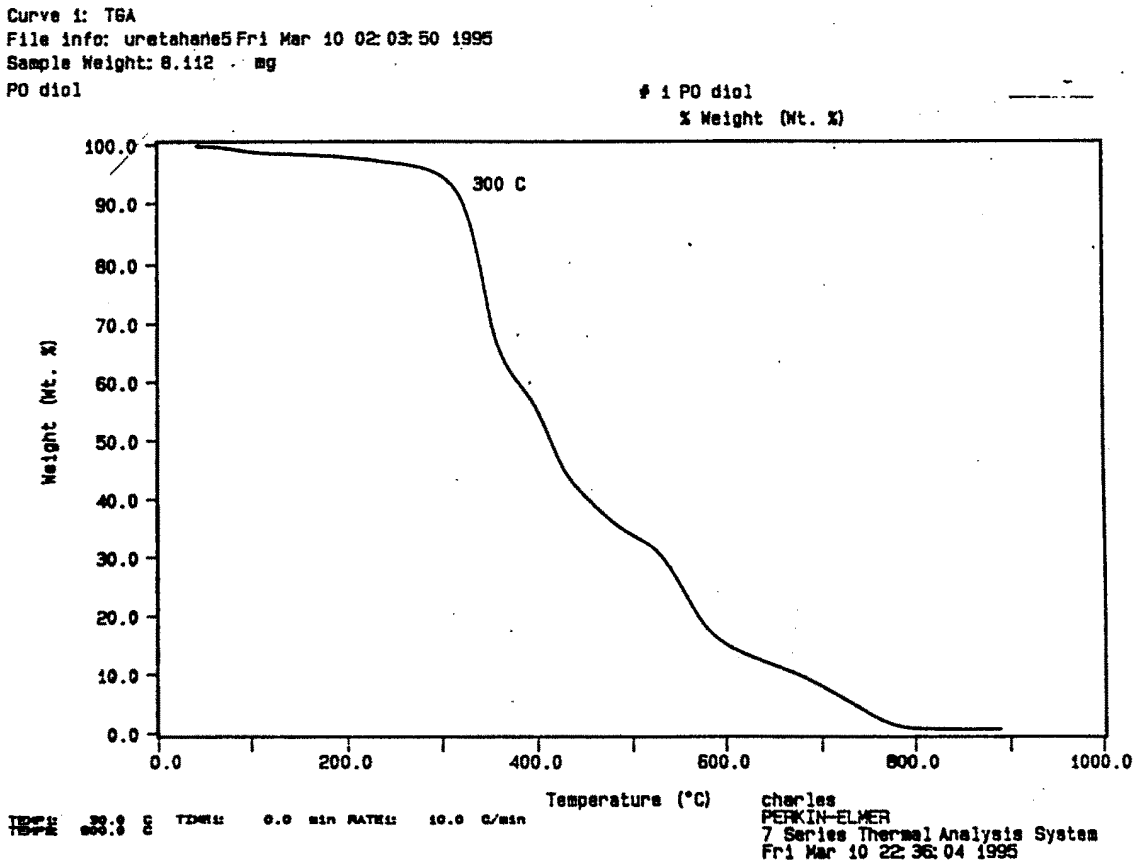

Figure 5.3-4 TGA traces of a Segmented Polyurethane with EBHPPO as Chain Extender

5.4 Poly(Arylene Ether Ketone Ketones)

5.4.1 Introduction

There has recently been an increasing interest in arylene ether ketones[5, 6]. Materials of this class of engineering plastics are constantly being designed, because of their scientific and commercial importance. The interest in poly(arylene ether ketones) can be attributable to their valuable characteristics. These include excellent thermal stability, high melting transitions and good mechanical properties, which are maintained well above 250^{o}C. Moreover, their resistance to most common solvents and ionizing radiations is outstanding. The good mechanical properties of these materials are mainly due to their high degree of crystallinity.

Poly(arylene ether ketones) have found a wide variety of high technology applications ranging from injection molded parts for use at high temperatures or in aggressive environments, to insulation for high performance wires and cables and to composite materials for aerospace components.

The synthesis of polymers of this type can in principle proceed via two routes: The base protonated nucleophilic displacement by a phenol or a halogeno- or nitrobenzophenone[7.8] and the acid-protonated electrophilic condensation of an aromatic carboxylic acid or acid chloride with an aromatic ether. Early investigation of the electrophilc route failed to yield high molecular weight polymers because of the premature crystallization from the solvent (e.g. dichloromethane) then employed[9]. It was not until condensation was carried out using boron trifluoride as catalyst in anhydrous hydrofluoric acid as solvent that high molecular weight was achieved in an electrophilic synthesis of a crystalline polyether ketone. Nucleophilc substitution synthesis was similarly unsuccessful until a solvent (diphenylsulfone) was discovered[10] that enabled very high temperatures (300-340 ^{o}C) to be used. This allowed the polymer to remain in solution until high molecular weight was achieved. Later on, aromatic polyether ketones were synthesized by using a reversibly modified monomer to generate a more soluble, amorphous polymer, which only crystallized on subsequent hydrolytic removal of the modifying acetal function[11]. When

strong acids such as hydrofluoric acid are used as solvents, the carbonyl group is protonated, which allows the polymer to remain in solution even at low temperatures. The electrophilic condensation can then take place and high molecular weight polymers can be obtained. Unfortunately, the use of hydrofluoric acid is extremely hazardous; it is volatile, corrosive and toxic. Some less hazardous alternatives such as polyphosphoric acid/aluminum chloride[12] and phosphorus (V) oxide in methane sulphonic acid[13] have been recently investigated, but only moderate molecular weight polymers were obtained (inherent viscosity 0.65) after several trials. More recently it has been reported that the superacid solvent trifluoromethane sulfonic acid (CF_3SO_3H) promotes the condensation of carboxylic acids with activated rings to give para-substituted ketones in high yields. Since trifluoromethane sulfonic acid is relatively non-volatile (b.p. 162^{o}C), not corrosive to glassware, non-oxidizing, nonsulfonating and, once neutralized, is not much more toxic than any other chemicals, it is now being investigated as catalyst and as solvent in many laboratories[9].

In our research, we decided to introduce a phosphine oxide unit into a pol(arylene ether ketone ketone), to improve on its solubility and allow the synthesis of higher molecular weight materials.

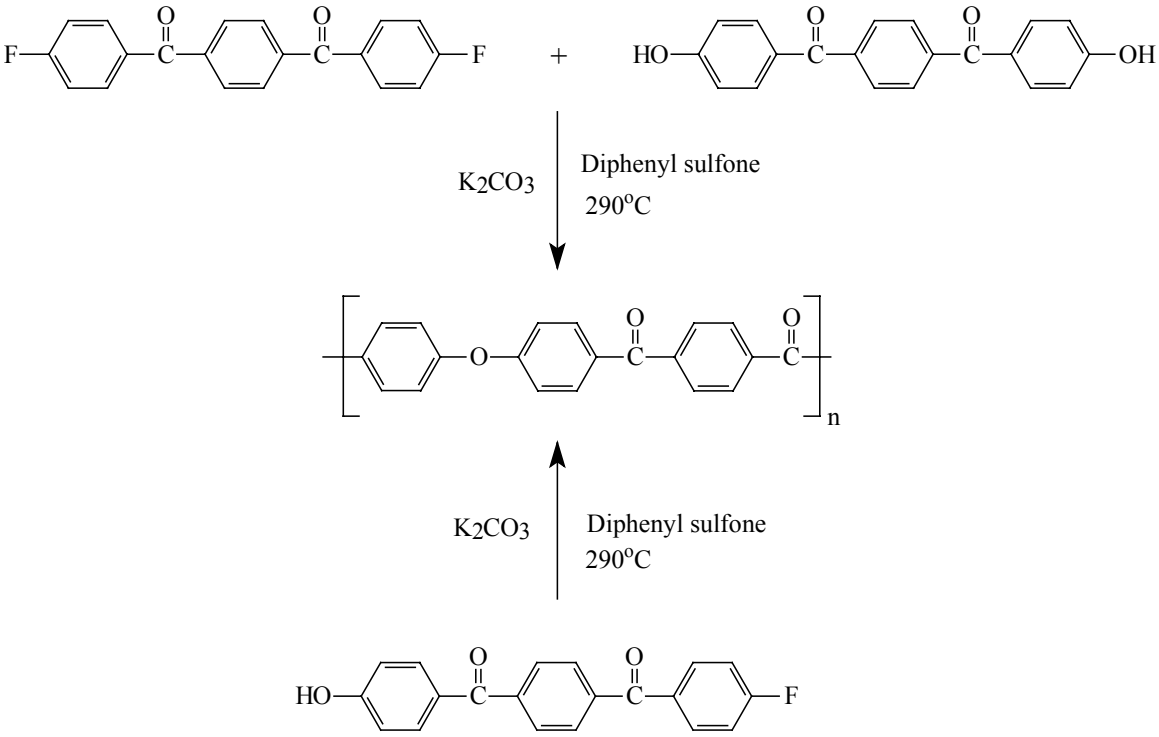

Scheme 5.4-1 Nucleophilic aromaticsubstitution synthesis of a poly(arylene ether ketone ketone)

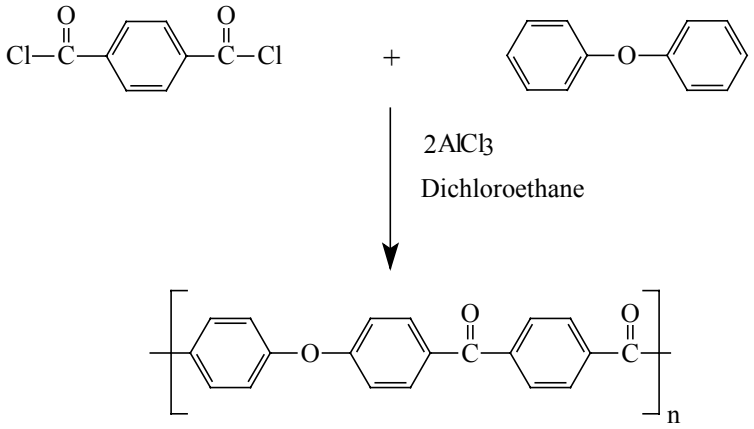

Scheme 5.4-2 Electrophilic polyacylation synthesis of a poly(arylene ether ketone ketone)

5.4.2 Experiments

Dichloromethane (150 ml), alumium chloride (13.3g, 0.10 mol), terephthaloyl chloride (10g, 0.05 mol) and diphenyl ether (8.5g, 0.05 mol) were placed in a 500 ml round bottom, three-neck flask, fitted with a mechanical stirrer, a nitrogen inlet, a reflux condenser and a gas outlet connected to a vessel containing a sodium hydroxide solution (to neutralize the HCl gas generated by the reaction). The reaction mixture was heated to reflux on an oil bath for two hours. The the contents of the flask were then precipitated into methanol. The solid precipitate was filtered, washed several times with water and dried in a vacuum oven at 150^{o}C. The yield was essentially quantitative. Similar reaction conditions were applied with the phosphine oxide monomer (BPPPO) substituted for one half and all the diphenyl ether. The results for this series of preparations are shown in Table 5.4-1.

5.4.3 Results and Discussion

Phosphorus NMR (Figure 5.4-1) confirmed the polymerization of the novel phosphine oxide-containing polymer. The occurrence of an additional peak on the spectrum can be ascribed to ortho substitutions on the phenyl ring, which sometimes occur during Friedel-Crafts type reactions.

The solubility of the crystalline poly(arylene ether ketone ketone) was improved by the introduction of the phosphine oxide moiety. Dynamic thermogravimetric data (Figure 5.4-2) indicate that polymers containing phosphine oxide units had higher char yields

than the control poly(arylene ether ketone ketone), which suggests their possible use for flame resistance applications. The thermal stability of the control polymer was somewhat low, which could be readily ascribed to its low molecular weights.

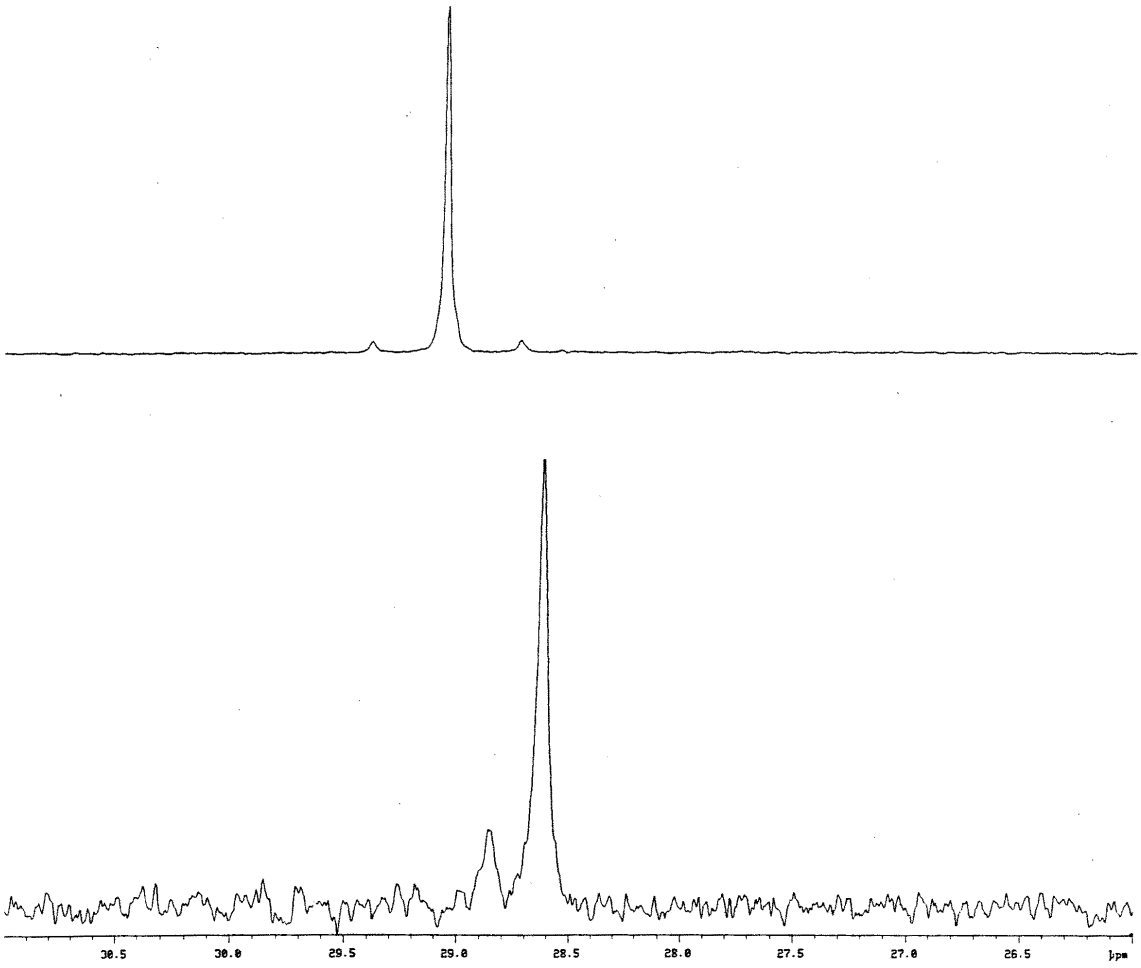

Figure 5.4-1 Phosphorus NMR of the poly (ether ketene) with all BPPPO in the repeat unit (bottom) and of the pure BPPPO monomer (top).

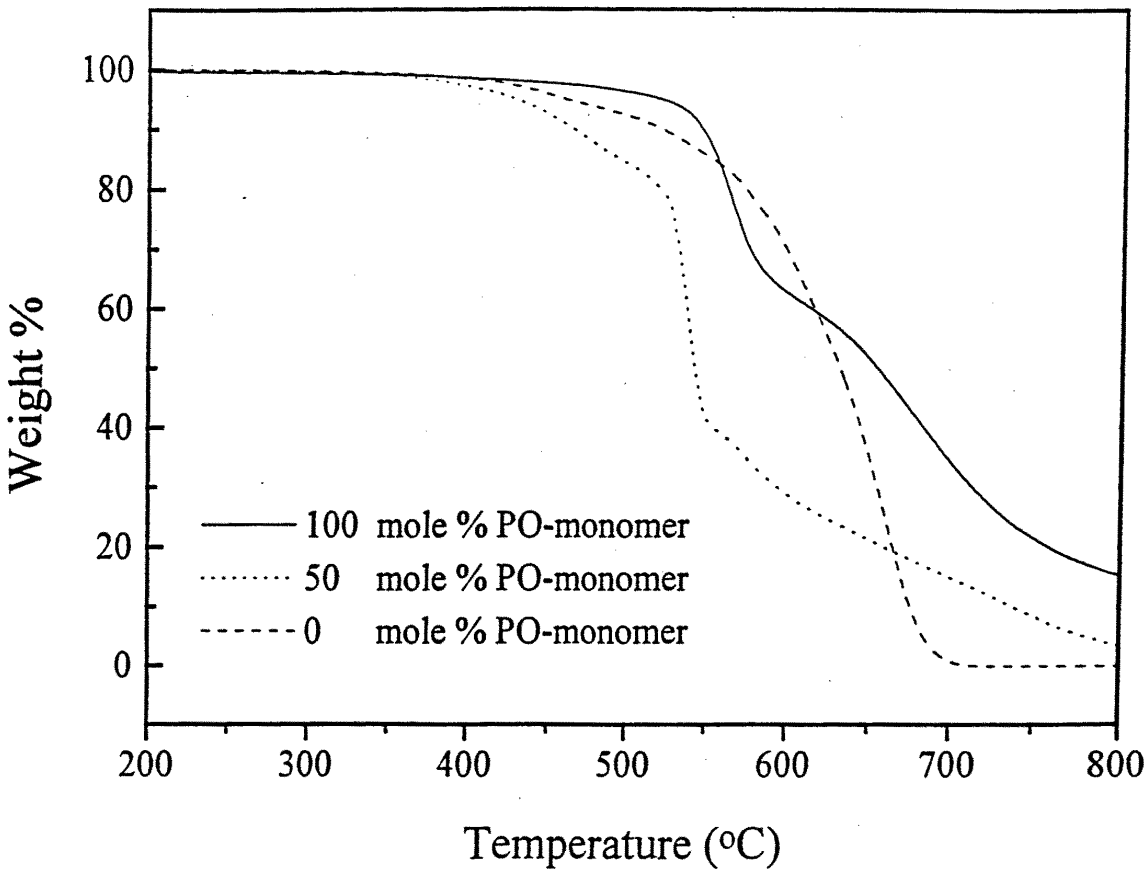

Figure 5.4-2 Thermogravimetric analysis of the poly(arylene ether ketone ketone)

Table 5.4-1 Data on attempted electrophilic substitution polymerizations with a phosphorus containing monomer and a control.

Mole ratio of Monomers* TC:DPE:BPPPO	Temp at 5% weight loss** (° C)	Char Yield at 750° C (%)	Solubility in Dichloroethane
1:1:0	460	0	Insoluble
1:0.5:0.5	428	13	Soluble
1:0:1	509	22	Soluble

* TC= Terephthaloyl chloride; DPE = Diphenyl ether; BPPPO = Bis(4-phenoxyphenyl) phenyl phosphine oxide
** Heating at 10^{o}C/min in air

5.5 Polyimides

5.5.1 Introduction

Aromatic polyimides are step growth polymers derived from aromatic tetracarboxylic acid dianhydrides and aromatic diamines. The heterocyclic imide units generate polymers with chain rigidity and imparts high chain interactions, which have earned polyimides their classification as high performance polymers. They are well known for their outstanding thermal stability, mechanichal and electrical properties[14, 15]. They are used in the electrical and aerospace industries in the forms of films and moldings. They are also used as adhesives, gas separation membranes, composite matrices, coatings and foams. Their applications are expected to increase dramatically in the next millennium. However, most aromatic polyimides are not processable, due to their insolubility and high glass transition temperatures (T_g). Thus they are usually processed in their soluble precursors forms and then imidized thermally or chemically[17-20]. One soluble polyimide precursor is is the corresponding poly(amic acid) which is widely used in the fabrication of all kinds of devices because of the simplicity of its synthesis. However a poly(amic acid) exits in equilibrium with its anhydride and amine parents, which makes its chain length sensitive to any temperature or moisture variations.

Another soluble polyimide precursor is the poly(amic alkyl ester). This precursor has high hydrolytic stability, due to the absence of equilibration with the parent monomers. For this reason, the poly(amic alkyl ester) route has gained considerable importance in the synthesis of polyimides[21,22].

In this section, the synthesis of polyimide containing ether and phosphine oxide units will be described. Those units create angular bonds in the polymer chain and also allow some rotation of the aromatic rings, thus improving polymer solubility and processability. In addition to this, the phosphine oxide moiety improves flame resistance properties of polymers.

5.5.2 Synthesis of Phosphine Oxide Containing Poly(Ether Imides), Ultem™ type.

A typical synthetic reaction for the synthesis of a poly(ether imide), Ultem™ type is depicted in Scheme 5.4-1. In the synthesis of phosphine oxide containing poly(ether imides), phosphine oxide monomers (DAMPO or DAPPO) were used as partial or total replacement for the usual diamine component, *m*-phenylene diamine (*m*-PDA). The poly(amic alkyl ester) route was selected for this system[23,24]. An example for the synthesis of an Ultem type poly(ether imide) (Mn = 20,000) with 50% of the DAMPO monomer is given below.

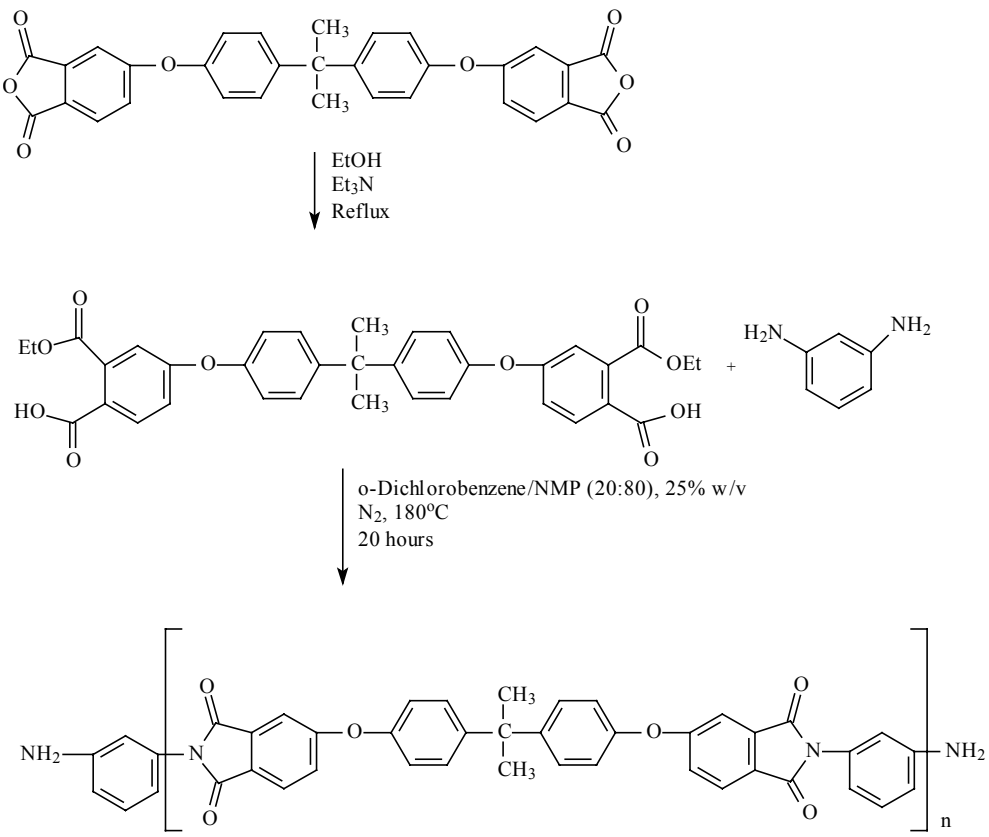

Scheme 5.5-1 Synthesis of an amine terminated poly(ether imide), Ultem type

BTDA (15.39g, 0.03 mol), ethanol (140 ml) and triethyl amine (2ml) were loaded in a 250 ml 3-necked round bottom flask euipped with a over head stirrer, reverse Dean-Stark trap,and a reflux condender with a nitrogen outlet. The mixture was heated to reflux on an oil bath and stirred for about one hour until a clear solution was obtained. The clarity of the solution denotes the formation of the ester acid. The ethanol and the triethyl amine were then stripped by distillation. Then *m*-PDA (1.87 g, 0.017 mol) and DAMPO (3.76g, 0.015 mol), NMP (60 ml) and *o*-dichlorobenzene 20 ml) were added to afford a 25% solution. The trap was filled with *o*-dichlorobenzene, and the reaction mixture was heated to approximately 180^{o}C for 20 hours. The viscous polymer was then cooled to 80^{o}C, and diluted with NMP to 15%weight solid. The polymer was precipitated into methanol, by means of a blender, filtered and dried under vacuum at 180^{o}C for 24 hours. The characterizations of the polymers are shown in Table 5.5-1

5.5.3 Synthesis of Thermoplastic Poly(ether imide) Modifiers

The synthesis of the thermoplastic modifiers proceeded in a manner similar to that described in section 5.5.2 above, except for the fact that no portion of the phosphine oxide containing monomers were used as a substitute for the *m*-phenylene diamine (MDA).

A Systematic series of amine terminated poly(ether imides) were synthesized as shown in Scheme 5.5-1, with the expected molecular weigths of Mn = 10,000, Mn = 15,000 and Mn = 20,000. This last molecular weight (20,000) corresponds to the molecular weight of their commercial homolog, Ultem™. The polymers were characterized by titration, ^{1}H NMR, and gel permeation chromatography (GPC). The results are summarized in Table 5.2-2.

5.5.4 Results and Discussion

Dynamic thermogravimetric analyses of the polymers are shown in Figure 5.5-1 and 5.5-2 for DAMPO and DAPPO phosphine oxide containing poly(ether imides), respectively. The molecular weight data, 5% weight loss temperatures, percent char yield and glass transition temperatures of the polymers are summarized in Table 5.5-1. The phosphine oxide containing poly(ether imides) were of high molecular weight, which illustrates the high purity of the monomers involved in their syntheses. The molecular weight control was outstanding. All the phosphine oxide containing polymer molecular weights were close to their expexted values (Mn = 20,000). The polydispersities (Mw/Mn) were consistent with that of most condensation polymers, since their values were close to 2. The glass transition temperatures, were all around 215^{o}C. Clearly, the transitions (T_g) of phosphine oxide containing poly(ether imides) were close those of the control.

The thermo oxidative stabilities (5% weight loss temperatures) of phosphine oxide containing poly(ether imides) were comparable to those of the control polymer (~260^{o}C), as determined by dynamic thermogravimetric analyses. Phosphine oxide containing poly(ether imides) had higher char yields (30% to 54%) at 750^{o}C than the control (11.5%). The char yield increased with the percentage of the phosphine oxide monomer in the polymer. These results suggest the possible applications of phosphine oxide containing poly(ether imides) for flame resistance applications.

Amine terminated poly(ether imides) thermoplatic prepolymers were also synthesized. No phosphine oxide units were included in the modifiers. Their molecular weight characteristics are included in Table 5.5-2. The molecular weights of the modifiers all approached their expected values. The distributions (Mw/Mn) were consistent with those of typical condensation polymers. The molecular weights estimated

by titration, were comparable to those estimated by gel permeation Chromatography (GPC) and ^{1}H NMR, however, during the thoughening of the epoxy networks, only the molecular weights by titration were taken into account.

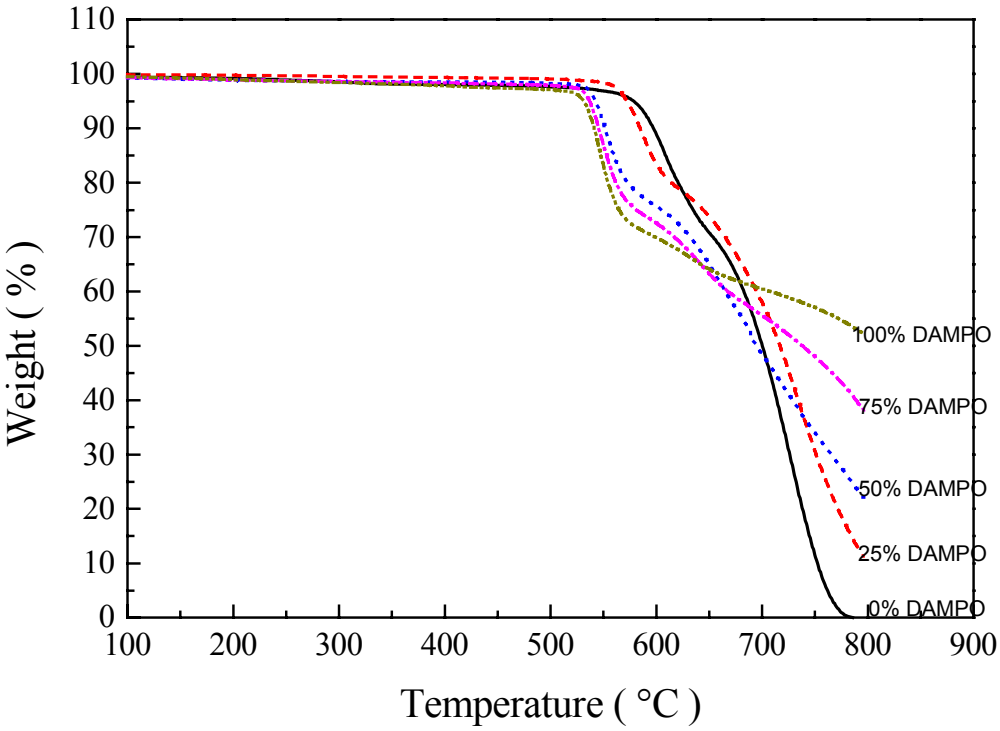

Figure 5.5-1 Dynamic TGA of DAMPO containing copolymers (in air, 10°C/min.)

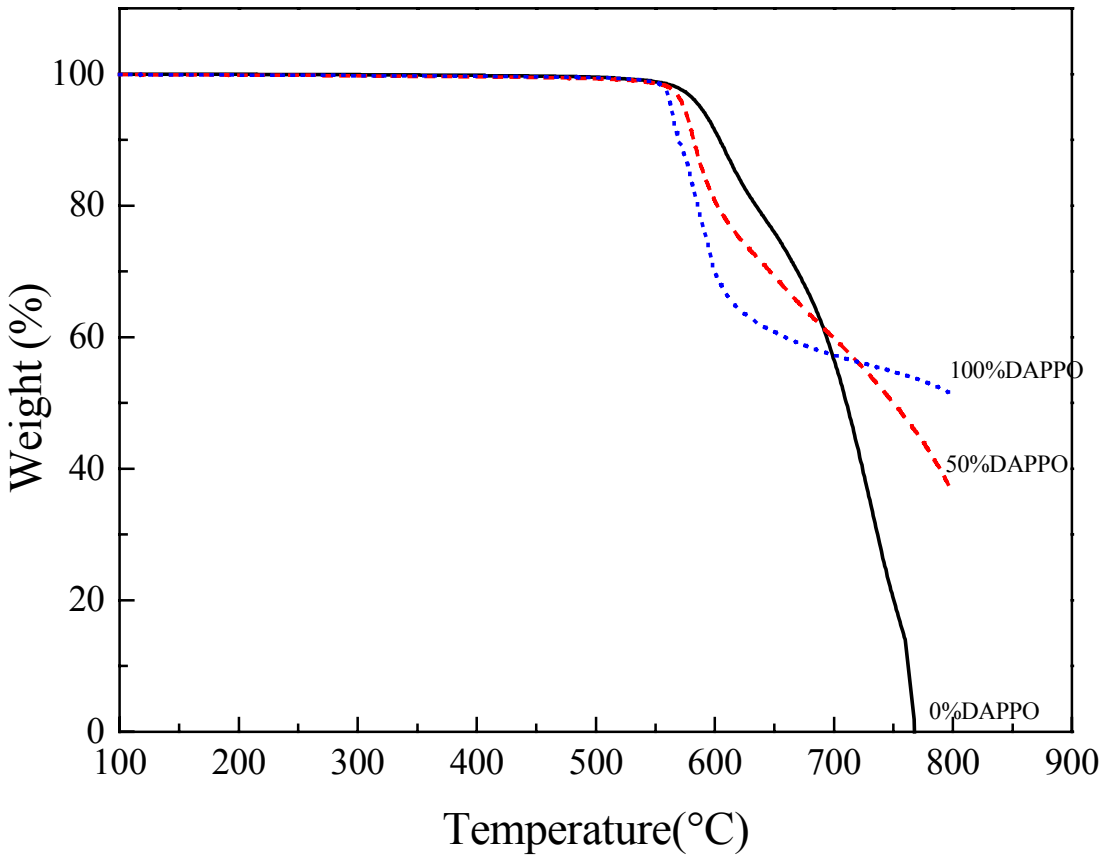

Figure 5.5-2 Dynamic TGA of DAPPO containing copolymers (in air, 10°C/min.)

Polymer % DAMPO	Target M_n (g/mol) $\times 10^{-3}$	M_n by GPC (g/mol) $\times 10^{-3}$	M_w/M_n	5 wt. % Loss Temp. TGA	% Char Yield TGA*	Tg (°C) (DSC)**
0 DAMPO	20	20.6	1.8	578	11.5	219
25 DAMPO	20	20.6	1.8	572	30	215
50 DAMPO	20	18.6	2.0	552	34	216
75 DAMPO	20	20.2	1.7	537	48	211
100 DAMPO	20	19.0	1.8	532	57	211
50 DAPPO	20	19.4	2.1	576	50	217
100 DAPPO	0	19.	1.9	563	54	217

* Heating at 10 C/min in air
** Heating at 10 C/min in N_2, second heat scan data

Table 5.5-1 Characterization of the phosphine oxide containing poly(ether imides)

Polymer	Intrinsic Viscosity[a] [η] dL/g	Molecular Weight by GPC			<M_n> by Titration ($\times 10^3$)	<M_n> by ^{1}H NMR ($\times 10^3$)
		<Mn> ($\times 10^3$)	<Mw> ($\times 10^3$)	<Mw>/<Mn>		
10K	0.347	13.0	25.0	1.9	11.8	
15K	0.441	16.3	30.9	1.9	14.9	
20K	0.470	19.7	38.3	1.9	19.3	17.8

a) In NMP at 25° C

Table 5.5-2 Characterization of the amine terminated thermoplastic polyimide modifiers (Ultem™ type)

5.6 Reference

65. Sivriev, C. and L. Zabski (1994) *Eur. Polym. J.*, **30(4)** 509.

66. Brinson, H. F. (1990) *Engineered Materials Handbook, Adhesives and Sealants*, Vol. 3, ASM International, p. 108.

67. Estes, G. M., S. L. Cooper and A. V. Tobolsky (1970) *J. of Macro. Sci. Rev. in Macro. Sci*., C4, 329.

68. Ji, Q., M. Muggli, C. Tchatchoua, S. Srinivasan, T. C. Ward and J. E. McGrath (1996) *Polym. Preprints* 37(1), 579

69. Ozarslan, O., E. Yildiz, T. Yilmaz, A. Gungor and A. Kuyulu

70. Ben-Haida, A. H. M. Colquhoum, P. Hodge and D. F. Lewis (1999) *Polymer*, **40**(18), 5173.

71. Johnson, R. N., A. G. Farham, R. A. Clendinning, W. F. Hale and C. N. Merriam, (1967) *J. Polym. Sci.*, A-1, **5**, 375.

72. Radlmann, V. E., W. Schmidt, and G. E. Nischk (1969) *Makromol. Chem*., **130**, 45.

73. Colquhoun, H. M. and D. F. Lewis (1988) Polymer, **29**, 1902.

74. Atwood T. E., P. C. Dawson, J. L. Freeman, L. R. J. Hoy, J. B. Rose and P.A. Taniland (1981) *Polymer*, **22**, 1096.

75. Kelsey, D. R., L. M. Robeson, R. A. Clendinning and C. S. Blackwell (1987) *Macromolecules*, **20**, 1204.

76. Niume, K., F. Toda. K. Uno, M. Hasegawa and Y. Ikura (1965) *J. Polym. Sci., Polym. Chem. Ed*., **20**, 1265.

77. Ueda M. and T. Kano (1985) *Makromol. Chem,. Rapid commun.*, 5, 833.

78. Wilson, D., H. D. Stenzenberger, P. M. Hergenrother (1990) Eds. Polyimides; Chapman and Hall, New York.

79. Ghosh, M. K., K. L. Mittal (1996) Eds. Polyimides: Fundamentals and Applications, Marcel Dekker, New York.

80. Sroog, C. E. (1991) *Prog. Polym. Sci*., 16:561.

81. Feger, C., M. M. Khojasteh, S. E. Molis (1996) Eds, Trends in material and applications. *Proc. 2nd Intern. Conf. Polyimide*, Mid-Hudson Section of Soc. Plastic Eng.

82. Czornyj, G., K. J. Chen, G. Silva-Prada, A. Arnold, H. A. Souleotis, S. Kim, M. Ree, W. Volksen, D. Dawson and R. DiPietro (1992) *Proc. Elect. Comp. Tech*. (IEEE), **42**, 682.

83. Ree, M., K. Kim, S. H. Woo and H. J. Chang (1996) *App.l Phys.*, **81**, 698.

84. Ree, M., D. Y. Yoon, W. J. Volksen (1991) *Polym. Sci. Part B: Polym. Phys*., **29**, 1203.

85. Houlihan, F. M. , B. J. Bahman, C. W. Wilkins and C. A. Pryde (1989) *Macromolecules*, **22**:4477.

86. Kim, Y., M. Ree. T. Chang, Y. Kim, M. Ree and T. Chang (1995) *Polym. Bulletin*, **34**:219.

87. Tan, B., C. N. Tchatchoua, L. Dong and J. E. McGrath (1998) *Polym. Adv. Technol*. **9**, 84-93.

88. Zhuang, H. (1998) Ph. D. Thesis, Virginia Polytechnic Institute and State University.

6 Chapter 6 CONCLUSIONS

In this work, several phosphine oxide containing monomers were sucessfuly synthesized. These monomers included bis(3-aminophenyl) methyl phosphine oxide(*m*-DAMPO), bis(3-aminophenyl) phenyl phosphine oxide (*m*-DAPPO), bis(3-aminophenoxy phenyl) phenyl phosphine oxide (*m*-BAPPO), and bis(3-aminophenoxy phenyl) methyl phosphine oxide (*m*-BAMPO). Modification of the existing synthetic procedures and work-up methods for those monomers resulted in increased yields and higher monomer purity than those achieved by previous investigators. Several novel monomers were synthesized as well.

The molecular structures of the monomers were confirmed by Fourier transform infrared spectroscopy, proton NMR spectroscopy, mass spectrometry and elemental analysis. Their high degrees of purity were determined by phosphous NMR, which revealed that only one type of phosphorus was present in each product therefore, there were no phosphorus containing impurities. Their purity was also determined by liquid chromatography and in some instances by potentiometric titration.

The monomers were subsequently used in the synthesis of high performance polymers, including epoxy networks, polyimides, poly(arylene ether ketone ketone)s, and poly(urea-urethanes). The polymers were characterized with respect to their structures and thermal properties. Polymers containing phosphine oxide units showed higher flame resistance than the controls, as assessed by dynamic thermogravimetric analysis, qualitative Bunsen burner tests developed in our laboratory, and externally performed cone calorimetric assays. The flame resistance seemed to increase with the phosphorus contents of the polymers in some tests, while the qualitative test showed that all the polymers were similarly flame resistant.

The introduction of the phosphine oxide moities into the polymer backbones did

not seem to proceed at the expense of other properties, such as glass transition temperature, thermostability and fracture behavior. In general, polymer properties were improved by the introduction of phosphine oxide units. Polymers containing phosphine oxide units showed weight loss onset temperatures similar to those of control samples.

Dramatic improvements of the TGDDM-DDS epoxy network fracture toughness were achieved through the means of amine terminal polyimide thermoplastic modification, with only a moderate decrease in flexural modulus. Fracture properties of these toughened networks were superior to those modified by their non-functionalized commercial homologues.

Solvent resistance of the toughened networks also was significantly higher when the thermoplastic modifiers were functionalized, when compared to that of the networks toughened by modifiers that were not funtionalized. Basically, all of the non-functionalized modifiers were extracted from the networks during the chemical insult, while amine terminated modifiers remained in the networks. These results were verified by scanning electron micrography (SEM) which showed etching of the sample surfaces, and Soxhlet extractions that indicated changes in the weight of the samples due to modifier removal.

Dielectric monitoring was an effective technique for following the curing process of epoxy resins. It was used to assess the relative gelation time and the vitrification time of the curing networks. The time between the beginning of the cure and vitrification was longest for 4,4'-DDS at 177^{o}C when reacted with Epon-828 for example, and was shortest for DAMPO. This was to be expected, due to differences in the structures of the diamines. Also, tetrafunctional epoxy resins cured much faster than the difunctional resins.

Transition temperatures were significantly higher for tetrafunctionl epoxy networks, than for those networks generated from Epon-828.

7 VITAE

Charles Ngassa Tchatchoua was born and educated in Cameroon (West Africa). His parents, John and Jeaninne Tchatchoua are farmers. He earned a Diploma of Advanced Education in Statistical Genetics from the University of Paris in 1987, after which he came to the United States and completed a Master Degree in Animal Science in 1992 at Virginia Polytechnic Institute. He started a graduate program in chemistry in the same school in 1992. Until the completion of his doctoral program in 1999, his has been a wonderful laboratory instructor for both general and organic chemistry courses. He is currently a post doctoral research associate in the department of chemistry at Virginia Polytechnic Institute and State University.